FGF Signaling in Tyrosine Kinase Inhibitor Resistance

By

Nathalie Javidi-Sharifi

A DISSERTATION

Presented to the Department of Cancer Biology

and the Oregon Health & Science University

School of Medicine

in partial fulfillment of

the requirements for the degree of

Doctor of Philosophy

August 2016

School of Medicine

Oregon Health & Science University

CERTIFICATE OF APPROVAL

This is to certify that the PhD dissertation of

Nathalie Javidi-Sharifi

has been approved

Table of Contents

iv

List of Figures

List of Tables

Abbreviations

A-loop	activation loop
ABL	Abelson tyrosine kinase
ALL	acute lymphocytic leukemia
AML	acute myeloid leukemia
ATP	adenosine triphosphate
BCR	break point cluster region
BM	bone marrow
c-Src	cellular proto-oncogene sarcoma tyrosine kinase
C-terminal	carboxy-terminal
CAR	CXCL12-abundant reticular cells
CLL	chronic lymphocytic leukemia
CML	chronic myeloid leukemia
CXCL12	C-X-C motif chemokine 12
DAG	diacyl glycerol
DFG motif	asparagine phenylalanine glycine motif
DGK	DAG kinase
DNA	deoxyribonucleic acid
ECV	extracellular vesicle
EGF	epidermal growth factor
EGFR	epidermal growth factor receptor
Eph	ephrin
ER	endoplasmic reticulum
ERK	extracellular signal-regulated kinase
ESCRT	endosomal sorting complexes required for transport
FGF	fibroblast growth factor
FGFR	fibroblast growth factor receptor

FL	FLT3 ligand
FLT-ITD	FLT3 internal tandem duplication
FLT3	fms-like tyrosine kinase 3
G-CSF	granulocyte colony stimulating factor
GIST	gastrointestinal stromal tumor
GM-CSF	granulocyte monocyte colony stimulating factor
HCL	hairy cell leukemia
HER2/neu	human epidermal growth factor receptor 2
HGF	hepatocyte growth factor
HMW	high molecular weight
HSC	hematopoietic stem cell
HSP	heat shock protein
iCCA	intrahepatic cholangiocarcinoma
IFN	interferon
Ig	immunoglobulin
IGF	insulin-like growth factor
IGF-1R	insulin-like growth factor receptor 1
IHC	immunohistochemistry
IL	interleukin
JAK	janus kinase
KD	kinase domain
KDM	kinase domain mutation
KO	knockout
LMW	low molecular weight
LSC	leukemia stem cell
MAPK	mitogen-activated protein kinase
MDS	myelodysplastic syndrome
MRD	minimal residual disease

MSC	mesenchymal stem cell
N-terminal	amino-terminal
NSCLC	non-small cell lung cancer
OSM	oncostatin M
PDGFR	platelet-derived growth factor receptor
PI3K	phosphoinositol-3-kinase
PKC	protein kinase C
PLC	phospholipase C
PMA	phorbol 12-myristate 13-acetate
PTB domain	protein tyrosine binding domain
RAR	retinoic acid receptor
RNA	ribonucleic acid
RT-PCR	reverse transcription polymerase chain reaction
RTK	receptor tyrosine kinase
SCF	stem cell factor
SCLL/EMS	stem cell leukemia/lymphoma
SDH	succinyl dehydrogenase
SH2 domain	Src homology 2 domain
siRNA	small interfering RNA
SQC	squamous cell carcinoma
STAT	signal transducer and activator of transcription
TGF	transforming growth factor
TKI	tyrosine kinase inhibitor
TMA	tissue micrarray
TNF	tumor necrosis factor

TYK2   tyrosine kinase 2

v-Src   viral proto-oncogene sacroma tyrosine kinase

VEGF   vascular endothelial growth factor

VEGFR   vascular endothelial growth factor receptor

Acknowledgements

I have been fortunate to be surrounded by an exceptional group of mentors and friends. I would like to thank my mentor Dr. Brian Druker for setting an inspiring example of excellence and devotion in the lab and with his patients, for providing me with opportunities to meet and learn from outstanding scientist, and most importantly for making a point of sharing his valued time and attention with me and other aspiring students. I would like to thank my mentor Dr. Jeff Tyner for his quiet brilliance and for teaching me important points on experimental design and how to bring a project to success. His insightfulness kept me on track while allowing me ample freedom to pursue my ideas. I would like to thank my mentor and friend Dr. Elie Traer for his continuing support and encouragement, and for his energy and enthusiasm that brings out the best in everyone. Especially during the last year, his mentorship has helped me grow as a scientist, and many pages of this thesis were filled thanks to our discussions. I am grateful to every member of my dissertation advisory committee: Dr. Rosalie Sears, Dr. Michael Heinrich, and Dr. Christopher Corless. I want to extend special thanks to Dr. Rosalie Sears for her interest in my scientific development. I would like to thank Dr. David Jacoby for his mentorship and seemingly unshakable trust in my abilities. I am also grateful to an exceptional mentor in the clinic, Dr. Craig Okada, for being a wonderful teacher and for making me excited for the next steps in my training.

I would like to thank the many former and current members of the Druker/Tyner labs, in particular my fellow graduate students David Edwards, Kevin Wantanabe-Smith, Chelsea Jenkins and Marilynn Chow, as well as Isabel English, Julia Maxson, Monika Davare and Christopher Eide.

I am grateful to my family for their support and love. Finally, I am most grateful to my husband Johannes Elferich. With him by my side, I feel I can do anything.

Abstract

This thesis describes fibroblast growth factor signaling in the development of resistance to tyrosine kinase inhibitor therapy in solid and hematologic malignancies, and in the maintenance of cancer-protective bone marrow stroma. Cell-extrinsic protection is emerging as a universal concept in cancer therapy. This promises to revolutionize the approach to targeted therapy, which previously centered on sequential employment of single inhibitors, or on drug combinations targeting several cell-intrinsic oncogene-activated pathways.

In this thesis, I demonstrate (i) that FGF2 enables persistence and outgrowth of gastrointestinal stromal tumor and chronic myeloid leukemia in the presence of imatinib, and of FLT3-ITD positive acute myeloid leukemia in the presence of quizartinib, (ii) provide evidence of clinical significance in all three malignancies, and (iii) define a role for FGF2 in the autocrine promotion of growth and maintenance of a cancer-protective phenotype in human bone marrow stromal cells. This includes the finding that FGF signaling promotes the production of exosomes in human bone marrow stroma, and the novel finding that FGF2 is conveyed from stroma to leukemia cells via exosomes. This work reveals FGFR signaling as a targetable pathway with the potential to modulate the microenvironment to prevent resistance.

1   **Introduction**

In this thesis, I will present my findings on the role of FGF2 (fibroblast growth factor 2) in microenvironment-mediated resistance to tyrosine kinase inhibitor therapy. The thesis will be divided into two parts; the first focusing on the paracrine protective function of FGF2 on three different cancers, and the second introducing FGF2 as an autocrine regulator of protective bone marrow stromal cells.

My research has demonstrated that FGF2 confers protection to a number of malignancies during exposure to tyrosine kinase inhibitor therapy. These malignancies arise in different organ systems, namely the bone marrow in the case of Acute and Chronic Myeloid Leukemias (AML and CML), and autonomic pacemaker cells of the gastrointestinal tract in the case of Gastrointestinal Stromal Tumor (GIST). A common feature of these malignancies is that their proliferation and survival is driven by mutational activation of receptor tyrosine kinases. I will discuss the individual receptors and their role in oncogenesis in introductory chapters pertaining to each malignancy. In this chapter, I will introduce receptor tyrosine kinases as oncogenes and targets for therapy. I will discuss the impact of tyrosine kinase inhibitors on cancer therapy and on provoking a paradigm shift in basic cancer research. Short-lived responses and the development of resistance remain the most widespread challenges to this therapeutic approach. The discussion here will focus on the role of cell-extrinsic factors in

protection and resistance. In addition to my own findings, FGF2 has been implicated in several types of therapy resistance. I will first provide an overview of fibroblast growth factor signaling, including a description of the ligand and receptor families, physiologic roles of FGF signaling, and then discuss pathologic dysregulation of these signaling pathways.

The second part of my thesis research focused on identifying the source, mode of delivery, and autocrine effect of FGF2 in bone marrow stroma. To this end, I will discuss the concept of the protective bone marrow niche in leukemia and its role in therapy resistance. Finally, I will introduce exosomes as versatile conveyors of cytokines, growth factors and nucleic acid between cancers cells and surrounding tissue. I will again comment on implications for therapy resistance and discuss exosomes as potential targets for cancer therapy.

1.1 Tyrosine kinases in cancer

In 1911, Peyton Rous discovered that tumors on the legs of chickens resulted from infection with a virus[1]. Several years later, Varmus and Bishop demonstrated that the oncogenic effect of the virus was due to a protein transcribed from viral RNA, but not viral in origin. The sequence encoding this oncogene had been acquired by the virus from cellular DNA[2]. The viral protein was named v-Src, and its cellular analog c-Src.

While the tyrosine kinase activity of the cellular form of Src was tightly regulated, the viral form became oncogenic through a constitutively activating mutation[3].

The human proteome contains more than 520 kinases and 130 phosphatases, exerting tight and reversible control on protein phosphorylation. Both of these enzyme categories can be subdivided into tyrosine- or serine/threonine-specific, based on their catalytic specificity. In addition, some possess dual specificity for both tyrosine and serine/threonine. The tyrosine kinase family numbers more than 90 genes in the human genome; 58 encode transmembrane receptor tyrosine kinases divided into 20 subfamilies, and 32 encode cytoplasmic, non-receptor tyrosine kinases in 10 subfamilies[4]. Kinases transfer a phosphate group from ATP to a tyrosine or serine/threonine residue on a protein. These phosphorylation events form the basis for intracellular signal transduction and are involved in pathways that promote growth and survival, cell cycle progression, differentiation, and apoptosis.

Tyrosine kinases can be broadly divided into two classes – receptor tyrosine kinases and intracellular kinases[5]-[7]. Receptor tyrosine kinases are single-pass transmembrane proteins with an extracellular ligand binding domain and an intracellular kinase domain. The aminoterminal extracellular part of the receptor contains globular domains such as immunoglobulin (Ig)-like domains, fibronectin type III-like domains, cysteine-rich domains, and EGF (epidermal growth factor)-like domains. The cytoplasmic portion consists of a juxtamembrane region, the tyrosine

kinase domain, and a carboxyterminal region. The tyrosine kinase domain contains the ATP-binding pocket, which contains an N-terminal and a C-terminal lobe connected by a hinge region. ATP binds in the cleft formed between the N- and C-lobes. A flexible activation loop (A-loop) starting with a conserved amino acid sequence Asp-Phe-Gly (DFG) controls access to the active site and undergoes a phosphorylation-dependent structural change that allows the kinase to become active[8], [9]. Normal activation is achieved by cytokines or growth factors binding to the extracellular domains of two receptors and inducing dimerization or oligomerization[10]. Ligands for receptor tyrosine kinases may either be monomers that allow binding of two receptors simultaneously, or may be dimers themselves. Receptors usually come together as homodimers, but heterodimers have been reported in a number of cases. Dimerization brings the two intracellular kinase domains into close proximity, allowing one to phosphorylate the A-loop of the other. This initial phosphorylation activates the kinase, resulting in additional auto- and trans-phosphorylation events. Phosphorylated tyrosine residues then serve as docking sites for a variety of downstream mediators[5].

Non-receptor tyrosine kinases are often associated with receptors. They respond to ligands that activate their respective receptors, including peptide hormones[11], cytokines[12], and immune signals[13] Other intracellular tyrosine kinases are activated by cell adhesion, calcium influx, or at a specific phase of the cell cycle. Dimerization is necessary for some but not all non-receptor tyrosine kinases. For example, JAK (janus

kinase) family kinases form homo- or heterodimers upon binding to cytokine receptors[7], [14], [15], whereas Src family kinases do not need to dimerize, but depend on the removal of an inhibitory phosphorylation to become active[16].

Tyrosine-phosphorylated residues on receptor and non-receptor tyrosine kinases serve as docking sites for Src homology-2 (SH2) and protein tyrosine-binding (PTB) domain-containing proteins[17]. This results in a cascade of phosphorylations and in the release of messenger molecules, greatly amplifying the signal initiated by one ligand molecule. Multiple cytoplasmic signaling pathways, including the Ras/Raf mitogen-activated protein kinase pathway, the phosphoinositol 3'-kinase/Akt pathway, the signal transducer and activator of transcription 3 pathway, the protein kinase C pathway, and scaffolding proteins may be activated[18]. The signaling cascade ultimately reaches the nucleus, where it induces transcription of a specific subset of genes. In normal cells, activation of a signaling pathway is tightly regulated at many levels. The action of tyrosine phosphatases is directly opposed to that of tyrosine kinases, removing phosphorylations and returning proteins to an inactive state[19]. Besides this, other mechanisms for inhibition of receptor tyrosine kinases include ligand-induced receptor endocytosis, initiation of negative feedback loops, and heterodimerization with kinase-

dead receptors[20].
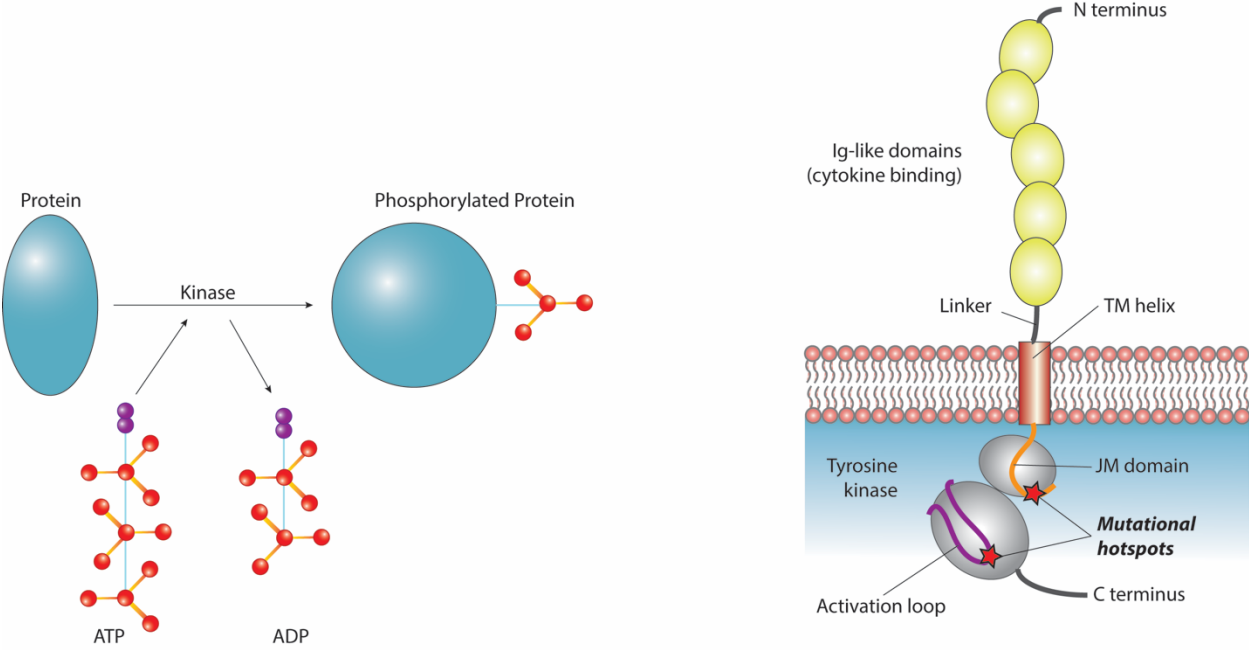
Figure 1.1.1 Tyrosine kinases.
Kinases transfer a phosphate group from ATP to an amino acid residue of a substrate protein.
Receptor tyrosine kinases are compoased of an intracellular kinase domain, regulatory
juxtamembrane domain, transmembrane helix, linker, and extracellular domain for ligand
binding and oligomerization.

1.1.1 Oncogenic activation of tyrosine kinases

Mutation or overexpression of over half of the known receptor tyrosine kinases has been associated with human malignancies. A tyrosine kinase can turn into an oncogene through several mechanisms, all resulting in constitutive activation of a pathway that is normally tightly regulated. Constitutive activation of a tyrosine kinase can result from genetic alterations. Mutations may be introduced by gene transfer from a virus, genomic rearrangements creating fusion proteins, gain-of-function point mutations, or small deletions. Commonly, gain-of-function mutations include deletion of, or mutations within, the extracellular domain, changes in the kinase domain, or alterations of the C-terminal region[21].

A non-mutated receptor kinase may become transforming if it or its ligand are aberrantly or excessively expressed. Overexpression of the receptor leads to constitutive kinase activation by increasing the concentration of dimers/ oligomers. This mechanism has been described for HER2/neu/ErbB2[22] and EGFR[23], which are often amplified in breast and lung cancer, respectively.

Lastly, a tyrosine kinase may be aberrantly activated even in absence of mutation or overexpression if negative regulators in the signaling pathway are dysfunctional. For example, the tyrosine phosphatase PTEN is mutated in several human cancers. PTEN acts as a tumor suppressor by downregulating the proliferative or mitogenic signals

transmitted germline mutations of PTEN are predisposing to a familial cancer syndrome, Cowden disease. Cancers in Cowden syndrome include breast cancer, thyroid cancer, brain tumors, and multiple hamartomas[24].

Tyrosine kinases not only act as tumor initiators or principal drivers of growth; they may also contribute accessory functions such as promoting vascularization. Vascular Endothelial Growth Factor Receptor (VEGFR) is expressed primarily in endothelium. The ligand, VEGF, is expressed in developing vasculature and in response to damage or hypoxic stress. High VEGFR levels have been detected in glioblastoma, adenocarcinoma of the gastrointestinal tract, and some leukemias. Similarly, the ligand is detected in high levels in solid tumors surrounding areas of hypoxia and necrosis[25].
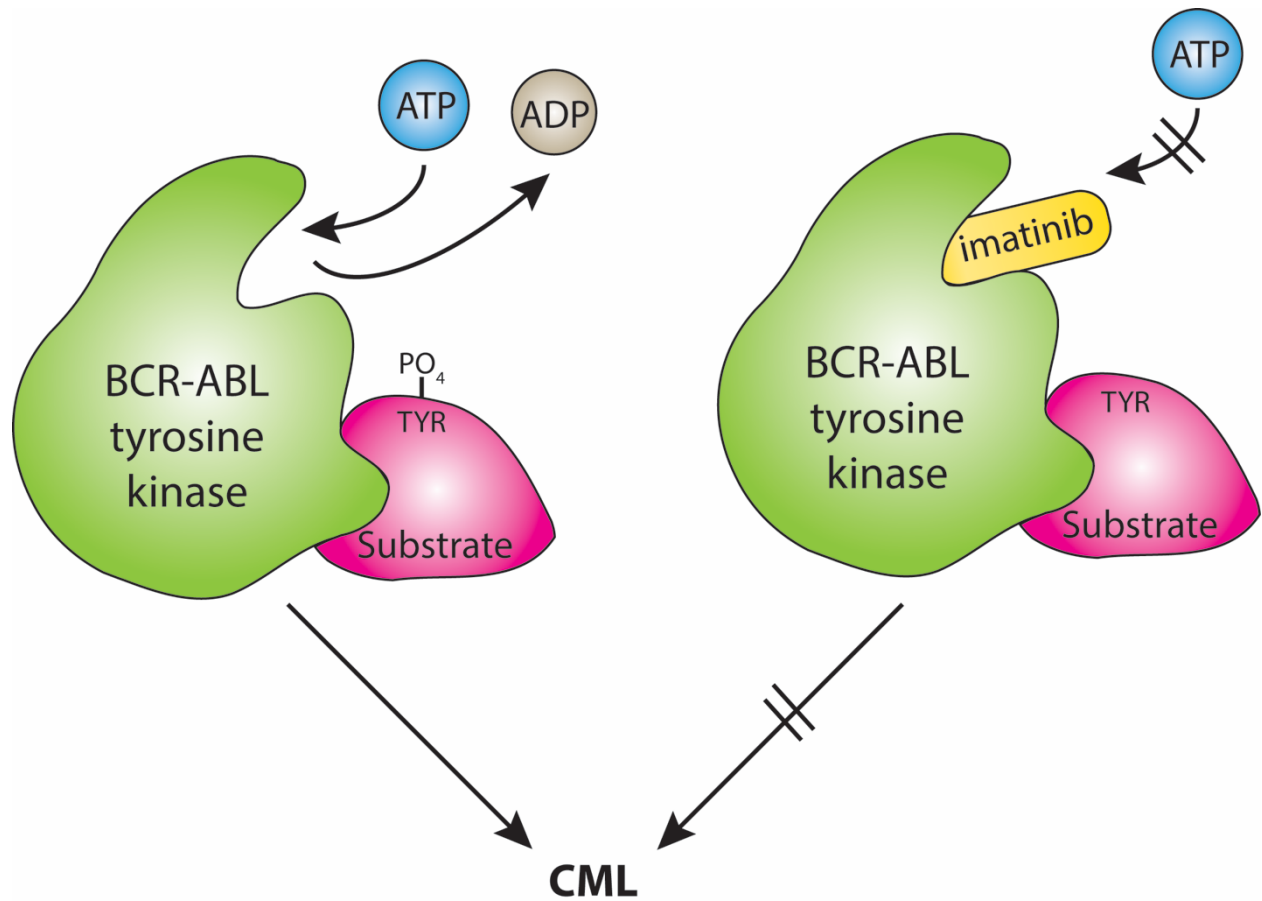
Figure 1.1.2 Oncogenic activation of tyrosine kinases on the example of BCR-ABL.
In the case of BCR-ABL, the uncontrolled phosphorylation and activation of signaling mediators results in chronic myeloid leukemia, or CML.

1.1.2   Tyrosine Kinase Inhibitors

Inhibition of a deregulated, oncogenic tyrosine kinase can prevent the proliferation of tumor cells in vivo and is in some cases sufficient to slow or halt tumor progression. The degree of initial success of a tyrosine kinase inhibitor depends on several considerations:

1) Does the targeted kinase drive or contribute to proliferation and survival of the cancer cell?

2) How potent and specific is the inhibitor?

3) Are there toxic effects resulting from either off-target inhibition of other kinases or from inhibition of the wild type form of the targeted kinase in normal cells?

4) What is the clinically achievable dose (considering solubility, tissue distribution, cell permeability and metabolism) of the inhibitor?

In short, the design and clinical implementation of an inhibitor requires the identification of a dysregulated protein or pathway, the characterization of the patient population whose disease is driven by this abnormality and who is thus likely to benefit from therapy, and subsequently the design or appropriation of safe and effective compounds for this application. Tyrosine kinase inhibitors are now the standard of care for several types of cancer. Insights into the biology of signal transduction pathways and rational design of small molecules to inhibit those pathways have significantly

improved progression-free survival and overall survival. Importantly, these therapies also often produce fewer adverse effects than conventional chemotherapy and thereby help to maximize patients' quality of life[26].

To date, 28 small molecule kinase inhibitors have been approved by the US Food and Drug Administration (Figure 1.4.1), with 15 of these approvals occurring between January 2012 and February 2015. The vast majority are tyrosine kinase inhibitors. Most small molecule tyrosine kinase inhibitors perturb ATP binding through interaction with the cleft between the C-lobe and N-lobe of the ATP binding site. Kinase inhibitors are irreversible or reversible. The former covalently bind to a cysteine residue close to the ATP-binding site. The latter can be further divided into four main types based on the conformation of the binding pocket and the DFG motif they preferentially bind. Type I inhibitors are ATP-competitive and bind the active forms of kinases. Type II inhibitors bind the inactive forms of kinases. Type III inhibitors bind an allosteric pocket adjacent to the ATP binding site. Type IV inhibitors bind an allosteric site distant from the ATP pocket. 26 of the 28 approved inhibitors are reversible and most are type I or type II inhibitors[27], [28].

The dogma that the kinase domain and ATP binding site in particular were too conserved to allow specific targeting was first challenged in the 1980's with the development of specific EGFR inhibitors[29] and has been almost completely eroded by now. However, the high sequence similarity does pose considerable challenge to the

development of potent inhibitors against desirable targets and minimal interactions with other kinases. A large number of inhibitors interact with more than one target. Promiscuous inhibitors are controversial, since they, as in the case of midostaurin[30], have proven to be useful clinical therapies. Indeed, it may become clear that instead of absolute specificity, inhibitors with a favorable selectivity profile will be more suitable for cancer treatment.

Small molecule drugs are not the only means of inhibiting a tyrosine kinase. Other types of targeted therapy include monoclonal antibodies and antisense inhibitors of growth factor receptor. The inhibition of BCR-ABL and KIT by imatinib represents the paradigm for tyrosine kinase inhibitor therapy, and will be discussed in chapters 2.1.2 and 2.2.2.
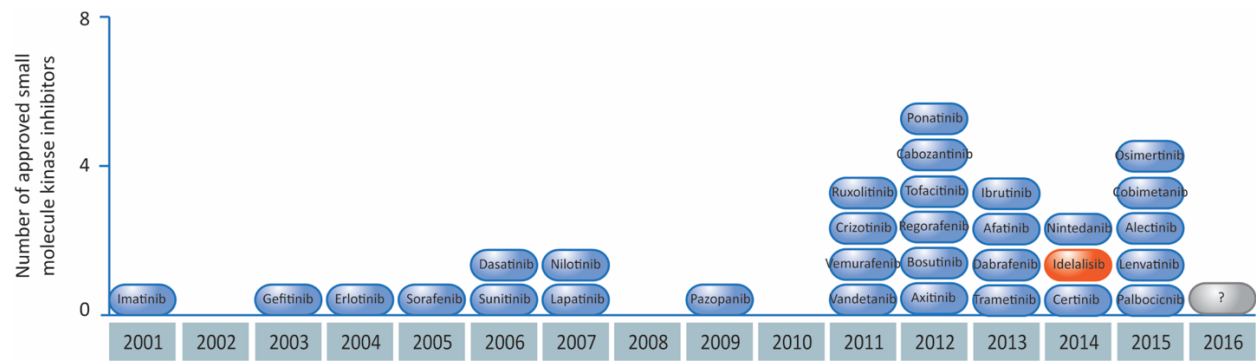
Figure 1.1.3 FDA-approved small molecule tyrosine kinase inhibitors (July 2016).
Adapted from[27], [28]

1.1.3 Resistance to TKI therapy

In clinical trials, highly selective or specific blocking of only one kinase has repeatedly been associated with limited or sporadic responses. This restricted efficacy remains a major challenge and prompts inquiry into the mechanisms of resistance. The problem underlying all types of resistance is the failure of initial therapy to eradicate a sufficient number of cells to prevent disease recurrence. Even in cases where the therapy succeeds in shrinking the bulk of the tumor, a population of cells that survives, called minimal residual disease (MRD), often remains and finds refuge in protective microenvironments. Not surprisingly, MRD levels above a certain threshold predict relapse in acute lymphoblastic leukemia (ALL) and acute myeloid leukemia (AML)[31], [32]. In ALL, the level of MRD is inversely proportional to the length of remission[33]. Cells that survive in a protective niche are continually exposed to the selective pressure of therapy. This eventually leads to the development of acquired resistance in the surviving cells and outgrowth of the MRD population, causing disease relapse.

Acquired resistance may develop either through secondary mutations in the targeted kinase (for example BCR-ABL T315I[34], EGFR T790M[35], and various mutations in HER2, PIK3CA and AKT), or through upregulation of bypass pathways (overexpression of MET or HER3, activation of IGF-1R, deletion or silencing of PTEN)[36]. Further examples will be given in chapters 2.1.3, 2.2.3, and 2.3.3, where resistance of specific cancer types to tyrosine kinase inhibitors are discussed.

1.1.1.1 *Environment-mediated resistance*

Environment-mediated resistance, where cancer cells are transiently protected from apoptosis or growth inhibition, is a major contributor to MRD[37]. This form of drug resistance is induced by signaling events that are initiated by factors present in the tumor microenvironment. These factors can be soluble cytokines, chemokines and growth factors secreted from tumor stroma, or cell adhesion-mediated processes induced by tumor cell integrins interacting with fibroblasts or components of the extracellular matrix[38]-[40].

Contact-dependent environment-mediated resistance is recognized as an important mechanism in hematologic malignancies. In a mouse model of AML, alpha4beta1 integrin was shown to promote MRD, and blocking this interaction in addition to standard therapy resulted in a 100% survival rate[37], [41]. In a group of patients with AML, high alpha4beta1 integrin levels were correlated with poor outcome. When AML cells with high integrin expression were isolated and cultured in vitro, they proved to be sensitive to chemotherapy, indicating that this is a case of environment-dependent protection[42]. Interestingly, another group found increased alpha4beta1 integrin expression in relapsed compared to primary AML, suggesting that higher expression may have been selected for during treatment[41].

Studies in the past assumed that major changes necessary for environment-mediated protection took place primarily in the tumor cells themselves. Stromal cells were expected to play a passive role, for example by providing a scaffold for malignant cells to adhere to and activate survival signaling. However, stroma experiences considerable selective pressures due to two reasons: First, stroma is exposed to the same abnormal conditions as the tumor, including hypoxia, altered nutrient delivery, and of course chemotherapy. Second, in addition, stroma is exposed to any factors secreted by tumor cells. These conditions cause the stroma to become increasingly abnormal and to develop a cooperative relationship with the tumor that contributes to protection and the development of resistance[25]. In support of this mechanism, human bone marrow stroma from healthy donors only protects myeloma cells from mitoxantrone if the two cell types are co-cultured[43]. Interleukin 6 and stromal cell-derived factor 1, both of which have been shown to mediate resistance to several cytotocix agents in various malignancies in vitro[44]-[46], are both expressed more highly in tumor-associated stroma than in normal bone marrow stroma[47].

1.1.1.2 *Approaches to overcoming environment-mediated resistance*

In an important review, Hanahan and Weinberg reasoned that six hallmarks of cancer are necessary for malignancy: autocrine promotion of growth, insensitivity to growth inhibitors, evasion of apoptosis, limitless replicative potential, sustained angiogenesis, and tissue invasion and metastasis. In addition, the authors noted that tumors exist in a

complex interplay with surrounding tissue, including vasculature, fibroblasts, and immune cells. They therefore envisioned cancer therapy as a multi-pronged approach that would target several of these hallmarks in both cancer cells and surrounding tissues[48].

Limited clinical studies have used compounds that block environment-mediated protective signaling as secondary treatments, with the goal of overcoming resistance after primary therapy. Because microenvironmental protection precedes acquired resistance, these strategies would probably be more effective if used as an initial, preventative treatment in conjunction with the primary therapy. Adhesion-mediated protection has been targeted with some success in mouse models of multiple myeloma, where a blocking antibody against alpha4 integrin showed strong synergy in reducing tumor burden in combination with melphalan chemotherapy[49].

Targeting stroma-mediated paracrine resistance pathways with tyrosine kinase inhibitors has shown promising results in preclinical models using cell lines or patient specimens. A VEGFR antagonist can prevent interleukin-6 (IL-6) production in stroma co-cultured with myeloma cells, leading to a loss of stromal protection from dexamethasone chemotherapy[50]. IL-6 has been demonstrated to mediate chemoresistance in several types of cancer either in an autocrine or in a paracrine manner. It is of particular relevance to the research presented in this thesis that FGFR

inhibitors have also been shown to block the production of IL-6 by bone marrow stromal cells[51], [52].

1.2 Fibroblast growth factor signaling

Fibroblast growth factors (FGFs) and their receptors are involved in angiogenesis, wound healing, and embryonic development. FGFs are important for both the maintenance of differentiation potential in stem cells and for precursor differentiation along various lineages. I will limit my discussion to a brief introduction of FGF receptor and ligand family members and a more detailed account of FGF2 trafficking, as this is of relevance in my research. Although I will discuss the role of FGF receptors and ligands in cancer and therapy resistance in this chapter, please also reference chapter 1.3.1 for the role of FGF2 in the maintenance and functional regulation of mesenchymal stem cells, which is likely inextricably linked to environment-mediated resistance, as discussed in chapter 1.1.

1.2.1 FGF receptor family

FGF receptors are single pass transmembrane tyrosine kinases that consist of a ligand binding extracellular domain, a transmembrane domain, and an intracellular tyrosine kinase that is separated into two parts by an insertion domain. There are four highly homologous Fgfr genes in mammals. Except for the Fgfr4 gene, all Fgfrs encode multiple splice variants[53]. Fgfr1 in particular has been speculated to encode up to 256

different splice isoforms. Splice sites affect both the intracellular and the extracellular domains. FGFR3 and FGFR4 have three Ig-like domains, whereas FGFR1 and FGFR2 can have two or three depending on splicing. The major splice variants of FGFR1, 2 and 3 differ in the second half of Ig-loop III, and are thus named IIIb and IIIc. These changes dictate varying ligand affinity and specificity[54].

The FGF signaling complex contains several cofactors with essential regulatory functions. Heparan sulfate plays two roles in FGF signaling. Extracellular matrix heparan sulfate acts as a depot for FGF that stabilizes and limits access to receptors. Heparan sulfate in the cell membrane is an integral part of the FGF receptor complex. It interacts with receptor and ligand and has been shown to determine ligand affinity and specificity, as well as downstream signaling. Heparan sulfate promotes complex formation with FGFR1 and FGF2 that has 2:2:2 stoichiometry[55].

Endocrine FGFs (see 1.2.2) bind to the same FGFRs as paracrine/autocrine homologues, but only in presence of membrane-anchored proteins called Klotho co-receptors. As an example, alphaKlotho binds to FGFR1 and forms a new binding site at the joint interface, which binds FGF23[56]. FGF23 controls mineral metabolism, specifically phosphate secretion in the kidney. BetaKlotho, on the other hand, controls high affinity binding of FGF19 and FGF21 to FGFR4 and regulates cholesterol/bile acid, lipid and glucose metabolism in adipocytes[57]. Interestingly, the Klotho co-receptors not only change the affinity of FGF receptors to accommodate endocrine FGFs, they also redirect

downstream signaling away from mitogenic pathways and towards metabolic

signaling[58].
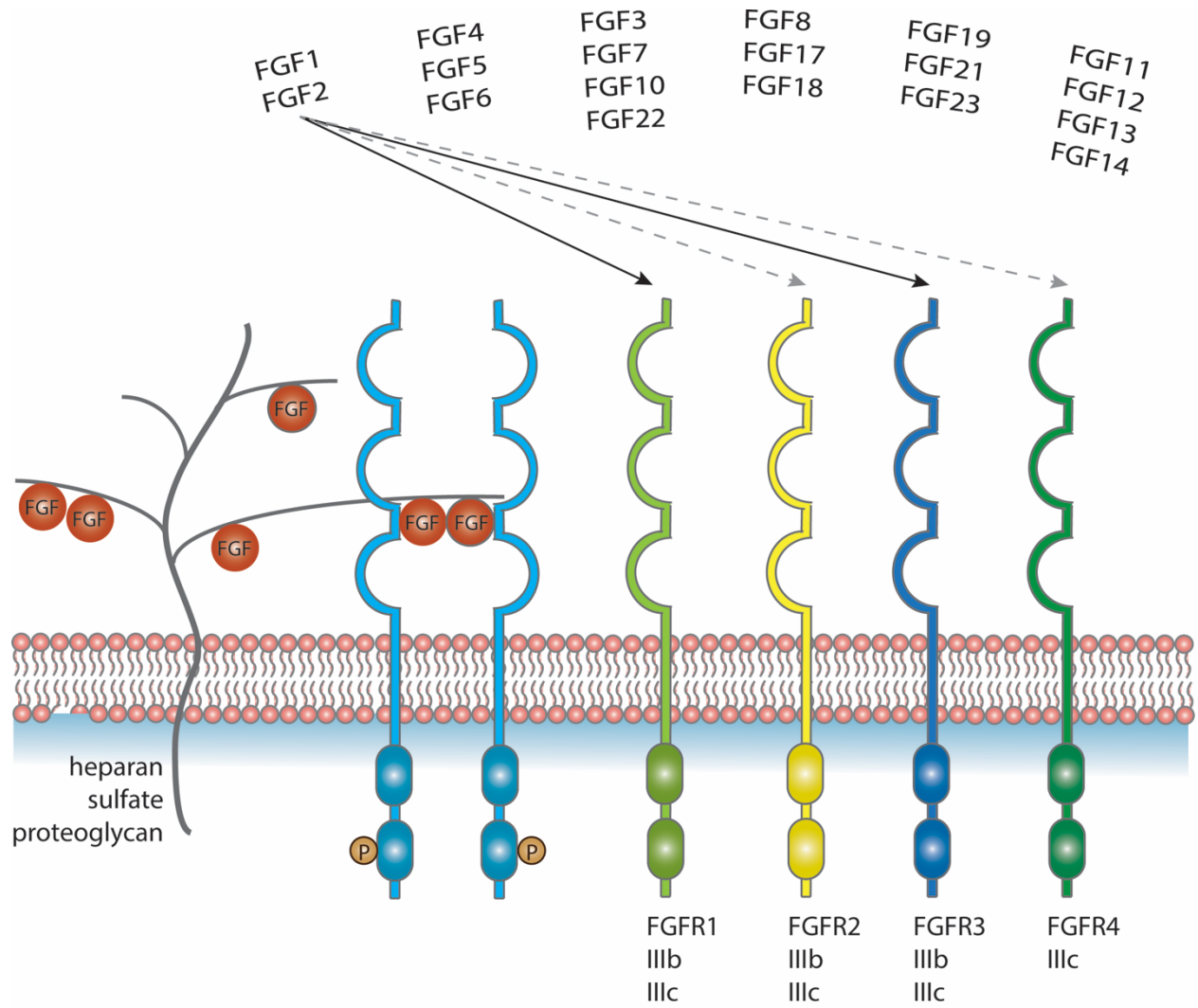
Figure 1.2.1 FGF receptor and ligand family members.
Arrows display the affinity of ligand FGF2 for FGF receptors. Splice isoforms dictate varying ligand affinity. Heparan sulfate proteoglycan binds ligands and acts a a co-receptor, promoting FGF receptor complex formation.

1.2.2 FGF ligands and FGF2 trafficking

The first two members of the fibroblast growth factor family, FGF1 (also called acidic FGF) and FGF2 (also called basic FGF), were discovered in the 1970s and named for their ability to stimulate fibroblast proliferation and their respective isoelectric points[59], [60]. Subsequently, 20 more members were identified on the basis of sequence homology[61]. It soon transpired that 'fibroblast growth factor' was not a fitting name for all members of this vast family, given that receptors for some of the FGFs are not even expressed by fibroblasts.

The FGF family can be divided into paracrine/autocrine- and endocrine-acting FGFs. The first group comprises FGF1-10, FGF16-18, FGF20 and FGF22. The second group comprises FGF19, FGF21 and FGF23. There is also a small group of non-canonical FGFs, FGF11-14, which do not bind FGF receptors at all, but exert their function by interacting with ion channels[62]-[64].

FGF2 occurs as low and high molecular weight isoforms, translated from a common mRNA by the use of alternative translation-initiation codons. The low molecular weight (LMW) isoform of FGF2 is 18 kDa in size. LMW FGF2 is found in both the nucleus and the cytoplasm and can also be secreted. High molecular weight (HMW) FGF2 varies in weight between 22 and 34kDa depending on the translation initiation site. HMW FGF2 is found in the nucleus and exerts its function independent of FGFRs[65], [66]. Most

FGFs have an N-terminal signal peptide for endoplasmic reticulum (ER) import and classical secretion. However, several FGFs, including FGF1 and FGF2, do not have a signal peptide and are secreted in an unconventional manner[67]. FGF2 interacts with phosphoinositides at the inner plasma membrane and oligomerizes to form a membrane pore. Subsequently, heparan sulfate on the outer plasma membrane can act as traps for FGF2 molecules, resulting in immobilization on the cell surface[68]. Two reports exist of FGF2 release by microvesicles. The first study found that after serum stimulation, FGF2 clusters under the plasma membrane and is subsequently released by microvesicle budding. FGF2 did not appear to be bound by heparin, but appeared to be contained inside vesicles[69]. The second study found that astrocytes produce extracellular structures that contain FGF-2 and VEGF, together with ß1- integrin. Based on size and content, the authors classified the structures as microvesicles, but could not exclude exosomes[70].

1.2.3   FGF Signaling Pathways

Important downstream signaling pathways of all four FGFRs include PLC-gamma, MAPK and PI3K. Only PLC-gamma can bind directly to phosphorylated residues at the C-terminus of the FGFRs[71]. MAPK and PI3K pathway components need to be recruited with the help of the membrane-anchored adaptor protein FGF receptor substrate 2alpha (FRS2alpha)[72]. CRK, an adaptor protein that recruits ERK, has also

been reported to bind to FGFRs[73].
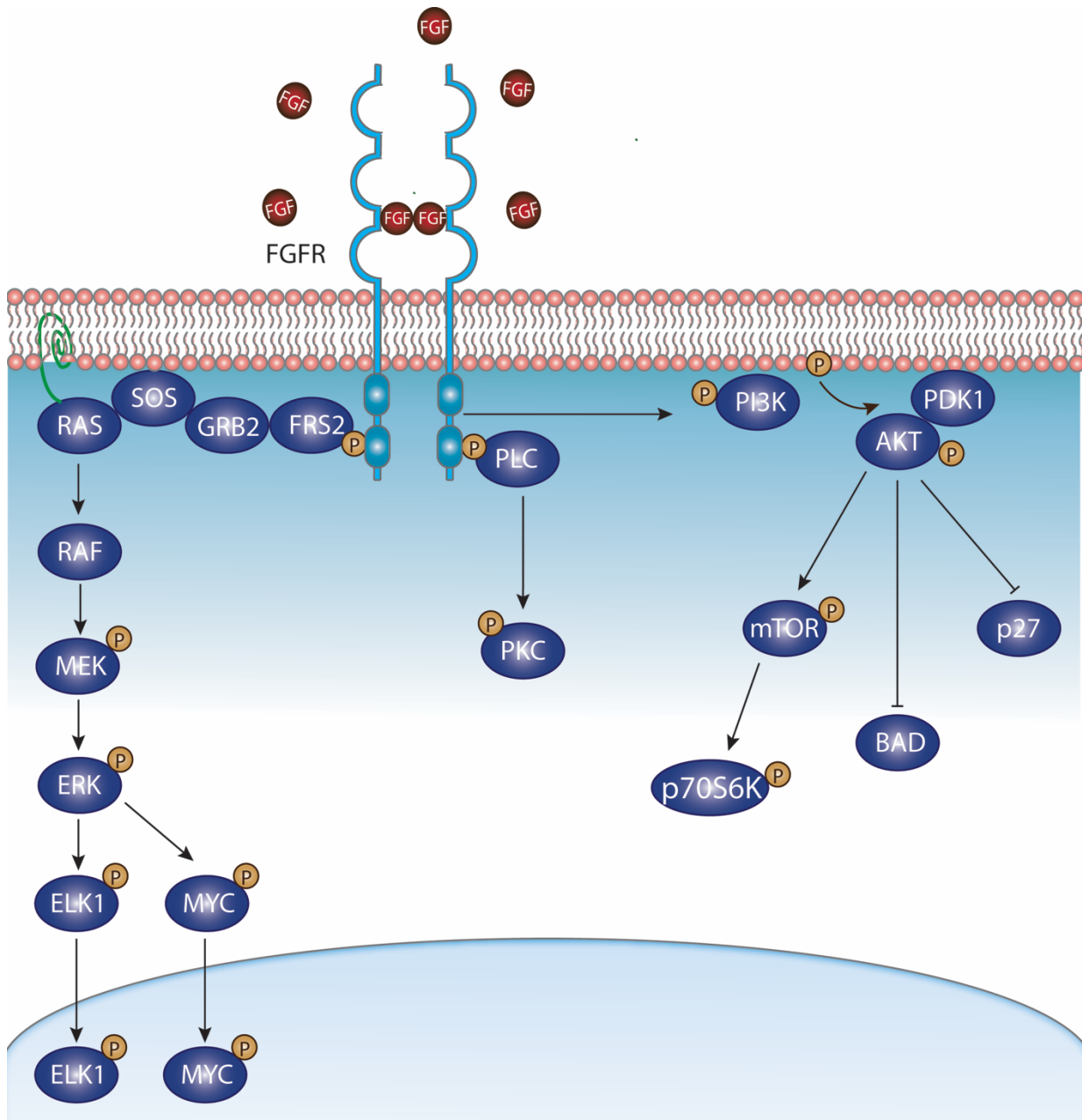
Figure 1.2.2 FGFR and downstream signaling.
A complex is formed among the FGF ligand, heparan sulfate (not shown), and FGFR to cause receptor dimerization and transphosphorylation at several tyrosine residues in the intracellular portion of the FGFR. Subsequent downstream signaling occurs via the intracellular receptor substrates FRS2 and PLCγ, leading ultimately to upregulation of the Ras-dependent MAPK and Ras-independent PI3K–Akt signaling pathways.

1.2.4 Physiologic roles of FGF signaling

In the embryo, FGFs and FGFRs are expressed in cell- and location-specific, tightly regulated patterns that change rapidly as development proceeds[74]. In adult organisms, components of FGF signaling are expressed in a cell type-specific manner and are important for tissue homeostasis and function. Abnormal expression of FGFs and FGFRs is associated with developmental disorders and adult pathologies. Interestingly, therapeutic manipulation of the FGF signaling axis has been attempted either with antagonists (in cancer) or with agonists or ectopic delivery of FGF (in traumatic injury).

Both FGF1 and FGF2 have been extensively studied in wound healing. FGF1 induces macrophages, epithelial cells and endothelial cells to secrete cytokines and migrate towards the area of injury[75]. Both FGF1 and FGF2 promote growth and differentiation of fibroblasts and angiogenesis[76]. In addition, FGF1 suppresses collagen production and therefore prevents scar formation[77], [78]. Recombinant FGF2 has been used to accelerate the healing of fresh and chronic wounds in several clinical trials in China and has shown success in diverse wound types, such as burn trauma, skin ulcers, chronically ischemic tissue and peripheral artery disease. FGF1 has also been shown to elicit modest nerve regeneration after spinal cord injury. FGF7, which only binds FGFR2b, has been used to promote healing of mouth sores after chemotherapy and irradiation[61].

FGF signaling is essential for cardiomyocyte homeostasis. Connexin 43, which is required for the maintenance of gap junctions, is phosphorylated in response to FGF stimulation[79]. FGF has shown cardioprotective effects in animal models of heart failure as well as in some clinical trials[80], [81]. FGF2 improved left ventricle function in pigs with chronic myocardial ischemia[82] and suppressed the progression of heart failure in rats[83]. In patients with coronary heart disease, infusion of recombinant FGF2 improved myocardial function and reduced angina. However, a larger, double-blind placebo-controlled trials did not confirm these findings, and further studies are needed to determine the efficacy of FGF in the treatment of patients with heart failure[84].

Endocrine FGFs are emerging as novel targets for therapies against obesity, diabetes, and cardiovascular disease. The endocrine-acting FGF21 has been shown to regulate energy homeostasis through activating of FGFR1 on adipocytes[85]. FGF21 is released by the liver, but also by other tissues, in response to both starvation and obesity. When administered to mice, both FGF21 and FGF19 dramatically reversed obesity and type 2 diabetes[86]. Studies of tissue-specific FGFR1 knockout mice revealed that this regulation depends on FGFR1 activation on adipocytes[87], and that FGF21 promotes adiponectin release from adipocytes[88].

For further details on the role of FGFs, and FGF2 in particular, on hematopoiesis and the maintenance of the bone marrow microenvironment, please see the last paragraph in chapter 1.3.

1.2.5 FGF receptor knockout mouse models

Knockout models of FGFR1 are generally lethal during late embryogenesis[89]. The only exception is a model with genetic modification in exon 8, preventing expression of the IIIb splice variant. This mouse model displays no obvious phenotype[90]. By contrast, genetic modification that prevents the expression of IIIc is lethal due to gastrulation defects. Embryonically lethal models of FGFR1 knockout reveal that FGFR1 is required for early postimplantation growth of the embryo, as well as axial organization, mesodermal patterning and limb bud formation[91].

Knockout of FGFR2 results in death during early embryogenesis, with abrogated growth of the inner cell mass, no visceral endoderm or placental formation[92]. Genetic modification that prevents the expression of FGFR2 IIIb leads to death at birth, with impaired limb growth and severe dysgenesis of multiple organs[93]. FGFR2 IIIc-deficient mice, on the other hand, are viable but exhibit delayed ossification of the skull and dwarfism in the long bones and axial skeleton[94].

Interestingly, FGFR3 knockout mice are viable and exhibit bone overgrowth and decreased bone mass, as well as early arthritis and deafness[95], [96]. Knockout of the

IIIb isoform leads to no obvious phenotype, while lack of IIIc recapitulates the skeletal overgrowth and decreased bone mineral density[96].

Finally, the knockout mouse model of FGFR4 is morphologically normal[97].

1.2.6 Receptor and ligand dysregulation in cancer

Overexpression of FGF ligand or receptor, as well as mutations in FGF receptors, has been reported in many cancers including head and neck, prostate, hepatocellular carcinoma, melanoma, lung, breast, bladder, and endometrial cancer (Table 1.4.1 and [98], [99]). Activating point mutations in FGFR3 have been found in over 60% of non-invasive bladder cancer[100]. In addition, mutations of FGFRs can prevent receptor endocytosis[101]. Alternative splicing may also promote tumorigenesis. FGFRIIIb is typically expressed on mesenchymal cells and IIIc on epithelial cells. When IIIc is expressed in bladder and prostate cancers, it leads to autocrine activation and increased invasiveness[102]. Amplification of chromosome 8p11-12, the region which encompasses Fgfr1, is also frequent in prostate cancer and more rarely in breast cancer. FGFR2 overexpression has also been reported in breast cancer[98].

FGFRs are expressed on all cells of hematopoietic origin, and dysregulated receptor expression has been reported in several hematologic cancers. Multiple myeloma is the most extensively studied example. 15 to 20% of multiple myeloma cases harbor a t(4;14)(p16.3;q32) translocation, bringing Fgfr3 under the influence of an IgH enhancer

region and leading to FGFR3 overexpression[103]. Although the clinical implications are still unclear, in vitro FGFR3 overexpression has been shown to promote multiple myeloma cell proliferation and survival[104]. A number of confirmed activating mutations in FGFR3 are also found in multiple myeloma. Interestingly, endothelial cells isolated from the bone marrow of multiple myeloma patients also express more FGFR2 and FGF2 compared to normal human umbilical vein endothelial cells, indicating an autocrine and paracrine function of the FGF system in this disease[105], [106]. The 8p11 myeloproliferative syndrome (EMS), also called stem cell leukemia/lymphoma (SCLL), is defined by a translocation that involves the kinase domain of Fgfr1 and most frequently the zinc finger gene ZNF198. The disease is characterized by a BCR-ABL-negative myeloproliferative syndrome concurrent with a precursor T cell lymphoma, and often progresses to acute myeloid leukemia[107].

Elevated production of FGF ligands has been associated with high grade disease and disease progression (Table 1.4.2 and [108]). For example, in prostate cancer, FGF8 and its receptors are overexpressed and create an autocrine signaling loop that leads to proliferation and dysplasia and independence from tumor stroma. High levels of FGF8 are associated with decreased patient survival. FGF8 also contributes to bone metastases in prostate cancer and is enriched in castration-resistant or chemotherapy refractory disease[109]-[111]. Further examples pertaining to FGF2 overexpression will be provided below.

Table 1.2.1 Summary of genetic aberrations in FGFRs in solid tumors and hematologic malignancies.

(SQC – squamous cell carcinoma, Adeno – adenocarcinoma, EMS – 8p11 myeloproliferative syndrome). Adapted from [98], [99].

Gene	Aberration	Cancer type
FGFR1	Mutation	Breast (rare), Lung (rare), Melanoma (rare), Glioblastoma (rare)
	Amplification	Lung (10–20% SQC & 3% Adeno), Breast (10–15%), Ovarian (~5%), Bladder (3%), Rhabdomyosarcoma (3%), Osteosarcoma (5%), Esophageal (9% SQC), Head & neck (10–17% SQC), Prostate (rare)
	Translocation	Lung (0.3–0.6% SQC), Glioblastoma multiforme (3%), EMS, CML (rare)
FGFR2	Mutation	Lung (3% SQC), Endometrial (10–16%), Gastric cancer (rare), Melanoma (rare), Cervical (rare)
	Amplification	Gastric (4–10%), Breast (~4%)
	Germline SNP	Second intron SNP: increased incidence of breast cancer
	Translocation	Lung (0.3% SQC), iCCA (~16%), Metastatic breast (rare), Metastatic prostate (rare)
FGFR3	Mutation	Lung (3% SQC), Bladder (50–60% non-muscle invasive type, 10–15% invasive type), Cervical (5%), Prostate (3%), Spermatocytic seminoma (7%), Multiple myeloma (rare), Head & neck (rare), Seborrheic keratosis (39%), Testicular (rare)
	Translocation	Lung (1–3.5% SQC), Lung (0.5% Adeno), Bladder (6% muscle-invasive), Glioblastoma (3-7%), Multiple myeloma (15-20%), Leukemia
FGFR4	Mutation	Rhabdomyosarcoma (8%), Glioblastoma multiforme (rare), Endometrial (rare), Lung (rare), Breast (rare)
	Amplification	Colorectal (5%), Prostate (18% of T1 tumors, 29–41% of T2-T4 tumors)

1.1.1.3 Roles of FGF2 in malignancy

Although, as indicated above, many members of the FGF and FGFR families have been associated with malignancy, FGF2 is the most studied ligand and has been revealed as an important regulator of cell growth and differentiation. Several studies have shown that FGF2 is a key oncogenic factor in the tumor microenvironment[108].

FGF2 has long been recognized as a potent pro-angiogenic factor. FGF2 stimulates endothelial cells in a paracrine manner after release from tumor and stromal cells. In addition, FGF2 plays an autocrine role in endothelial cells. Endothelial cells primarily express FGFR1, and activation by FGF2 leads to endothelial cell proliferation, migration, protease production and angiogenesis[112], [113]. Importantly, FGF2 has been shown to compensate for VEGF-induced angiogenesis in the setting of VEGFR inhibition[114]. In addition to supporting tumor vasculature, FGF2 may contribute to cancer progression by acting directly on tumor cells. FGF2 is overexpressed and/or released from tumor, endothelial, or stromal cells, and thus acts in an autocrine or paracrine manner on cancer cells. FGF2 secreted by stromal fibroblasts induces tumor cell proliferation. In addition, FGF2 has an autocrine role in activating tumor fibroblasts[108].

Growing evidence points to FGF2 as an important factor in hematopoiesis and hematologic malignancies. Again, FGF2 directly induces stem cell proliferation and

differentiation, but also promotes proliferation of stromal cells in the bone marrow. FGF2 stimulation of stem or neoplastic cells can be autocrine or paracrine. For example, lymphoma cells express both FGF2 and FGFRs. In Hodgkin lymphoma, increased expression of FGF2 and FGFRs is associated with poor prognosis and chemoresistance[115], [116]. In ALL, urinary FGF2 levels are elevated before induction chemotherapy, variable during therapy, and normal when complete remission is achieved[117]. A large study found elevated FGF2 levels in the plasma of patients with ALL, AML, CML, CLL, and myelodysplastic syndrome (MDS)[118]. Another report demonstrated significantly elevated FGF2 levels in newly diagnosed AML. Induction chemotherapy again resulted in decreased FGF2 levels[119]. In MDS, FGF2 levels in the serum are significantly higher in patients whose disease is at high risk for leukemic transformation[120]. A summary of studies investigating the clinical relevance of FGF2 levels in hematologic malignancies is provided in table 1.4.2. In bone marrow stroma, FGF2 induces the production of IL-6, which in turn stimulates the production of FGF2. In several cancer types, IL-6 and FGF2 appear to be involved in paracrine and autocrine feedback loops that promote disease progression and chemoresistance[52], [116], [121]. As already mentioned in chapter 1.1.3.2, targeting this crosstalk may be a promising approach to target environment-mediated resistance. Further evidence pertaining to FGF2 in therapy resistance will be provided below.

Table 1.2.2 Studies evaluating FGF2 as a prognostic biomarker in cancer patients with hematological tumors.
Adapted from [108]. Reproduction permitted under the Creative Commons Attribution License (CCAL).

Cancer Type	Specimen Type	FGF2 Expression Pattern	Prognosis/ Associated with
Acute Lymphoblastic Leukemia (ALL)	Untreated, treated plasma	Increased 1.4 fold in tumors vs. normal controls	-
	Untreated urine	Increased 8 fold in tumors vs. normal controls	-
Acute Myeloid Leukemia (AML)	Untreated, treated plasma	Increased 1.2 fold in tumors vs. normal controls	-
	Untreated BM biopsy	Increased 1.6 fold in tumors vs. normal controls	No significant correlation between FGF2 and MVD
Chronic Lymphocytic Leukemia (CLL)	Untreated, treated plasma	Increased levels in 54% of tumors vs. normal range in healthy controls	-
	Untreated, treated plasma	Increased 9 fold in tumors vs. normal controls	-
	Urine	Increased 2 fold in tumors vs. controls	-
	Peripheral blood (cell lysates and plasma)	Increased 64 fold in tumors with high risk vs. normal controls	No significant correlation between FGF2 and factors other than stage of disease
Chronic Myeloid Leukemia (CML)	Untreated, treated plasma	Increased levels in 44% tumors vs. normal range in healthy controls	-
	Untreated, treated plasma	Increased 1.6 fold in tumors vs. normal controls	-
Hairy Cell Leukemia (HCL)	Untreated, treated serum and BM aspirates	Increased FGF2 levels in 44% of tumors vs. normal range in healthy controls	-

Hodgkin's Lymphoma	Lymph node tissue	85% tumors positive	-
	TMA (NS)	Increased 246 fold in PO tumors vs. normal lymph node controls Increased 10 fold in GO tumors vs. normal lymph node controls	-
	Untreated, treated serum	FGF2 levels in tumors were normal	No significant change in FGF2 levels relative to pre-therapy values
Multiple Myeloma	BM aspirates	Increased FGF2 expression in tumors (13.5 pg/ml) vs. absent in controls	-
	Plasma cells	Increased 6.7 fold in active MM patients vs. non-active ones	No significant correlation between FGF2 and BM neovascularization
	Untreated, treated serum	Increased FGF2 levels in tumors vs. controls. Decreased 0.3 fold in treated patients with CR vs. untreated patients	Significant correlation between FGF2, VEGF, HGF, and B2M
Non-Hodgkin's Lymphoma	Untreated, treated serum	Increased 2 fold in tumors vs. controls. No correlation between FGF2 at diagnosis and after treatment	Correlated with bulky disease
	Biopsy	Positive expression in 23.1% of tumors	Decreased 0.5 and 0.4 fold months OS and PFS respectively, in FGF2 positive vs. negative tumors; correlated with bulty disease
	BM biopsy	7% positive FGF2 in tumors	-
	Untreated, treated serum	Increased in untreated tumors vs. controls; no significant change in FGF2 relative to untreated sample values	-

1.1.1.4 FGF2 in therapy resistance

High levels of FGF2 in serum and tumor are associated with relapse and/or recurrence in several cancers including bladder, breast, esophageal and Hodgkin lymphoma[108]. In a rat model of metastatic prostate cancer, the increased resistance of metastases over primary disease to chemotherapy with paclitaxel, doxorubicin and 5-fluorouracil was dependent on extracellular FGF2 produced by the metastatic microenvironment[122]. Other evidence that FGF2 may be involved in clinical drug resistance is provided by studies on fludarabine resistance in chronic lymphocytic leukemia (CLL)[123]. FGF2 levels in patient-derived or cell line CLL cells correlate with fludarabine resistance in vitro. Addition of exogenous FGF2 induces or further potentiates resistance when added to FGF-low or -high CLL cells, respectively.

FGF2 has been found to alter the levels of Bcl-2 and Bax family proteins to modulate the threshold for drug-induced apoptosis. Bcl-2 and its homologues are apoptosis regulators that regulate the permeability of mitochondrial outer membranes. They can be either pro-apoptotic (Bax, BAD, Bak among others), or anti-apoptotic (Bcl-2 and Bcl-XL among others). Bcl-2 and Bcl-XL are upregulated by FGF2 in small cell lung cancer cells, where FGF2 mediates resistance to etoposide[124]. FGF2 also interacts with other anti-apoptotic proteins. Endothelial cells upregulate the expression of survivin in response to FGF2, which is associated with protection from multiple chemotherapeutic drugs[125]-[127].

It is becoming clear that FGF2 is not only protective against broad-acting

chemotherapeutic agents, but also in several instances of tyrosine kinase inhibitor

therapy. In non small cell lung cancer cell lines, EGFR inhibitor treatment with gefitinib

increases the expression of FGFR2 and FGFR3 and well as FGF2. This leads to autocrine

reactivation of the ERK pathway, leading to cell survival and invasion, and reducing

the sensitivity gefitinib[128], [129]. FGFR activation is also an escape mechanism in

human lung cancer cells resistant to afatinib, another EGFR inhibitor[35]. In a similar

study of human melanoma cell lines, prolonged exposure to the B-RAF inhibitor

vemurafenib induced secretion of FGF2 and led to FGFR3 activation and re-activation

of the MAPK pathway[130]. In this thesis, I will describe FGF2-induced resistance to

tyrosine kinase inhibitors in three additional cancers. Collectively, these reports

strengthen the literature in support of FGF2 as an important mediator of protection and

resistance in multiple settings.

Nevertheless, it is important to note that FGF2 is likely not unique in this capacity. A

study of 41 receptor tyrosine kinase-driven human cancer cell lines found that most

cells could be rescued from sensitivity to their respective tyrosine kinase inhibitors by

exposure to one or more receptor tyrosine kinase ligands. The ligands HGF, FGF and

neuregulin 1 were the most broadly protective. Many tested cell lines could be rescued

from treatment sensitivity by as many as four different ligands. These ligands had in

common that they induced reactivation of the PI3K-AKT and/or MAPK pathways. This

report confirms a recurrent theme in resistance against tyrosine kinase inhibitors – the compensation for signaling downstream of the targeted kinase through activation of another, ligand-dependent receptor[131]. This argues strongly that we should take into account the expression of not only the driving oncogenic kinase, but that of other receptors and their ligands to inform treatment strategies that anticipate resistance mechanisms. Strategies to narrow down the set of potentially protective signaling pathways should include consideration of receptors previously implicated in resistance, such as MET and AXL, as well as consideration of the receptor expression profile in the given cancer.

1.1.1.5 FGFR inhibitors

With the exception of AZD4547 and to a lesser extent BGJ398 and PD173074, most FGFR inhibitors, including dovitinib (CHIR258), nintedanib (BIBF 1120), lenvatinib, brivanib, orantinib (TSU-68) and lucitanib (E3810), inhibit multiple receptor tyrosine kinases[99]. Indeed, the first generation of FGFR inhibitors, which includes brivanib, lucitanib, orantinib and nintedanib, was designed to target VEGFR or platelet-derived growth factor receptors (PDGFRs). These agents exert antiangiogenic and anti-tumor effects through the inhibition of VEGFR and FGFR. Since FGFR has been found to compensate for VEGFR in promoting angiogenesis[114], the dual activity may be fortuitous in preventing resistance. On the other hand, these multi-targeted inhibitors are often less potent against FGFRs over the other kinases and exhibit multiple side effects. Several

companies are developing FGFR-selective inhibitors, including the covalent irreversible

inhibitors named FGFR inhibitors 2 (FIIN-2) and 3 (FIIN-3). FIIN-2 and 3 can inhibit the

gatekeeper mutants of FGFR1 and 2, which confer resistance to first-generation

inhibitors[132]. The first irreversible inhibitor (TAS-120) is now being evaluated in a

phase I clinical trial for patients with solid tumors or multiple myeloma[133].

Dovitinib is a multi-target inhibitor of FGFR1-3, VEGFR1-3 and PDGFR. Phase I

studies suggested that dovitinib has a tolerable safety profile at therapeutic

doses. Dovitinib was evaluated in a phase II trial of HER2-negative metastatic

breast cancer with FGFR1 amplification. The results showed limited activity with

responses correlating with the level of FGFR1 amplification[134].

Lucitanib is an inhibitor of FGFR1-3, VEGFR1-3 and PDGFR. A phase I/IIa

demonstrated responses in FGFR1 amplified breast cancer, and in tumors often

responsive to VEGFR inhibitor therapy such as renal cell and thyroid cancer.

Further phase II trials in patients with breast cancer and other solid tumors

showing FGFR dysregulation are ongoing[135], [136].

AZD4547 is a newer FGFR inhibitor, with over 100-fold selectivity of FGFRs over

VEGFR. A phase I trial in patients with advanced solid tumors is ongoing, and a

phase II trial to test the efficacy of AZD4547 in combination with an aromatase

inhibitor is currently recruiting patients with ER+ breast cancer. AZD4547 is also

included in a phase II/III trial that employs genomic screening to assign therapies in NSCLC and squamous cell lung cancer[137].

BGJ398 is a selective FGFR inhibitor with some activity (70-100-fold difference) against VEGFR. Safety and efficacy are being evaluated in a phase I trial in patients with advanced solid tumors harboring FGFR1, 2 or 3 mutations or amplifications. Preliminary results are encouraging, as a lung cancer patient with FGFR1 amplification exhibited a 33% reduction in tumor size. The most recent adverse events were gastrointestinal events and fatigue. A frequent observation in clinical trials using more selective FGFR inhibitors has been hyperphosphatemia due to inhibition of FGF23 signaling in the kidney. AZD4547 also had this effect[138]-[140].

JNJ-42756493 is a selective and highly potent FGFR inhibitor that in initial phase I studies exhibited concerning side effects, but whose tolerability was improved on an intermittent schedule. Among 23 patients with advanced solid tumors harboring FGFR alterations, four had confirmed responses (glioblastoma, urothelial and endometrial cancers) and 16 patients had stable disease. Further studies are ongoing[141], [142].

INCB05828 is another potent inhibitor of FGFR1, 2 and 3 currently under evaluation in a phase I clinical trial for advanced malignancies[143].

In addition to kinase inhibitors, several strategies have been developed to block ligand-receptor interaction, including antibodies against FGFs or FGFRs, ligand traps, and ligand mimetics. The advantage of monoclonal antibodies is their isoform specificity, which should minimize common side effects associated with inhibition of all FGFRs. Despite promising results in in vitro models and animal studies, very few monoclonal antibodies have progressed to clinical trials. The FGFR3 antibody MFGR1877S is one of the few that has been evaluated in two separate phase I trials; one in t(4;14) multiple myeloma, and one in advanced solid tumors. In multiple myeloma, MFGR1877S was well-tolerated, and although no objective responses were observed, stable disease was observed in 3 patients[144]. A preliminary report on the solid tumor study documented long-lasting stabilization in 4 of 10 patients with bladder cancer[145].

1.3   Bone marrow microenvironment

In solid malignancies, the tumor microenvironment has long been recognized as an essential accessory to the establishment, growth, and dissemination of disease. This paradigm applies to leukemias as well, where abnormalities in a stem or progenitor cell alter the homeostasis between supportive cells and normal blood cell progenitors. Leukemias originate from a hierarchy of neoplastic stem cells that differ in self-renewing capacity. Neoplastic or leukemic stem cells (LSCs) arise from transformed normal hematopoietic stem cells (HSCs) or from hematopoietic progenitor cells that have re-acquired self-renewal capacity during transformation.

HSCs have to balance enormous production needs (over 500 billion blood cells are produced every day) with the need to regulate precise percentages of blood cell types in the circulation. It is estimated that humans possess approximately 10,000 HSCs, with about 1000 contributing to hematopoiesis at any given time[146]. The healthy bone marrow microenvironment is uniquely adapted to support HSCs, creating what is known as the stem cell niche. In addition to HSCs, the bone marrow contains mesenchymal stem cells (MSCs), osteoprogenitors, osteoblasts, osteocytes, and chondrocytes, as well as other stromal cell populations that may regulate hematopoiesis, such as neuronal cells, glial cells, and adipocytes. The bone marrow is also highly vascularized, and endothelial cells contribute to the maintenance of HSCs (Figure 1.4.2 and [147]).

HSC are found predominantly close to vasculature, and this location has implicated stromal cells in the perivascular region as niche cells[148]. Perivascular stromal cells are a heterogeneous population characterized by high CXCL12 expression, a chemokine that plays a crucial role in maintaining HSC function. CXCL12 positive stromal cells can be divided into three overlapping sub-populations: CXCL12-abundant reticular (CAR) cells, nestin-GFP positive stromal cells and leptin receptor positive stromal cells[149]. In addition to CXCL12, these cells express SCF and angiopoietin[150].

The cell populations discussed in the previous paragraph can be considered the immediate progeny of MSCs. Thus, MSCs are defined as self-renewing cells that can

generate cells of osteoblast, chondrocyte, adipocyte, and fibroblast lineages. Currently, no strategy exists to prospectively identify a pure MSC population. However, minimal criteria for the characterization of MSCs have been defined by the Mesenchymal and Tissue Stem Cell Committee of the International Society for Cellular Therapy: MScs must be plastic-adherent in culture, must express CD73, CD90 and CD105, and must lack expression of CD11b, CD14, CD34, CD45, CD79alpha, and HLA-DR, and must have full differentiation capacity[151]. Recently, the requirement for MSCs to be adherent has been called into question, as mesenchymal progenitors were expanded in suspension, and appeared to maintain a less committed phenotype than those cultured on plastic[152]. In human bone marrow, CD146 marks a population of stromal cells that is enriched for MSCs[153]. PDGFRalpha and CD51 have more recently been identified as markers of human MSCs. These cells support HSC expansion in vitro[154].
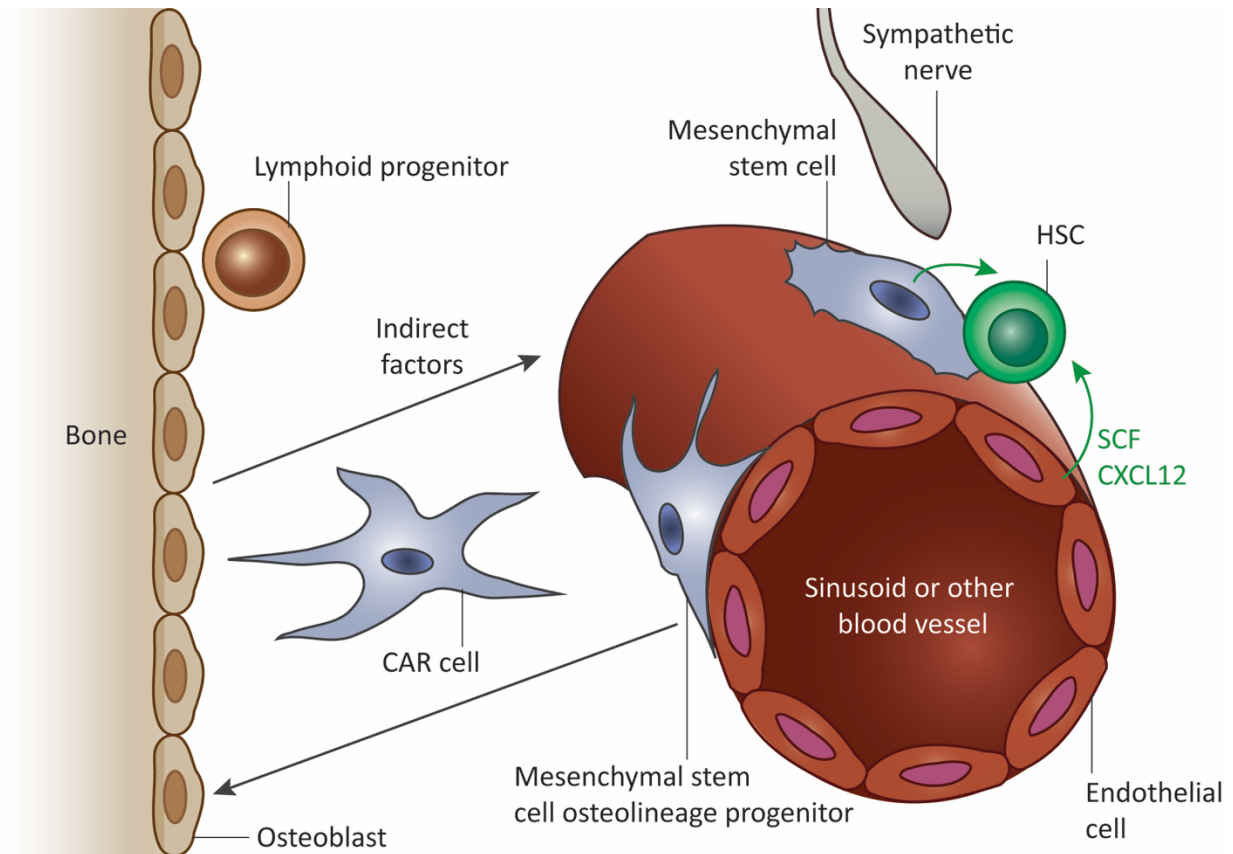
Figure 1.3.1 Hematopoietic stem cells (HSCs) in the bone marrow niche.
HSCs are found mainly adjacent to sinusoids in the bone marrow, where endothelial cells and mesenchymal stem cells promote HSC maintenance by producing SCF, CXCL12 and probably other factors. Perivascular stromal cells, which probably include CXCL12-abundant reticular (CAR) cells contribute to this niche. It is likely that other cells also contribute. These probably include cells near bone surfaces in trabecular-rich areas. Other cell types that regulate HSC niches include sympathetic nerves, non-myelinating Schwann cells, macrophages and osteoclasts. The extracellular matrix and calcium also regulate HSCs. Osteoblasts do not directly promote HSC maintenance but do promote the maintenance and perhaps the differentiation of certain lymphoid progenitors by secreting CXCL12 and probably other factors. Early lymphoid restricted progenitors thus reside in an endosteal niche that is spatially and cellularly distinct from HSCs. Adapted and reprinted by permission from Macmillan Publishers Ltd: Nature [154], copyright 2014.

1.3.1 FGF signaling in hematopoiesis

FGFs can regulate hematopoiesis directly by acting on hematopoietic cells, and indirectly by stimulating stromal cells to produce hematopoietic cytokines[155]. FGF2 induces proliferation of bone marrow stromal cells and promotes the release and/or synthesis of cytokines that stimulate megakaryopoiesis[156]. This is supported by the observation that an IL-6 blocking antibody abrogates the FGF2-induced enhancement of megakaryocyte colony formation[157]. FGFs play important roles in MSC differentiation and have been implicated both in adipogenesis and osteogenesis[158]. The osteogenic transcription factor Runx2 can be upregulated by FGF2, FGF4, and FGF8[159]. In addition, FGF2 can induce alkaline phosphatase activity and promote mineralization[160]. In terms of adipogenic differentiation, FGF1, FGF2, and FGF10 have been shown to promote adipogenesis when adipogenic conditions are provided[161]. Therefore, FGF2 exerts dual roles in regulating adipogenic and osteogenic differentiation. Importantly, FGF2 also promotes the maintenance of MSC self-renewal capacity, including extended lifespan in vitro, longer telomere length, and pluripotency.

FGF2 KO mice exhibit normal steady state hematopoiesis. However, a study showed that HSCs in these mice are unable to recover fully from myeloablative insults. The

authors propose that FGF2 expands and maintains stromal cells, including perivascular

Nestin+ supportive stromal cells, that facilitate HSC expansion by secreting SCF, and

exit from quiescence by downregulating CXCL12 via mir-31. Upregulated SCF levels

activate KIT, which is highly expressed by FGF2-induced HSCs. FGF2 is revealed as an

important regulator of stress hematopoiesis, undergoing a dramatic upregulation after

marrow insult, and leading to an expansion of MSCs and subsequently HSCs[162].

As indicated above, bone marrow endothelial cells are an important part of the stem cell

niche. FGF signaling plays an important role in maintaining endothelial integrity.

Endothelial cell-specific knockout of FGFR1/2 leads to impaired endothelial integrity

and exposure of HSCs to peripheral blood, which augments their differentiation and

compromises long-term self-renewal capacity[163].

1.3.2   Mesenchymal stem cells in the leukemic niche

LSCs localize to the same niche as their non-neoplastic counterparts, and thus compete

with normal HSCs. MSCs control the fate of LSCs similarly to HSCs, including

quiescence, resistance to apoptotic stimuli and resistance to drugs. These pathways are

regulated most efficiently when LSCs are in contact or in close proximity to MSCs[164].

For example, CD44, which binds extracellular matrix proteins, is essential for the

homing and establishment of CML and AML in several mouse models[165]. The

addition of an anti-CD44 monoclonal antibody to dasatinib led to a reduction of CML

blasts, suggesting that dislodged leukemia cells are more sensitive to

chemotherapy[166]. Direct cell-to-cell contact inhibits leukemic cell proliferation and

activates survival pathways leading to protection from chemotherapy[167]. As

indicated in chapter 1.1.3.1, cell-contact mediated protection can also promote resistance

to tyrosine kinase inhibitors.

Interestingly, the bone marrow microenvironment can even be the initiator of abnormal

HSC behavior. Mice lacking retinoic acid receptor (RAR) gamma have increased

granulocyte/macrophage progenitors. However, when wild-type HSCs were

transplanted into these mice, the mice still developed myeloproliferation[168]. It was

later shown that increased TNFalpha secretion in the bone marrow contributed to the

aberrant proliferation. In another mouse model, Dicer1, which is required for

microRNA processing, was disrupted in osteoprogenitors. Mice developed a

myelodysplasia-like syndrome and several progressed to AML with new genetic

abnormalities[169]. These data are the first evidence that stromal cells can be the

inciting abnormality.

1.4   Exosomes in cancer

Extracellular vesicles, including exosomes and microvesicles, are emerging as a form of

intercellular communication with important roles in physiological processes as well as

in cancer. Extracellular vesicles can transfer proteins, RNA transcripts, microRNAs, and

even DNA to neighboring cells or to distant tissues. Microvesicles can be as large as 0.2-1 um in diameter, while exosomes are typically much smaller, ranging in size from 0.04-0.1 um[170]. These two classes of extracellular vesicles are formed through distinct mechanisms. Microvesicles are shed from the plasma membrane by budding and fission. Conversely, exosomes do not initially form at the plasma membrane (Figure 1.4.3 and [171]). They are produced through inward budding in a late endosome called the multivesicular body assisted by ESCRT (endosomal sorting complex required for transport) machinery. The multivesicular body is re-routed to the cell surface, where it fuses with the plasma membrane and releases the exosomes[172]. Several markers, including CD63, CD81, CD9, tsg-101, syndecan-1, MHC molecules, ALIX, and HSP70, have been used to identify exosomes at different stages of their biogenesis[170]. In addition to the ESCRT-mediated exosome biogenesis described above, ceramide and nSMase2 (neutral sphingomyelinase 2; the rate limiting enzyme of ceramide biosynthesis) seem to be able to mediate exosome formation, loading, and release[173].

Both microvesicles and exosomes have been implicated in cancer progression. Microvesicles shed from cancer cells have been shown to activate fibroblasts and alter the tumor microenvironment, as well as stimulating tumor angiogenesis[174], [175]. Likewise, exosomes have been implicated in mediating the communication between stromal cells and surrounding cancer cells, and the education of bone marrow-derived cells, which in turn affects the development of the pre-metastatic niche[176], [177].

Extracellular vesicles generated by some cancer cells contain signaling molecules such as Ras and EGFR[178], [179], and different RNA species that regulate the expression of proteins that stimulate cell growth and survival[180]. Two studies in glioblastoma were the first to demonstrate that extracellular vesicles could transfer functionality from one cancer cell to another. In the first study, microvesicles from patient sample glioblastoma were taken up by the U87 glioblastoma cell line and stimulated their growth, likely through translation of oncogenic RNA transcript contained in the vesicles[181]. The second study showed that not only transcript, but functional protein, in this case the growth-promoting EGFRvIII receptor, could be transferred via extracellular vesicles, and promote accelerated growth in U87 cells[182]. This suggests that extracellular vesicles may help the propagate the oncogenic phenotype among heterogeneous cell populations in a tumor.

Extracellular vesicles can also have a significant impact on the function and behavior of cells in the tumor microenvironment. For example, vesicles shed from breast cancer cells are taken up by normal mammary epithelium and fibroblasts and enhance their proliferation, survival, and anchorage-independent growth[183]. In gastrointestinal stromal tumor, oncogenic KIT-containing exosomes have been shown to activate signaling in normal smooth muscle progenitor cells to support tumor invasiveness[184]. Interestingly, the transfer of information via extracellular vesicles between cancer cells and the microenvironment is reciprocal. For example, stromal cells associated with

breast cancer release vesicles that contribute to chemoresistance and tumor re-initiation[177]. Another study demonstrated that exosomes secreted from fibroblasts associated with oral cavity squamous cell carcinoma contain TGFbeta receptor II, which contributes to TGFbeta-responsiveness in cancers cells at the edge of the tumor, resulting in growth arrest, increased metastatic capacity and drug resistance[185].

Extracellular vesicles have been heavily implicated in the creation of the pre-metastatic niche. For example, exosomes from metastatic melanoma cells increased vascular leakiness and enhanced the metastasis of melanoma cells in a mouse xenograft[186]. A similar role for extracellular vesicles was found in a model of metastatic pancreatic ductal carcinoma[176]. Extracellular vesicles also seem to determine tropism of various cancers for different metastatic organ sites. The presence of different integrins on vesicles regulated uptake in different organs, suggesting that they could serve as metastatic markers[187].

1.4.1 Exosomes in the hematopoietic niche

The role of exosomes in leukemias is not as well studied as their role in solid malignancies. Nevertheless, the limited studies have highlighted a possible role in leukemia development and progression. Exosomal microRNA in the serum is correlated with AML xenograft growth kinetics and can serve as a minimally invasive early biomarker of AML[188]. Another study found that leukemia patients develop severe

bleeding as a result of diffuse activation of the clotting cascade. Tissue factor has been found in extracellular vesicles of patients with advanced malignancies[189]-[191]. Primary AML and AML cell lines release exosomes that can be taken up by murine OP9 bone marrow stromal cells. The exosomes transfer IGF-1R mRNA to the stromal cells[192]. Recently, a study showed that CLL-derived exosomes are incorporated into endothelial and mesenchymal stem cells, and that this transfer causes an inflammatory phenotype in the recipient cells and transforms stromal cells into cancer-associated fibroblasts. The endothelial cells also showed increased angiogenic potential[193].

It has been established that mesenchymal stem cells are a rich source of extracellular vesicles, and that these vesicles share some of the unique properties of MSCs themselves[194]. For example, MSC-derived exosomes reduce pro-inflammatory cytokines in patients with treatment-refractory graft-versus-host disease[195]. In addition, extracellular vesicles derived from MSCs elicit cardioprotection and decrease the damage caused by ischemia in animal models of ischemia and reperfusion injury[196]. Despite these findings, little is known about MSC-derived exosomes in cancer. However, initial reports suggest that they may play a role in therapy resistance. In multiple myeloma, exosomes from bone marrow stromal cells have been found to provide protection from apoptosis when myeloma cells are exposed to bortezomib. Stromal exosomes alter the expression and activity of p38, p53, c-Jun, N-terminal kinase, and the AKT pathway[197]. This study is the first indication that exosome-mediated

crosstalk between leukemia and bone marrow stromal cells is reciprocal and can contribute to drug resistance, however, the function of MSC-derived exosomes in hematopoietic malignancies remains otherwise largely unexplored.

1.4.2 Regulation of exosome biogenesis and release

As exosomes are derived from the endocytic pathway, endocytosis can be considered the first step in exosomal biogenesis. Cancer cells frequently express abnormal levels of transmembrane receptors and associated structural and signaling components. The plasma membrane is highly dynamic, and receptors have a high turnover rate[101]. As receptors are marked for recycling or degradation, they enter the endocytic pathway, transitioning from early endosomes to multivesicular bodies and potentially to exosomes for subsequent release. Indeed, the rate of endocytosis of lipid rafts is directly correlated with the rate of exosome release. Cancer cell-specific properties such as lipid composition of the plasma membrane, receptor expression and activation status and reactions to hypoxia are all likely to influence the quality and quantity of exosome biogenesis[198]. There is great interest in inhibiting exosome-mediated enhancement of metastasis. The focus has been on blocking the production of exosomes by tumor cells in a relatively unspecific manner. For example, it has been shown that exosomes from 4T1 cancer cells are released in a Rab27a-dependent manner, and inhibition of Rab27a results in decreased primary tumor growth and metastatic potential[199]. However, silencing of Rab27a and b inhibits production of exosomes in many cell types including

HeLa cells[200]. Even less specifically, exosome production can be inhibited by blocking

H/Na and Na/Ca channels. Blocking of Ca-channels can be achieved with amiloride.

Amiloride has been shown to inhibit exosome biosynthesis in vitro and in vivo, and in

combination with cyclophosphamide, reduced the activity of myeloid-derived

suppressor cells[201]. Beyond this, we have not yet capitalized on our understanding of

the exosome biogenesis pathway to develop strategies that specifically target one cell

type.
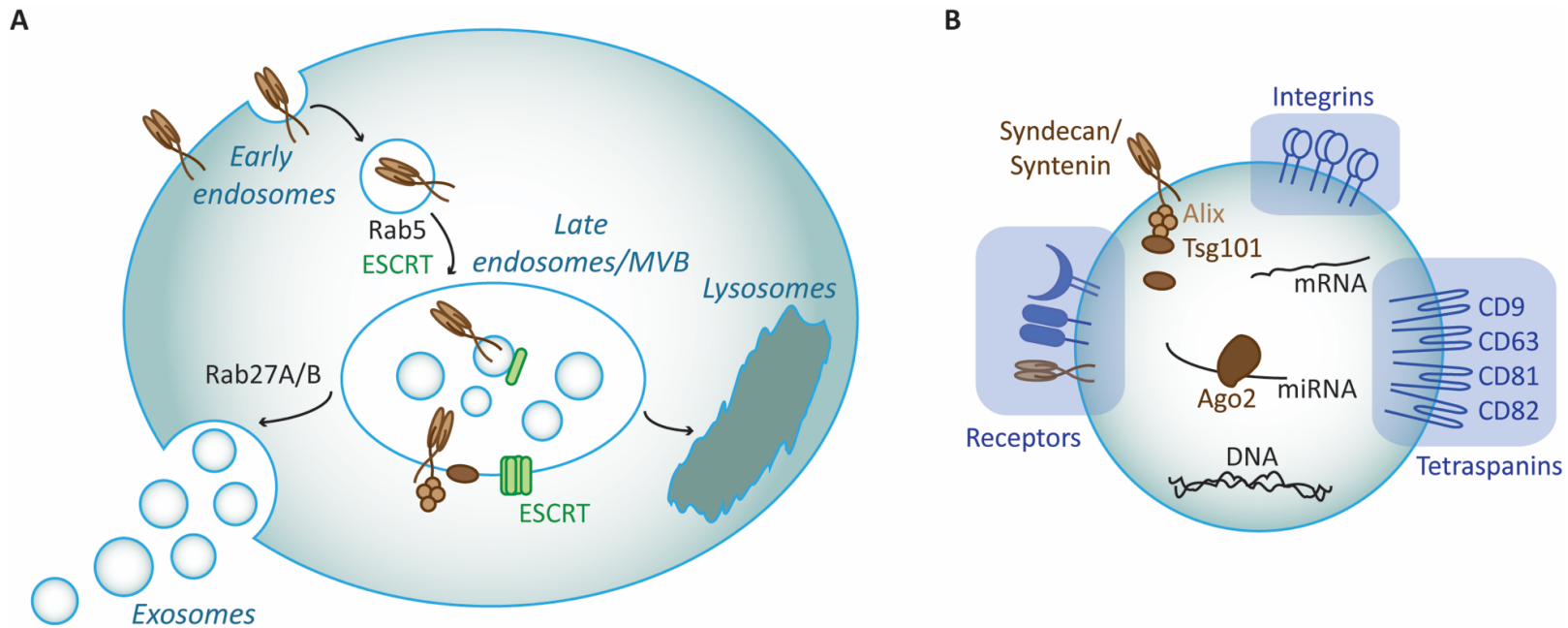
Figure 1.4.1 Overview of EV biogenesis and functions.
A. Exosome biogenesis. Exosomes are derived from multivesicular bodies (MVBs). Exosome generation is initiated through inward budding of early endosomes leading to MVB formation. Exosomes are released when MVBs fuse with the cell membrane to release their cargo. ESCRT proteins, together with additional factors such as syntenin and syndecans, mediate the biogenesis of MVBs and the sorting of specific cargo to MVBs. Rab proteins regulate maturation and fusion of MVBs with the plasma membrane. Fusion of the MVB and release of exosomes are regulated and are known to require phospholipase D, calcium and Rabs 11 and 27A and B. B. Exosome constituents. Exosomes are composed of a lipid bilayer, and they contain specific receptors on their surface reflecting their cells of origin (i. e. tetraspanins and integrins). Exosomes can be identified by the presence of specific ESCRT components such as tsg101 and Alix. They also contain various molecules including protein, lipid, DNA and RNA (including miRNAs bound to Argonaute-2 (Ago2). Adapted and reprinted by permission from John Wiley and Sons: Cellular Microbiology [171], copyright 2014.

2   Paracrine mechanisms of FGF-mediated resistance

This chapter is based on three manuscripts describing the paracrine protective action of

FGF2 on three different cancer types. Data not included in the original publications is

shown in sections 2.1.3.2 and 2.1.3.8.

2.1 Crosstalk between KIT and FGFR3 Promotes Gastrointestinal Stromal Tumor Cell Growth and Drug Resistance.

Nathalie Javidi-Sharifi, Elie Traer, Jacqueline Martinez, Anu Gupta, Takehiro Taguchi, Jennifer Dunlap, Michael C. Heinrich, Christopher L. Corless, Brian P. Rubin, Brian J. Druker, Jeffrey W. Tyner

2.1.1 Abstract

Kinase inhibitors such as imatinib have dramatically improved outcomes for patients with gastrointestinal stromal tumor (GIST), but many patients develop resistance to these treatments. Although in some patients this event corresponds with mutations in the GIST driver oncogenic kinase KIT, other patients develop resistance without KIT mutations. In this study, we address this patient subset in reporting a functional dependence of GIST on the FGF receptor FGFR3 and its crosstalk with KIT in GIST cells. Addition of the FGFR3 ligand FGF2 to GIST cells restored KIT phosphorylation during imatinib treatment, allowing sensitive cells to proliferate in the presence of the drug. FGF2 expression was increased in imatinib-resistant GIST cells, the growth of which was blocked by RNAi-mediated silencing of FGFR3. Moreover, combining KIT and FGFR3 inhibitors synergized to block the growth of imatinib-resistant cells. Signaling crosstalk between KIT and FGFR3 activated the MAPK pathway to promote resistance to imatinib. Clinically, an IHC analysis of tumor specimens from imatinib-resistant GIST patients revealed a relative increase in FGF2 levels, with a trend toward increased expression in imatinib-naïve samples consistent with possible involvement in drug resistance. Our findings provide a mechanistic rationale to evaluate existing FGFR inhibitors and multikinase inhibitors that target FGFR3 as promising strategies to

improve treatment of patients with GIST with de novo or acquired resistance to imatinib.

2.1.2 Introduction

1.1.1.6 *GIST clinical perspective*

Gastrointestinal stromal tumors (GIST) are the most common mesenchymal neoplasms of the gastrointestinal tract with 5,000 to 6,000 new cases in the United States each year. They originate from interstitial cells of Cajal or their stem cell precursors, also known as GI pacemaker cells as they interface between autonomic nerves and smooth muscle cells of the GI tract[202]. GISTs occur throughout the GI tract with the most common locations being the stomach (60%), jejunum and ileum (30%), and colorectum (less than 5%). Approximately ¼ of gastric and ½ of intestinal GISTs are metastatic, most commonly to the abdominal cavity and liver. GISTs usually occur in adults over 50. The most common symptom of GIST is GI bleeding. If possible, tumors are resected. In cases of unresectable or metastatic disease, tyrosine kinase inhibitors against KIT and/or PDGFRA achieve complete or partial remission in the majority of patients.

1.1.1.7 *Oncogenic signaling in GIST*

The importance of the receptor tyrosine kinase KIT was first established when germline loss-of-function point mutations proved deleterious for normal hematopoiesis and mast-cell development, melanogenesis, gametogenesis, and development of the

interstitial cells of Cajal[203]. Gain of function mutations in KIT are associated not only

with GIST, but also with several other highly malignant tumors in humans, such as

mast-cell and myeloid leukemias, seminomas, and dysgerminomas. KIT mutations in

GIST cluster in exon 11, which encodes the juxtamembrane domain of KIT. The

mutations cluster around the autophosphorylation sites at Tyr568 and 570, leading to

de-repression and autophosphorylation in absence of ligand[204]. KIT is highly

expressed and carries activating mutations in most cases of GIST. The majority of GISTs

with wild-type KIT have activating mutations in PDGFRA[205], [206]. Activation of the

PI3K pathway downstream of mutant KIT/PDGFRA is essential for GIST cell growth

and survival[207]. In addition, MAPK pathway signaling is activated downstream of

KIT, and plays a pivotal role in tumorigenesis through the stabilization of the

transcription factor ETV1 and activation of an oncogenic transcriptional program[208].

1.1.1.8 TKI therapy in GIST

Until fifteen years ago, GIST was regarded as a chemotherapy-resistant disease, with

little to no improvement in survival with the use of conventional chemotherapy[209].

The introduction of targeted tyrosine kinase inhibitor (TKI) therapy has revolutionized

the clinical management of GIST and exemplifies the success of targeted therapy in

solid tumors. 80% to 90% of patients with GIST with unresectable or disseminated

disease initially attain at least disease stabilization, or complete or partial response to

imatinib[210]. A dose of 400 mg per day is the current first0line treatment for patients

with metastatic GIST, unless the tumor harbors a gatekeeper mutation in exon 18 of

PDGFRA (D842V) which confers resistance to imatinib. In patients with KIT exon 9

mutations, increasing the dose to 800 mg per day has shown a significant improvement

in progression-free survival[210]. Imatinib is now also routinely used in a neoadjuvant

or adjuvant setting[211].

1.1.1.9   *Resistance to TKI therapy in GIST*

Nearly 50% of GIST cases treated with imatinib develop secondary resistance in the first

2 years. Most frequently, secondary resistance is due to acquisition of additional

mutations in KIT or PDGFRA that decrease the binding affinity for imatinib[207], [212].

However, another mechanism that is likely to account for acquired resistance in a

subset of GISTs is activation of pathways other than KIT and PDGFRA, thereby

bypassing the inhibitory effects of KIT/PDGFRA-targeted small molecules. One third of

the patients can be stabilized by increasing the imatinib dose to 800 mg per day[213].

Sunitinib is the standard of care for patients who progress on or cannot tolerate

imatinib[214]. Regorafenib has been approved for third-line treatment of GISTs that

progressed on imatinib and sunitinib after demonstrating improved progression-free

survival compared to imatinib re-challenge or placebo[215], [216].

Masitinib is under evaluation as a second-line therapy in comparison to sunitinib. Initial

results are promising and a phase III trial is recruiting patients. Ponatinib is another

multi-kinase inhibitor that targets KIT, PDGFRA, BCR-ABL, and FGFRs and was first studied in CML, and now is being evaluated for GIST. The management of patients with a PDGFRA D842V mutation remains a particular challenge. Crenolanib is an inhibitor of Imatinib-resistant PDGFRA kinases including D842V in GIST patients; a phase II trial has been initiated to treat this population. Inhibitors of downstream pathway kinases (PI3K and MAPK) are under evaluation. Heat shock protein (HSP) protects KIT from degradation and agents targeting HSP 90 are under investigation for Imatinib resistant GISTs.

A group of KIT/PDGFRA wild-type patients show high expression of IGF-1R in their tumors. This is due to deficient succinyl dehydrogenase (SDH) complex function[217]. Therefore, lisitinib, a TKI against IGF-1R, was investigated in a phase II trial in wild-type GISTs. No objective response was observed, however, this could be because patients without SDH deficiency were included in the trial.

Here, we delineate a new resistance mechanism to imatinib in a resistant GIST cell line with no secondary KIT or PDGFRA mutations. We demonstrate dependence on FGFR3 in multiple GIST cell lines and show that resistance can be induced in sensitive lines by exposure to FGF2. Resistance could be overcome by combined inhibition of FGFRs and KIT, providing new actionable targets in imatinib-refractory disease.

2.1.3 Results

1.1.1.10 FGFR3 dependence in GIST cell lines

GIST T1 cells harbor a heterozygous deletion of KIT exon 11 and consequently exhibit high sensitivity to imatinib with potent suppression of cell proliferation at concentrations ranging from 100 to 1,000 nmol/L.[218] The GIST 10R cell line grew out as a colony after 2 months treatment of GIST T1 cells with 10,000 nmol/L imatinib. Consequently, GIST 10R cells exhibit no IC50 at concentrations of imatinib up to 10,000 nmol/L, although an IC25 is still apparent at 100 nmol/L (Figure 2.1.1 A). Interestingly, GIST 10R cells do exhibit reduced phosphorylation of KIT and its downstream signaling molecules after exposure to 1,000 nmol/L imatinib (Figure 2.1.1 B), and no secondary mutations were found in KIT, indicating that drug resistance in GIST 10R cells must be due to alternative mechanisms. The fact that inhibition is equal at equal concentrations of imatinib is likely due to the fact that GIST 10R does not carry additional mutations in KIT that should render this primary drug target less susceptible to inhibition. In addition, comparative RNA sequencing between GIST T1 and 10R revealed no point mutations or remarkable changes in gene expression that would explain drug resistance in these cells. To investigate possible alternative therapeutic targets in these cells, we transfected GIST T1 and 10R cells with a panel of siRNAs that collectively target the entire tyrosine kinase gene family in addition to NRAS and KRAS (93 genes total; refs. 19, 20). As expected, siRNA against KIT significantly reduced the relative number of

proliferating GIST T1 cells (Figure 2.1.2 A). We also observed a significant reduction in

proliferation after silencing of colony stimulating factor 1 receptor, tyrosine kinase 2

(TYK2), and FGFR3. Polo-like kinase 1 plays a critical role in mitosis in all cells and was

used as a positive control for effective siRNA-mediated silencing. Interestingly, GIST

10R cells retained residual sensitivity to KIT silencing (Figure 2.1.2 B); however,

silencing of TYK2 and FGFR3 reduced growth more significantly. To confirm

reproducible and significant sensitivity to silencing of these genes, we independently

assessed cell proliferation after silencing of KIT, FGFR3, and TYK2 compared with

nontargeting siRNA. We confirmed the differential effect of KIT siRNA on GIST 10R

and T1 cells (Figure 2.1.2 C). KIT silencing significantly impacted both cell lines, but this

impact was much less pronounced in GIST 10R cells than in GIST T1 cells. We also

confirmed that both cell lines were sensitive to FGFR3 silencing to a comparable degree.

For reference, FGFR3 phosphorylation and expression levels are compared in all cell

line models in Figure 2.1.1 C. Expression of FGFR3 after treatment of GIST 10R and T1

cells with four individual siRNA duplexes also resulted in reductions of GIST cell

viability (Figure 2.1.3). To determine whether this impact on relative number of viable

cells was predominantly an effect on cell growth or an induction of apoptosis, we also

stained cells with Annexin V after silencing of KIT, FGFR3, or TYK2. Although we

observed minor increases in Annexin V staining after silencing of each gene, these

changes were markedly less than the reduction observed in overall numbers of viable

cells, indicating that reduced cell growth is largely responsible for the observed phenotype (Figure 2.1.1 D).

1.1.1.11 TYK2 dependence in GIST cell lines

After observing sensitivity to TYK2 knockdown in both GIST T1 and 10R cells (Figure 2.1.2), we sought to define the connection between TYK2 signaling and other relevant targets, such as KIT and FGFR3. We were able to confirm that both TYK2 and STAT1 were activated after treatment with FGF1 (Figure 2.1.4 A), as well as FGF2 (Figure 2.1.4 B). TYK2 phosphorylation was not increased following stimulation with SCF (Figure 2.1.4 C). Although JAKs were first identified as components of cytokine signaling, there are reports of JAK kinase association with RTKs, such as EphA4[219]. We therefore asked whether TYK2 was directly associated with FGFR3. Indeed, we observed an association of TYK2 with FGFR3 by co-immunoprecipitation (Figure 2.1.4 D). In contrast, TYK2 did not co-IP with KIT in this setting (Figure 2.1.4 E). Although we cannot exclude a possible interaction between KIT and TYK, overall, these results support a role for TYK2 in FGF signaling.

1.1.1.12 Crosstalk between KIT and FGFR3

We next sought to understand the role of FGFR3 in maintenance of GIST T1/10R cell growth. First, we treated both cell lines with 1,000 nmol/L imatinib for 2 hours and then detected the active, phosphorylated forms of KIT and FGFR3, as well as total protein, on

an immunoblot analysis (Figure 2.1.5 A). Surprisingly, in both cell lines, we observed a

reduction in phospho-KIT and phospho-FGFR3 after imatinib treatment. To confirm

that the reduction in phospho-FGFR3 was not due to an off-target effect of imatinib, we

silenced KIT in GIST 10R and again assessed FGFR3 phosphorylation by immunoblot

analysis (Figure 2.1.5 B). Phosphorylation was again reduced, indicating that FGFR3

activation in GIST cells is dependent on KIT activity. Next, we asked whether the

connection between KIT and FGFR3 was reciprocal, so that FGFR3 inhibition or

silencing would affect KIT activity. We treated GIST 10R cells with the FGFR inhibitor

PD173074 at 1,000 nmol/L for 2 hours and performed immunoblot analyses (Figure 2.1.5

C). Phospho-FGFR3 and total FGFR3 protein levels were markedly reduced after

treatment with PD173074. Importantly, KIT is not a reported target of PD173074, yet

phospho-KIT was reduced after treatment in both cell lines. To rule out direct inhibition

of KIT as the source for reduced phosphorylation, we silenced FGFR3 using siRNA in

GIST 10R cells and assessed KIT phosphorylation by immunoblot analysis (Figure 2.1.5

D). Again, phospho-KIT was reduced after FGFR3 silencing, suggesting that reciprocal

crosstalk exists between KIT and FGFR3 in GIST cells. In addition, we stimulated KIT

and FGFR3 by the addition of ligand for each receptor (SCF and FGF2, respectively) and

observed increased phosphorylation for both KIT and FGFR3 in GIST 10R and, to a

lesser degree, in GIST T1 (Figure 2.1.5 E and F). Although FGF1 is the prototypic ligand

of FGFR3, FGF2 also binds and activates FGFR3[55]. We observed a similar increase in

phosphorylation of FGFR3 and KIT in response to FGF1 (Figure 2.1.6 A); however, FGF2 elicited a more dramatic protective effect after imatinib treatment (Figure 2.1.7 A-C) compared with FGF1 (Figure 2.1.6 B). We thus chose to conduct subsequent experiments using FGF2.

Reciprocal crosstalk between two RTKs may result from indirect interaction (mediated by a common downstream kinase), or direct interaction through the formation of heterodimers or other receptor clustering. To test the hypothesis that the crosstalk between KIT and FGFR3 is direct, we co-transfected HEK 293 cells with plasmids containing KIT and FGFR3 wild-type cDNA. We performed immunoprecipitation with a KIT-specific antibody, followed by immunoblotting for FGFR3 (Figure 2.1.5 G). We observed co-immunoprecipitation of KIT and FGFR3, suggesting a direct interaction between these RTKs. The reverse co-immunoprecipitation was not successful, likely because there is no antibody suitable for immunoprecipitation of FGFR3 available to us.

1.1.1.13 *FGF2-mediated protection of imatinib-sensitive GIST cells*

We reasoned that presence of ligand, in particular FGF2, in the cell culture media might dampen the response of GIST T1 cells to imatinib. Consequently, we treated GIST T1 cells with a gradient of imatinib concentrations with or without a constant concentration of ligand (Figure 2.1.7 A). In the absence of ligand, GIST T1 cells were extremely sensitive to imatinib, with an IC50 of 40 nmol/L. In the presence of SCF, the

IC50 was increased slightly, however, at higher concentrations of imatinib, cell

proliferation was not improved. In contrast, the addition of FGF2 increased cell

proliferation in the presence of imatinib dramatically, with no IC50 even at

concentrations as high as 10,000 nmol/L. Of note, the combination of FGF2 and SCF

conferred a further increase in viability at low concentrations of imatinib. Similar results

were observed using a different, KIT-sensitive GIST-derived cell line, GIST 882 (Figure

2.1.7 B). We also cultured GIST T1 cells with 1,000 nmol/L imatinib in the presence or

absence of 10 ng/mL SCF or FGF2 (Figure 2.1.7 C). Viable cells were counted every 2 to

3 days for 19 days. As expected, culture with SCF did not confer any growth advantage

over cells cultured with imatinib and a vehicle control. The addition of FGF2, however,

increased the number of viable cells starting at day 4. Importantly, cells not only

persisted in the culture, but, after a lag phase, continued to divide and exceeded the

number initially plated on day 0. We hypothesized that the desensitization of GIST cells

to imatinib is indeed mediated through the interaction between KIT and FGFR3, and

not the result of an alternative survival pathway replacing KIT signaling. To this end,

we measured GIST T1 cell growth after KIT silencing in the presence or absence of FGF2

with the hypothesis that presence of KIT protein would be required for FGF2 rescue

(Figure 2.1.7 D). As predicted, rescue of cell growth by FGF2 was ineffective after KIT

knockdown, indicating that FGF2 rescue requires presence of both KIT and FGFR3. We

also showed that inhibition of FGFR3 by PD173074, which inhibits GIST T1 cell

proliferation with an IC50 of 300 nmol/L, can be partially reversed by the addition of

SCF (Figure 2.1.8) and that SCF rescue is ineffective after silencing of FGFR3 (Figure

2.1.7 D). To test whether desensitization to imatinib is, indeed, mediated by FGFR3, we

performed siRNA knockdown of FGFR1, FGFR2, and FGFR3 in GIST T1, and

subsequently treated with imatinib and FGF2 Figure 2.1.7 E). Knockdown of FGF

receptors was confirmed via real-time RT-PCR (Figure 2.1.9). FGF2 rescue of imatinib

sensitivity remained effective after FGFR1 and FGFR2 silencing; however, FGFR3

silencing ablated the response to FGF2, implicating FGFR3 but not FGFR1 or FGFR2 in

FGF2-mediated drug resistance. We next treated GIST T1 cells with 0, 50, or 500 nmol/L

imatinib and stimulated cells with SCF or FGF2. At baseline, KIT phosphorylation was

responsive to both SCF and FGF2 stimulation. The response to SCF was conserved in

the context of 50 nmol/L imatinib treatment, but was markedly decreased after

treatment with 500 nmol/L imatinib. In contrast, FGF2 still restored KIT

phosphorylation at 500 nmol/L (Figure 2.1.7 F). To ensure that this observation was not

specific to the cell line GIST T1, we repeated this experiment in the cell line GIST 882

(Figure 2.1.7 G). Again, we observed that KIT phosphorylation in GIST 882 was

completely ablated at 500 nmol/L imatinib without FGF2 stimulation, but could be

partially restored by the addition of FGF2. We subsequently sought to determine the

effects of FGF2 stimulation on downstream signaling in the setting of imatinib

treatment (Figure 2.1.7 H). Analysis of AKT and MAPK pathway activation revealed

that both pathways are inhibited after imatinib treatment. However, although AKT phosphorylation remained inhibited after the addition of FGF2, MEK1/2 and ERK1/2 phosphorylation was restored.

1.1.1.14 Synergy between FGFR and KIT inhibition in resistant GIST cells

We hypothesized that combination treatment using imatinib and the selective FGFR inhibitor PD173074 may restore imatinib sensitivity in resistant GIST cells. Accordingly, we performed dose–response curves in the imatinib-resistant GIST 10R cells using imatinib and PD173074 alone as well as a constant, equimolar ratio combination of the two drugs (Figure 2.1.10 A). We then determined the combination index (CI) for each dose point using the Chou–Talalay method to quantify synergy. Figure 2.1.10 B shows CI values plotted against the log of drug dose. Over the entire dosing curve, the CI values ranged from 0.0005 to 0.004, indicating an extremely high degree of synergy between the two drugs.

We next wanted to determine whether signaling pathways activated downstream of FGFR3 might also exhibit synergy with KIT inhibition. To this end, we treated GIST 10R cells with combinations of imatinib and PLX-4720, a B-Raf inhibitor (Figure 2.1.11), AZD-6244, a MAPK inhibitor (Figure 2.1.10 C), and PI103, a PI3K inhibitor (Figure 2.1.10 D). Combination of imatinib with inhibitors of the RAF/MAPK pathway exhibited significant synergy at all concentrations tested. In contrast, combination of imatinib

with inhibitors of the PI3K-AKT pathway did not result in synergy with imatinib.

Combined treatment with imatinib and AZD-6244, in particular, led to a decrease in cell

growth similar to that observed after imatinib and PD173074 treatment, suggesting that

the MAPK pathway is a key mediator of imatinib resistance in GIST 10R cells.

1.1.1.15 MAPK signaling in imatinib resistance

We performed immunoblot analysis to assess phosphorylation of AKT, c-Raf, MEK, and

ERK in GIST 10R and T1 cells after 2-hour treatment with 1,000 nmol/L imatinib (Figure

2.1.12 A). In both cell lines, AKT phosphorylation was equivalently reduced after

treatment. However, we observed divergent effects on MAPK pathway activation.

Phosphorylation of c-Raf was reduced less markedly in GIST 10R compared with GIST

T1 cells. Even more strikingly, phosphorylation of MEK and ERK was abolished in GIST

T1 after imatinib treatment, but increased in GIST 10R. To determine whether this

feedback mechanism could be solely regulated at the receptor level, or whether it might

also be regulated after direct inactivation of the downstream PI3K signaling, we treated

GIST 10R cells with the PI3K inhibitor PI103 and asked whether the same increased

phosphorylation of MAPK signaling resulted (Figure 2.1.12 B). No increase in c-Raf,

MEK, or ERK phosphorylation was observed after inhibition of PI3K. To assess whether

FGF receptors are involved in mediating this MAPK feedback mechanism, we inhibited

KIT and FGFRs, either by the dual inhibitor CHIR-258 (dovitinib; Figure 2.1.12 C), or by

a combination of imatinib and PD173074 (Figure 2.1.12 D). We found that MAPK

activation was abrogated in both cases, providing a mechanistic basis for the synergy observed in Figure 2.1.10.

1.1.1.16 *FGF2 levels in GIST patient samples*

Because our data suggest that FGF2 can promote imatinib resistance in GIST cells, we wanted to determine whether FGF2 levels are higher in GIST 10R than GIST T1 cells and whether this may underlie the resistance of GIST 10R cells to imatinib. It is well recognized that FGF2 associates with heparan sulfate in the extracellular matrix. We were thus unable to detect it in supernatant but found it present in cell lysate. Evaluation of FGF2 protein levels did reveal increased levels of FGF2 in GIST 10R cells compared with GIST T1 (Figure 2.1.13 A). Subsequently, we investigated whether silencing of FGF2 in GIST 10R cells changes cell growth when compared with treatment with nontargeting siRNA. Indeed, we observed a significant decrease in cell growth after GIST 10R cells were treated with FGF2 siRNA (insert in Figure 2.1.13 B). We next asked whether siRNA-mediated knockdown of FGF2 would resensitize these cells to imatinib. Silencing of FGF2 dramatically shifted the IC50 for imatinib in GIST 10R cells (Figure 2.1.13 B), indicating that FGF2 contributes to imatinib resistance in GIST 10R and that the inhibition of FGF signaling restores the response to imatinib in a resistant GIST cell line. Knockdown of FGF2 expression was confirmed via real-time RT-PCR (Figure 2.1.14). We sought to examine whether increased levels of FGF2 correlated with KIT activation in GIST patient samples. We obtained a panel of six frozen tissue

specimens from GI stromal tumors with confirmed activating mutations in KIT exon 11.

Five of the tumors were treatment naïve at the time of biopsy, while one patient had

received 4 to 5 weeks of imatinib before the tumor being removed. The treatment was

discontinued 3 to 4 days before surgery. We performed immunoblot analyses for

activated KIT and FGFR, as well as FGF2 levels in these samples (Figure 2.1.13 C) and

observed increased FGF2 in specimen TB-7248, which had been exposed to imatinib.

The pan-phospho-FGFR antibody yielded immunoblot analyses with lower background

and was thus chosen here for use on tumor lysates. Concurrent with high FGF2 levels,

we observed a high degree of phosphorylated KIT and FGFR. This observation is

consistent with our model of FGF2-mediated reactivation of KIT. We sought to validate

these findings in a larger number of GIST samples by performing IHC staining for FGF2

on ten sections of formalin-fixed paraffin-embedded tissue (Figure 2.1.13 D). An

illustration of the quantification process is provided in Figure 2.1.15. Samples not

previously exposed to treatment were segregated by mitotic rate and tumor size

according to the Fletcher risk table into low-risk and intermediate/high-risk categories.

Figure 2.1.13 E–G provides examples of IHC staining in treatment naïve, low-risk

disease, as well as two cases of imatinib exposed tumor samples. Overall, low risk was

associated with low FGF2 staining, whereas intermediate/high-risk and treatment

exposure or resistance were associated with elevated levels, warranting further study of

FGF2 levels in even larger cohorts of primary GIST patient specimens in the future.

1.1.1.17 FGF2 in infiltrating immune cells

Increased FGF2 levels in imatinib pre-treated and resistant GIST could be due to intra-

tumoral upregulation, upregulation in tumor-associated smooth muscle or fibroblasts,

or a result of tumor infiltration by FGF2-expressing immune cells. FGF2 is expressed in

bone marrow stroma and contributes to therapy resistance against imatinib and

AC220in CML and FLT3-ITD positive AML, respectively([220] and chapter 2.3). FGF2 is

also found in mast cells and can be released through degranulation[221]. We therefore

performed immunofluorescence staining of paraffin-embedded GIST tissue for FGF2

together with markers for immune cells to determine the source of FGF2 (Figure 2.1.16).

Co-staining of FGF2 and CD45, a marker of all myeloid lineage immune cells, revealed

overlapping signal in samples from imatinib pre-treated samples, but not in resistant

samples. Immune cell infiltration and FGF2 staining was minimal in untreated samples.

We next stained for FGF2 together with the neutrophil marker CD15, and observed the

same pattern. In pre-treated samples (example in Figure 2.1.16 A), FGF2 was localized

to tumor-infiltrating neutrophils, while in imatinib resistant samples (example in Figure

2.1.16 B), FGF2 staining was tumor-intrinsic. Although we are not aware of reports of

FGF2 expression in neutrophils, studies show that neutrophils express several FGFRs,

most prominently FGFR2, and respond to FGF2 with chemotaxis, transendothelial

migration, and priming[222]. Therefore, the expression of FGF2 in response to damage

produced by chemotherapy may recruit further FGF2-positive cells to the tumor microenvironment, creating a protective conditions for the cancer cells under attack.

2.1.4 Discussion

Our study describes for the first time a functional cooperation between FGFR3 and KIT in human GIST and analyzes the molecular mechanisms that underlie this cooperation. The findings provide insight into the protective potential of FGF signaling in GIST and into the signal transduction pathways that mediate resistance to small-molecule inhibitors of KIT in these tumors. Moreover, this represents a new mechanism of resistance in this setting that can account for GIST patients progressing on imatinib in the absence of a secondary resistance mutation in KIT.

1.1.1.18 MAPK signaling in GIST

Here, we present one of the first accounts of FGF2-mediating resistance to targeted therapy. Recently, activation of FGFR3 and the downstream MEK/ERK pathway was also implicated in resistance to a targeted agent, the B-RAF inhibitor vemurafenib, in melanoma[130]. The protective effect of FGF2 in this setting is mediated by the MAPK pathway and downstream activation of ribosomal protein S6 kinase 2[124], [223]. Similarly, an autocrine signaling loop was identified in NSCLC, where FGFRs and their ligands were coexpressed and provided an alternative pathway to EGFR signaling in cells treated with gefitinib[224]. This correlates well with our finding that MAPK

pathway members are preferentially activated after FGF2 stimulation in the presence of imatinib in GIST T1 cells. Similarly, this pathway remained active in GIST 10R cells during imatinib treatment, and these cells could be resensitized by combined imatinib and MAPK inhibitor treatment. The Raf/MEK/ERK signaling pathway is already recognized as an important driver of cell proliferation, survival, and angiogenesis in GIST, as evidenced by an ongoing phase II multicenter trial of the Raf inhibitor sorafenib in imatinib- and sunitinib-resistant GIST. Selective inhibition of this pathway also inhibited proliferation and induced apoptosis and cell-cycle arrest in patient-derived GIST xenograft lines[225]. Taken together with our observations, this underscores the potential of the Raf/MEK/ERK signaling pathway as potential future targets of molecular therapy in GIST. Shortly after publication of this manuscript, another study demonstrated FGF-mediated reactivation of MAPK signaling as a resistance mechanism in GIST. This study found downregulation of negative regulators of the FGF signal transduction pathway, such as DUSP6 and Sprouty (SPRY) proteins in GIST cells after imatinib treatment. This suggests that low FGF signaling activity is due to high levels of ERK activity in untreated GIST cells, and that inhibition of KIT results in relief of feedback inhibition and increased responsiveness to FGF ligands. The same study demonstrated improved efficacy of imatinib when combined with the FGFR inhibitor BGJ398 in patient-derived mouse xenografts[226].

Interestingly, a recent paper showed that TYK2 is required for the full activation of

ERK1/2 after FGF2 stimulation. JAK/STAT activation has been observed in GIST with

conflicting relevance for cell survival[212], [227] and TYK2 specifically is involved in

mediating FGF-induced drug resistance[228].

1.1.1.19 *Heterogeneous receptor crosstalk*

We propose that, in addition to preferential activation of the MAPK pathway, FGFR3

activation partially restores KIT activity. In the setting of overexpression of both

receptors, we demonstrated an interaction between the two receptors. Although these

data are supportive of a direct interaction between KIT and FGFR3, this is only one

mechanism potentially underlying the crosstalk observed in GIST cells, and other

possibilities such as the involvement of downstream mediators should not be

discarded. Receptor crosstalk and heterodimerization to circumvent targeted therapy

have been explored extensively in the setting of EGFR inhibition. EGFR can interact

with other RTKs such as MET, ERBB2, and IGF-1R. These mechanisms were identified

at the clinical and preclinical level in NSCLC and breast cancer. Overexpression and

activation of EGFR can promote transphosphorylation of MET in lung and epidermal

carcinoma cell lines. Activation of MET occurs in an EGFR-ligand dependent manner in

the setting of EGFR overexpression, or independently of ligand in glioblastomas

expressing a constitutively active EGFR variant. Xenograft models of glioblastoma

require targeting of both EGFR and MET to achieve growth inhibition[229]. The

crosstalk between KIT and FGFR3 we present in this paper involves two hitherto unconnected signaling pathways, which are highly relevant to human cancers. Our findings are consistent with the biology reported for crosstalk in other systems. Although no previous reports exist of transactivation between KIT and FGFR3, there is evidence that FGFRs can crosstalk with other RTKs. For example, the cytoplasmic domains of FGF receptors and EphA4 can interact and transphosphorylate each other[230].

1.1.1.20 Clinical trials of FGFR inhibitors in GIST

In light of the propensity of FGF2 to desensitize GIST cells to the short- and long-term effects of imatinib, we suggest that FGF2 expression in treated tumors provides the basis for the development of resistance. Future studies should determine the mechanism of FGF2 upregulation and examine the dynamics of FGF2 expression with imatinib treatment. This would provide valuable information to identify patient populations who may be at risk of FGF-mediated resistance, either by constitutive overexpression or by sustained upregulation in response to therapy. Our observations are an added incentive to pursue targeted treatment that combines inhibition of KIT with antagonism of protective signaling from autocrine loops or the tumor stroma. This strategy could be especially powerful with screening to identify patients at risk for microenvironment-induced resistance. A current trial evaluates a pan-FGFR inhibitor

BGJ398 in combination with imatinib in untreated advanced GIST (NCT02257541), but no results are available yet.

In summary, we show for the first time that the FGFR3 pathway crosstalks with KIT, and that FGF2 mediates survival and outgrowth of GIST cells during imatinib treatment. We further elucidate the molecular mechanisms of FGF2-mediated drug rescue. Our data suggest that incorporation of FGFR3 inhibitors to combination therapeutic regimens may be beneficial in overcoming clinical resistance to targeted therapies for some patients with GIST.
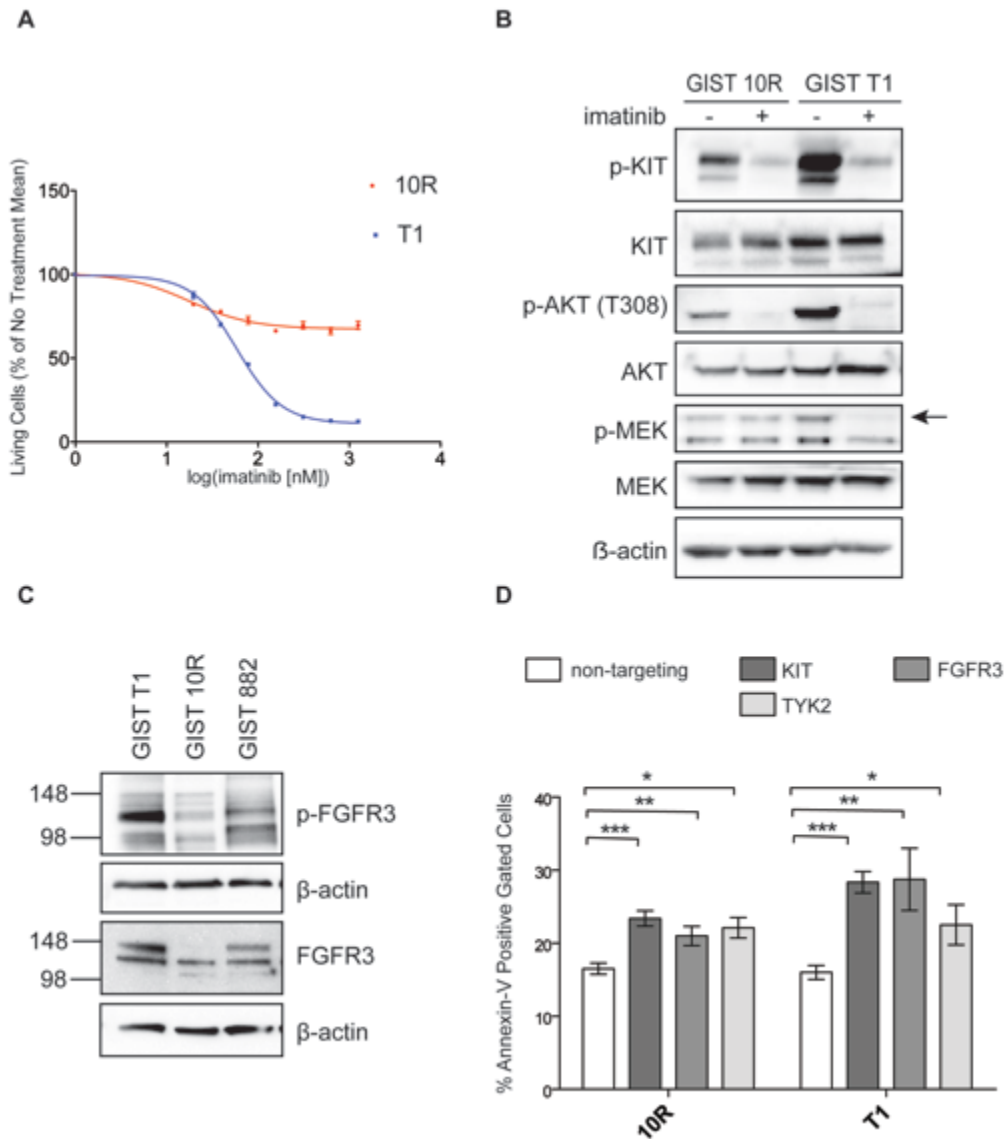
Figure 2.1.1 Response of GIST cell lines to imatinib.
A, GIST T1 and 10R cells were treated with a dose gradient of imatinib for 48h. The percentage of living cells was assessed via MTS assay and normalized to vehicle treated controls. B, GIST T1 and 10R cells were treated with 1uM imatinib for 2h before lysis and analysis of phospho- and total KIT, phospho- and total AKT, and phospho- and total MEK (arrow denotes band corresponding to MEK), and β-actin by immunoblot. C, GIST T1, 10R, and 882 cell lysates were analyzed for phospho- and total FGFR3 and β-actin by immunoblot. D, Target validation comparing the effect of KIT, FGFR3, and TYK2 silencing on apoptosis of GIST cells (as determined by Annexin V staining). The bars represent the mean ± s.e.m. between independent experiments, each containing 3 replicates (n=3). The P values for the t tests are indicated by asterisks (*): *.01 ≤ P < .05; **.001 ≤ P < .01; ***P < .001
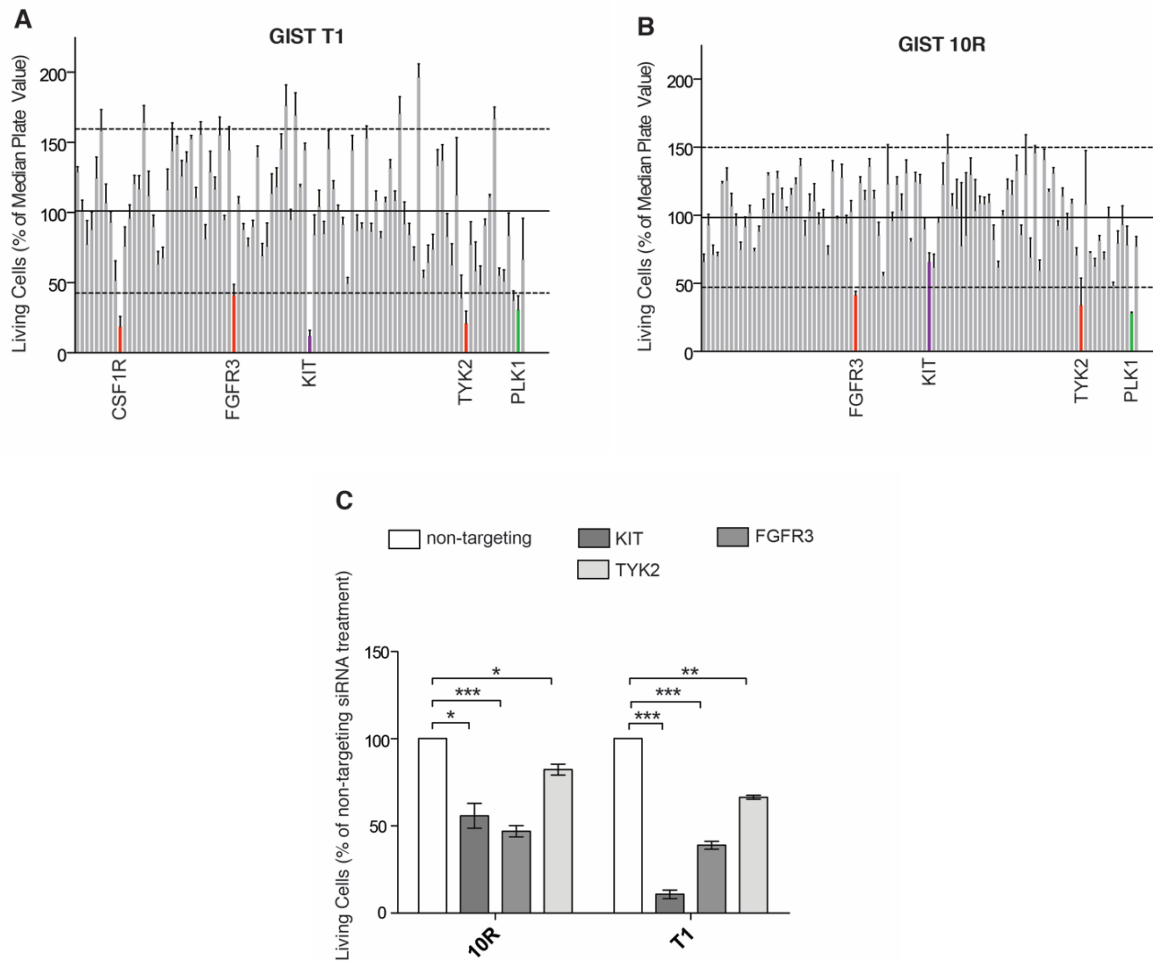
Figure 2.1.2 GIST cell sensitivity to siRNA-mediated knockdown of the receptor tyrosine kinome and target validation.

A, the cell line GIST T1 was transfected with siRNA pools individually targeting each member of the receptor tyrosine kinome. The cell viability was calculated by normalizing the cell proliferation (as determined by the MTS assay) after 96 hours of treatment to the median plate value. B, the imatinib-resistant cell line GIST 10R was treated and analyzed analogous to GIST T1 in A. C, target validation comparing the effect of KIT, FGFR3, and TYK2 silencing on proliferation of GIST cells (as determined by the MTS assay). The bars represent the mean) ± SEM between independent experiments, each containing three replicates (n = 3). The P values for the t tests are indicated by asterisks: 0, 0.01 P < 0.05; 00, 0.001 P < 0.01; 000, P < 0.001. Viability measures for all tested siRNA constructs can be found in Table 2.1.

Table 2.1.1 Raw siRNA screening results.
GIST cells were incubated with 1 µM siRNA from an siRNA library individually targeting each member of the tyrosine kinase family as well as N-RAS, K-RAS, and single and pooled non-specific siRNA controls. Cell viability was determined by MTS assay at day 4 post-transfection. T-tests compare the averages of 3 wells for each individual siRNA to the average value for non-specific siRNA.

GENE	GIST 10R VIABILITY	S.E.	T-TEST	GENE	GIST T1 VIABILITY	S.E.	T-TEST
ABL1	54.199147	12.996323	0.162034	ABL1	110.453552	11.829257	0.587068
ABL2	62.200914	12.237678	0.190794	ABL2	97.145110	12.437642	0.967966
TNK2	87.369299	4.156724	0.540892	TNK2	100.727741	2.171145	0.889110
ALK	52.037912	2.211095	0.010718	ALK	82.919952	4.706872	0.346897
AXL	90.946715	1.798207	0.525923	AXL	102.174796	25.947564	0.851313
BLK	90.141223	3.454169	0.439850	BLK	167.632220	3.423164	0.053868
BMX	119.353239	4.540757	0.152575	BMX	174.387538	3.212982	0.043234
BTK	113.438469	2.775573	0.045129	BTK	96.646326	3.163089	0.916928
TP53RK	93.257324	1.114245	0.764280	TP53RK	35.131096	4.804994	0.035489
CSF1R	62.334844	5.494367	0.007790	CSF1R	23.937780	11.499719	0.010326
CSK	118.222388	1.085112	0.090043	CSK	158.195685	19.078867	0.186247
DDR1	116.682557	8.184607	0.280135	DDR1	142.094297	13.023212	0.279711
DDR2	100.059454	11.951745	0.812769	DDR2	131.568374	6.652861	0.168080
STYK1	90.401285	17.424488	0.856320	STYK1	75.370886	1.892725	0.289158
EGFR	157.429200	9.954692	0.062586	EGFR	257.608466	13.468299	0.032898
EPHA1	139.946197	10.395656	0.115205	EPHA1	148.845417	7.485080	0.161668
EPHA2	119.974743	14.564031	0.353199	EPHA2	105.762031	4.034724	0.744152
EPHA3	126.288759	17.951444	0.323482	EPHA3	39.332500	1.393610	0.069196
EPHA4	137.183168	29.193887	0.352185	EPHA4	73.173149	5.262518	0.372080
EPHA7	142.516972	29.444393	0.310072	EPHA7	90.474164	4.612303	0.630510
EPHA8	106.828667	4.581502	0.173874	EPHA8	131.632161	12.071412	0.251641
EPHB1	108.165980	2.209413	0.188878	EPHB1	130.500248	12.475189	0.313115
EPHB2	105.137537	3.596461	0.416885	EPHB2	157.564181	10.013596	0.123606
EPHB3	99.789406	5.082749	0.722497	EPHB3	124.917742	16.020416	0.336466
EPHB4	109.795344	2.518402	0.245625	EPHB4	145.713494	4.505683	0.154396
EPHB6	115.026850	3.280885	0.177811	EPHB6	142.906463	15.843185	0.014243
ERBB2	106.135163	4.953826	0.431698	ERBB2	172.262121	7.143545	0.077920
ERBB3	100.578044	4.880770	0.680460	ERBB3	140.665389	3.699197	0.085379
ERBB4	114.895792	8.284005	0.311456	ERBB4	108.309580	6.304185	0.708674
FER	57.235965	9.240955	0.134266	FER	52.162201	4.364787	0.095711
FES	133.278816	5.017919	0.075132	FES	156.194997	20.836801	0.035150
FGFR1	90.044075	6.713076	0.735708	FGFR1	95.423541	26.511190	0.873680
FGFR2	101.333429	8.062735	0.708997	FGFR2	122.372766	29.581753	0.217999
FGFR3	86.549674	2.615463	0.428955	FGFR3	34.537648	13.763793	0.009256
FGFR4	125.529832	2.848478	0.047160	FGFR4	68.093355	5.456650	0.254662
FGR	78.976423	4.395671	0.210491	FGR	108.350209	17.010871	0.769961
FLT1	95.654887	2.843957	0.960783	FLT1	53.651646	8.972469	0.189826
FLT3	88.391304	9.498601	0.662513	FLT3	93.316677	7.231557	0.854813
FLT4	116.871199	4.004019	0.176532	FLT4	115.182992	11.568292	0.561731
FRK	92.155441	4.089117	0.801659	FRK	76.100305	2.971968	0.300938
FYN	104.818438	1.235911	0.261044	FYN	68.112586	5.141761	0.273340
HCK	108.165777	4.516488	0.138881	HCK	109.314732	4.800838	0.654509
IGF1R	100.554221	5.306317	0.162075	IGF1R	98.985992	5.554429	0.975174
INSR	64.021584	1.201968	0.057011	INSR	144.868148	9.980038	0.221986
ITK	103.708830	2.383008	0.343905	ITK	199.734236	16.030589	0.078729
JAK1	94.983628	5.192484	0.969518	JAK1	42.169731	7.497872	0.052911
JAK2	73.536888	3.044353	0.026453	JAK2	97.154184	4.924543	0.944645
JAK3	66.157225	2.352011	0.021264	JAK3	85.750411	7.848824	0.620913
KDR	68.271820	2.165916	0.026170	KDR	108.585855	11.008884	0.719809
KIT	92.741199	7.428937	0.587842	KIT	18.129921	5.086818	0.021140
LMTK2	98.742223	1.904364	0.524965	LMTK2	57.863749	2.074238	0.167071
LCK	75.273591	1.904015	0.056832	LCK	101.056155	5.178020	0.900947
LTK	106.067989	1.490529	0.168246	LTK	137.360388	24.801004	0.432572
LYN	93.498757	2.227901	0.761311	LYN	198.145928	22.614593	0.125487
MATK	105.158934	2.340570	0.280434	MATK	177.170733	18.568688	0.155803
MERTK	100.460148	5.177563	0.541647	MERTK	142.454267	7.107121	0.160829
MET	91.257588	1.594839	0.595042	MET	72.141860	1.763555	0.271830
MST1R	74.310891	2.861367	0.041723	MST1R	30.954340	2.412070	0.046355
MUSK	87.884908	7.032125	0.393245	MUSK	66.213334	12.454584	0.111088
NTRK1	103.234344	3.239000	0.251910	NTRK1	96.218778	16.460498	0.950502
NTRK2	111.044945	4.123328	0.027249	NTRK2	113.293356	10.887449	0.633806
NTRK3	110.023704	3.253719	0.047057	NTRK3	219.626949	6.817043	0.030228
PDGFRA	86.739476	2.159385	0.201536	PDGFRA	62.025066	6.101944	0.242917
PDGFRB	73.554301	5.015724	0.019729	PDGFRB	62.799583	3.784634	0.184380
PTK2	55.660349	8.456934	0.006245	PTK2	30.727903	5.215381	0.028819
PTK2B	109.138220	3.565278	0.046187	PTK2B	129.734669	10.982739	0.355257
PTK6	111.999473	6.345057	0.155649	PTK6	191.085489	16.669841	0.108800
PTK7	112.844579	1.528331	0.074320	PTK7	135.153848	14.196242	0.329722
PTK9	90.654063	4.684035	0.360044	PTK9	114.690844	9.504497	0.549853
PTK9L	91.474647	4.328550	0.281375	PTK9L	66.453178	5.808730	0.103416
RET	115.977136	1.606418	0.101712	RET	144.938300	4.777253	0.158267
ROR1	108.365476	0.650302	0.156650	ROR1	69.092548	0.859322	0.212192
ROR2	124.122270	5.757140	0.033460	ROR2	224.373183	26.224908	0.099741
ROS1	78.400393	4.901618	0.017629	ROS1	32.303751	3.276480	0.044438
RYK	94.889764	3.294861	0.948155	RYK	66.932054	3.003864	0.163007
SRC	98.794960	3.123227	0.440059	SRC	97.859226	10.766874	0.985874
SYK	99.235681	4.545200	0.597887	SYK	126.926691	10.499579	0.406201
TEC	113.278692	3.982445	0.020172	TEC	199.445502	16.902144	0.085830
TEK	95.807297	5.522499	0.854855	TEK	55.369830	3.146900	0.156007
TIE	96.300050	5.340494	0.520271	TIE	51.336493	4.005220	0.075919
TNK1	93.617962	5.191832	0.891997	TNK1	166.479722	10.410534	0.032861
TXK	84.588545	4.564675	0.042768	TXK	54.735346	19.588455	0.105308
TYK2	86.423205	3.010993	0.437914	TYK2	-20.294042	24.991982	0.080079
TYRO3	114.977496	1.912068	0.108310	TYRO3	93.086854	18.793068	0.107516
YES1	95.115048	4.668640	0.995253	YES1	61.782378	5.867500	0.182767
ZAP70	89.622980	4.965049	0.077949	ZAP70	60.971160	6.968816	0.258249
NRAS	123.412414	1.444071	0.068580	NRAS	117.899285	12.710776	0.570577
KRAS	89.456485	7.161601	0.470955	KRAS	91.554479	2.559433	0.761972
EPHA5	104.470927	5.271862	0.514012	EPHA5	84.864572	10.497174	0.504695
EPHA6	68.493017	1.537585	0.060652	EPHA6	25.642827	5.082676	0.030317
SRMS	92.464597	2.005078	0.780707	SRMS	55.990906	2.131731	0.108127
AATK	125.728877	5.132925	0.009328	AATK	111.012601	8.972097	0.348250
LMTK3	93.939279	7.838877	0.555451	LMTK3	76.213659	22.315567	0.399028
NON-SPECIFIC	95.138311	6.597348	N.A.	NON-SPECIFIC	98.302348	16.932041	N.A.

81

GIST 10R

GIST T1
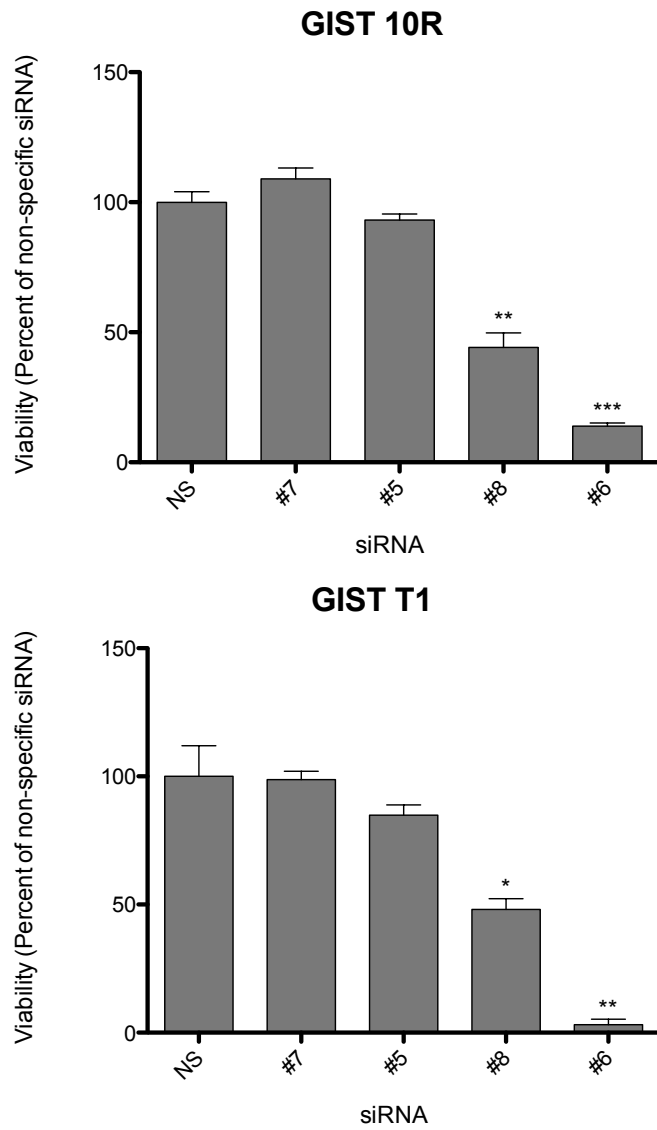
Figure 2.1.3 Testing of individual FGFR3 siRNA duplexes.
GIST cells were transfected with non-specific siRNA or siRNA duplexes targeting three different regions of FGFR3 (#5, 6, 7, 8). After 4 days, cells were subjected to an MTS assay to measure cell viability. Values represent percent mean (normalized to non-specific control wells) ± SEM. (n=3). The P values for the t tests are indicated by asterisks (*): *.01 ≤ P < .05; **.001 ≤ P < .01; ***P < .001
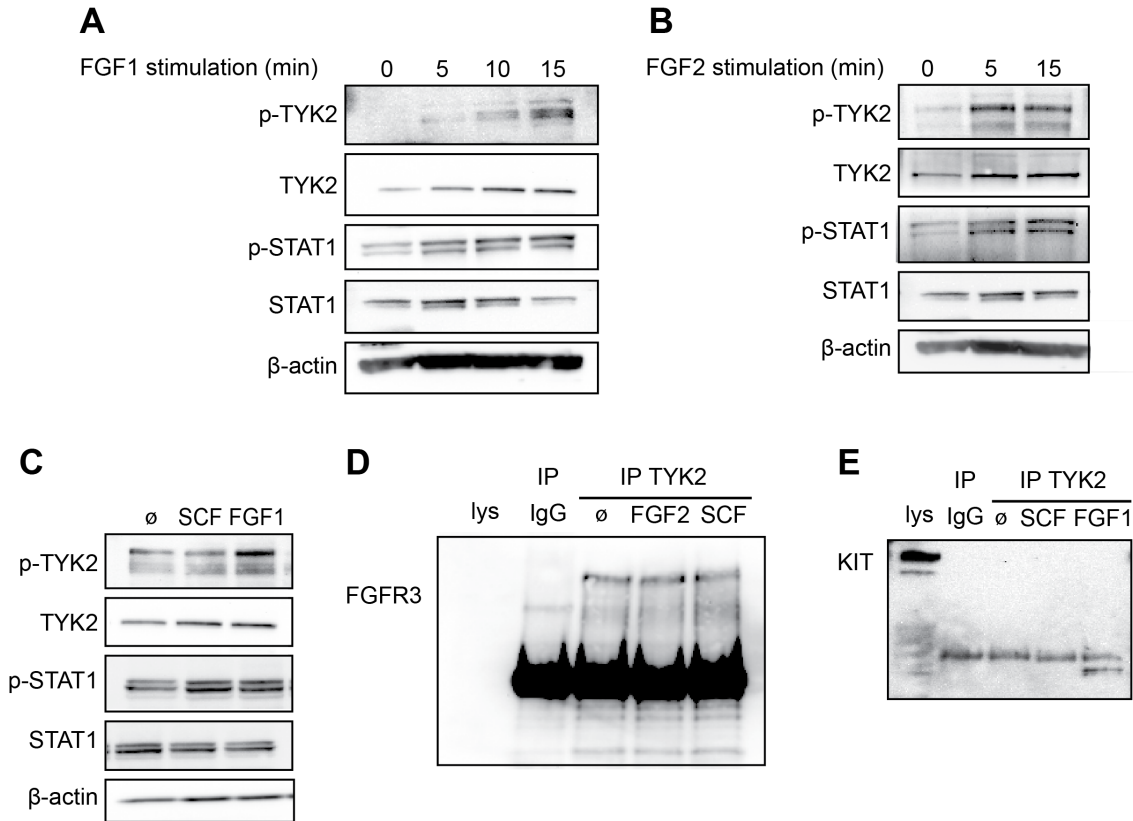
Figure 2.1.4 TYK2 signaling downstream of FGFR3.
A, GIST T1 cells were stimulated with 100 ng/ml FGF1 for 0, 5, 10, or 15 minutes and cell lysates were subjected to immunoblot analysis using antibodies specific for phospho- and total TYK2, phospho- and total STAT1, and β-actin. B, GIST T1 cells were stimulated with 100 ng/ml FGF2 for 0, 5, or 15 minutes and cell lysates were subjected to immunoblot analysis using antibodies specific for phospho- and total TYK2, phospho- and total STAT1, and β-actin. C, GIST T1 cells were stimulated with 100 ng/ml SCF or FGF1 for 15 minutes and cell lysates were subjected to immunoblot analysis using antibodies specific for phospho- and total TYK2, phospho- and total STAT1, and β-actin. D, GIST T1 cells were exposed to 100ng/ml FGF2 or SCF for 15 minutes. Cell lysates were immunoprecipitated with IgG isotype control or antibody against TYK2. Whole cell lysates as well as immunoprecipitates were subjected to immunoblot analysis using an antibody specific for FGFR3. E, GIST T1 cells were exposed to 100ng/ml SCF or FGF1 for 15 minutes. Cell lysates were immunoprecipitated with IgG isotype control or antibody against TYK2. Whole cell lysates as well as immunoprecipitates were subjected to immunoblot analysis using an antibody specific for FGFR3.
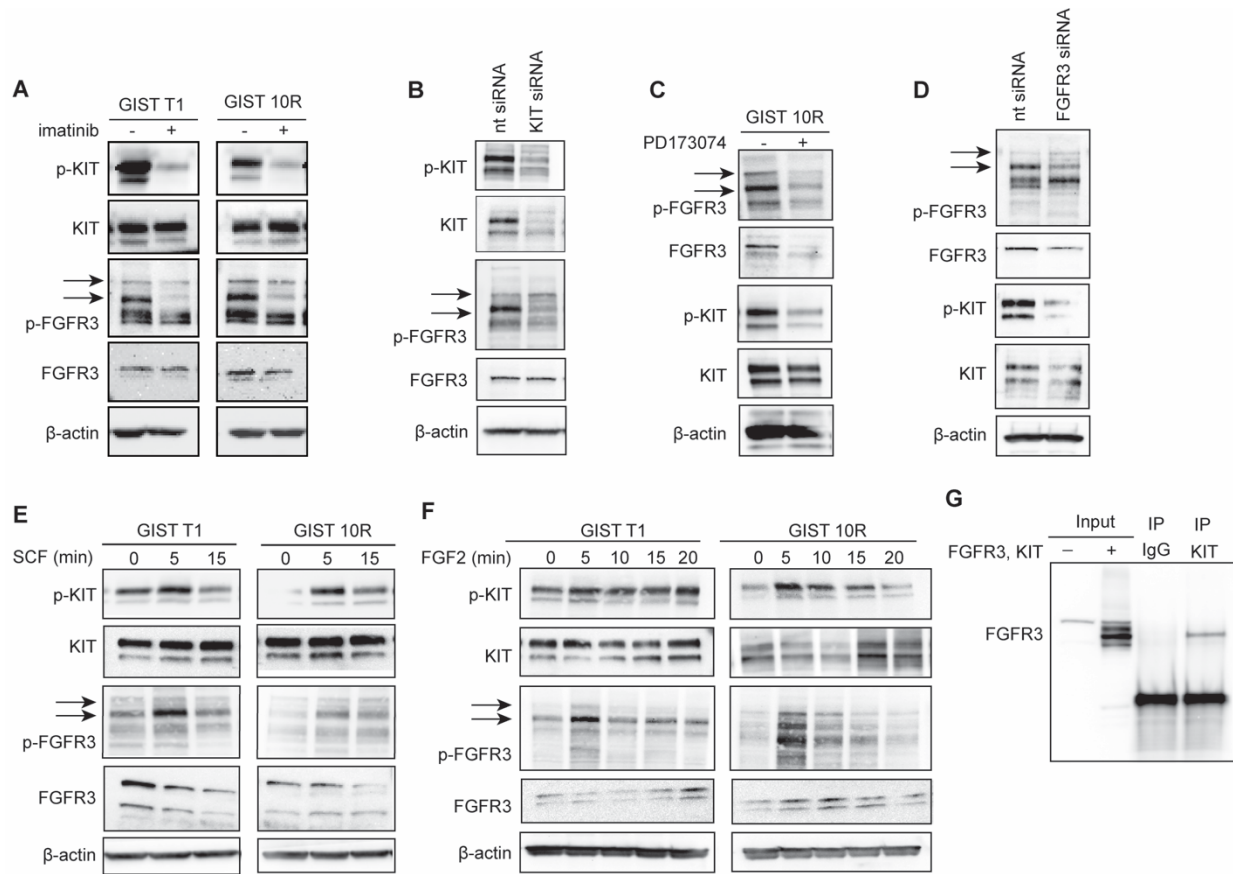
Figure 2.1.5 Crosstalk between KIT-and FGFR3-signaling after inhibition or stimulation.
A, GIST cell lines were treated with 1 mmol/L imatinib (+) or medium (-) for 2 hours. Levels of total and phospho-KIT and FGFR3 as well as b-actin were assessed by immunoblot analysis. Phospho-FGFR3 bands are indicated by arrows. B, GIST cell lines were treated with siRNA against KIT or a nontargeting control pool (nt siRNA) for 96 hours and cell lysates were subjected to immunoblot analysis. C, GIST cell lines were treated with 1 mmol/L of the FGFR-inhibitor PD173074 (+) or media (-) for 2 hours. Levels of total and phospho-KIT and FGFR3 as well as b-actin were assessed by immunoblot analysis. D, GIST cell lines were treated with siRNA against FGFR3 or a nontargeting control pool (nt siRNA) for 96 hours and cell lysates were subjected to immunoblot analysis. E, GIST T1 and 10R cell lines were stimulated with 100 ng/mL SCF for 0, 5, or 15 minutes and cell lysates were subjected to immunoblot analysis. F, GIST T1 and 10R cell lines were stimulated with 100 ng/mL FGF2 for 0, 5, 10, 15, or 20 minutes and cell lysates were subjected to immunoblot analysis. G, HEK 293 cells were transfected with plasmids for the overexpression of KIT and FGFR3. After 48 hours, cell lysates were immunoprecipitated with IgG isotype control or antibody against KIT. Whole-cell lysates as well as immunoprecipitates were subjected to immunoblot analysis using an antibody specific for FGFR3.
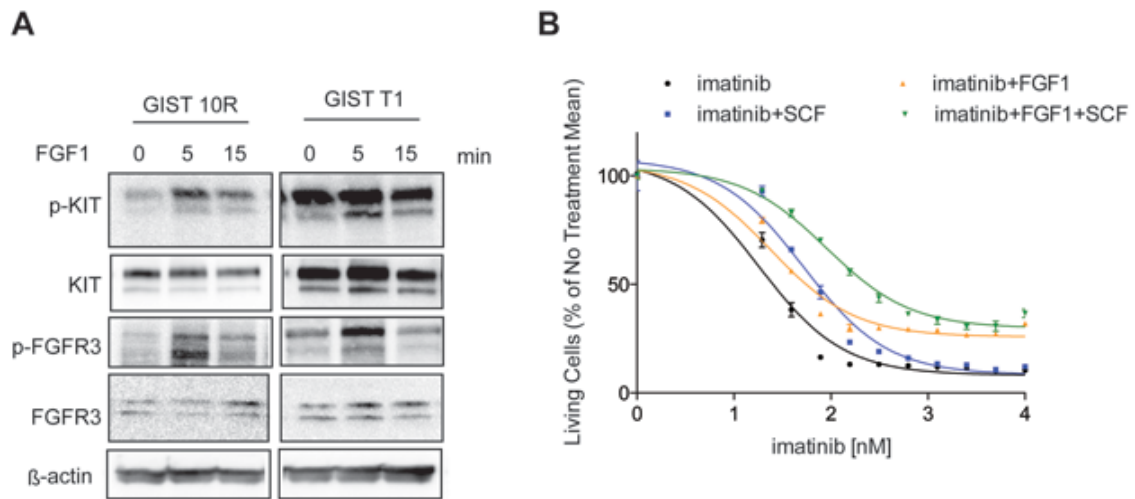
Figure 2.1.6 FGF1 restores KIT phosphorylation and rescues GIST cells from imatinib inhibition. A, GIST T1 cells were treated with media alone or FGF1 (100 ng/ml) for 5 or 15 minutes. Cell lysates were subjected to immunoblot analysis using antibodies specific for total or phospho-KIT and FGFR3 as well as β-actin. B, GIST T1 cells were treated with a dose gradient of imatinib in the presence of 10ng/ml SCF, FGF1, SCF+FGF1, or media (no ligand). After 48 h, viability was assessed by MTS assay and normalized to ligand treatment in the absence of drug. The bars represent the mean ± s.e.m. between replicates (n=3).
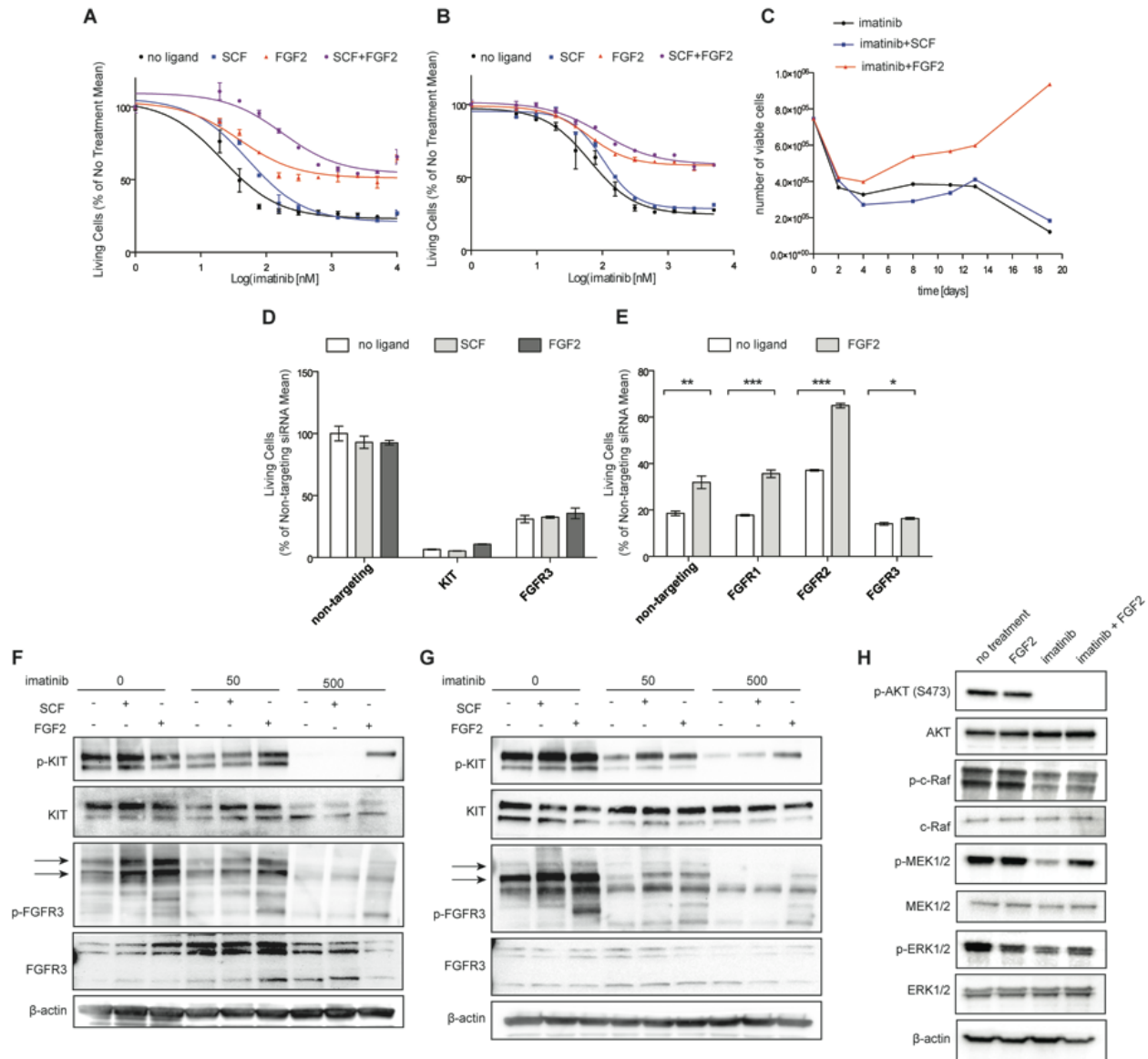
Figure 2.1.7 FGF2 rescues GIST cell lines from KIT inhibition in an FGFR3-dependent manner.
A, GIST T1 cells were treated with a dose gradient of imatinib in the presence of 10 ng/mL SCF, FGF2, SCF+FGF2, or media (no ligand). After 48 hours, viability was assessed by the MTS assay and normalized to ligand treatment in the absence of drug. B, GIST 882 cells were treated and analyzed analogous to GIST T1 in A. C, resistance in the presence of FGF2 leads to outgrowth of GIST T1 cells in a 20-day culture with imatinib. Cells were cultured with 1 mmol/L imatinib and 10 ng/mL ligand. Viable cell counts were obtained by flow cytometry using PI exclusion. Data are representative of three experiments. D, GIST T1 cells were transfected with nontargeting, KIT, or FGFR3 siRNA and cultured for 48 hours before the addition of 10 ng/mL FGF2. After an additional 48 hours, viability was assessed by the MTS assay and normalized to no treatment. E, GIST T1 cells were transfected with siRNA-targeting members FGFR1, FGFR2, or FGFR3 or with nontargeting siRNA, and cultured for 48 hours. Cells were treated with imatinib (1000 nmol/L) in the presence of FGF2 (10 ng/mL) and cell viability was assessed after an additional 48 hours. F,

86

GIST T1 cells were treated with a dose gradient of imatinib for 2 hours and then stimulated with media alone or media containing SCF (100 ng/mL) or FGF2 (100 ng/mL) for 5 minutes. Cell lysates were subjected to immunoblot analysis. G, GIST 10R cells were treated with a dose gradient of imatinib for 2 hours and then stimulated with media alone or media containing SCF (100 ng/mL) or FGF2 (100 ng/mL) for 5 minutes. Cell lysates were subjected to immunoblot analysis. Phospho-FGFR3 bands are indicated by arrows. H, GIST T1 cells were treated with imatinib for 24 hours, and stimulated with FGF2 (100 ng/mL) for 5 minutes. Phosphorylation was assessed using antibodies specific for total and phospho AKT, MEK1/2, ERK1/2, and b-actin. The bars represent the mean ± SEM between replicates (n 1⁄4 3). The P values for the t tests are indicated by asterisks: 0, 0.01 P < 0.05; 00, 0.001 P < 0.01; 000, P < 0.001.
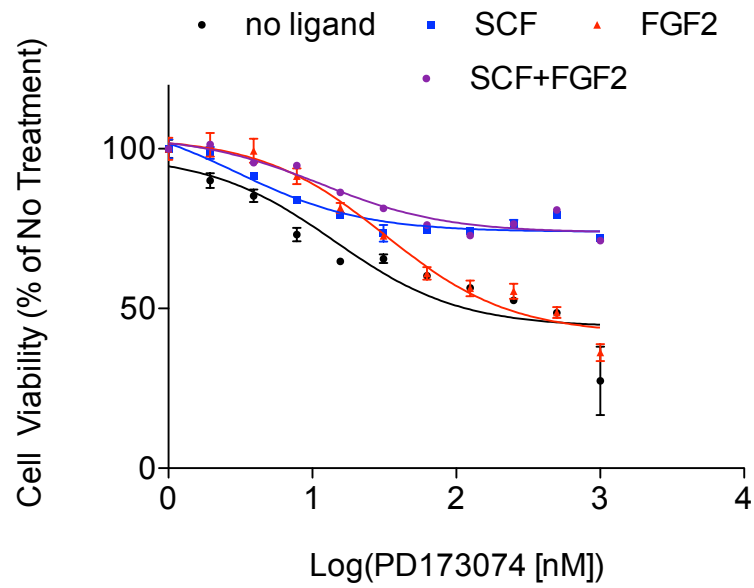
Figure 2.1.8 SCF rescues GIST cells from FGFR inhibition.
GIST T1 cells were treated with a dose gradient of PD173074 in the presence of 10ng/ml SCF, FGF2, SCF+FGF2, or media (no ligand). After 48 h, viability was assessed by MTS assay and normalized to ligand treat ment in the absence of drug. The bars represent the mean ± SEM between replicates (n=3).
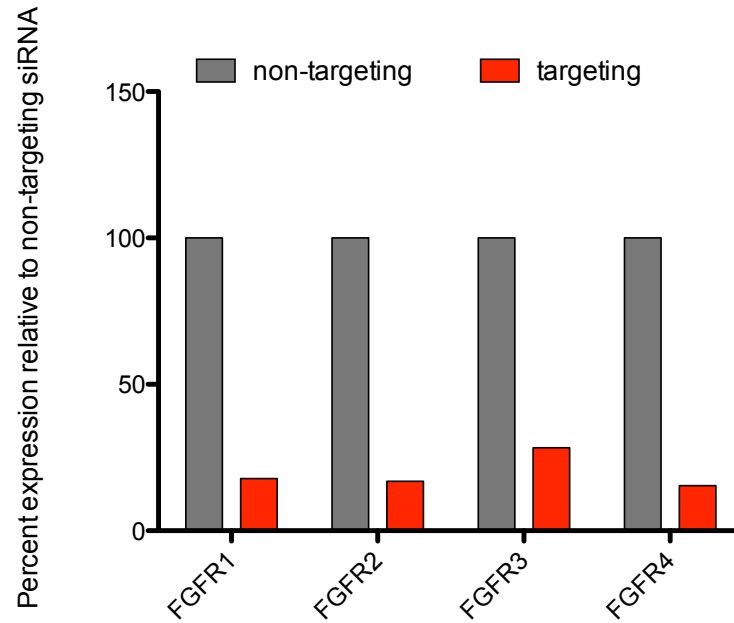
Figure 2.1.9 FGFR expression levels after siRNA knockdown.
GIST cells were transfected with non-targeting or FGFR siRNA and cultured for 48 h. RNA expression level was quantified by real time RT-PCR.
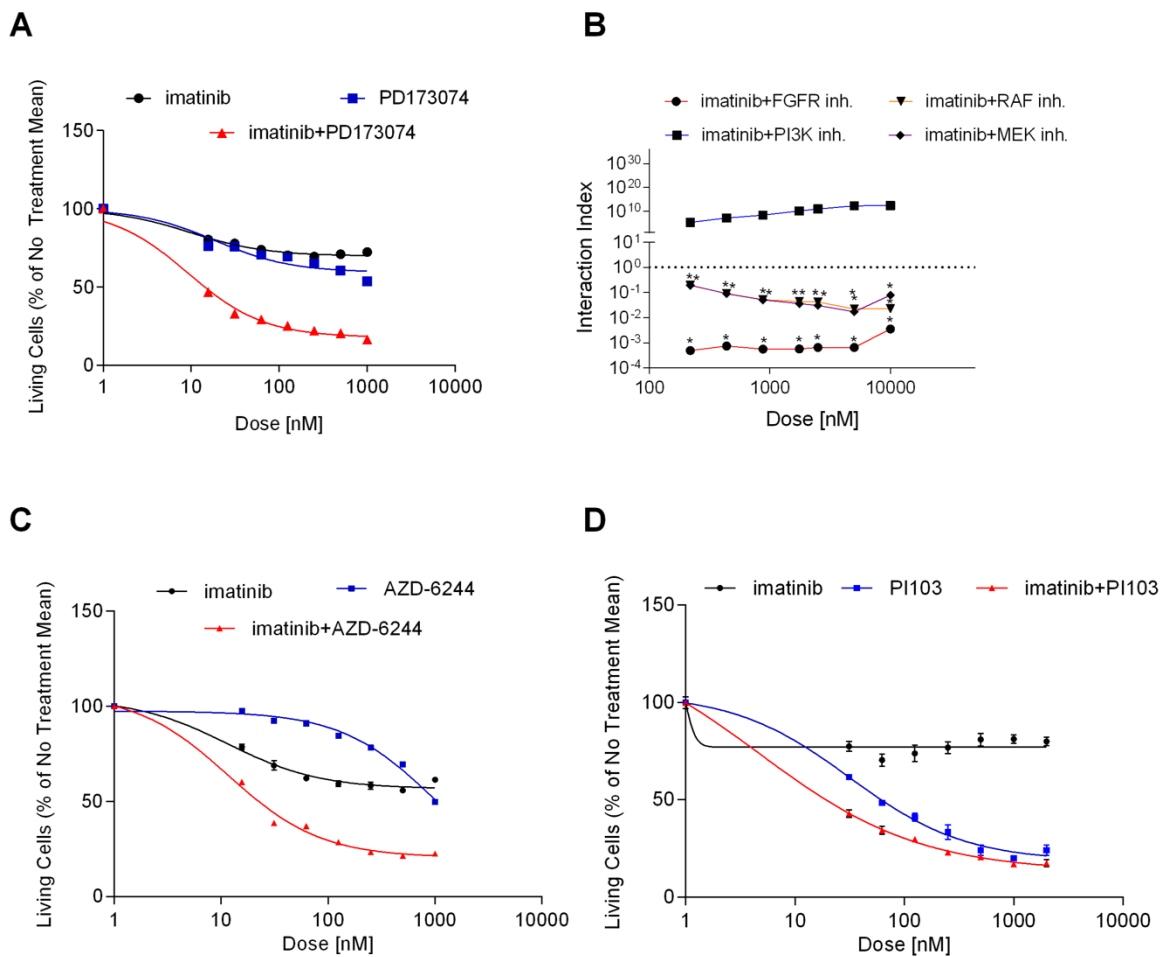
Figure 2.1.10 Combination of FGFR inhibitor or MAPK pathway inhibitors with imatinib restores sensitivity in GIST 10R cells.

A, GIST 10R cells were treated with combinations of imatinib with PD173074 (FGFR inhibitor; 1:1 ratio). Cells were cultured in drug dilutions for 48 hours and viability was quantified by the MTS assay. B, combination indices were calculated for each concentration point of each drug curve. Asterisks mark combinations that show significant synergy (upper limit of interaction index below 1). C, GIST 10R cells were treated with combinations of imatinib with AZD-6244 (MEK inhibitor; 1:1 ratio). Cells were cultured in drug dilutions for 48 hours and viability was quantified by the MTS assay. D, GIST 10R cells were treated with combinations of imatinib with PI103 (PI3K inhibitor; 1:10 ratio). Cells were cultured in drug dilutions for 48 hours and viability was quantified by the MTS assay.
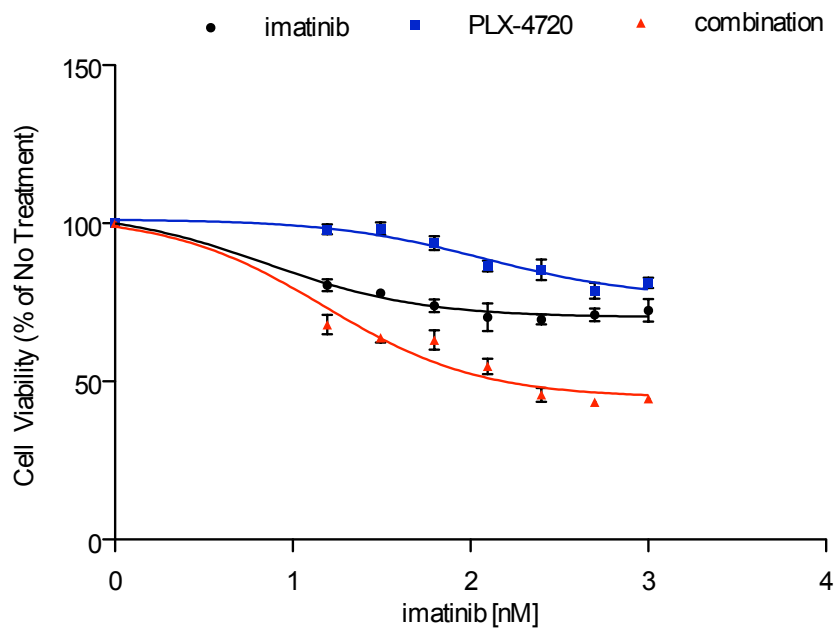
Figure 2.1.11 Combination of B-Raf inhibitor with imatinib.
GIST 10R cells were treated with combinations of imatinib with PLX-4720 (B-Raf inhibitor; 1:1 ratio). Cells were cultured in drug dilutions for 48 h and viability was quantified by MTS assay. The bars represent the mean ± SEM between replicates (n=3).
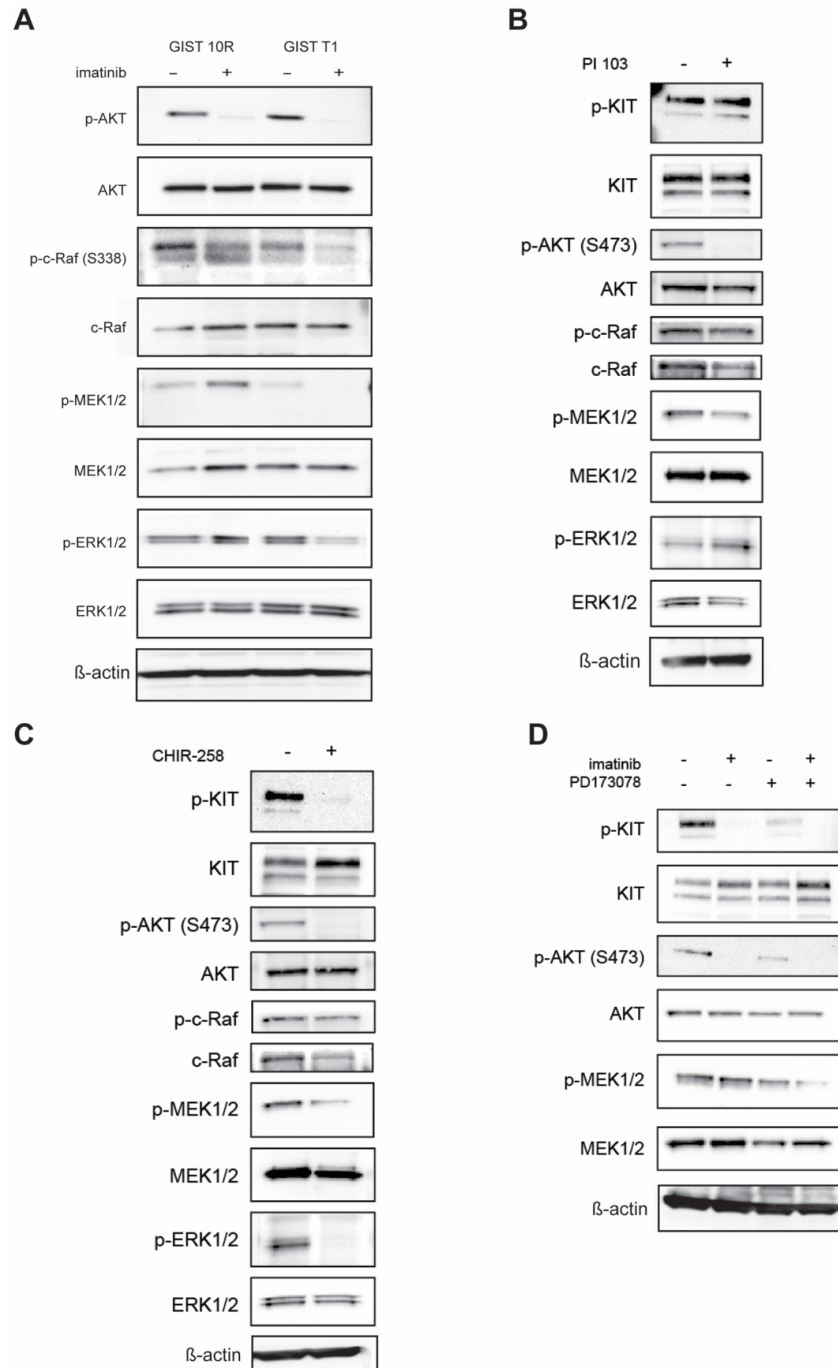
Figure 2.1.12 The MAPK pathway is upregulated downstream of FGFRs in resistant GIST cells in response to imatinib.

A, GIST T1 and GIST 10R cells were treated with imatinib for 2 hours and cell lysates were subjected to immunoblot analysis using antibodies specific for total or phospho-AKT, C-RAF, MEK1/2, ERK1/2, or b-actin. B–D, GIST 10R cells were treated with the PI3K inhibitor PI103 (B), the multikinase inhibitor CHIR-258 for 2 hours and cell lysates were subjected to immunoblot analysis (C), or a combination of imatinib and PD173074 (D).
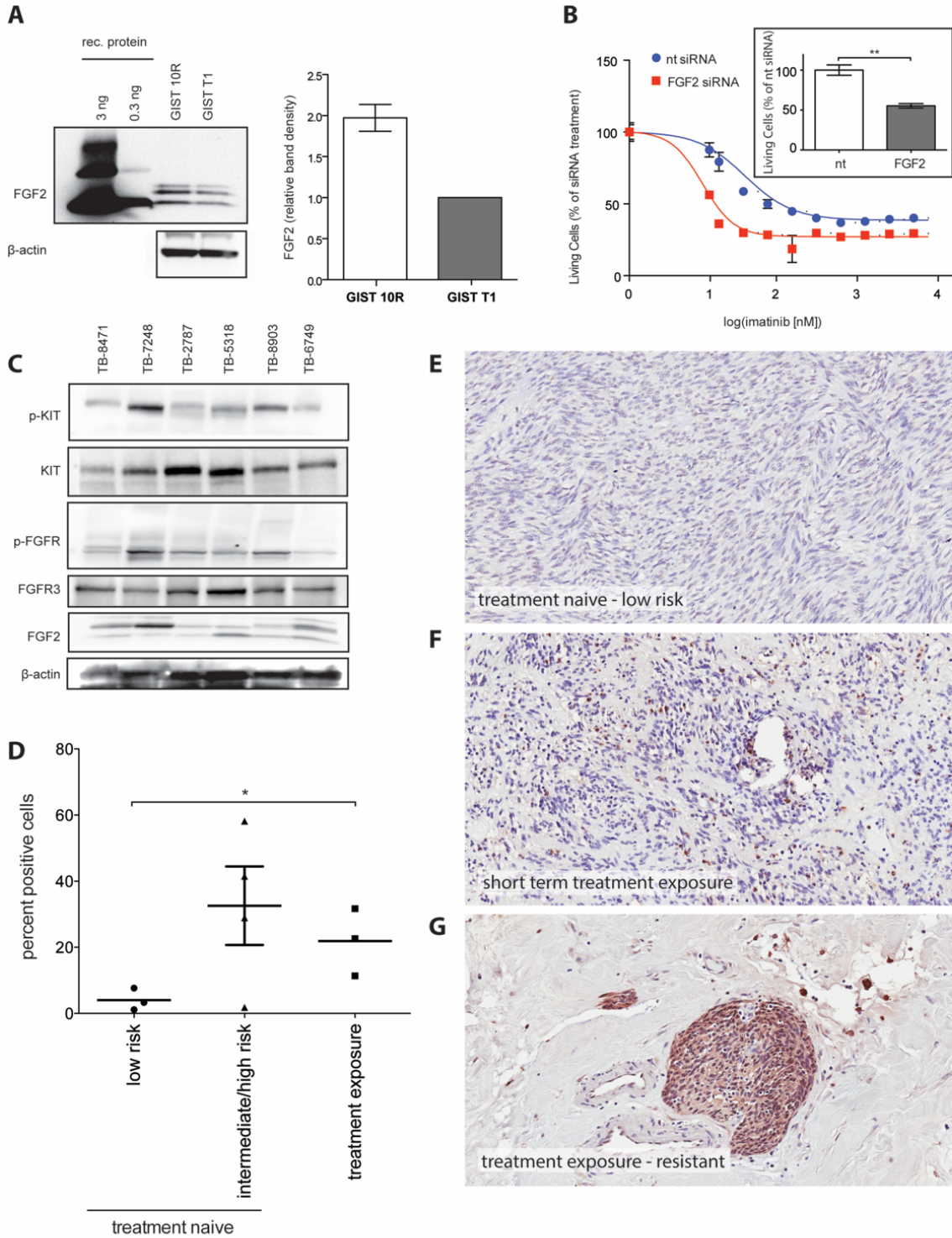
Figure 2.1.13 FGF2 is overexpressed in GIST 10R cells and a pretreated patient sample.
A, cell lysates from untreated GIST 10R and GIST T1 cells were subjected to immunoblot analysis using antibodies specific for FGF2 or b-actin. Recombinant FGF2 is included for comparison.

Sample blot is shown. FGF levels on immunoblot analyses were quantified as bioluminescence units relative to actin and normalized to levels in GIST T1 cells for comparison. B, GIST 10R cells were transfected with nontargeting or FGF2 siRNA and cultured for 48 hours. An imatinib gradient was added to cells and viability was assessed after another 48 hours. For comparison, viability was normalized to the effect of the respective siRNA alone. The effect of siRNA alone on viable cell number is shown in the inset. The bars represent the mean ± SEM between replicates (n = 3). GIST 10R cells were transfected with nontargeting or FGF2 siRNA and cultured for 96 hours. Viability was determined by the MTS assay. The P value is indicated: 00, 0.001 P < 0.01. C, frozen GIST tissue samples were prepared for immunoblot analysis and probed with antibodies specific for total and phospho KIT, FGFR, FGF2, or b-actin. D, GIST tumor FFPE samples were subjected to IHC staining for FGF2. Staining was quantified using ImageScope software. 0, 0.01 P < 0.05. E, example of IHC staining for FGF2 on a treatment naive, low-risk tumor sample. F, IHC staining for FGF2 on a tumor sample after short-term exposure to imatinib. G, example of IHC staining for FGF2 on an imatinib exposed, resistant tumor sample.
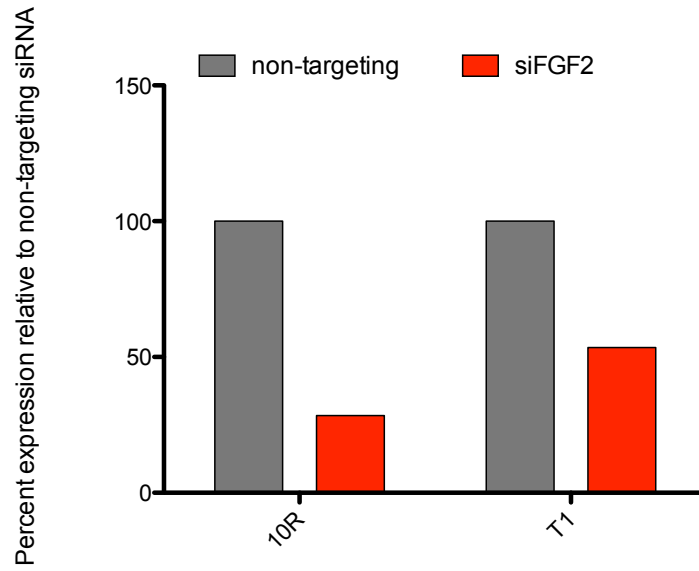
Figure 2.1.14 FGF2 expression levels after siRNA knockdown.
GIST cells were transfected with non-targeting or FGF2 siRNA and cultured for 48 h. RNA expression level was quantified via real time RT-PCR.

Percent Positive Nuclei	58.2544
Intensity Score	1
(3+) Percent Nuclei	2.19327
(2+) Percent Nuclei	16.5222
(1+) Percent Nuclei	39.539
(0+) Percent Nuclei	41.7456
Average Positive Intensity	191.651
Average Negative Intensity	220.948
(3+) Nuclei	3937
(2+) Nuclei	29658
(1+) Nuclei	70974
(0+) Nuclei	74935
Total Nuclei	179504
Average Nuclear RGB Intensity	134.567
Average Nuclear Size (Pixels)	104.286
Average Nuclear Size (um^2)	25.7078
Area of Analysis (Pixels)	71621153.
Area of Analysis (mm^2)	17.65549157362425

Figure 2.1.15 Illustration of patient tissue analysis using the Aperio ScanScope CS Slide Scanner.
A, Whole tumor tissue selected for analysis. B, Results of analysis using the nuclear-9 algorithm.
C, Unmarked tissue. D, Annotated tissue after analysis.

96
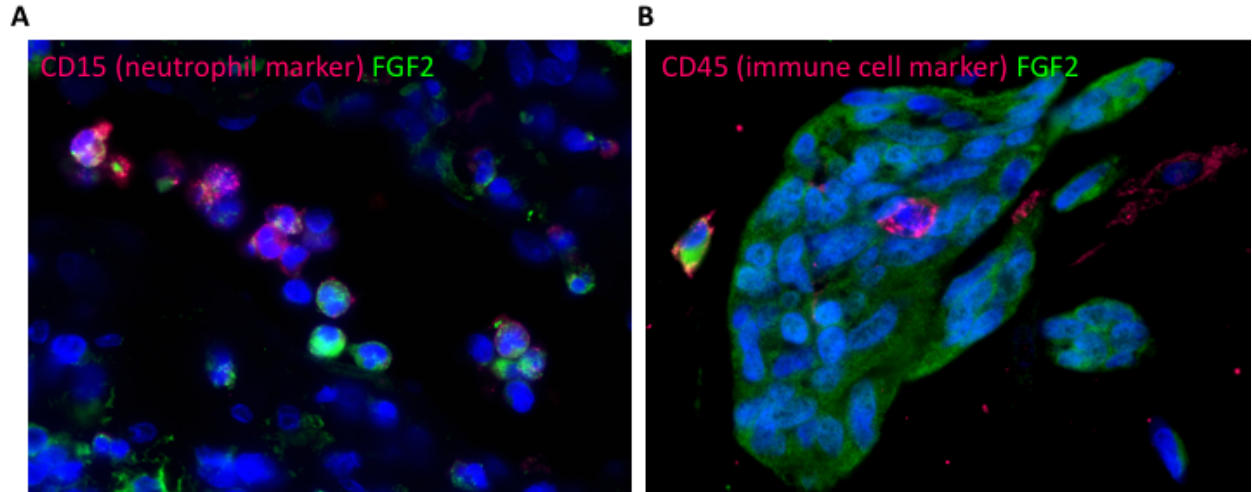
Figure 2.1.16 FGF2 is present in neutrophils in pre-treated GIST samples and in tumor cells in a resistant sample.

A, Example of a pre-treated, imatinib-responsive GIST tumor FFPE sample subjected to immunofluorescence staining for FGF2 shown in green and neutrophil marker CD15 shown in red. B, Example of an imatinib-refractory GIST tumor FFPE sample subjected to immunofluorescence staining for FGF2 shown in green and immune cell marker CD45 shown in red.

2.2   Ponatinib overcomes FGF2-mediated resistance in CML patients without kinase domain mutations.

Elie Traer, **Nathalie Javidi-Sharifi**, Anupriya Agarwal, Jennifer Dunlap, Isabel English,

Jacqueline Martinez, Jeffrey W. Tyner, Melissa Wong, Brian J. Druker

2.2.1 Abstract

Development of resistance to kinase inhibitors remains a clinical challenge. Kinase domain mutations are a common mechanism of resistance in chronic myeloid leukemia (CML), yet the mechanism of resistance in the absence of mutations remains unclear. We tested proteins from the bone marrow microenvironment and found that FGF2 promotes resistance to imatinib in vitro. Fibroblast growth factor 2 (FGF2) was uniquely capable of promoting growth in both short- and long-term assays through the FGF receptor 3/RAS/c-RAF/mitogen-activated protein kinase pathway. Resistance could be overcome with ponatinib, a multikinase inhibitor that targets BCR-ABL and FGF receptor. Clinically, we identified CML patients without kinase domain mutations who were resistant to multiple ABL kinase inhibitors and responded to ponatinib treatment. In comparison to CML patients with kinase domain mutations, these patients had increased FGF2 in their bone marrow when analyzed by immunohistochemistry. Moreover, FGF2 in the marrow decreased concurrently with response to ponatinib, further suggesting that FGF2-mediated resistance is interrupted by FGF receptor inhibition. These results illustrate the clinical importance of ligand-induced resistance to kinase inhibitors and support an approach of developing rational inhibitor combinations to circumvent resistance.

2.2.2 Introduction

1.1.1.21 CML clinical perspective

Chronic myelogenous leukemia (CML) was first described by two pathologists, Rudolf

Virchow and John Hughes Bennett, in 1845[231], [232]. Their reports are seminal in the

field of leukemia as a whole, as they were the first to include a microscopic examination

of their patients' blood. Although Bennett's observation slightly predated Virchow's,

the latter introduced the term "weisses Blut", later amended to "leukhemia". CML

accounts for approximately 20% of all cases of adult leukemia. CML is a neoplastic

disorder of hematopoietic stem cells, where an excess of white blood cells is found in

the bone marrow and the peripheral blood. During the chronic phase of the disease,

cells undergo normal maturation. Without treatment, the disease transitions to an acute

or blast phase within approximately 4 years. In this phase, cells originating from the

malignant progenitor loose the ability to terminally differentiate[233], [234].

1.1.1.22 Oncogenic signaling in CML

The vast majority of CML cases harbors a translocation between chromosomes 9 and

22[235], [236]. This translocation juxtaposes the breakpoint cluster region on

chromosome 22 with the ABL tyrosine kinase from chromosome 9. This results in the

fusion protein BCR-ABL, in which the first exon of ABL is replaced by BCR sequences

usually of a length of 902 or 927 amino acids[237]. BCR-ABL has increased tyrosine

kinase activity compared to normal ABL[238], [239]. The fusion protein is able to transform hematopoietic progenitor cells in culture, confer ligand-independent growth to IL-3-dependent cell lines, and recapitulate the disease phenotype of CML in mice[240], [241].

BCR-ABL kinase activity confers altered adhesion to stromal cells and extracellular matrix[242], increased proliferation, and decreased apoptosis to a hematopoietic stem or progenitor cell, leading to a massive increase in myeloid cells and premature release of myeloid progenitors from the bone marrow[243]. The RAS pathway has been implicated in BCR-ABL mediated proliferation[244], and STAT-5 activation leads to upregulation of the antiapoptotic protein BCL-XL. The AKT pathway may also promote survival by promoting inactivation of the proapoptotic protein BAD[245].

1.1.1.23 TKI therapy in CML

Before the introduction of imatinib, treatments available to patients were limited to hydroxyurea, interferon α (IFN-α) or allogeneic stem cell transplantation. Since only a fraction of patients responded to this type of chemotherapy, and transplant donors were limited, only 20% of patients could be cured using old regimens[233], [234]. For patients in blast crisis, the median survival was two to three months[246], [247]. Imatinib was the first drug designed to inhibit BCR-ABL kinase activity and was initially found to have significant activity in preclinical models[248], [249]. In a phase III

randomized trial comparing imatinib to IFN-α and Ara-C, 97% of patients randomized

to imatinib had a complete hematologic response, although the majority of patients still

had detectable BCR-ABL transcript levels by RT-PCR[250], [251]. Shortly thereafter,

imatinib was established as first-line treatment of CML.

1.1.1.24 Resistance to TKI therapy in CML

Several mechanisms of resistance to imatinib have been described. A useful

classification is to separate cases where BCR-ABL continues to be inhibited from cases

where BCR-ABL maintains or regains kinase activity. The first group includes

decreased drug uptake, increased drug efflux, or upregulation of signaling molecules

such as the Ras-Raf-MEK-ERK and Src family kinase pathways. The second group

includes amplification or overexpression of BCR-ABL or point mutations in the ABL

kinase domain[34]. Point mutations are the most common mechanism of imatinib

resistance in CML. More than 100 different mutations have been described in the ATP-

binding site, the catalytic loop and the activation loop. Four amino acid replacements

account for 60% of point mutations found at relapse: Thr315Ile ('gatekeeper' mutation),

Tyr253Phe, Glu255Lys.Val, and Met351Thr[252].

The second generation BCR-ABL inhibitors dasatinib, nilotinib, and bosutinib have

been approved by the FDA in response to the problem of acquired resistance[246], [253].

Unfortunately, none of them is effective against the gatekeeper mutation. Ponatinib, a

third generation BCR-ABL inhibitor, showed efficacy. Ponatinib was rationally designed to bypass the steric restrictions of the T315I mutation, allowing it to fit in the binding pocket of BCR-ABL, and has shown impressive clinical activity in patients with mutated BCR-ABL kinase domain[254]. Unfortunately, FDA approval was revoked due to adverse effects in phase III trials.

In contrast, a subset of CML patients are resistant to imatinib, dasatinib and nilotinib and do not have mutations of the kinase domain. In these patients, the mechanism of resistance is unclear, and thus there have been no clear strategies to develop novel therapies for these patients. Recent evidence suggests that the bone marrow microenvironment provides a sanctuary for leukemia cells and may provide important survival cues for leukemia cells[255]. The bone marrow microenvironment comprises soluble proteins, extracellular matrix, and specialized cells, including fibroblasts, osteoblasts, and endothelial cells, that promote the survival of hematopoietic cells within specialized niches[256].

We hypothesized that the marrow microenvironment may be involved in mediating resistance to imatinib—particularly in the absence of mutations of the BCR-ABL kinase domain—so we tested cytokines, growth factors, and soluble proteins that are expressed by cells in the bone marrow microenvironment for their ability to protect CML cells from imatinib.

2.2.3 Results

1.1.1.25 FGF2-mediated protection of CML cells

Selected proteins present in the microenvironment (Agarwal et al, manuscript in preparation) were plated at 3 concentrations: 100 ng/mL, 10 ng/mL, and 1 ng/mL with the CML cell line K562 in the presence of 1 μM imatinib. Viability was assessed with an MTS assay and the results were ranked according to greatest viability at 100 ng/mL (Figure 2.2.1 A). The 2 most protective proteins in this initial assay were FGF2 and FGF1. To confirm these findings, we repeated the assay at lower doses comparing some of the most protective proteins (FGF2, FGF1, and IFN-γ) along with proteins previously reported to be important in mediating resistance in CML including interleukin-6[257], G-CSF[258], granulocyte macrophage colony-stimulating factor[259], and placental-derived growth factor (data not shown)[260]. We confirmed that FGF2 was the most protective protein in 48-hour culture (Figure 2.2.1 B).

We reasoned that short-term improvement in viability may be overcome by longer imatinib exposure, so we tested the effects of FGF2 in long-term cell culture. K562 cells were cultured with 1 μM imatinib in media alone or supplemented with 10 ng/mL FGF2. We also tested IFN-γ because it was protective in our short-term assay and G-CSF for comparison. Media, IM, and growth factors were replaced every 2-3 days. After a few weeks, only FGF2-supplemented K562 cells were able to slowly resume growth

and expansion, indicating an acquired imatinib resistance (Figure 2.2.1 C). Notably, this resistance did not occur immediately but on average took about 3-4 weeks. FGF2-mediated growth was highly significant by 2-way analysis of variance, and resistant cells continued to grow indefinitely in FGF2-supplemented culture.

1.1.1.26 *FGFR3 mediates FGF2 protection*

To evaluate the mechanism of FGF2-mediated resistance, we examined the effect of FGFR inhibitors in combination with FGF2 and imatinib. K562 cells were grown in media alone or with 10 ng/mL FGF2 and exposed to increasing gradients of the selective FGFR inhibitor PD173074 or the JAK/FGFR inhibitor AZD1480. Both inhibitors were able to block FGF2-mediated protection from imatinib in a dose-dependent manner (Figure 2.2.2 A-B). There was a modest increase of K562 viability with FGF2 in the absence of imatinib that was blocked by FGFR inhibition, but PD173074 itself had no adverse effect on K562 viability in the absence of FGF2 (Figures 2.2.2 and 2.2.3). Similarly, preincubation of FGF2 with blocking antibodies prevented binding and subsequent activation of FGFR, and thus protection from imatinib (Figure 2.2.2 C).

Because multiple FGFRs are expressed on K562 cells, we used siRNA pools targeting FGFR1-4 to knockdown expression of each receptor and then treated cells with imatinib in the presence or absence of FGF2. FGF2 protected K562 cells from imatinib in the context of FGFR1, FGFR2, and FGFR4 silencing; however, K562 cells treated with

siRNA targeting FGFR3 did not exhibit FGF2-mediated protection, indicating that FGF2 binds FGFR3 to mediate this protective effect (Figure 2.2.2 D; Figure 2.2.5). Further confirmation that FGFR3 was specifically activated and responsible for protection was obtained by using siRNAs targeting the tyrosine kinome[261], [262]. In the presence of FGF2 and imatinib, siRNAs targeting both ABL1 and FGFR3 significantly decreased viability (Figure 2.2.2 E), providing genetic evidence that BCR-ABL and FGFR3 are critical survival pathways in the presence of IM and FGF2. As expected, in the absence of FGF2 and imatinib, siRNA targeting ABL1 was the only siRNA that significantly reduced viability of K562 cells (Figure 2.2.5).

1.1.1.27 Synergy between FGFR and BCR-ABL inhibition

We next turned our attention to the long-term resistant cultures depicted in Figure 2.2.1 C, henceforth denoted as K1-K5. Because the resistant cells were grown in continuous 1 μM imatinib concentration, we wanted to evaluate a range of both IM and PD173074 concentrations to test for synergy of these inhibitors. We created a 64-well matrix with an imatinib gradient on 1 axis overlaid with a PD173074 gradient on the other, and then evaluated viability in triplicate after 48 hours of treatment. Viability of long-term cultures was assessed 48 hours after fresh media, FGF2, and imatinib were replaced. The results are depicted as surface plots (Figure 2.2.3 A-D), and the data are presented again in linear form to highlight the response to each drug individually and in fixed combination (Figure 2.2.3 E-H).

As anticipated, unmanipulated K562 cells respond uniformly to increasing doses of imatinib, and PD173074 had no effect on their growth (Figure 2.2.3 A,E). When K562 cells were cultured with FGF2 and imatinib for 48 hours, there was an expected increase in viability at lower concentrations of imatinib (~1 μM), which was attenuated by FGFR inhibitor (Figure 2.2.3 B,F). Of the long-term cultures, 4 of 5 developed dependence on FGF2 signaling (K1 shown, similar data for K3 and K4 in Figure 2.2.4) and became sensitive to PD173074, yet profoundly insensitive to imatinib, even at high concentrations (Figure 2.2.3 C,G). The combination of imatinib and PD173074 was highly synergistic in these long-term cultures (Table 2.2.1), indicating that both BCR-ABL and FGFR3 are important for survival when FGF2 is present. This was also confirmed genetically with siRNA (Figure 2.2.5). In contrast, a single long-term culture, K2, remained sensitive to imatinib, but only at higher doses than the parental K562 cells (Figure 2.2.3 D,H). K2 was far less sensitive to FGFR inhibition alone but there was synergy between the 2 compounds at higher doses of imatinib (Table 2.2.1).

Ponatinib is a recent ABL inhibitor that was rationally designed to circumvent the gatekeeper T315I mutation,[263] yet ponatinib is also a multikinase inhibitor with activity against FGFR[264], [265]. Therefore, we predicted that ponatinib would be uniquely effective against FGF2-dependent long-term cultures (K1, K3-K5). We compared the ABL inhibitors imatinib, dasatinib, nilotinib, and ponatinib (Figure 2.2.3 I-L) and found that ponatinib was indeed the only drug effective against FGF2-

dependent cultures (K1 shown, K3 and K4 in Figure 2.2.4). Notably, ponatinib only became effective around 10 nM, which is near the reported half maximal inhibitory concentration (IC50) of ponatinib against cell lines with FGFR overexpression[264]. In contrast, the IC50 of ponatinib for BCR-ABL is much lower and comparable to dasatinib[263]. Thus, ponatinib efficacy cannot be rationalized solely by its inhibition of BCR-ABL, which occurs at least 10-fold lower (Figure 2.2.3 I) than the doses of efficacy noted here (between 10 and 100 nM).

1.1.1.28 MAPK signaling in FGF2-mediated imatinib resistance

We then analyzed potential downstream signaling pathways using a phospho-kinase array to determine the mechanism of survival in these long-term cultures. In parental K562 cells, imatinib decreased both phospho-STAT5 and phospho-ERK1/2 signal (Figure 2.2.6 A) consistent with the known regulation of these pathways by BCR-ABL[266]. In FGF2-dependent cultures, phospho-STAT5 remained suppressed—consistent with inhibition of BCR-ABL by imatinib—yet phospho-ERK1/2 was partially restored. This suggested that activation of the mitogen-activated protein kinase pathway was important for survival. We did not identify activation of any other signaling pathways using the phospho array.

FGFR3 and downstream signaling pathways were analyzed by western blot. As expected, K562 cells treated with imatinib have reduced phospho-BCR-ABL, phospho-

STAT5, RAS-GTP, phospho-c-RAF, phospho-MEK, and phospho-ERK (Figure 2.2.6 B, lane 2 compared with lane 1). Surprisingly, the addition of FGF2 in short-term culture was able to restore some phosphorylation of BCR-ABL and STAT5. Inhibition by PD173074 reversed this effect (Figure 2.2.6 B, lanes 3 and 4). In contrast, phosphorylation of BCR-ABL and STAT5 were absent in long-term FGF2-dependent culture K1 (Figure 2.2.6 B, lane 5), whereas RAS-GTP and downstream kinases were phosphorylated. The amount of total FGFR3 protein was also reduced, consistent with proteolysis and internalization of the FGFR3 receptor after binding by FGF2[267]. Addition of PD173074 specifically inhibited RAS/c-RAF/MEK/ERK, indicating dependence of this pathway on FGF2-FGFR3 stimulation (Figure 2.2.6 B, lane 6 compared with lane 5).

In contrast, in the single K2 culture, there was restoration of phospho-BCR-ABL and downstream phospho-STAT5 signaling despite 1 μM imatinib (Figure 2.2.6 B, lane 7). RAS and downstream pathways were reactivated, but this did not occur downstream of FGFR3 because there was no relation to PD173074 treatment (Figure 2.2.6 B, lane 8). Because KD mutations are a well-described mechanism of resistance in CML[34], [268], we sequenced the ABL KD but found no mutations in K2 or any of the long-term cultures (data not shown). We also sequenced the FGFR3 receptor and found no activating mutations to explain the development of resistance. Of note, the total amount of BCR-ABL protein also increased in K2, yet messenger RNA levels did not

dramatically increase in these cells by quantitative polymerase chain reaction (data not shown).

1.1.1.29 FGF2 in bone marrow biopsies of CML patients with TKI resistant disease

Ponatinib was recently evaluated in a phase I clinical trial and found to be surprisingly effective in patients without KD mutations[254]. We suspected that if FGF2 promoted resistance in these patients, it would be relatively increased in bone marrow samples compared with ponatinib-responsive patients with KD mutations. We collected available bone marrow biopsies from patients on the ponatinib clinical trial at our institution and evaluated FGF2 expression by immunohistochemistry (IHC). Most patients were previously treated with multiple ABL inhibitors and the majority responded to ponatinib treatment, with the exception of 1 patient who only had a transient response to ponatinib and is presented separately (Table 2.2.2). Bone marrow samples from patients undergoing joint replacement surgery were used as normal controls. The FGF2 staining was quantified using Aperio ImageScope software (Figure 2.2.9).

Consistent with previous reports, we found that FGF2 in normal marrow is expressed primarily in the supportive marrow stromal cells (Figure 2.2.8)[269], [270]. Bone marrow samples from CML patients at diagnosis had a modest but statistically significant increase in FGF2 staining compared with normal controls (Figure 2.2.8 D). Ponatinib-

responsive patients without KD mutations had increased FGF2 in their marrow compared with patients with mutations (P = .033). Qualitatively, FGF2 was increased in supportive stromal cells, but also present in hematopoietic progenitors (arrows, Figure 2.2.8 B). The presence of FGF2 in some CD45+ hematopoietic cells was confirmed with immunofluorescence (Figure 2.2.11). Interestingly, ponatinib treatment decreased marrow FGF2 staining concurrently with clinical response to ponatinib (Figure 2.2.8 B-C as representative examples), and FGF2 returned to a predominantly stromal localization, similar to normal controls. This decrease was statistically significant in comparison with ponatinib-responsive patients with KD mutations (Figure 2.2.8 E). To further analyze the protective effects of FGF2 in primary cells, we plated CML CD34+ cells in methocult in the presence of FGF2 and imatinib. We found that at 5 µM imatinib, FGF2 10 ng/mL was able to increase CFU-GM colony number in all samples tested. To normalize for the variable response to imatinib between patient samples, we evaluated the average increase in c[130]olony number promoted by FGF2, which was statistically significant (P = .016).

2.2.4 Discussion

Activation of FGFRs is known to be a driver in numerous malignancies, including FGFR1 fusions in 8p myeloproliferative neoplasms[271], [272], t(4;14) translocation with FGFR3 upregulation in multiple myeloma[273], [274], FGFR3 mutations in bladder carcinoma[275], and most recently FGFR1/FGFR3 fusions in glioblastoma[276].

However, it is becoming more apparent that ligand activation of FGFR is also an important mechanism of resistance to kinase inhibitors. Autocrine secretion of FGF2 and activation of FGFR1 was recently reported to promote resistance to gefitinib in lung cancer cell lines[128], [129], and activation of FGFR3 by either exogenous FGF2 or FGFR3 activating mutations in melanoma cell lines was shown to promote resistance to B-RAF inhibitors. A recent screen tested the ability of secreted ligands to promote resistance to kinase inhibitors in multiple cell lines and found that FGF2, hepatocyte growth factor, and neuregulin 1 were the most "broadly active" ligands[131], defining a class of ligands that can drive resistance to kinase inhibitors.

FGF2 was not just protective in short-term culture, but, more importantly, FGF2 effectively promoted imatinib resistance in long-term culture as well (Figure 2.2.1). The development of imatinib resistance took about 1 month, suggesting that either a small subpopulation of cells was capable of using FGF2 as a growth molecule and/or a genetic/epigenetic event was required to resume growth in the presence of FGF2. Most of the long-term cultures (K1, K3-K5) became dependent on FGF2-FGFR3 signaling, and as a result were very sensitive to PD173074 treatment (Figure 2.2.3) or removal of FGF2 ligand (data not shown). However, a single long-term culture, K2, was able to restore BCR-ABL signaling in the presence of FGF2 and 1 μM imatinib, and had increased BCR-ABL protein (Figure 2.2.6). Of note, the K2 long-term culture was sensitive to FGFR inhibitors at earlier time points during outgrowth (data not shown), suggesting that

FGF2 can also act indirectly as a bridge to reactivation of BCR-ABL, although notably this did not occur through mutation of BCR-ABL itself.

1.1.1.30 FGF2 upregulation in stress hematopoiesis

FGF2 is produced by bone marrow stromal cells (Figure 2.2.8) and plays an active role in hematopoiesis in vitro[155], [156], [277], [278]. FGF2 is thought to be secreted from stromal cells into the extracellular matrix where it binds to proteoglycans and promotes hematopoiesis[279]. We found that FGF2 was significantly increased in the bone marrow of patients without KD mutations who subsequently responded to ponatinib treatment (Figure 2.2.8). Most of the increased FGF2 in these patients was localized in stromal cells and thus it is likely that FGF2 acts in a paracrine manner, similar to other reported models of ligand-induced resistance.42 In support of the paracrine model, we did not find any increased production of FGF2 in long-term resistant K562 cultures. However, by immunofluorescence, there was some detectable FGF2 in some hematopoietic cells themselves (Figure 2.2.8 B; Figure 2.2.11), which could either be internalized FGF2 from adjacent stroma or produced by the cells themselves, so we cannot formally exclude an autocrine mechanism in patients.

The events that trigger increased expression of FGF2 in the marrow are not yet clear, but recent studies suggest a potential mechanism. FGF2 knockout mice were initially described to have a mild phenotype with respect to normal hematopoiesis[280], but

recent studies have identified FGF2-FGFR signaling as critical for stress

hematopoiesis[162], [281], [282]. In stress hematopoiesis, FGF2 stimulates expansion of

both supportive marrow stromal cells and hematopoietic stem/progenitor cells to

regenerate the marrow. There is evidence that stress hematopoiesis is a frequent event

in CML, because up to 35% of CML patients treated with imatinib (and newer agents)

develop transient cytopenias[283]. In contrast, cytopenias are far less prominent in

imatinib-treated patients with gastrointestinal stromal tumors[284], suggesting that this

is not purely a drug effect. We examined FGF2 in the marrow of newly diagnosed CML

patients treated with imatinib and found a highly variable, but consistent increase in

FGF2 from marrow biopsies taken 6-18 months after initiation of imatinib (2.2.10). We

suspect that FGF2 likely decreases in most patients as they return to normal marrow

homeostasis and has no clinical impact. However, we propose that in some patients a

sustained feed-forward FGF2 expression can promote FGF2 expression in stromal cells

in an autocrine manner and survival of CML cells in a paracrine manner (the CML cells

themselves may induce FGF2 expression), eventually leading to overt imatinib

resistance (Figure 2.2.8 G). In this proposed model, the normal regeneration of the

marrow after imatinib treatment is hijacked by CML cells, similar to what has been

described in other malignancies[25]. Ponatinib overcomes FGF2-mediated resistance

and also interrupts the feed-forward FGF2 loop in the stroma, leading to a

normalization of FGF2 expression (Figure 2.2.8 C,E).

1.1.1.31 Combined BCR-ABL and FGFR inhibitors in clinical trials

In the recent phase I and II ponatinib trials, an impressive 62% and 49% of patients without detectable KD mutations achieved a major cytogenetic response.8,9 Taken together with our data, this suggests that FGF2-mediated resistance potentially accounts for a substantial number of resistant patients. Although ponatinib is clinically effective for these patients, the recent discovery of serious arterial thrombotic events in 11.8% of patients[254] prompted the US Food and Drug Administration to suspend sales of ponatinib, and clinical trials were put on hold. The mechanism of increased thrombotic events remains unclear; however, this makes rational combinations of selective kinase inhibitors (such as ABL and FGFR inhibitors) an attractive option to treat patients without T315I mutations and avoid toxicity of multikinase inhibitors.

Our results also provide a strong rationale to define the critical ligand-RTK pathways of resistance in other kinase-driven malignancies. This is of particular clinical relevance in the case of protective ligands such as FGF2 and hepatocyte growth factor, because effective inhibitors[285], [286] are available to interrupt these survival signals, and many more are in development. In comparison with CML, malignancies driven by activated kinases such as FLT3, HER2, B-RAF, and epidermal growth factor receptor tend to have an initial response to kinase inhibitors, but the majority of patients develop resistance[287]-[292]. Compared with CML, mutations of the KD tends to be a less frequent mechanism of resistance in other malignancies, and ligand-RTK pathways are

thus more likely to mediate resistance. Identification of critical ligand-RTK pathways of resistance has the potential to rationally develop combinations of kinase inhibitors that circumvent resistance. This is critical if we are to achieve durable responses, akin to that of CML, in malignancies that routinely develop resistance to kinase inhibitors.
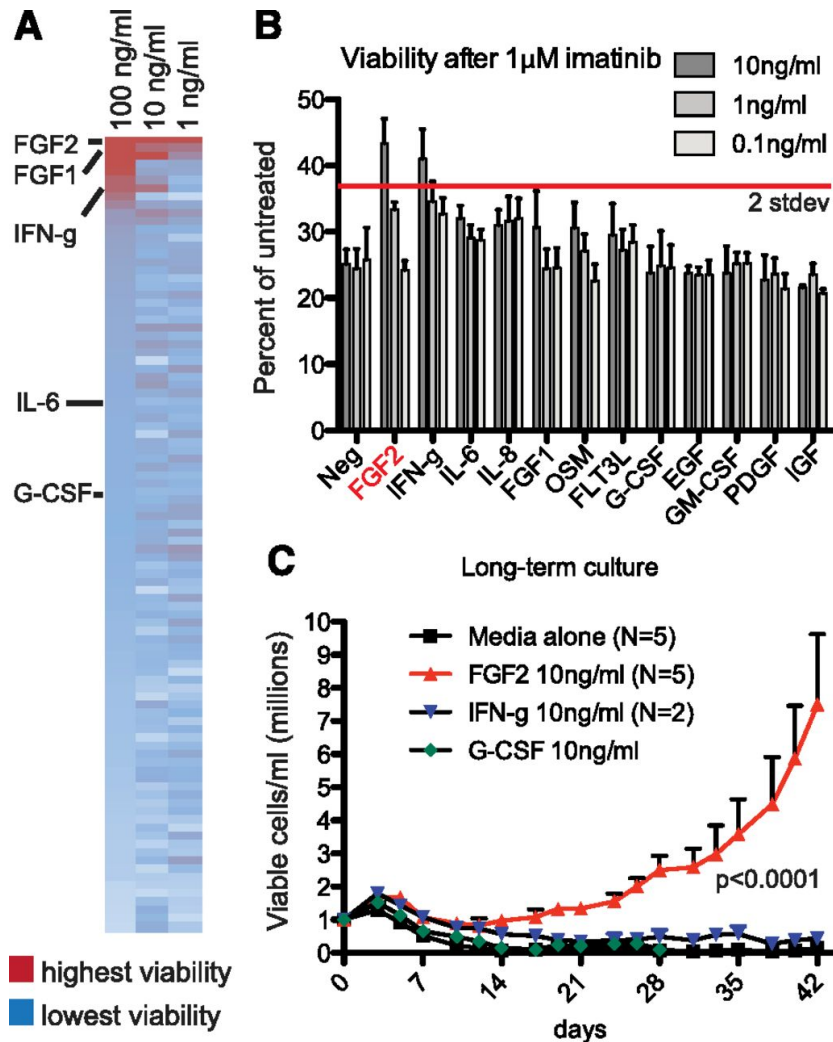
Figure 2.2.1 Microenvironmental screen identifies FGF2 as a protective molecule for K562 cells in the presence of imatinib; FGF2 promotes long-term K562 outgrowth and imatinib resistance. A, K562 cells were added to a 384-well plate containing cytokines, chemokines, growth factors, and small proteins to screen for factors that would promote growth in the presence of 1 μM imatinib. Viability was measured using MTS reagent and the results sorted according to viability at 100 ng/mL concentration. The highest 2% of values are indicated in red and lowest 2% in white, with gradients indicating subsequent highest and lowest values, respectively. B, K562 cells were cultured in 10, 1, and 0.1 ng/mL of recombinant proteins plus 1 μM imatinib. Viability was assessed after 48 hours with MTS reagent and data plotted as percent of the respective untreated control. All wells were plated in triplicate with standard deviation indicated in error bars. The red line represents 2 standard deviations of imatinib-treated K562 cells (11.8%, n = 9). C, K562 cells were cultured in 1 μM imatinib alone and with FGF2, IFN-γ, or G-CSF as indicated. Fresh media, imatinib, and cytokines were replaced every 2-3 days over the indicated time. Viable cells were analyzed using Guava ViaCount. EGF, epidermal growth factor; GM-CSF, granulocyte macrophage colony-stimulating factor; IGF, insulin-like growth factor; IL, interleukin; Neg, negative control; OSM, oncostatin M.

Figure 2.2.2 FGF2 protection of K562 cells is mediated by FGFR3.
K562 cells were cultured in media without and with 10 ng/mL FGF2 and exposed to a titration of FGFR inhibitors. A, PD173074: 25, 50, or 100 nM or B, AZD1480: 0.5, 1, or 2 µM and in combination with 1 µM imatinib as indicated. Viability was measured by MTS assay after 48 hours. Cells not exposed to imatinib were normalized to untreated K562 cells. Imatinib-treated

cells were compared with their respective untreated control (eg, media alone, FGF2, 25 nM PD173074). C, Blocking FGF2 Ab (Millipore bFM-1) at 100 μg/mL, 10 μg/mL, or 1 μg/mL was added to media with or without 10 ng/mL FGF2 and preincubated for 1 hour at 37°C. K562 cells were then added with or without 1 μM imatinib and viability measured by MTS. Viability is presented as the percent of untreated control for each condition. D, K562 cells were electroporated with siRNAs targeting FGFR1, FGFR2, FGFR3, FGFR4, and a nonspecific (NS) control. After 48 hours, the cells were pelleted and resuspended in media with or without FGF2 ± 1 μM imatinib and viability assessed by MTS after 48 hours. At 48 hours, a portion of the cells were lysed and analyzed by Western Blot for FGFR3 to evaluate protein expression (lower panel and supplemental Figure 2 for quantitative polymerase chain reaction). *Indicates $P < .01$ by Student t test. E, K562 cells were electroporated with pools of siRNAs targeting the tyrosine kinome as described previously[261], [262] and incubated with 10 ng/mL FGF2 and 1 μM imatinib. Viability was assessed after 72 hours by MTS; the dark gray horizontal line indicates 2 standard deviations below the mean for all siRNAs. ABL1 and FGFR3 siRNA are denoted as the only 2 siRNA pools that reduced viability below 2 standard deviations.
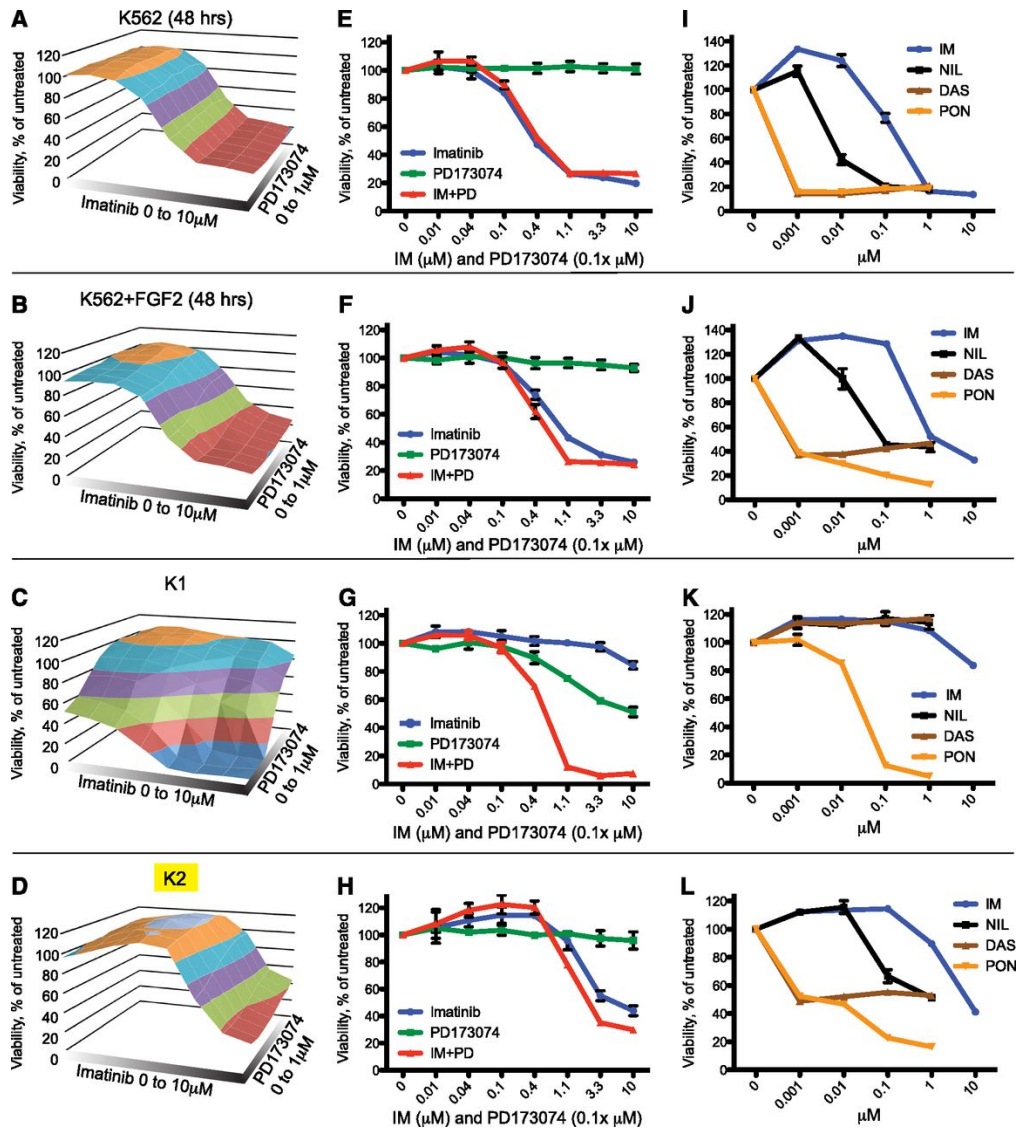
Figure 2.2.3 Long-term imatinib resistance occurs via FGF2-dependent or -independent mechanisms, and FGF2-dependent resistance can be overcome by FGFR inhibition.
A-D, K562 cells with and without 10 ng/mL FGF2 and 2 long-term imatinib-resistant K562 outgrowths in 10 ng/mL FGF2 (Figure 1, denoted as K1 and K2) were exposed to a matrix of an imatinib gradient (0, 0.01, 0.04, 0.1, 0.4, 1.1, 3.3, 10 µM) combined with the FGFR inhibitor PD173074 (PD; 0, 0.001, 0.004, 0.01, 0.04, 0.11, 0.33, 1 µM). Viability was measured after 48 hours and average viability graphed as a surface plots using untreated as reference with colors denoting 20% increments. E-H, Viability from surface plots indicating drug curves to imatinib (IM) alone, PD173074 alone, and combination to highlight synergy. Calculation of the combination index for relevant drug concentrations is included in Table 2.2.1. I-L, K562 cells with and without 10 mg/mL FGF2, K1, and K2 in 10 mg/mL FGF2 were exposed to indicated concentrations of imatinib, dasatinib (DAS), nilotinib (NIL), and ponatinib (PON). Viability was measured after 48 hours. All experiments were done in triplicate with average viability scaled to untreated condition (100%). Error bars represent standard deviation.
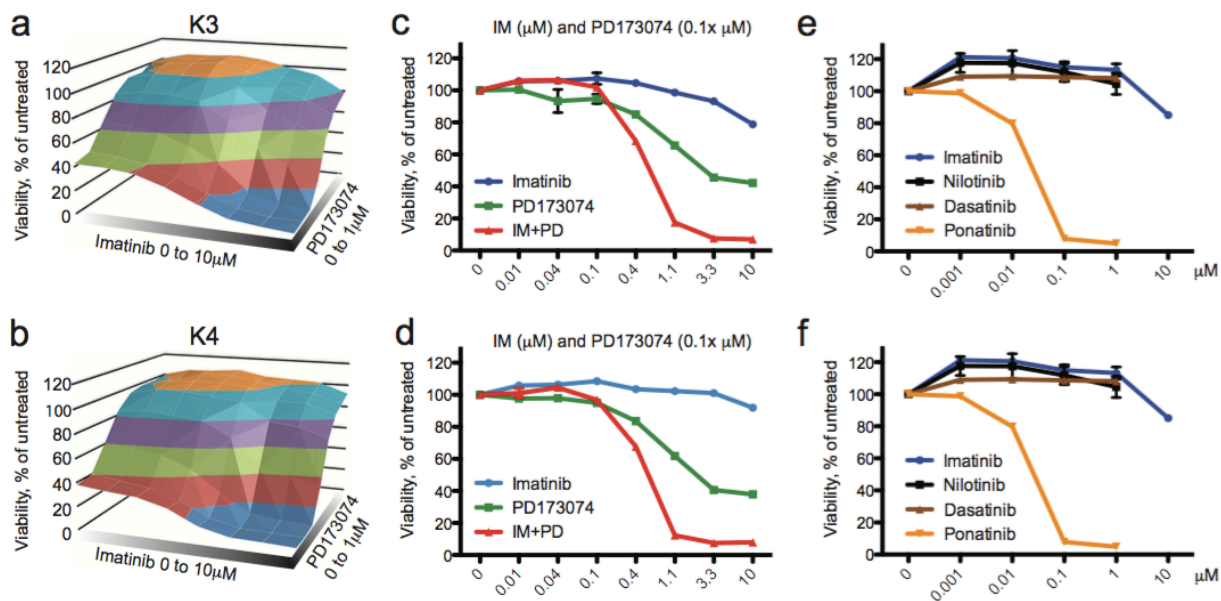
Figure 2.2.4 Long-term imatinib resistance via FGF2-dependent mechanism can be overcome by FGFR inhibition.

A-B, The long-term imatinib-resistant K562 outgrowths in 10ng/ml FGF2 (K3 and K4) were exposed to a matrix of an imatinib gradient (0, 0.01, 0.04, 0.1, 0.4, 1.1, 3.3, 10 μM) combined with the FGFR inhibitor PD173074 (0, 0.001, 0.004, 0.01, 0.04, 0.11, 0.33, 1 μM). Viability was measured after 48 hours and average viability graphed as a surface plots using untreated as reference. C-D,) Viability from surface plots indicating drug curves to imatinib, PD173074, and combination to highlight synergy. e-f) K3 and K4 in 10mg/ml FGF2 were exposed to indicated concentrations of imatinib, dasatinib, nilotinib and ponatinib. Viability was measured after 48 hours. All experiments were done in triplicate with average viability scaled to untreated condition (100%). Error bars represent standard deviation.

Table 2.2.1 Calculation of combination indexes to evaluate synergy.
Viability data as presented in Figure 2.2.3 E-H, representing K562, K562 + 10 ng/ml FGF2, K1 + 10 ng/ml FGF2, and K2 + 10 ng/ml FGF2 treated with fixed combination of Imatinib and PD173074, were analyzed by Chou Talalay method to calculate the combination index. Values less than 1 indicate synergy. The data is color coded with green representing numerical values >1 (no synergy), yellow indicates values from 0.1-1 (intermediate synergy), and orange indicates values <0.1 (highly synergistic). The script for running the R program was kindly provided by James Korkola of the Gray lab.

Imatinib (nM)	PD173074 (nM)	Combination Index			
		K562	K562+FGF2	K1	K2
123	12	429692854.8	0.231603201	0.165316116	25660.0657
370	37	1.03553E+13	0.317336224	0.154081803	1.909163468
1111	111	5.68079E+15	0.393802049	0.04386517	0.175817111
3333	333	1.58963E+16	1.155276731	0.069363995	0.131950487
10000	1000	5.69758E+16	3.36745879	0.254916735	0.325633491
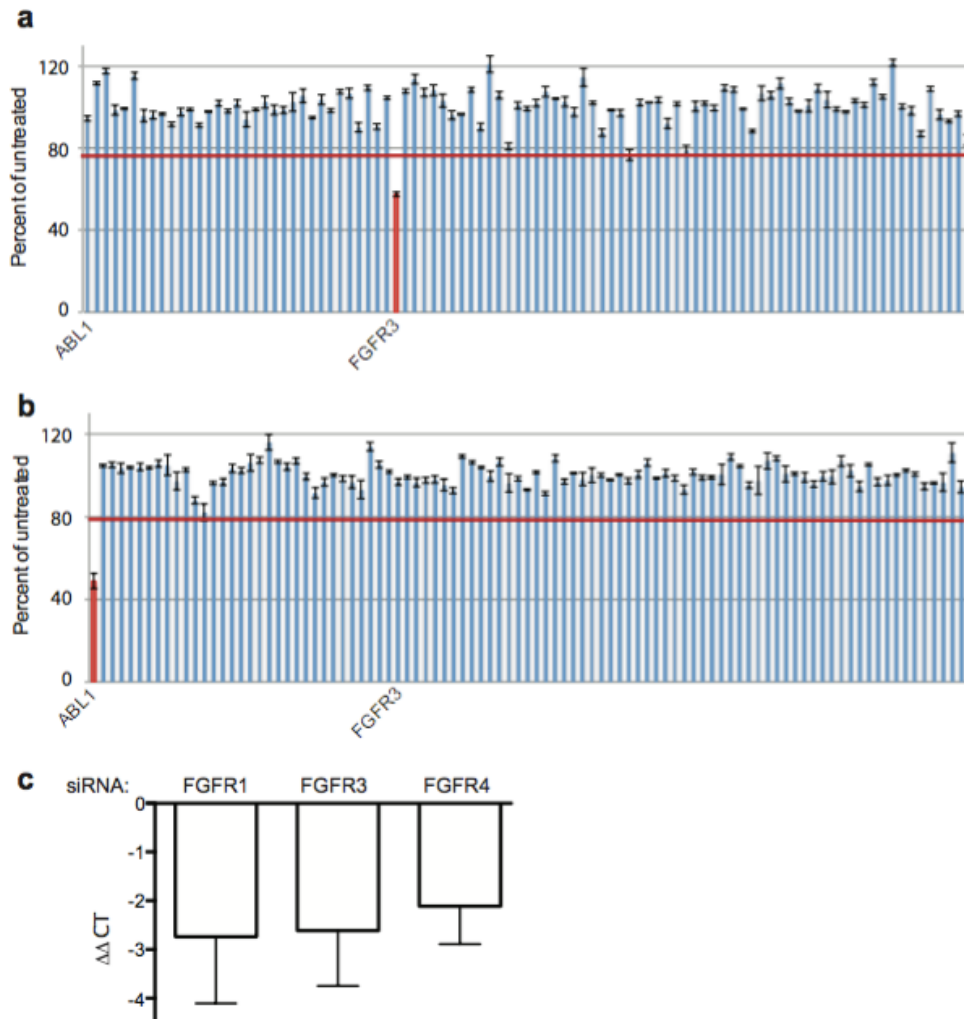
Figure 2.2.5 FGF2 protection of K562 cells is mediated by FGFR3 in long-term cultures.
A, The FGF2-dependent K3 long-term culture was electroporated with pools of siRNAs targeting the tyrosine kinome[261], [262] and incubated with 10 ng/ml FGF2 and 1 µM imatinib. Viability was assessed after 72 hours by MTS. The red line indicates two standard deviations of the mean for all siRNAs. FGFR3 siRNA is denoted in red as the siRNA pools that reduced viability below 2 standard deviations. B, A control electroporation of K562 with pools of siRNAs targeting the tyrosine kinome with K562 cells in media alone. SiRNA targeting BCR- ABL (pooled siRNA against ABL1) reduced viability indicating effective knock-down with siRNA and is indicated in red. Without the selective pressure of imatinib and available FGF2, there was no change in viability with siRNA targeting FGFR3. C, Taqman primers were used to evaluate mRNA of FGFR1-4 in K562 cells electroporated with targeted siRNAs. GusB was used to calculate the ΔCT for each FGFR. FGFR3 was the most abundant FGFR transcript in K562 cells whereas FGFR2 was of such low expression that the data could not be reliably interpreted and was excluded. The ΔΔCT was calculated for FGFR1, 3, and 4 and plotted with standard deviation. A value of 0 indicates no change in expression. Each QPCR reaction was run in triplicate following manufacturers protocol (Life Technologies, Grand Island, NY).
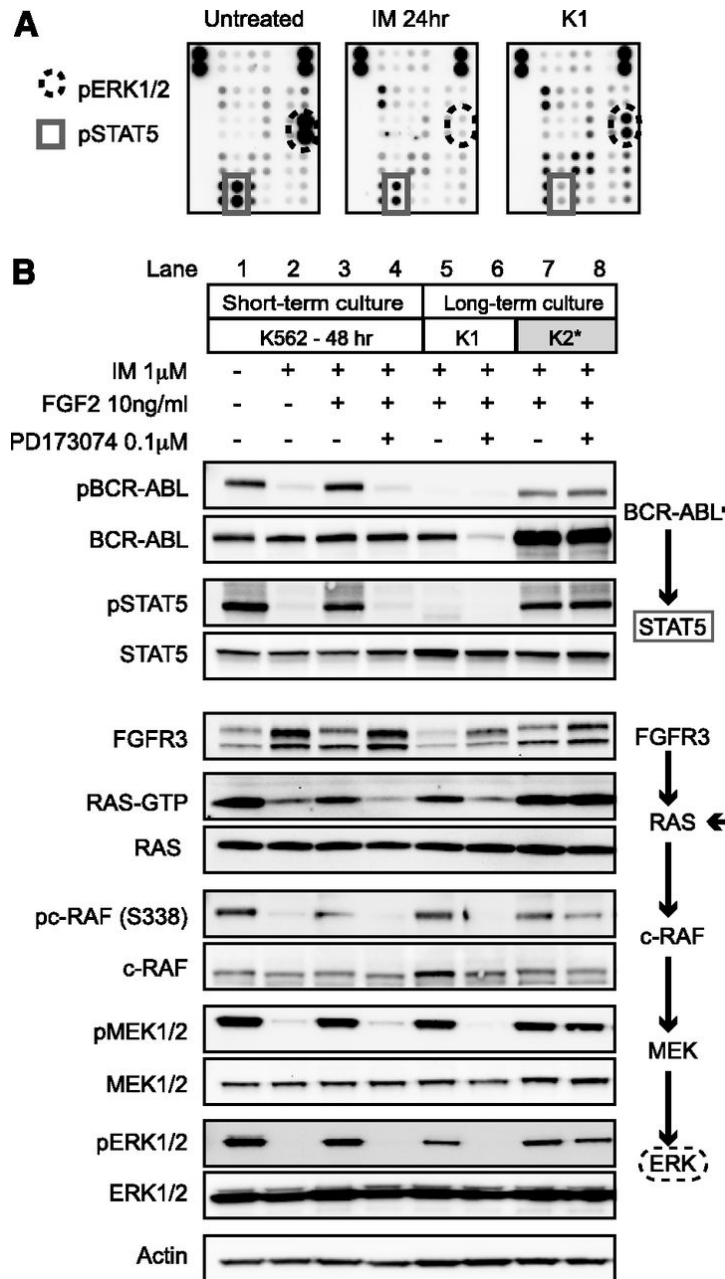
Figure 2.2.6 FGF2-dependent resistance is mediated by activation of FGFR-RAS-RAF-MEK-ERK pathway, whereas FGF2-independent resistance is mediated by reactivation of BCR-ABL.
A, Untreated K562 cells, K562 cells treated for 24 hours with 1 μM imatinib, and K1 cells after 1 month of culture in 10 ng/mL FGF2 and 1 μM imatinib were lysed and used to probe a human phospho-kinase array (Proteome Profiler, RnD). The dots corresponding to pERK1/2 and pSTAT5 are indicated. B, K562 cells were treated for 48 hours in the indicated conditions under short-term culture conditions. The long-term cultured cells were grown continuously in imatinib and FGF2 as described in Figure 1. Cell lysates were collected 48 hours after replacement of media, FGF2, and inhibitor (IM and PD173074). The cells were then lysed as described with western blot analysis as in Methods. RAS-GTP was evaluated at 24 hours using immunoprecipitation.

124
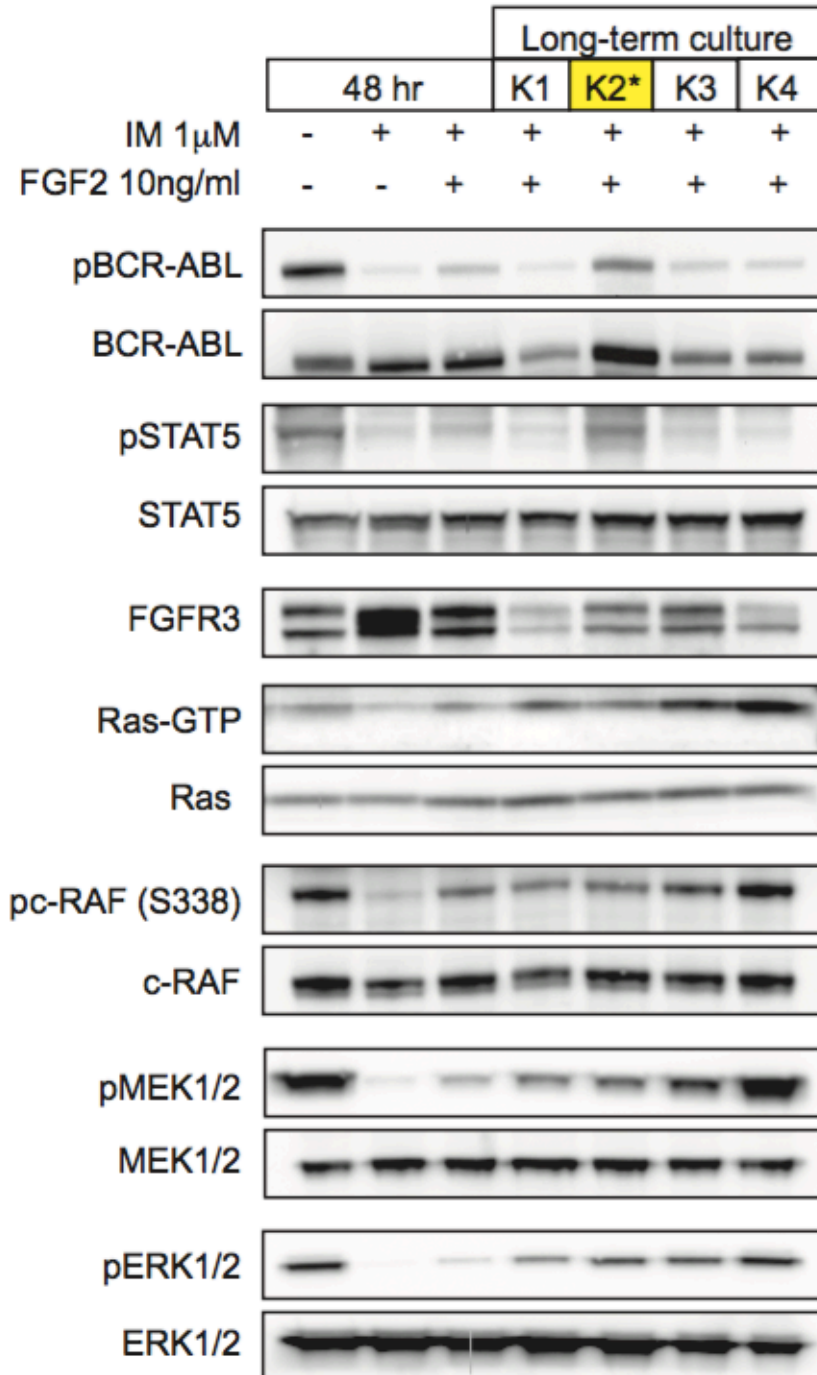
Figure 2.2.7 Western blot of activated pathways in K562 cells and long-term imatinib-resistant cultures.

K562 cells and resistant K1-K4 long-term imatinib-resistant cultures were treated for 48 hours in the indicated conditions. The cells were then lysed as described with Western blot analysis per Materials and Methods. Ras-GTP was evaluated at 24 hours using immune-precipitation.
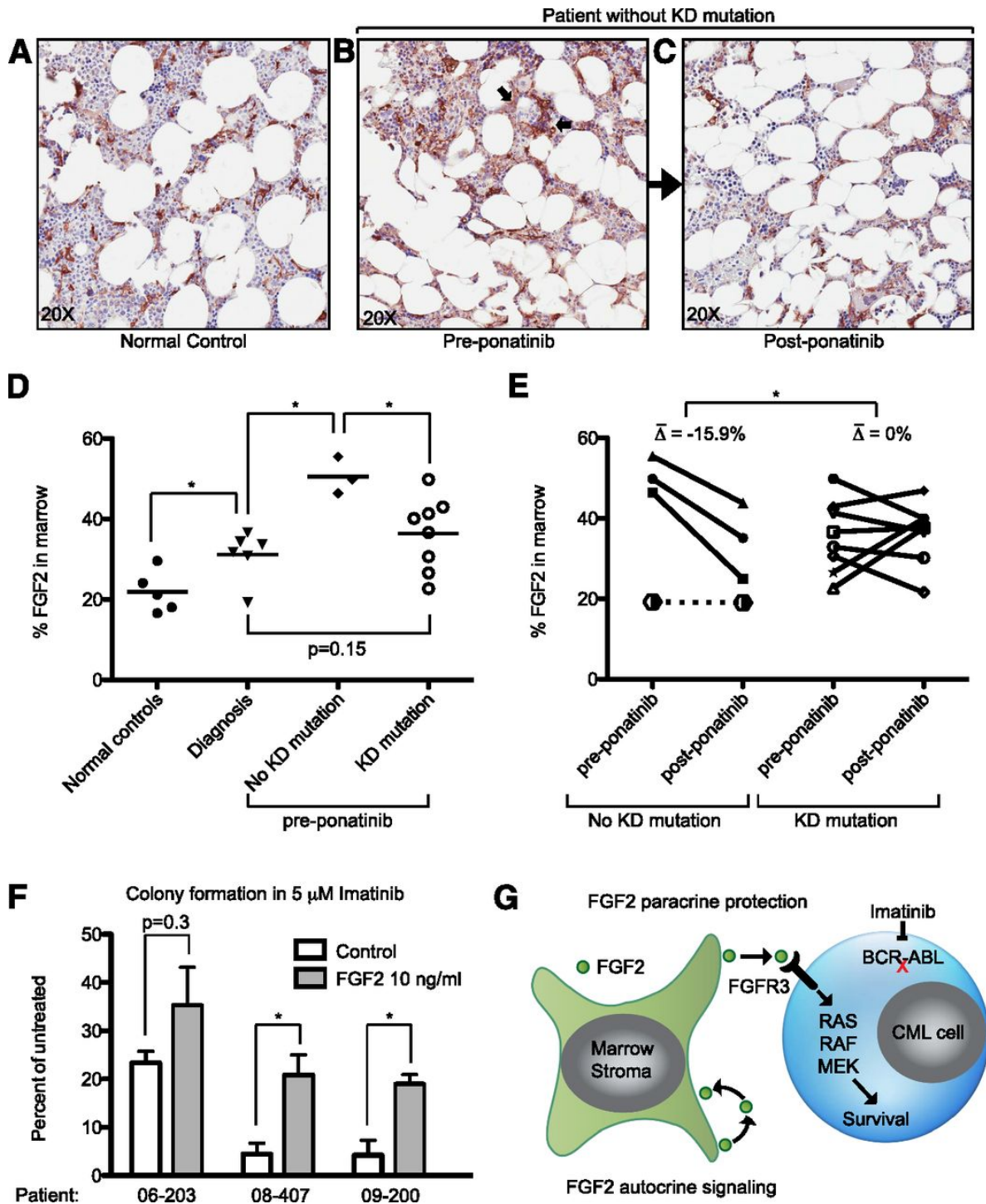
Figure 2.2.8 FGF2 is increased in the bone marrow of patients without KD mutations and decreases with ponatinib treatment.
Bone marrow core biopsies obtained from normal controls (surgical joint replacement patients), CML patients at diagnosis, tyrosine kinase inhibitor resistant patients before ponatinib therapy (pre-ponatinib), and responsive patients post-ponatinib were collected and evaluated for FGF2

by IHC as described in Methods. Representative images of A, normal control, B, pre-ponatinib marrow of a patient without KD mutation, and C, the same patient post-ponatinib. FGF2 is normally expressed in marrow stroma (A); arrows indicate nonstromal areas of increased FGF2 in resistant patients (B). D, IHC images from normal controls, patients at diagnosis, and pre-ponatinib patients who responded to ponatinib (with and without KD mutations) were analyzed with Aperio ImageScope software to quantify FGF2 staining. The line indicates the median value. Statistically significant differences were evaluated using a 2-tailed Student t test. E, Paired IHC analysis of pre- and post-ponatinib bone marrow of patients treated with ponatinib (same as D). Patients without KD mutations had an average decrease of 15.9% in FGF2 staining, whereas patients with KD mutations were more variable. The differences pre- and post-ponatinib were analyzed by the 2-tailed Student t test for significance. A single patient without KD mutations who failed imatinib, dasatinib, nilotinib, and ponatinib is plotted with a dotted line for comparison (see Table 1). F, CD34+ cells from newly diagnosed CML patients were resuspended in methocult H4534 ± FGF2 10 ng/mL and ± 5 µM imatinib. Cells were plated in triplicate, cultured for 14 days, and then CFU-GM colonies were counted. The data are presented as the percent of untreated control (control or FGF2). The differences between control and FGF2 were analyzed by 2-tailed Student t test for significance. *P < .05. G, Model of FGF2 paracrine protection of CML cells based upon data in this article and previous publications regarding FGF2 autocrine/paracrine stromal cell signaling.

Table 2.2.2 Patient characteristics.

Bone marrow biopsies from patients who responded to ponatinib were evaluated both before therapy and after response to ponatinib. A single patient who developed resistance to ponatinib within 6 months of therapy is shown for comparison. The clinical characteristics are listed as well as the quantitation of the FGF2 present in the marrow by Aperio ImageScope software (Figure 2.2.9). BOS, bosutinib; TKI, tyrosine kinase inhibitor.

Age	Gender	KD mutation	Previous TKIs	Prior years of therapy	%FGF2 preponatinib	%FGF2 postponatinib	Δ
56	M	None	IM, DAS	3	49.8	35.1	−14.7
67	M	None	IM, DAS, NIL	2	46.4	24.9	−21.5
31	M	None	IM, DAS	3	55.4	43.8	−11.7
54	M	L248V	IM, DAS, NIL	2	26.6	40.0	13.4
68	M	F317L/F359V	IM, DAS, NIL	2	43.0	46.9	3.9
62	M	F359V/M244V	IM, DAS, NIL, BOS	2	36.6	30.2	−6.5
70	F	F359C	IM, NIL	4	40.1	37.6	−2.5
47	M	T315I	IM, DAS	3	22.7	37.6	15.0
53	M	T315I	IM, DAS	4	41.3	36.8	−4.5
45	M	T315I	IM, DAS	3	30.6	21.6	−9.1
59	F	T315I	IM, DAS	4	49.8	40.0	−9.8
Nonresponder							
37	F	None	IM, DAS, NIL	4	19.2	19	0.2

Table 2.2.3 Bone marrow biopsies were repeatedly stained by IHC and quantitated for FGF2.
Bone marrow core biopsies from selected patient samples representing different analysis groups were evaluated for FGF2 by IHC as described in Methods. The percent FGF2 staining from each run are listed as well as the average and standard deviation. When multiple samples were available for analysis, the average staining was always used.

Patient	Treatment	FGF2 quantitation	Average	Standard Deviation
Normal control		32.7	29.6	2.9
		27.0		
		29.1		
IM responder		33.1	36.1	4.3
		39.1		
No KD mutations	pre-ponatinib	55.6	49.8	8.2
		44.0		
	post-ponatinib	35.3	35.1	0.2
		35.0		
KD mutations	pre-ponatinib	44.7	43.0	2.4
		41.3		
	post-ponatinib	47.3	46.9	0.6
		46.4		
T315I	pre-ponatinib	32.6	30.6	2.8
		28.6		
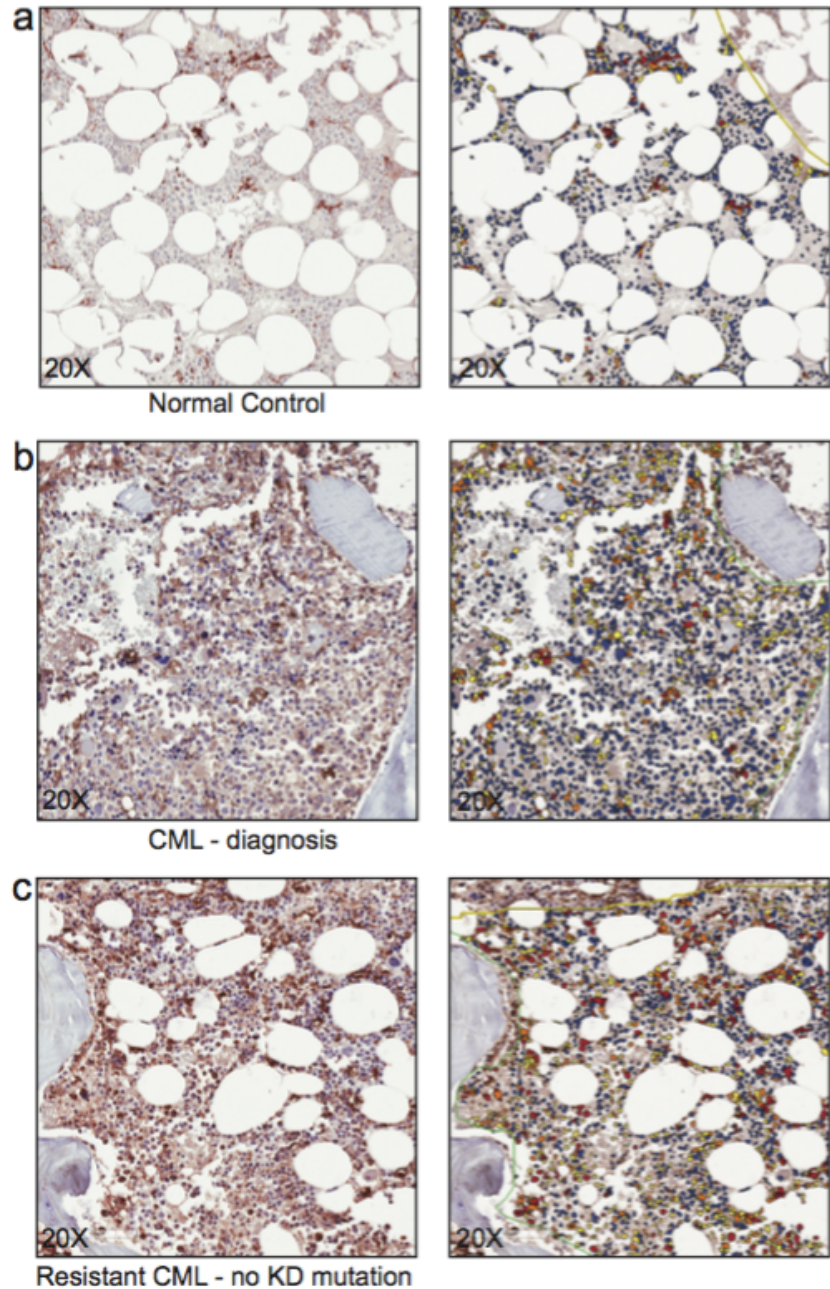
Figure 2.2.9 Examples of quantitation of FGF2 staining with Aperio ImageScope software.
Bone marrow core biopsies from A, normal control (surgical joint replacement patient), B, a CML patient at diagnosis, and C, a resistant patient without kinase domain (KD) mutations prior to ponatinib therapy were evaluated for FGF2 by IHC as described in Methods. The images were then quantitated for FGF2 staining using Aperio ImageScope software. Cells were automatically identified by nuclear hematoxylin stain and intensity of FGF2 staining indicated by blue (no staining), yellow (1+), orange (2+) and red (3+). Intact marrow was designated for quantitation with trabecular bone, edges, and crushed marrow excluded from analysis. The yellow line indicates the area selected for analysis.
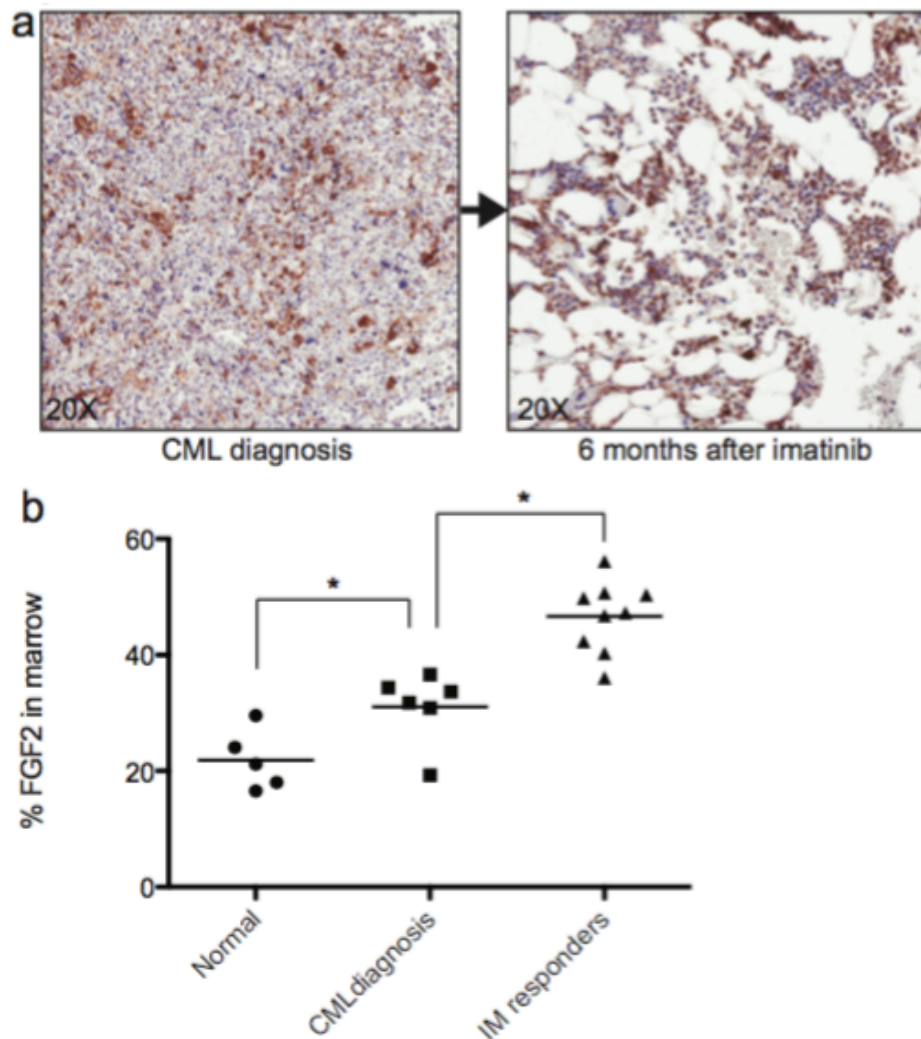
Figure 2.2.10 FGF2 increases in the marrow of patients who respond to imatinib.

Bone marrow biopsies of patients who responded to imatinib (no resistance) were evaluated for FGF2 by IHC as described in Methods and compared to FGF2 of normal controls and CML patients at diagnosis. Bone marrow biopsies of a CML patient at A, diagnosis and the same patient B, 6 months after initiating imatinib. Quantitation of FGF2 staining was 31.8% at diagnosis and increased to 46.8% after 6 months, however the overall cellularity of the marrow also decreased over that time as well. c) Comparison of normal controls, CML patients at diagnosis, and CML patients after response to imatinib (IM). Bone marrow biopsies at response ranged from 6-18 months after initiation of imatinib. The differences between patient samples were analyzed by 2- tailed t-test for significance. * indicates p value of <0.05.
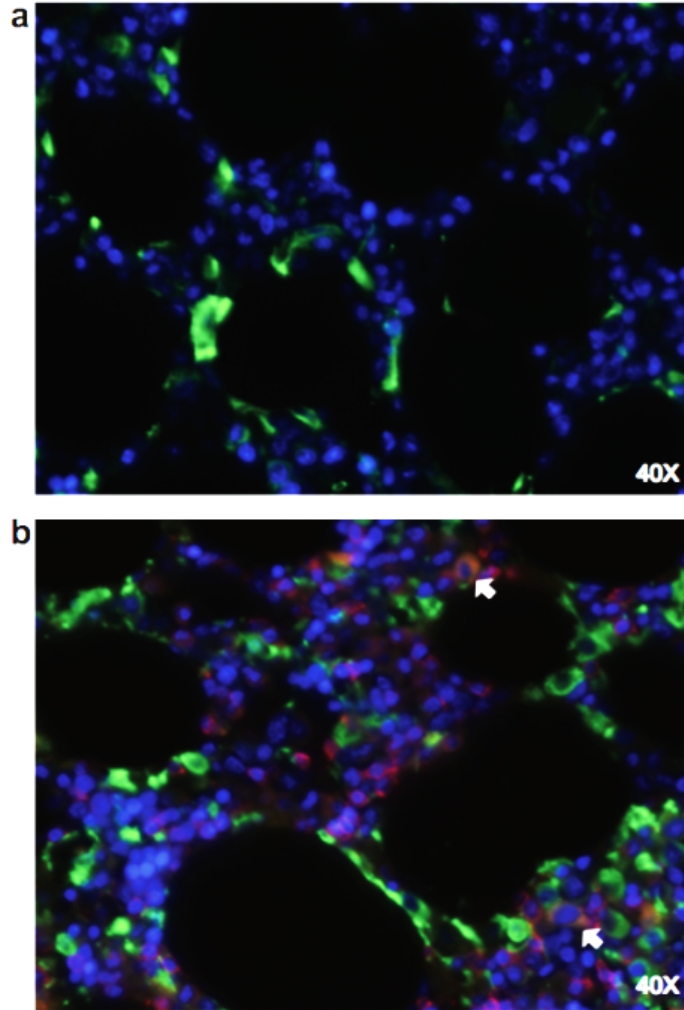
Figure 2.2.11 Immunofluorescence identifies bone marrow cells which co-express CD45+ and FGF2.

Bone marrow samples from normal controls and resistant CML patients were incubated overnight at 4°C with 1:500 rabbit primary antibody to FGF2 (SC-79, as described in Methods) and 1:200 mouse anti-CD45 antibody (HPA000440, Sigma-Aldrich, St. Louis, MO) overnight in Dako Antibody Diluent with Background Reducing Reagents. The following day the slides were washed and incubated with 1:200 Alexa Fluor 488 anti-rabbit antibody and 1:200 Alexa Fluor 594 anti-mouse antibody (Cell Signaling, Danvers, MA) for one hour at room temperature followed by DAPI staining to stain the nuclei (blue). The slides were mounted in NPG (n-propyl gallate) to preserve immunofluorescent signal. A, Normal marrow with anti- FGF2 alone (green) as a control. The FGF2 staining pattern is similar to Figure 2.2.8. B, Resistant CML sample prior to ponatinib stained with FGF2 (green), CD45 (red) and DAPI (blue). FGF2 is mostly restricted to CD45- stroma but two cells are indicated with arrows that clearly have both CD45+ and FGF2. These cells also have a clearly visible nucleus.

2.3 FGF2 from the bone marrow stroma promotes resistance to FLT3 inhibitors in acute myeloid leukemia

Elie Traer, Jacqueline Martinez, **Nathalie Javidi-Sharifi**, Anupriya Agarwal, Jennifer Dunlap, Isabel English, Tibor Kovacsovics, Jeffrey W. Tyner, Melissa Wong, and Brian J. Druker

2.3.1 Abstract

Potent FLT3 inhibitors, such as quizartinib (AC220), have shown promise in treating acute myeloid leukemia (AML) with FLT3 internal tandem duplication (ITD) mutations, however, responses are not durable and resistance develops within months. Evidence suggests that the bone marrow microenvironment provides sanctuary to leukemia cells. Selected microenvironmental proteins were tested for their ability to protect FLT3-ITD+ MOLM14 cells from AC220. FLT3 ligand (FL) and fibroblast growth factor 2 (FGF2) were found to be the most protective. FL directly attenuated AC220 inhibition of FLT3, consistent with previous reports. In contrast, FGF2 promoted resistance through activation of FGFR1 and downstream MAPK pathway, and resistant cells responded synergistically to combined FGFR1 and FLT3 inhibition. Removing FL or FGF2 from ligand-dependent resistant cultures transiently restored sensitivity to AC220, but accelerated the acquisition of secondary resistance through mutational and non-mutational re-activation of FLT3 and RAS/MAPK signaling. FLT3-ITD AML patients treated with AC220 developed increased expression of FGF2 in marrow stromal cells over time, with FGF2 expression peaking during early resistance, prior to overt clinical relapse and/or detection of resistance mutations. Thus we propose a two-step model in which initial resistance is mediated by extrinsic FGF2 and/or FL from the microenvironment, followed by evolution of ligand-independent resistance. These

134

results support a strategy of early combination therapy that targets early survival signals from the bone marrow microenvironment, in particular FGF2, to improve the depth of response in FLT3-ITD AML.

2.3.2 Introduction

1.1.1.32 FLT3 ITD AML clinical perspective

Over 20% of AML patients under the age of 60 carry an internal tandem duplication (ITD) in the transmembrane domain of the FMS-like tyrosine kinase 3 (FLT3) gene[293]. The presence of FLT3-ITD is associated with poor prognosis and high risk of relapse after chemotherapy or stem cell transplant[294]. FLT3-ITD+ AML characteristically relapses after a shorter first remission than other subtypes[295]. Patients who are refractory to induction chemotherapy or who relapse after a remission of less than 6 months have an expected long-term survival of 0-3%. Patients who attain a remission of 6 months or longer can expected to achieve a second remission in 20% of cases and have a 5-10% chance of long-term survival[296]. Several FLT3 inhibitors have been developed and evaluated in clinical trials. While a rapid clearance of blasts in the peripheral blood is frequently achieved, most inhibitors only attain limited effects on bone marrow blasts.

1.1.1.33 Oncogenic signaling in FLT3 ITD AML

FLT3 is a class III receptor tyrosine kinase expressed on early hematopoietic stem and progenitor cells, and is important for hematopoiesis. FLT3 is activated by its ligand, FLT3 ligand (FL), which promotes receptor dimerization and growth via activation of STAT5, Ras/MAPK and Akt pathways[297]. FLT3 is frequently mutated in acute myeloid leukemia (AML). The most common genetic alteration is the internal tandem duplication (ITD) in the juxtamembrane domain of the protein[298], which disrupts the autoinhibitory mechanism of the juxtamembrane domain and results in chronic FLT3 activation[299]. FLT3-ITDs are present in ~20% of newly diagnosed AML and lead to increased risk of relapse[294], [300]. FLT3 is also frequently mutated by point mutations in the activation loop of the protein, most commonly at D835, and is present in ~10% of newly diagnosed AML[301], [302], however, the prognostic significance of these kinase domain mutations (KDMs) is less clear.

1.1.1.34 TKI therapy in FLT3 ITD AML

The multi-kinase inhibitor midostaurin demonstrated some encouraging activity against FLT3-ITD+ AML. The administration of midostaurin resulted in a greater than 50% reduction of peripheral blood or bone marrow blasts in 42% (FLT3 wild type) and 71% (FLT3-ITD) of patients[303]. Studies combining midostaurin with conventional chemotherapy or with a hypomethylating agent also demonstrated enhanced

antileukemic activity[304], [305]. Lestauranib, an inhibitor of Trk receptors, JAK2 and FLT3, showed activity in phase I and phase II trials[291], but no improvement in remission rates due to poor FLT3 inhibition in vivo when following salvage chemotherapy[295]. Sorafenib, an inhibitor of VEGFR, PDGFR, Raf and FLT3, achieved remarkable initial responses, however, the response was lost in most patients after 72 days[306].

Recently, a more potent FLT3 inhibitor, quizartinib (AC220), was developed and demonstrated a 50% composite complete remission rate in phase II clinical trials[307]. AC220 is now in phase III trials in comparison to salvage chemotherapy in relapsed FLT3-ITD AML. However, despite a higher response rate, the durability of AC220 response is still quite limited, and most patients develop resistance after a few months of therapy.

1.1.1.35 *Resistance to TKI therapy in AML*

Similar to resistance in CML, FLT3 point mutations have been shown to decrease affinity of AC220 for its target, leading to clinical resistance[306], [308], [309]. In particular, mutations of the "gatekeeper" residue F691L and mutations in the activation loop (the region around D835) confer resistance to AC220 both in vitro and in vivo[308]. In contrast, resistance also occurs in the absence of FLT3 mutations, although the nature of this resistance is less clear.

Recently, the ligand for FLT3 (FL) was also found to promote resistance to FLT3 inhibitors[310]. FL ligand expression increases during therapy with FLT3 inhibitors, providing one potential explanation of why leukemia cells in the bone marrow are relatively more resistant to FLT3 inhibitors[310]. However, FL is likely not the only component of the bone marrow microenvironment that provides sanctuary to leukemia cells. We hypothesized that other proteins from the bone marrow microenvironment would promote resistance to FLT3 inhibitors and tested known microenvironmental cytokines, growth factors, and soluble proteins for their ability to protect MOLM14 cells from AC220 treatment. Fibroblast growth factor 2 (FGF2) was one of the most effective proteins in promoting survival of MOLM14 cells in the presence of AC220, and led to resistance in extended cultures. FGF2 is highly expressed by bone marrow stromal cells and plays an active role in hematopoietic colony formation in vitro[155], [156], and hematopoiesis in vivo[162], [281].

We recently identified FGF2 as a microenvironmental protein that can promote resistance to imatinib in CML in the absence of kinase domain mutations[220]. Moreover, FGF2 has been implicated in promoting resistance in multiple kinase-driven solid tumors[129]-[131], [219], suggesting that FGF2/FGFR activation is a conserved mechanism of resistance. Here, we determine the mechanism of FGF2-mediated resistance in FLT3 ITD AML and contrast it with resistance induced by FL.

2.3.3 Results

1.1.1.36 FGF2- and FL-mediated protection of AML cells

To screen for microenvironmental factors that protect AML cells from FLT3 inhibitors, we cultured MOLM14 cells with graded concentrations of selected proteins expressed in the bone marrow microenvironment (Agarwal et al., manuscript in preparation) in the presence of 10 nM AC220. Viability was assessed after two days by MTS assay and averaged over all concentrations (1, 10, and 100 ng/ml). Proteins that increased viability >2 standard deviations are highlighted in red (Figure 2.3.1 A). The most protective molecule in this screen was FL, which has been previously reported to attenuate the effect of FLT3 inhibitors[310], providing an internal positive control. Two of the other top hits in our screen were FGF2 and FGF1, also known as basic FGF and acidic FGF respectively. We confirmed the results using lower concentrations (1 ng/ml and 0.1 ng/ml) and found again that FL and FGF2 were the most protective overall (Figure 2.3.1 B). We focused our attention on FGF2, which is highly expressed in bone marrow[220], and FL as two distinct mechanisms of ligand-mediated resistance.

To test the protective effects of FGF2 and FL over a longer duration, MOLM14 cells were cultured over many weeks with 10 nM AC220, media, FL, and FGF2 replaced every 2-3 days. Addition of FL or FGF2 promoted outgrowth in all replicates (N=4) at around 6 weeks (Figure 2.3.1 C). In contrast, only 2/4 replicates cultured in media

without FGF2 or FL developed resistance, and it took nearly 12 weeks, providing strong

evidence that continuous exposure to protective ligand accelerates development of

resistance (see also Figure 2.3.10).

1.1.1.37 FGFR1 mediates FGF2 protection

To test if FGF2 protects cells through activation of an FGF receptor (FGFR), we treated

MOLM14 cells with the pan-FGFR inhibitor PD173074 in the presence of FGF2 and

AC220. Even at doses as low as 25 nM, PD173074 was able to attenuate the protective

effect of FGF2 (Figure 2.3.2 A). Since FGF2 is capable of binding multiple FGFRs[55], we

measured the relative expression of FGFRs 1-4 by Taqman qPCR and found that FGFR1

was the most highly expressed FGFR in MOLM14 cells (Figure 2.3.3). siRNA targeting

blocked the protective effect of FGF2 in the presence of AC220 (Figure 2.3.2 B), and

efficiently reduced mRNA levels and protein expression (Figure 2.3.3 B and Figure

2.3.2. C). In contrast, siRNAs targeting FGFR2, FGFR3, and FGFR4 had no effect on

FGF2 protection (Figure 2.3.2 B). To further test the role of FGFR1, we took advantage of

the fact that BaF3 cells do not express FGFRs 1-4[311]. BaF3 cells were initially

retrovirally transfected with FLT3 ITD[312], and then subjected to a second retroviral

infection with either an empty pMX vector or pMX containing human FGFR1. The cells

were selected by puromycin and expression of FGFR1 confirmed by Western blot

(Figure 2.3.2 D). When FLT3 ITD-dependent BaF3 cells were exposed to quizartinib,

FGF2 was only protective when FGFR1 was also expressed (Figure 2.3.2 F vs. 2.3.2 E),

again indicating that FGF2 signals through FGFR1 to exert its protective effect. We tested whether FGF2 protected two other FLT3 ITD AML cell lines (MOLM13 and MV-4-11) with lower FGFR expression from AC220 (Figure 2.3.4). We found no significant protective effect in these lines, again confirming that FGFR expression is a prerequisite for FGF2-mediated protection.

1.1.1.38 FGF2 protects a subset of FLT3 ITD AML patient samples

FGFR1 is the most highly expressed FGFR in cytogenetically normal AML, with expression comparable to FLT3 and AXL, another receptor tyrosine kinase reported to mediate resistance in FLT3 ITD AML[313], [314] (Figure 2.3.4). To test if FGF2 protects primary AML samples from AC220, we cultured fresh and thawed frozen viable primary AML cells with media alone (no ligand) or supplemented with FGF2. The cells were then treated with a gradient of AC220 and viability was assessed after 72 hours. FGF2 was highly protective of a subset of primary AML samples (example shown in Figure 2.3.2 G) and increased viability of AC220-treated samples in a dose-dependent and statistically significant manner (Figure 2.3.2 H).

1.1.1.39 Combined inhibition of FLT3 and FGFR overcomes resistance

MOLM14 cells grown in continuous 10 nM AC220 with FGF2 or FL eventually resumed exponential growth despite the presence of AC220 (Figure 2.3.1 C) and are henceforth referred to as FGF2- or FL-dependent resistant cultures. We tested the sensitivity of

these resistant cells to titrations of both AC220 and the FGFR inhibitor PD173074 by creating a 64-well matrix with a gradient of AC220 on one axis, and overlaying a gradient of PD173074 on the other axis. Viability was assessed after 48 hours by MTS and the results are shown as a surface plot of all 64 conditions, with corresponding linear graphs of AC220, PD173074, and an equimolar combination of AC220 and PD173074 to highlight synergy (Figure 2.3.5 A-C). Naïve MOLM14 cells were exquisitely sensitive to AC220 at low nM concentrations but were not affected by PD173074 treatment in the absence of FGF2 (Figure 2.3.5 A, see also Figure 2.3.6). In contrast, FGF2-dependent resistant cultures were protected from AC220 at higher AC220 concentrations, and the addition of PD173074 was highly synergistic in overcoming this protection (Figure 2.3.5 B and Table 2.3.1). FL-dependent resistant cultures had a shifted AC220 dose-response curve (Figure 2.3.5 C), but resistance was overcome by higher doses of AC220 (>10 nM), and PD173074 had minimal additional effect.

1.1.1.40 MAPK signaling in FGF2-mediated resistance

To explore the mechanism of resistance in FGF2- and FL-dependent resistant cultures, we first evaluated the FLT3 gene for known resistance mutations in the activation loop[308]. A single Y842C mutation was found in one FGF2-supplemented culture, but the remainder of the FGF2-dependent resistant cultures did not have mutations to explain AC220 resistance. We then performed Western blot analysis to analyze

phosphorylated FLT3 (pFLT3) at multiple sites, as well as the MAPK pathway, which is downstream of both FLT3 and FGFR1. AC220 treatment of naïve MOLM14 cells effectively abrogated pFLT3 at all phosphorylation sites, pSTAT5, and pERK1/2 (lanes 1 and 2, Figure 4A). The single FGF2-dependent resistant culture that developed a Y842C mutation had partial reactivation of FLT3 despite the presence of AC220 (FGF2 R-1, lane 3). FL-dependent resistant cultures also had partial restoration of pFLT3, consistent with previous reports[310] (lanes 7-10). In contrast, FGF2-dependent resistant cultures R-2 to R-4 maintained phosphorylation of ERK but there was little pFLT3. To test if alternative kinase pathways might be altered in either FGF2- or FL-dependent resistant cultures, we used a phospho-kinase array to assess 46 phosphorylated proteins, but found that only the MAPK signaling pathway was consistently restored in all FGF2- and FL-dependent resistant cultures (Figures 2.3.8 and 2.3.9).

1.1.1.41 FLT3 and MAPK pathway mutations in FGF2 outgrowth cultures

To evaluate whether FGF2- and FL-dependent resistant cultures remained dependent on ligand after four months of outgrowth, we split the FGF2- and FL-dependent cultures and removed ligand from one subset (Figure 2.3.10 B-C). Media and AC220 were replaced every 2-3 days and the number of viable cells was measured with media change. The time when cells resumed exponential growth is indicated in gray and plotted on a timeline with the initial extended culture experiment to allow comparison (Figure 2.3.1 C). The single FGF2-dependent culture with the FLT3 Y842C mutation

quickly resumed exponential growth, about one week after FGF2 was removed (Figure 2.3.10 B). The remainder of FGF2- and FL-dependent cultures also developed resistance after FGF2 was removed, and resumed exponential growth after about one month. Of note, resistance after removal of FGF2 or FL developed more rapidly than initial resistance (~2 months) in the presence of FGF2 or FL (Figure 2.3.10 B, C). The cultures were evaluated for FLT3 activation loop mutations by Sanger sequencing at early timepoints in resistance (4 and 6 months, Figure 2.3.11), and then again after 8 months using a next-generation sequencing panel of 43 genes frequently mutated in AML. Most of the FGF2- and FL-supplemented cultures did not have detectable resistance mutations during initial resistance, but removing FGF2 or FL greatly accelerated the acquisition of mutations. In addition, we identified frequent activating mutations of the RAS pathway, suggesting a strong selective pressure to reactivate RAS/MAPK signaling. The frequency of the KRAS G13D mutation was particularly notable and we suspect this mutation is present at a low level in the naïve MOLM14 cells, since 2/659 reads contained this mutation, although below the sensitivity of the assay to call a true mutation.

To confirm that the observed FLT3 mutations drive resistance, we compared the sensitivity of these cultures to multiple FLT3 inhibitors, including crenolanib, a FLT3 inhibitor that is not blocked by mutations in the activation loop[315]. The D839V and Y842C mutated cultures were resistant to AC220, sorafenib and ponatinib, but uniquely

sensitive to crenolanib (Figure 2.3.10 D). In contrast, resistant cultures without FLT3

mutation remained resistant to crenolanib (single example shown, FL R-1). All resistant

cultures remained sensitive to higher doses of FLT3 inhibitors suggesting the continued

importance of partial FLT3 signaling (Figures 2.3.5 and 2.3.10). In agreement with this

result, after withdrawal of cytokine, most resistant cultures had partial restoration of

FLT3 phosphorylation in addition to reactivation of MAPK signaling by Western blot

(2.3.12), providing further evidence that the primary routes of resistance are mediated

by FLT3 and RAS/MAPK.

1.1.1.42 *FGFR inhibitors in stromal co-cultures*

FGF2 is expressed in normal bone marrow stroma[220], [269]. We evaluated if FGFR

inhibitors could block the protective effects of FGF2-expressing stroma in co-culture

with MOLM14 to overcome FGF2-mediated resistance. We used the human bone

marrow stromal cell lines HS-5 and HS-27a, which are derived from the same person

but have distinct functional characteristics[316]. HS-5 also expresses much higher

amounts of FGF2 compared to HS-27a (Figure 2.3.13 A). We cultured MOLM14 cells in

media alone, with 10 ng/ml FGF2, or in transwells above HS-5 and HS-27a. The cells

were then treated with 10 nM AC220, 250 nM PD173074, or a combination, and assessed

for viability after four days. PD173074 alone had no effect on MOLM14 cell viability

(data not shown). MOLM14 cells cultured with recombinant FGF2 or in transwells over

HS-5 stroma were protected from effects of AC220 treatment, but protection could be

overcome by concomitant PD173074 treatment. In contrast, the protective effect of HS-27a was less substantial than HS-5, and was unchanged with addition of PD173074 (Figure 2.3.13 B). Since FGF2 is also reported to be an autocrine growth factor for stromal cells[162], [281], we removed the transwells and assessed viability of the underlying HS-5 and HS-27a cells. Only HS-5 growth was significantly attenuated by addition of PD173074 (Figure 2.3.13 C). In summary, addition of FGFR inhibitor overcomes protective effects of FGF2-expressing stromal co-cultures and also prevents autocrine growth of FGF2-expressing stroma.

1.1.1.43 FGF2 in bone marrow stroma during AC220 treatment

To test expression of FGF2 in FLT3-ITD AML patients, bone marrow core biopsies from patients on the AC220 trial at our institution were collected prior to treatment, during response to AC220, and at development of resistance. Clinical characteristics of patients with multiple bone marrow biopsies available for analysis are shown in Table 2.3.2. The marrow biopsies were stained for FGF2 by IHC. A normal bone marrow biopsy from a surgical hip repair is shown for comparison in Figure 2.3.14 A and a representative patient series is shown in Figure 2.3.14 B, with the peripheral blood and bone marrow leukemia burden shown above the stained bone marrow biopsies. Of note, in this particular patient an acquired FLT3 D835 mutation was detected at day 158. FGF2 was primarily expressed in the marrow stroma and not hematopoietic cells (CD45+) by immunofluorescence (Figure 2.3.15). The FGF2 staining was quantitated by Aperio

ImageScope software for all 10 patients during therapy and is shown in Figure 7C. FGF2 increased significantly during response to AC220, peaked with early resistance, and then decreased again after overt clinical resistance. We also investigated FLT3 mutations at the time of resistance: three of five patients acquired mutations in FLT3 during therapy; one patient had a D835 mutation prior to AC220; and three patients were bridged to allogeneic transplant (Figure 2.3.14 C and Table 2.3.2). Since FL expression is reported to be increased with FLT3 inhibitor treatment[310], we attempted FL staining by IHC with two different antibodies for comparison but were unable to obtain reliable staining for quantification.

2.3.4   Discussion

Although FLT3-ITD AML initially responds well to FLT3 inhibitors, the durability of response is short and resistance develops in about 4 months. Mutations in the activation loop of FLT3 are the most commonly described mechanism of clinical resistance to AC220[306], [308], [309] and in vitro mutagenesis screens were able to predict many of the mutations that develop clinically[308]. However, this approach still fails to address non-mutational mechanisms of resistance, including extrinsic mechanisms of resistance from the bone marrow microenvironment that can promote leukemia cell survival in the absence of kinase domain mutations. While FLT3 inhibitors induce a rapid clearance of leukemia blasts from the peripheral blood, the leukemic blasts within the bone marrow respond more slowly, providing strong clinical evidence that the leukemia cells

in the marrow are relatively protected from AC220. This protective effect has been reproduced in vitro using either marrow stromal cells[317]-[319], recombinant FL[310], and now recombinant FGF2.

We noted that FGF2- and FL-mediated resistance initially promoted resistance largely in the absence of mutations, but continued culture or removal of ligand greatly accelerated development and outgrowth of resistance mutations. This is analogous to the residual AML blasts that remain in the marrow at low level and then begin to proliferate in the marrow prior to overt clinical resistance. Taken together, our data supports a two-step model of resistance, where ligands from the microenvironment initially blunt the effect of FLT3 inhibitors, allowing leukemia cells time for survival and adaptation, which is then followed by microenvironment-independent resistance and clinical relapse.

1.1.1.44 Ligand-mediated protection and acquired resistance

Although recombinant FGF2 and FL promote resistance, the mechanism of protection is distinct. FGF2 bound to FGFR1, and FGF2/FGFR1 signaling in extended cultures led to increased dependence upon the FGFR1/MAPK signaling pathway for cell survival, as evidenced by the strong synergy between AC220 and the FGFR inhibitor PD173074. We investigated if there might be a direct interaction between FGFR1 and FLT3 using immunoprecipitation, but found no significant interaction (Figure 2.3.16). In

comparison, FL-dependent resistant cultures partially restored FLT3 and downstream MAPK signaling despite the presence of AC220. Removal of FGF2 and FL from ligand-dependent cultures resulted in mutational and non-mutational activation of both FLT3 and the MAPK pathway. Taken together, either partial restoration of FLT3 signaling or activation of the MAPK pathway through a compensatory pathway is sufficient for initial resistance and restores signaling homeostasis in the cells[310], [319], [320], which then leads to sustained activation through direct mutational or non-mutational mechanisms.

1.1.1.45 Predicting ligand-mediated resistance pathways through receptor expression and

physiologic damage response pathway analysis

It is becoming apparent that ligand-activation of FGFR is an important mechanism of resistance in cancers with activation of other oncogenic kinases. Autocrine secretion of FGF2 and activation of FGFR1 was recently reported to promote resistance to the EGFR inhibitor gefitinib in lung cancer cell lines[128], [129]. Similarly, activation of FGFR3 by either exogenous FGF2 or FGFR3 activating-mutations in melanoma cell lines was shown to promote resistance to B-RAF inhibitors[130]. FGF2 also promotes resistance to BCR-ABL inhibitors in CML[321] and KIT inhibitors in gastrointestinal stromal tumors[226], [322] providing evidence that this is a conserved pathway of resistance.

FGF2 is not uniquely capable of promoting resistance, however. A recent screen tested the ability of multiple ligands to promote resistance to kinase inhibitors in multiple cancer cell lines and found that FGF2, hepatocyte growth factor (HGF), and neuregulin 1 (NRG1) were the most "broadly active" ligands capable of promoting resistance to kinase inhibitors[131]. In particular, paracrine resistance to vemurafenib has been shown in B-RAF-mutated melanoma and resistant patients had increased serum HGF, as well as increased HGF expression in the stromal cells adjacent to the melanoma[323]. Growth arrest-specific 6 (GAS6) ligand-dependent activation of the receptor AXL is another mechanism of resistance that has recently been described[324], including in FLT3 ITD AML[313], [314]. Primary AML cells express both FGFR1 and to a lesser extent AXL, suggesting that different ligands are capable of mediating resistance in FLT3 ITD AML. Our results support the importance of ligand-RTK interaction as a general mechanism of kinase resistance; and FGF2 in particular as an important member of a class of ligands expressed in the tumor microenvironment that promote resistance.

Our results also suggest that targeting early survival pathways in treatment are more likely to reduce the residual leukemia in the microenvironment, and reduce the opportunity for subsequent development of resistance mutations. More potent FLT3 inhibitors are likely to overcome FL-mediated resistance, but early interruption of FGF2 signaling is also likely to be important since FGF2 expression in the bone marrow

stroma increases during AC220 treatment, providing even more external survival cues over time. Expansion of FGF2-expressing stroma is consistent with the recent discovery that FGF2 is an autocrine growth factor for marrow stroma (normally activated during stress hematopoiesis[162], [281] and our results suggest that this stress response is hijacked by residual AML cells for survival.

1.1.1.46 Clinical trials of FGFR inhibitors in AML

In CML, patients treated with ponatinib, which targets both BCR-ABL and FGFR, exhibited reduction of FGF2-expressing stromal cells over time, indicating that the stroma itself can be effectively targeted in patients[220]. Thus, FGFR inhibition can block both FGF2 paracrine survival signals to leukemia cells, and FGF2 autocrine signals to stroma, making the marrow stroma itself a therapeutic target by remodeling the leukemia cell niche. Optimally, clinical trials using a combination of FGFR inhibitors and novel FLT3 inhibitors that remain active against the common FLT3 activation loop mutations would 1) overcome paracrine FGF2-mediated resistance, 2) attenuate autocrine-stimulated expansion of FGF2-expressing stroma, and 3) circumvent development of the most common mutations that lead to resistance and relapse. This strategy has the potential to improve the durability of response to FLT3 inhibitors.
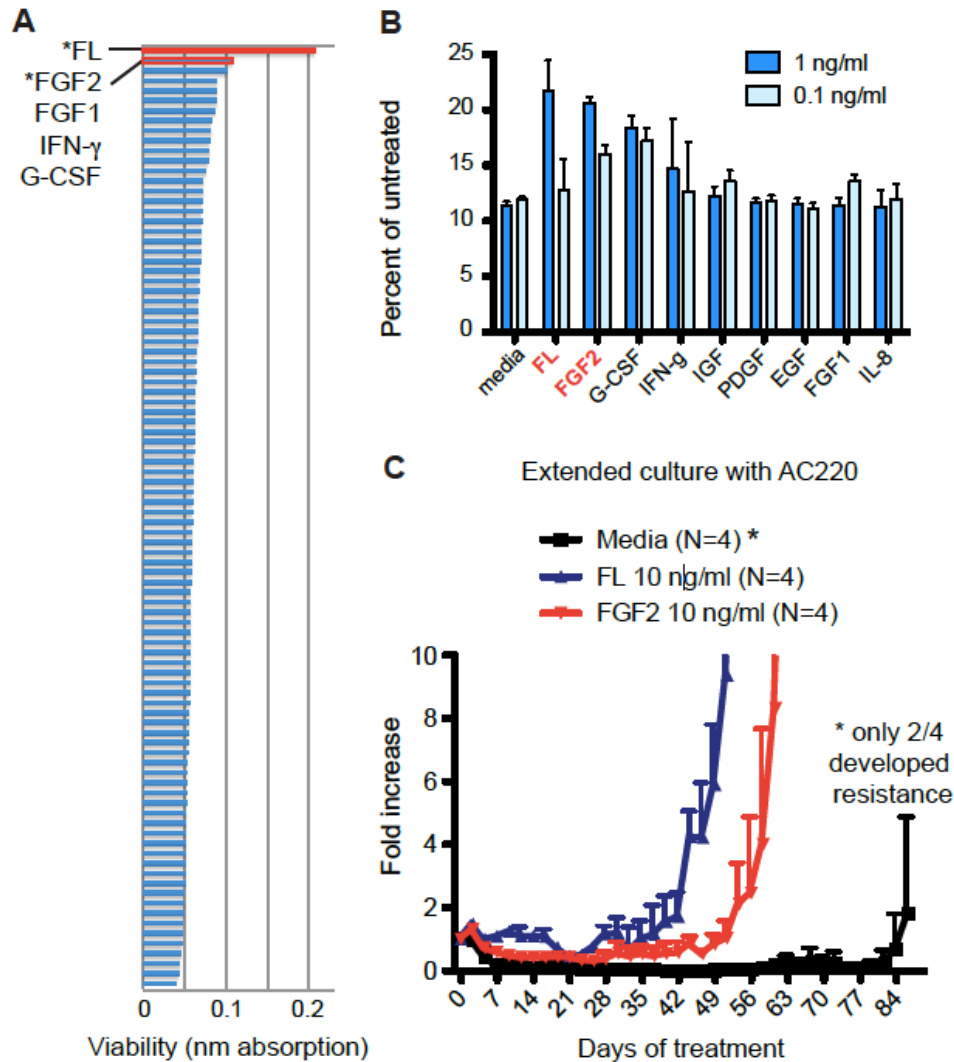
Figure 2.3.1 Microenvironmental screen identifies FL and FGF2 as protective molecules for MOLM14 cells, and they accelerate development of resistance in extended cultures.
A, MOLM14 cells were added to a 384-well plate containing cytokines, chemokines, and growth factors to screen for proteins that promote growth in the presence of 10 nM AC220 (quizartinib). Viability was measured using MTS reagent, and averaged over all concentrations (1, 10, and 100 ng/ml), and the results sorted according to highest average viability. Average viability >2 standard deviations above the mean are highlighted in red and by an *. B, MOLM14 cells were cultured in lower concentrations of recombinant proteins (1, and 0.1 ng/ml) in 96-well plates plus 10 nM AC220. Viability was assessed after 48 hours with MTS reagent and data plotted as percent of the respective untreated control. All wells were plated in triplicate with standard deviation indicated in error bars. C, MOLM14 cells were cultured continuously in 10 nM AC220 with FL, FGF2, or media alone as indicated (N=4 for each). Fresh media, AC220 and cytokine were replaced every 2-3 days over the indicated time period. Viable cell numbers were analyzed every 2-3 days with Guava ViaCount.
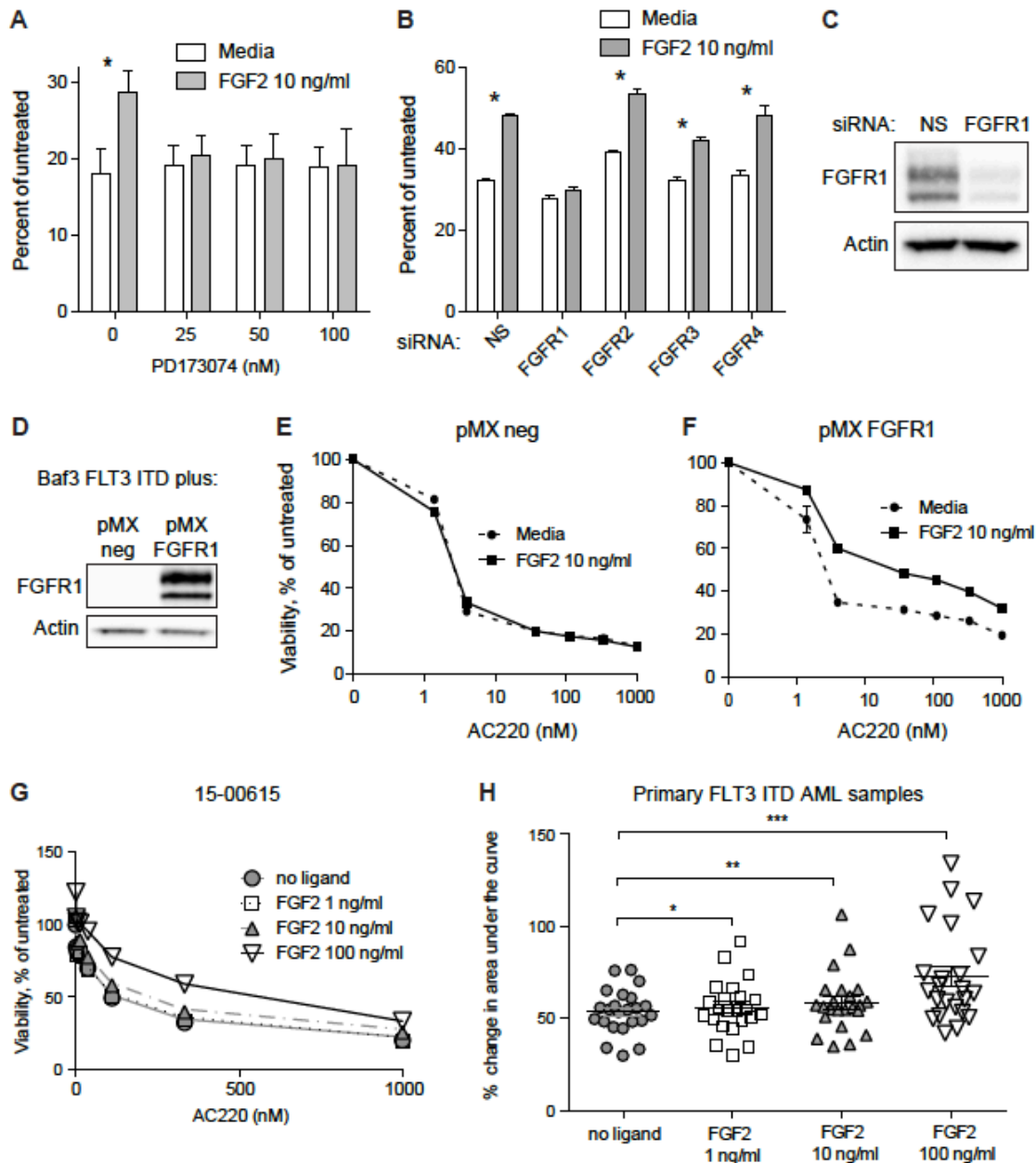
Figure 2.3.2 FGF2 protection of MOLM14 cells is mediated by FGFR1.
A, MOLM14 cells were cultured in media alone or media supplemented with 10 ng/ml FGF2, treated with 10 nM AC220, and exposed to doses of the FGFR inhibitor PD173074: 25, 50, 100 nM as indicated. Viability was measured by MTS assay after 48 hours and AC220 treated cells were compared to their respective untreated control (media alone, FGF2, 25 nM PD173074, etc.) B, MOLM14 cells were electroporated with siRNAs targeting FGFR1, FGFR2, FGFR3, FGFR4 and a non-specific (NS) control. After 48 hours the cells were pelleted and resuspended in media with or without FGF2 -/+ 10 nM AC220 and viability was assessed by MTS after 48 hours. * indicates p<0.01 by t test. C, MOLM14 cells were analyzed by Western blot for FGFR1 to evaluate protein

expression after siRNA (see supplemental Figure S1 for QPCR after knock-down). D, BaF3 cells expressing FLT3 ITD were retrovirally transfected with either empty pMX vector (pMX neg) or vector containing FGFR1, selected with puromycin, and analyzed by Western blot to show FGFR1 expression. The Baf3 cells with FLT3 ITD and E, empty pMX vector or F, pMX with FGFR1 were then treated with a gradient of AC220 in either media alone or supplemented with 10 ng/ml FGF2. Viability was assessed after 48 hours with MTS reagent and data plotted as percent of the respective untreated control. All cell line experiments were performed in triplicate, error bars indicate standard deviation. Fresh primary AML samples containing FLT3 ITD (5) and thawed frozen viable FLT3 ITD AML samples (see methods) were plated with media alone (no ligand) or with FGF2 at 1, 10 and 100 ng/ml concentration. The cells were then exposed to a gradient of AC220 and viability was measured after 72 hours by MTS. G, An example of FGF2-mediated protection during AC220 exposure in a primary AML sample. H, The area under the curve was calculated for 21 patient samples in the absence or presence of FGF2 ligand (see 2G) and graphed with mean and standard error of the mean shown. One-tailed t-tests were performed with p values indicated by *<0.05, **<0.005, and ***=0.0007.
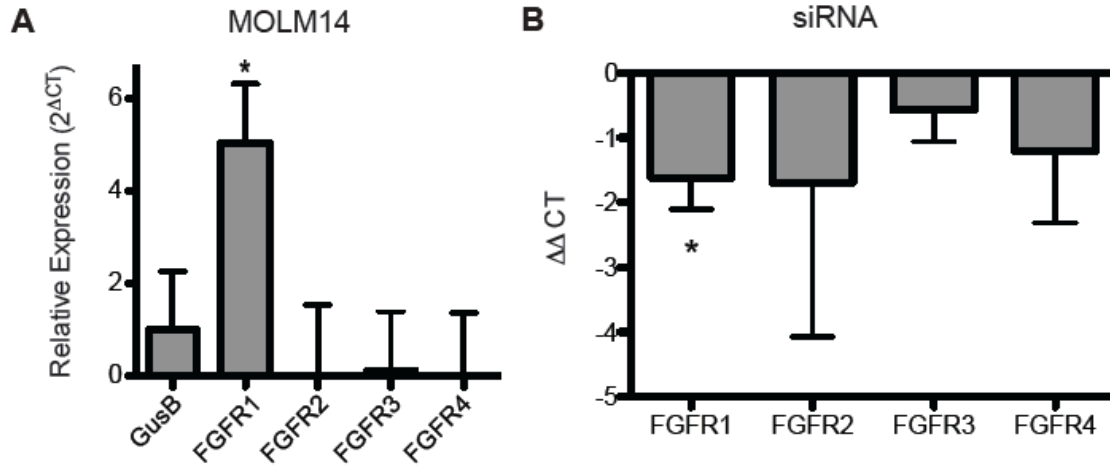
Figure 2.3.3 FGFR1 is the most highly expressed FGFR in MOLM 14 and siRNA knock down of FGFR mRNA.

A, Relative mRNA expression of FGFR1-4 was evaluated by QPCR and normalized relative to control mRNA GusB (value of 1). B, Taqman primers were used to evaluate mRNA of FGFR1-4 in MOLM14 cells electroporated with targeted siRNAs. GusB was used to calculate the ΔΔCT for each FGFR. The ΔΔCT was calculated for FGFR1, 2, 3, and 4 and plotted with standard deviation. A value of 0 indicates no change in expression. Each QPCR reaction was run in triplicate following manufacturers protocol (Life Technologies, Grand Island, NY).
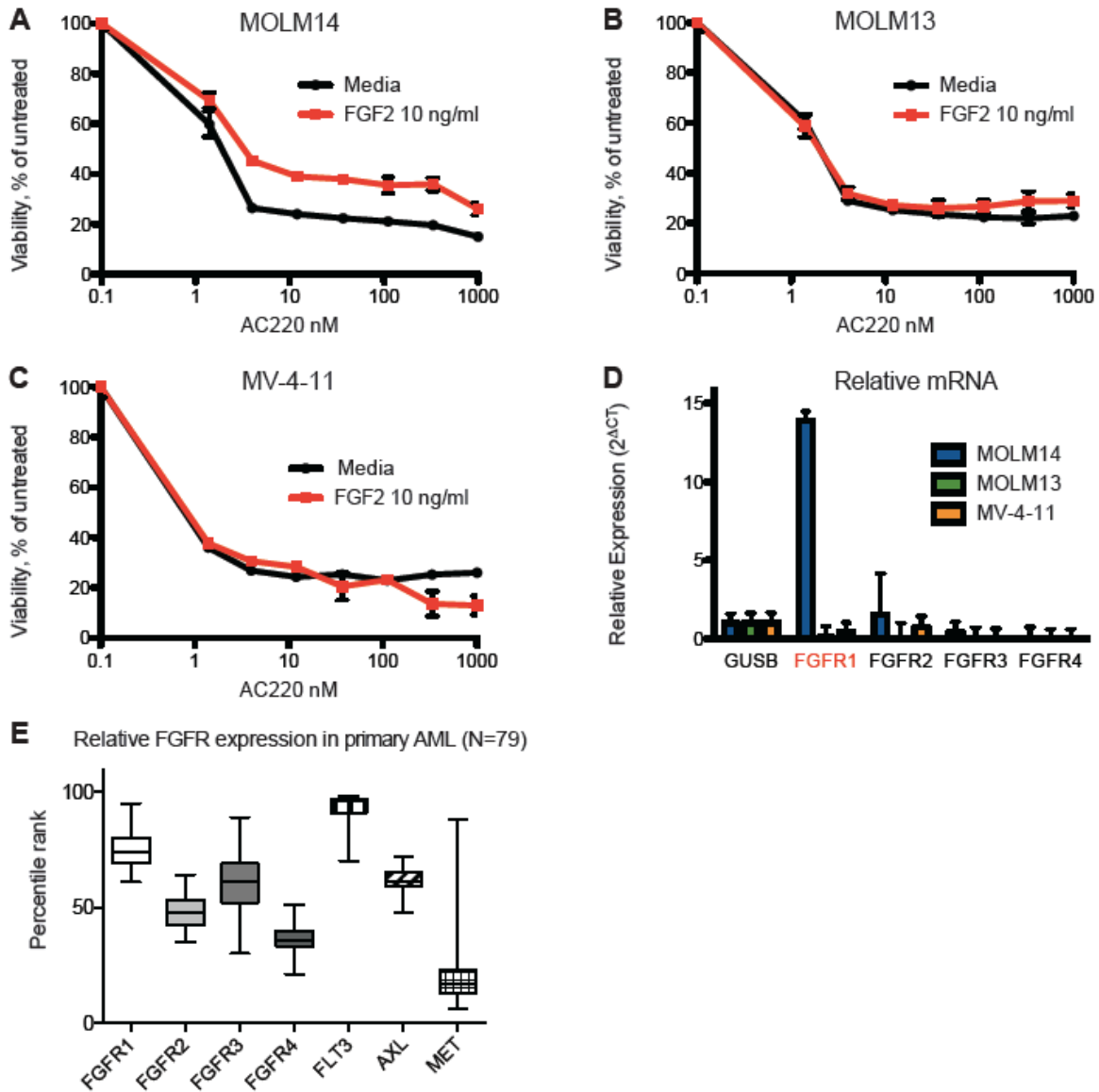
Figure 2.3.4 FGF2 protection from FLT3 inhibitors is dependent upon FGFR expression.
Three FLT3 AML cells lines were treated with AC220 in media alone or with 10 ng/ml FGF2: A, MOLM14, B, MOLM13, and C, MV-4-11. The human AML MOLM13 cell line was generously provided by Dr. Yoshinobu Matsuo (Fujisaki Cell Center, Hayashibara Biochemical Labs, Okayama, Japan) and cultured in RPMI with 20% FBS instead of 10%. The human AML cell line MV-4-11 was obtained from the American Type Culture Collection (Manassas, VA, USA) D, Relative mRNA expression of FGFR1-4 was evaluated by QPCR and normalized relative to control mRNA GusB (value of 1). All experiments run in triplicate, error bars indicate standard deviation. E, A test-sample set of cytogenetically normal AML samples (GDS3329, N=79[325]) was queried for relative expression of FGFRs 1-4, FLT3, AXL and MET. The percentile rank expression for all samples is shown using a box-and-whiskers plot.
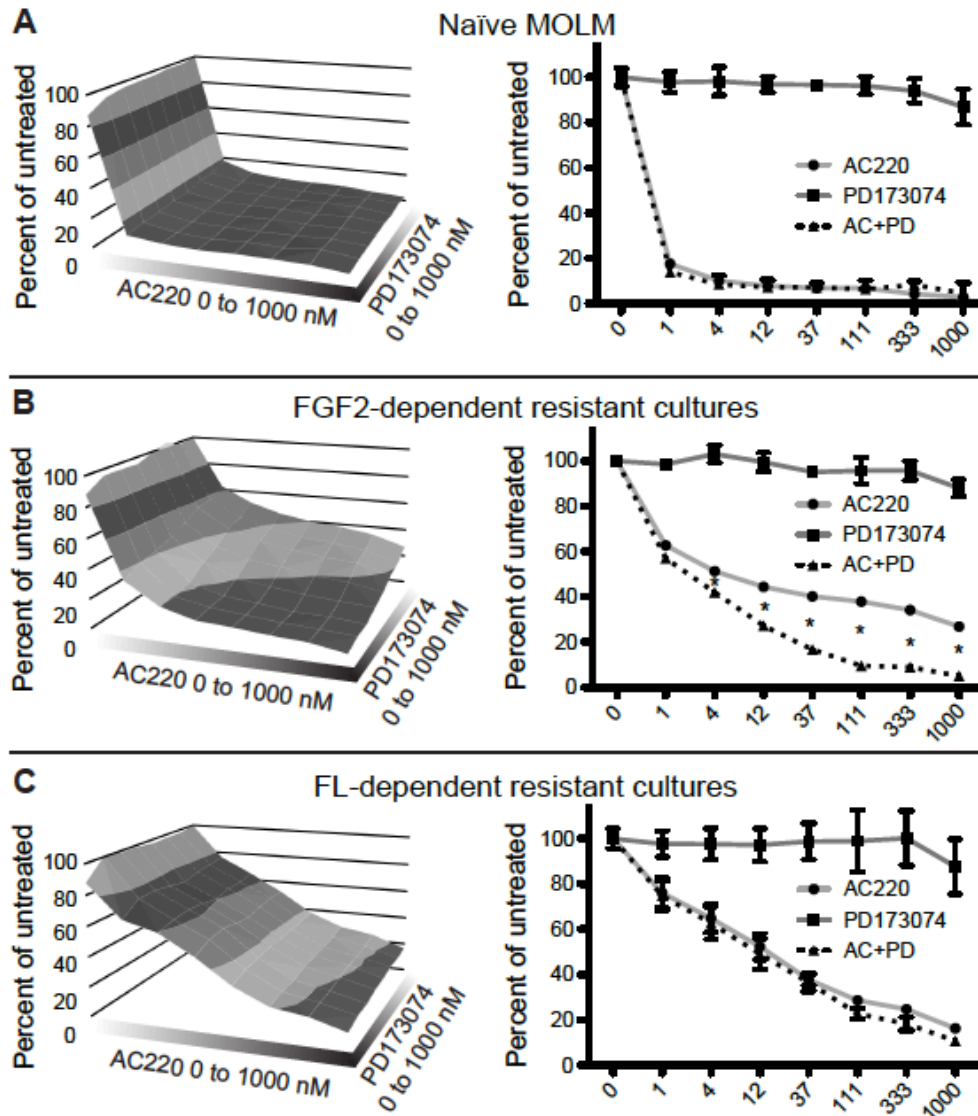
Figure 2.3.5 FGF2-dependent resistant cultures respond synergistically to combined FLT3 and FGFR inhibition.

A, Naïve MOLM14 cells in media alone were exposed to a matrix of an AC220 gradient (0, 1.4, 4, 12, 37, 111, 333, 1000 nM) combined with the FGFR inhibitor PD173074 (0, 1.4, 4, 12, 37, 111, 333, 1000 nM) and compared to B, FGF2- and C, FL-dependent resistant MOLM14 cells (Figure 2.3.1 C) in the same conditions. Viability was measured after 48 hours and average viability graphed as surface plots with gray scale denoting 20% increments. Separate graphs at right indicate viability in response to titrations of AC220 alone, PD173074 alone, and equimolar combination to highlight synergy. Calculation of the combination index for relevant drug concentrations is included in supplemental Table 2 and synergy is indicated by an *. All experiments were done in triplicate with average viability scaled to untreated condition (100%). Error bars represent standard deviation.

Table 2.3.1 Calculation of combination indexes to evaluate synergy.

Viability data as presented in Figure 2.3.5 B and C, representing AC220 and PD173074, were analyzed by Chou Talalay method to calculate the combination index using CompuSyn software. Values less than 1 indicate synergy. The data is color coded with green representing higher numerical values (no synergy) with yellow and orange indicating increased synergy (values <0.1 are highly synergistic).

		Combination Index	
AC220	PD173074	FGF2	FL
(nM)	(nM)	long-term	long-term
1.4	1.4	0.15253	1.12195
4.1	4.1	0.09498	0.85503
12	12	0.05107	0.65655
37	37	0.03199	0.63201
111	111	0.01863	0.34308
333	333	0.04671	0.53615
1000	1000	0.02815	0.35692
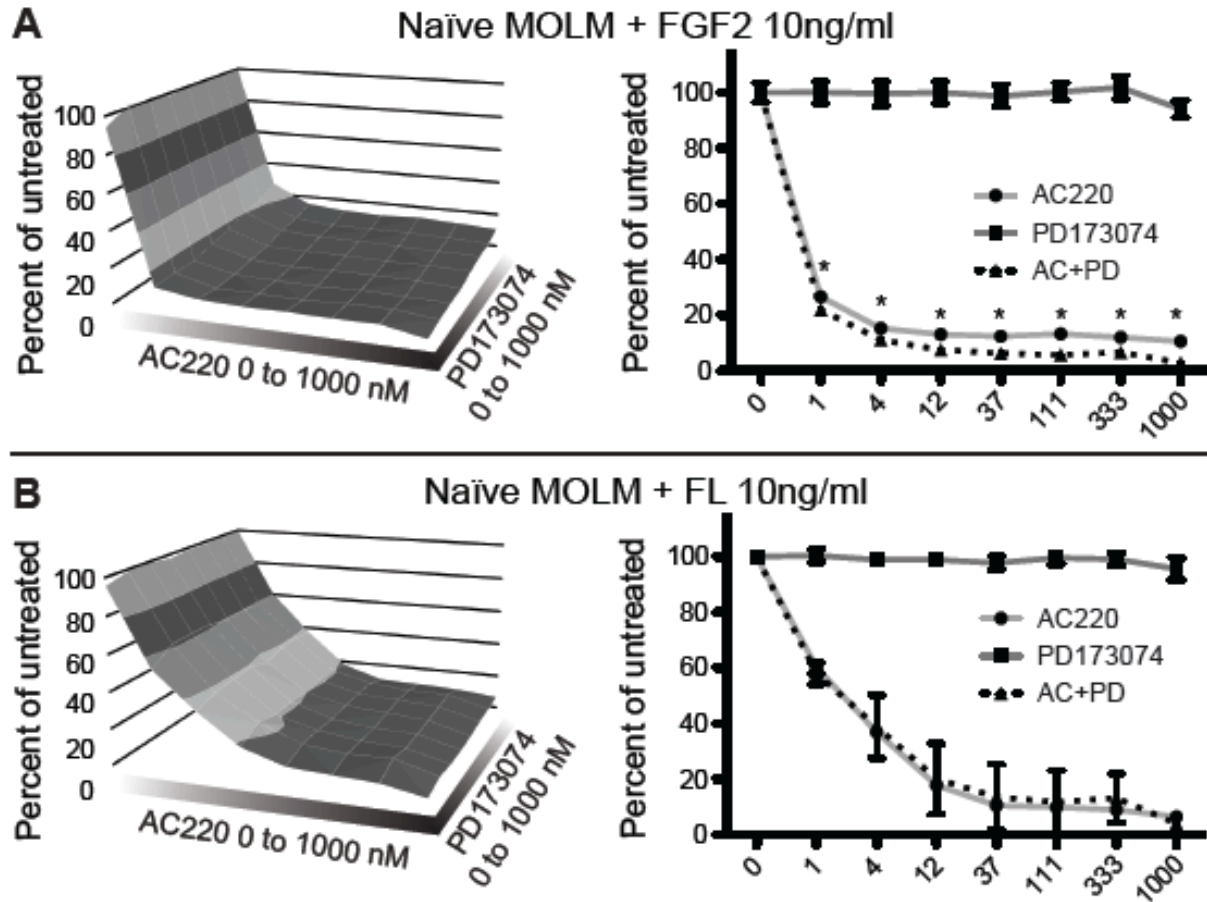
Figure 2.3.6 Matrix of AC220 and PD173074.
Naïve MOLM14 cells in media supplemented with A, 10ng/ml FGF2 or B, FL were exposed to a matrix of an AC220 gradient (0, 1.4, 4, 12, 37, 111, 333, 1000 nM) combined with the FGFR inhibitor PD173074 (0, 1.4, 4, 12, 37, 111, 333, 1000 nM). Only the cells with supplemented FGF2 had response to combination of AC220 and PD173074.
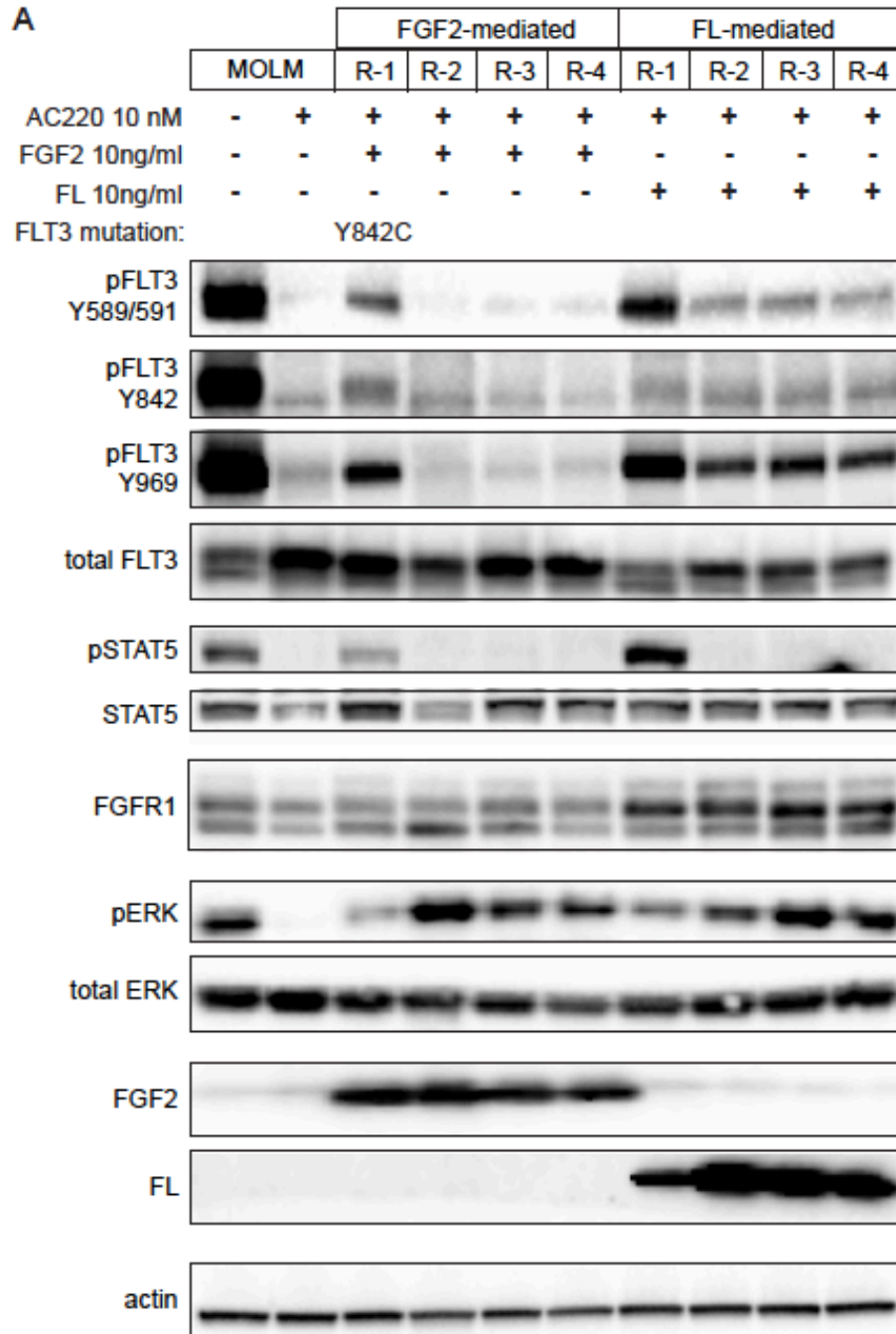
Figure 2.3.7 FGF2 and FL restore downstream FLT3 signaling, particularly the MAPK pathway.
A, Naïve MOLM14 cells were treated for 24 hours -/+ 10 nM AC220 (first two lanes) and compared to FGF2- and FL-dependent resistant cells (grown continuously in FGF2 or FL, lanes 3-10). The FGF2- and FL-dependent resistant cells were harvested 24 hours after addition of fresh media, recombinant protein and AC220. The cells were then lysed as described with Western blot analysis as per Materials and Methods. The FGF2-dependent resistant culture that developed a Y842C mutation is indicated.
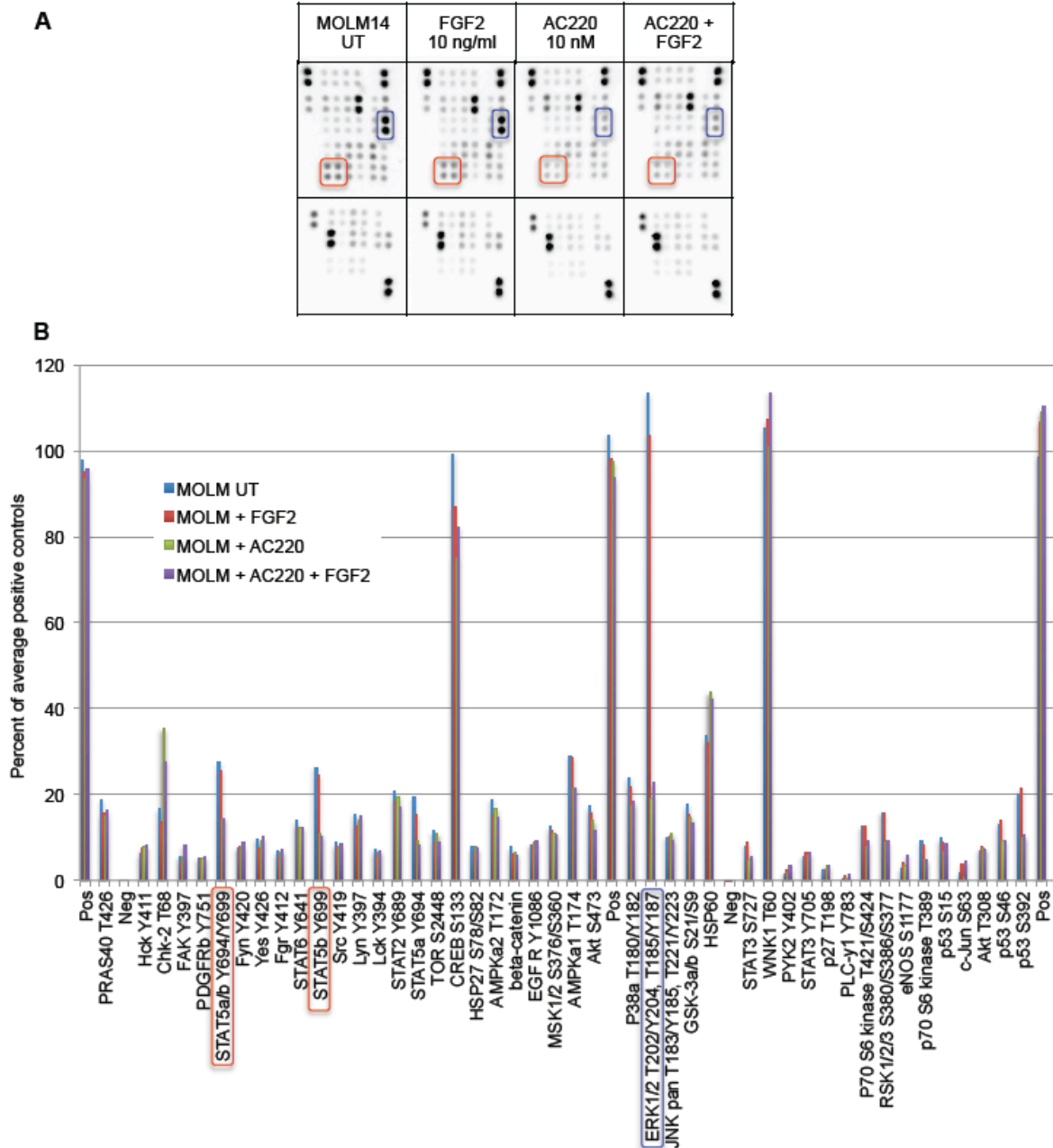
Figure 2.3.8 STAT5 and ERK are downstream targets of FLT3.
A, Untreated MOLM14 cells were incubated in media alone or media supplemented with 10 ng/ml FGF2 and then were left either untreated or treated with 10 nM AC220 for 24 hours. The cells were lysed and used to probe a human phospho-kinase array per manufacturer's instruction (Proteome Profiler, RnD). Each phospho-protein in the array contains a pair of spots. The pSTAT5 (two different antibodies) and the pERK spots are highlighted in red and blue, respectively, to demonstrate the effects of AC220 on these two phospho-proteins. B, The phospho-protein signals from panel A were quantified for each spot, values averaged (two spots per phospho-protein), then normalized to the positive and negative controls on the blots. The data is presented as percent of the positive control for each sample tested.
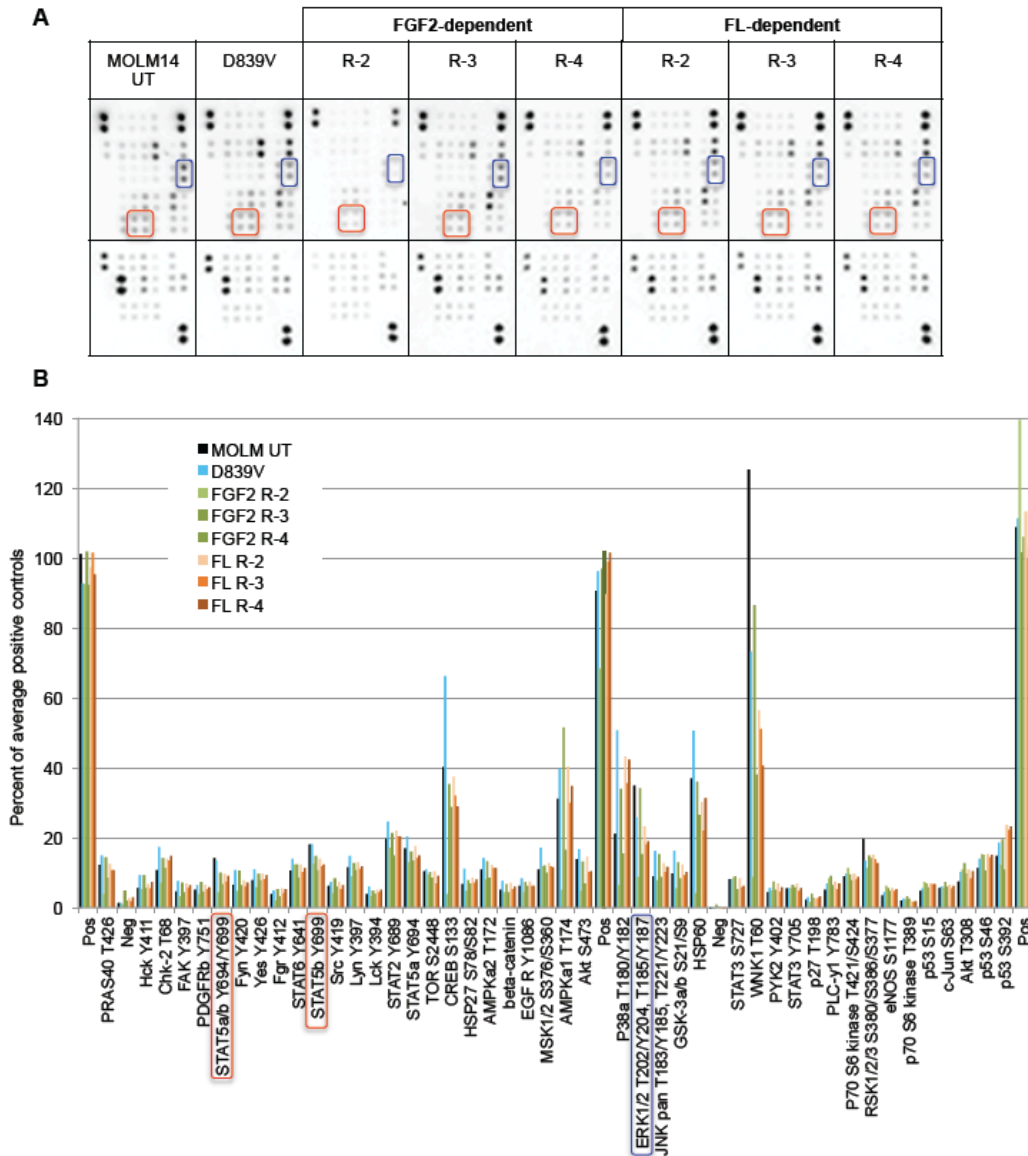
Figure 2.3.9 Resistant long-term cultures have very similar phosphorylated proteins to naïve MOLM14 cells.

A, Untreated MOLM14 cells, a long-term resistant culture that developed a D839V mutation, three FGF2-supplemented long-term cultures, three FL-supplemented long-term cultures were lysed and used to probe a human phospho-kinase array per manufacturer's instruction (Proteome Profiler, RnD). Each phospho-protein in the array contains a pair of spots. The pSTAT5 (two different antibodies) and the pERK spots are highlighted in red and blue, respectively. Naïve MOLM14 and resistant cells have largely the same phosphorylation pattern, particularly with respect to pERK. B, The phospho-protein signals from panel A were quantified for each spot, values averaged (two spots per phospho-protein), then normalized to the positive and negative controls on the blots. The data is presented as percent of the positive control for each sample tested.
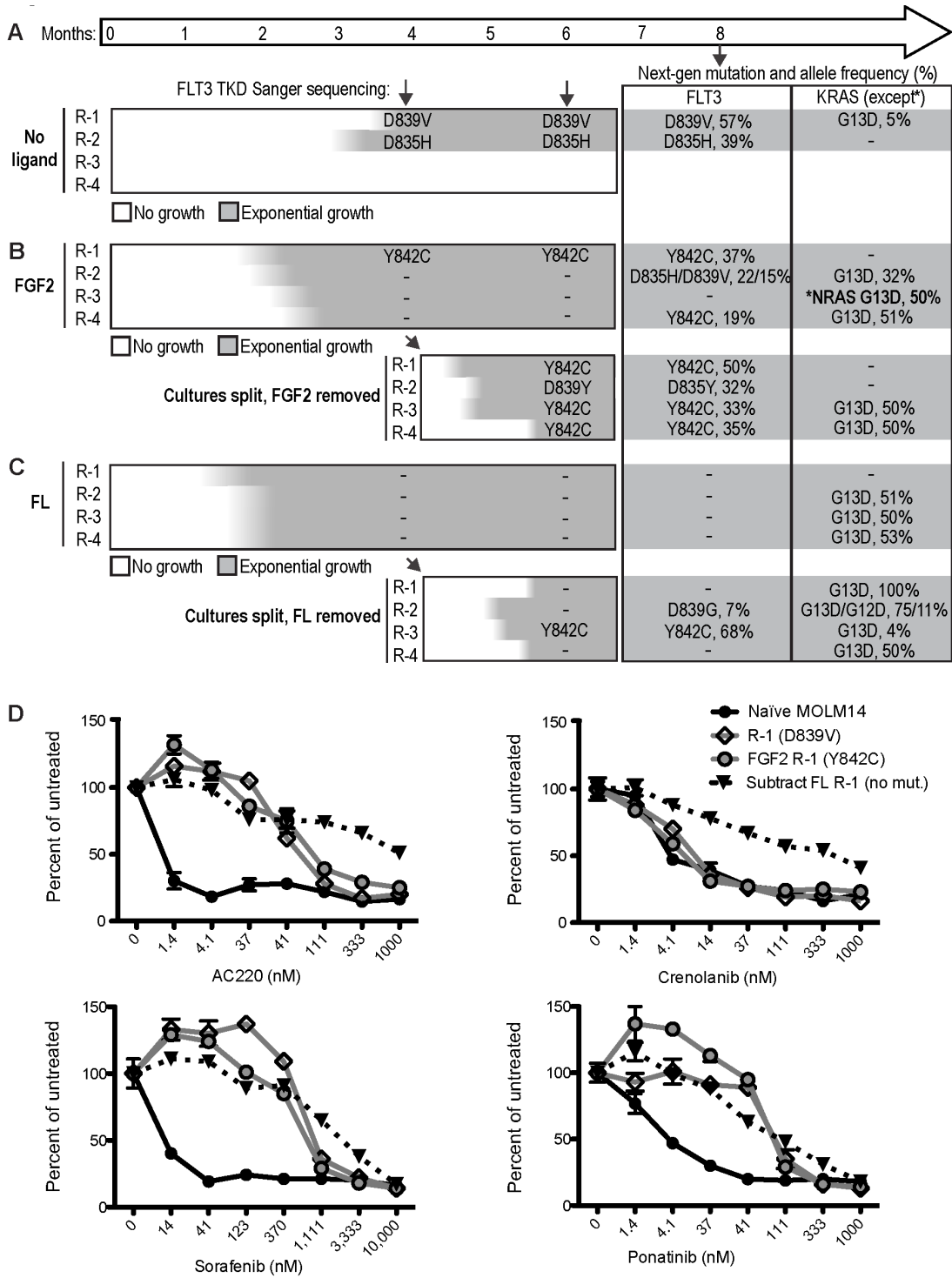
Figure 2.3.10 Removing FL or FGF2 from FGF2- or FL-dependent resistant cultures results in ligand-independent resistance mediated by mutation of FLT3, MAPK pathway genes, or through a non-mutational mechanism.

The time to development of exponential growth was plotted over time for the extended cultures in Figure 1C and time to acquisition of mutations by either Sanger or deep next-generation sequencing (average read depth ~1500) is indicated by arrows. If a mutation could not be detected it is indicated with -. All mutations detected by next-generation sequencing that were not present in naïve MOLM14 cells are shown on the right. Of note, the KRAS G13D C>T mutation was detected in 2/659 reads in the naïve MOLM14 cells and thus may be present at very low level. A, MOLM14 cells cultured in media alone (no ligand) developed exponential growth later than FGF2- and FL-dependent cultures (panels B and C) and were found to have resistance mutations, D839V and D835H, shortly after resuming exponential growth. B, FGF2-dependent and C, FL-dependent resistant cultures (cultured continuously in 10 ng/ml FGF2/FL and 10 nM AC220) were split at 4 months and $1x10^7$ cells placed into fresh media without recombinant protein with 10 nM AC220. Fresh media and 10 nM AC220 were replaced every 2-3 days over the indicated time period and viable cell number was analyzed using Guava ViaCount and plotted over time. D, Naïve MOLM14 cells, resistant cells with the FLT3 D839V mutation, FGF2-mediated resistant R1 cells with FLT3 D842C mutation, and non-mutated resistant MOLM14 cells (FL R1 after FL subtraction) were exposed to a gradient of FLT3 inhibitors: quizartinib, crenolanib, sorafenib, and sunitinib and viability was measured after 48 hours by MTS assay. Experiments in panel D were done in triplicate with average viability scaled relative to untreated cells (100%) and error bars represent standard deviation.
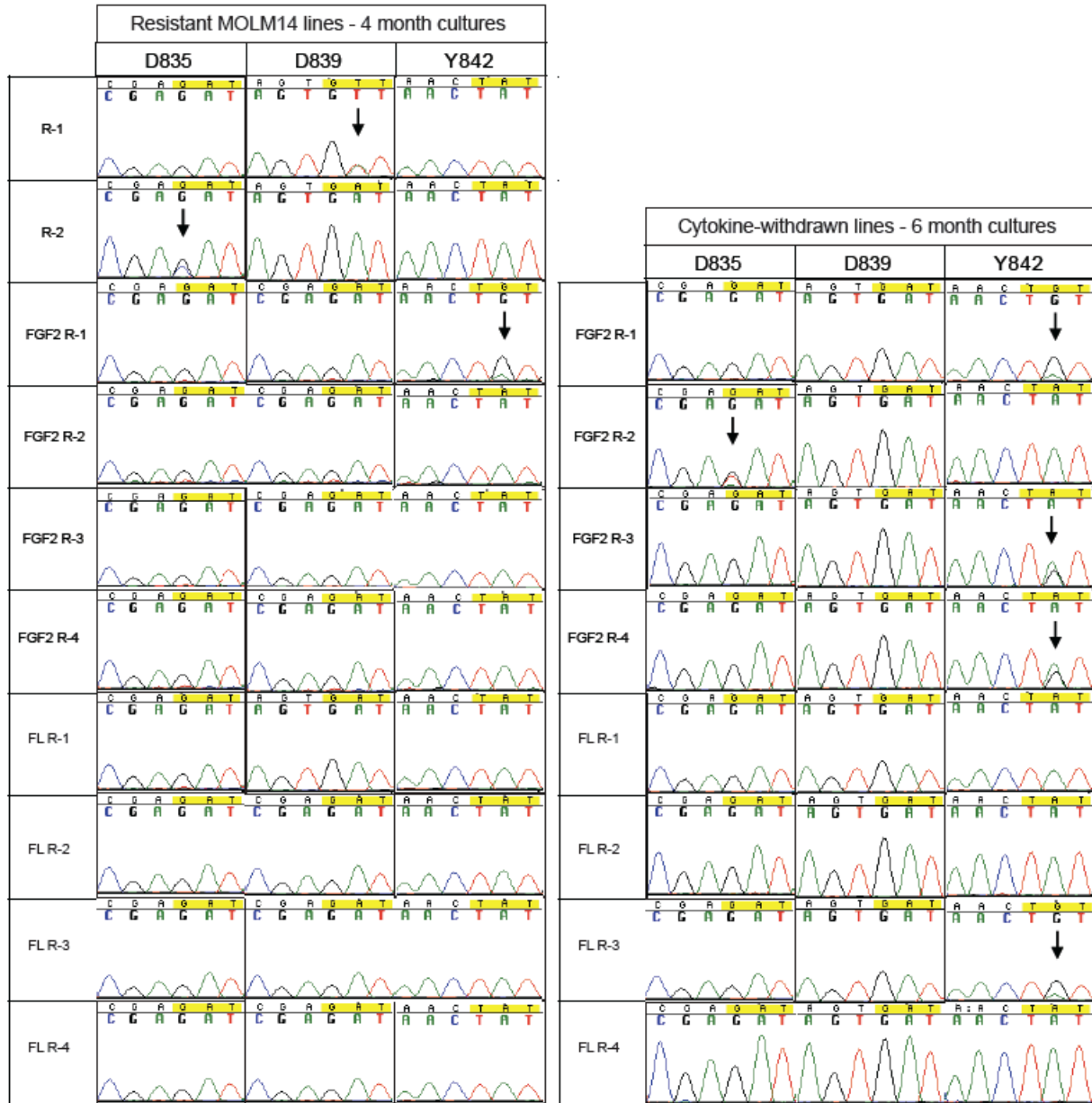
Figure 2.3.11 Identification of FLT3 point mutations by Sanger sequencing.
Primers were used to amplify the FLT3 kinase domain and for sequencing as previously described[308]. Sanger sequencing was performed and alignment to the native FLT3 sequence performed with Sequencher Software (Gene Codes Corporation, Ann Arbor, MI, USA).
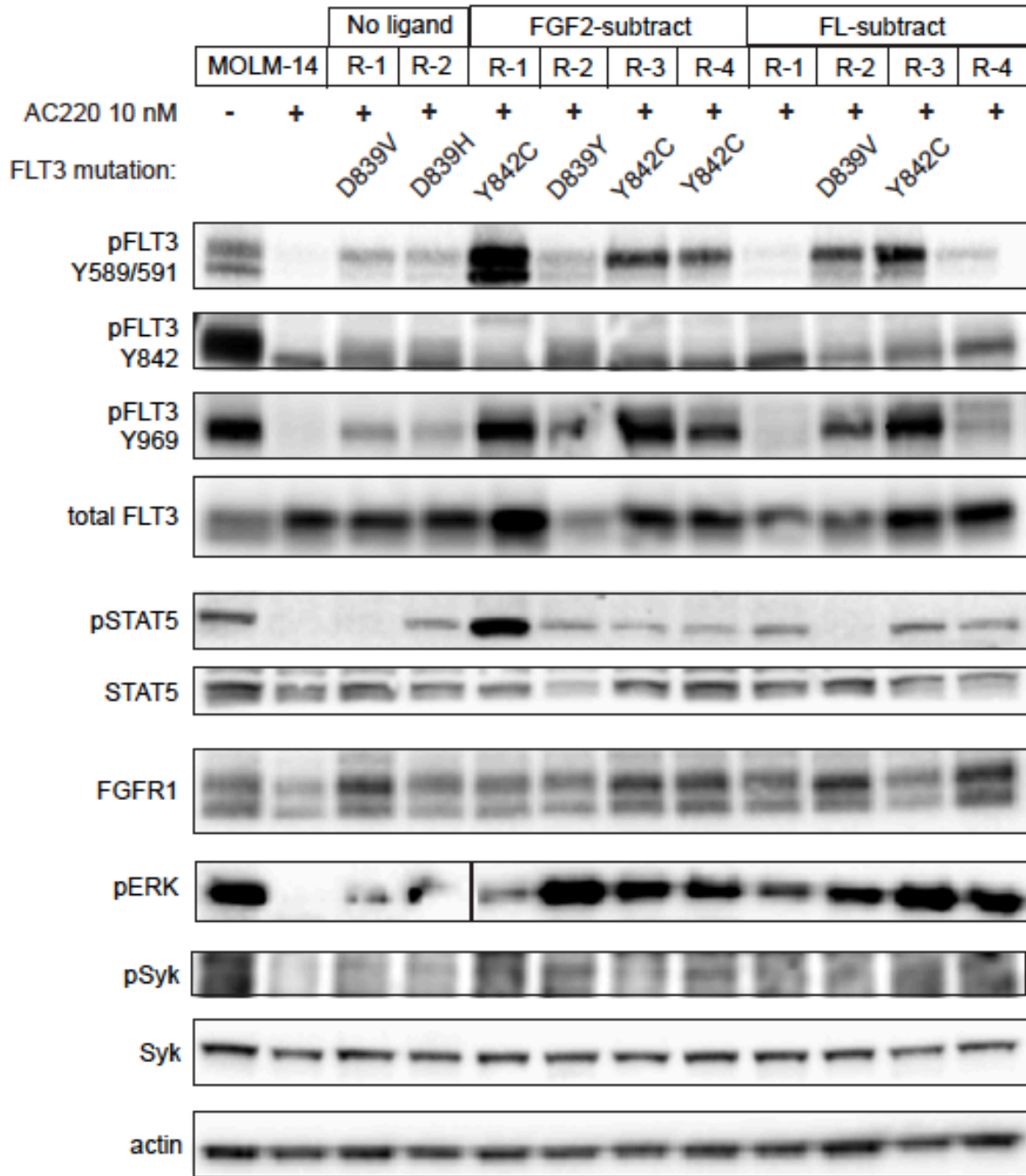
Figure 2.3.12 Removing FL or FGF2 from long-term resistant cultures results in partial reactivation of FLT3 either through point mutation or non-mutational activation.
Control MOLM14 cells were treated for 24 hours -/+ 10 nM AC220 (first two lanes). Long-term resistant cultures grown in absence of ligand (Figure 2.3.1 C) are shown in lanes 3 and 4. Long-term cultured cells grown continuously in FGF2 or FL were transitioned to fresh media and AC220 without ligand are shown in lanes 5-12. Mutations of FLT3 tyrosine kinase domain are indicated if present. All cells were prepared as per Materials and Methods.
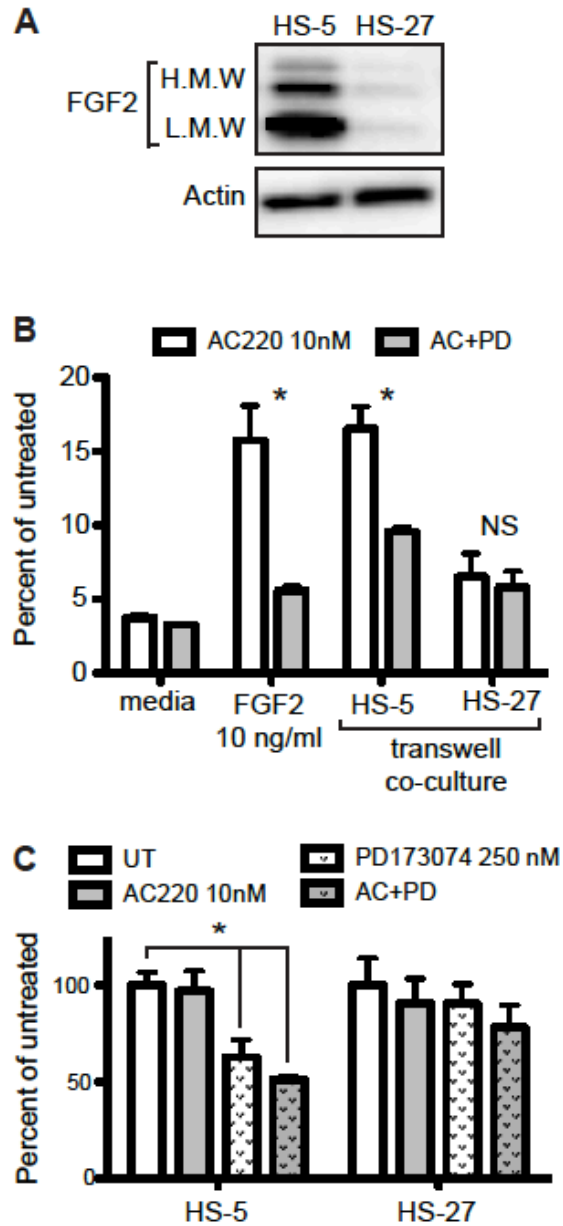
Figure 2.3.13 FGFR inhibitors overcome the protective effects of FGF2-expressing stroma (HS-5) in co-culture assays.
A, The human stromal cell lines HS-5 and HS-27 were analyzed for FGF2 expression by Western blot and labeled as in Figure 6D. B, MOLM14 cells were cultured in media alone, 10 ng/ml FGF2, or in 1 μm transwells over HS-5 or HS-27a stromal cell lines. The cells were treated with 10 nM AC220 and/or 250 nM PD173074 as indicated and MOLM14 cells were analyzed for viable cell number after 4 days. Viable cells were plotted as percentage of untreated control. C, The corresponding stromal cells from the transwell co-culture experiments were also evaluated by MTS assay for viability. Results are shown relative to the untreated condition. All experiments were done in triplicate, error bars represent standard deviation, and * indicates p<0.05.
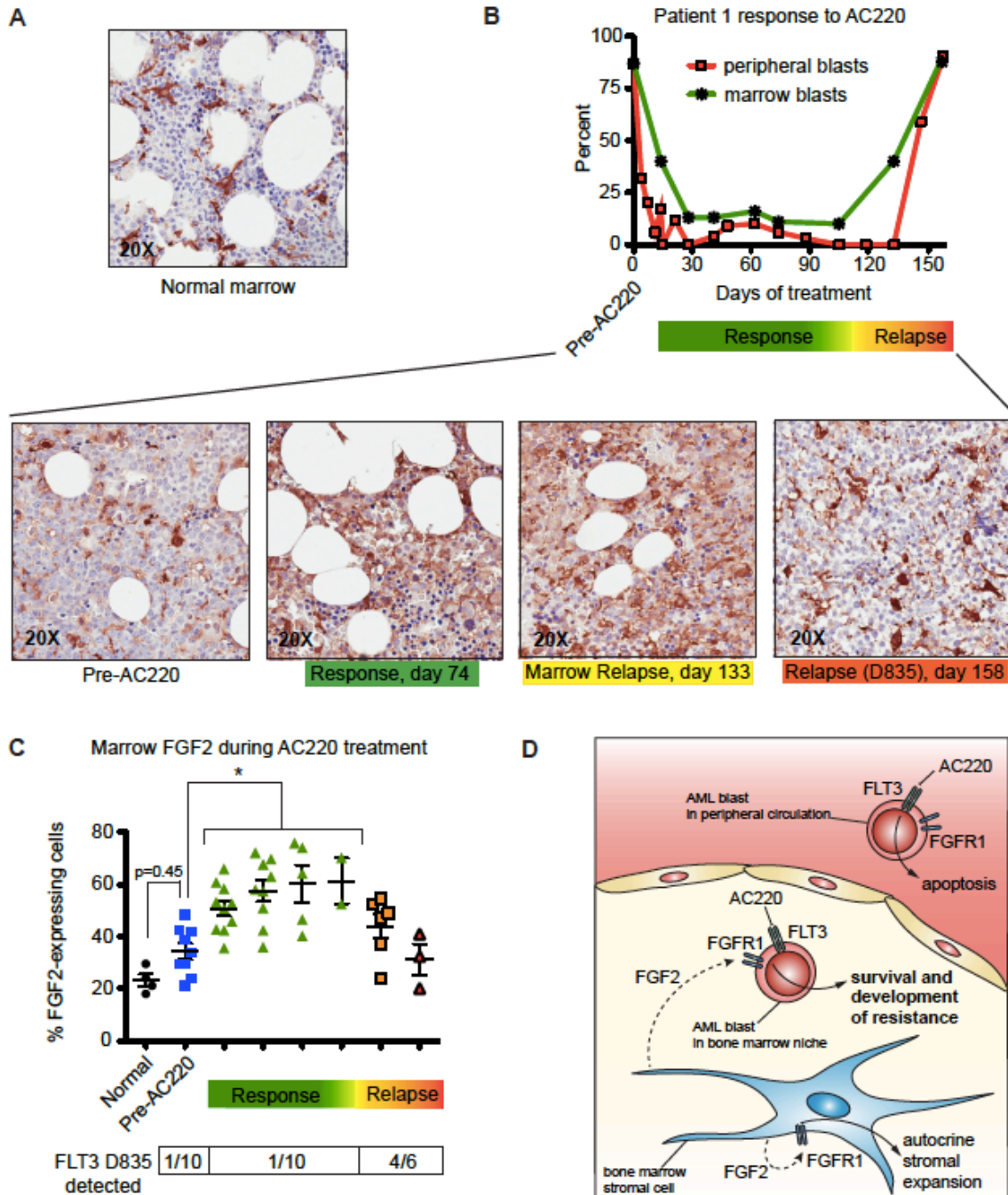
Figure 2.3.14 Bone marrow FGF2 increases during AC220 treatment and peaks prior to development of resistance.

A, Normal bone marrow biopsy (hip replacement) stained by immunohistochemistry (IHC) for FGF2 indicating stromal expression of FGF2 as described in Materials and Methods. B, Graph of peripheral blood and marrow blast percentage over time of representative patient treated with AC220. Response to therapy is indicated with green, early relapse in marrow indicated in yellow/orange, and peripheral blood relapse indicated in red. Sequential bone marrow biopsies

from this patient were stained for FGF2 by IHC and are shown below. This patient developed a FLT3 mutation at D835, which was detected at day 158 as indicated. C, Quantification of marrow FGF2 by IHC of all evaluable patients treated with AC220. The marrows were analyzed with Aperio ImageScope software to quantify total number of cells and percent that expressed FGF2. The line indicates the median value. Statistically significant differences were evaluated using a 2-tailed t-test. * indicates $p<0.05$. The number of patients and the presence or absence of FLT3 mutations are indicated below. Table 2.3.2 provides more detail about each patient. * indicates $p<0.05$. D, Model of FGF2 paracrine-mediated protection of leukemia cells.

Table 2.3.2 Patient characteristics studied by immunohistochemistry (IHC).
Patients treated with AC220 on phase II clinical trial with multiple bone marrow biopsies that were evaluable by IHC. Duration of AC220 considered continued decrease or stability in total marrow leukemia blasts. Marrows with increased leukemia blasts considered resistance (marrows usually one month apart). D835 mutations determined by PCR-based test (indicated as D835) or direct sequencing with mutated amino acid indicated (e.g. D835N). N/A indicates there were no D835 studies performed. Abbreviations: Ind=Induction, Cons=Consolidation, Salv=Salvage, and Allo SCT=Allogeneic stem cell transplant.

Age	Prior therapies	AC220 response (months)	D835 mutation pre-AC220	D835 mutation post-AC220	Clinical outcome
60	Ind	2	None	N/A	Allo SCT
66	Ind, Cons, Salv	3.5	None	ND	Allo SCT
66	Ind, Cons	4	None	None	Allo SCT
78	Decitabine	3	None	D835V	Resistance: 4 months
62	Ind, Cons	3	None	D835V and D835N	Resistance: 4 months
69	Ind, Cons	4	None	D835Y	Resistance: 5 months
71	Ind, Cons	5	None	None	Resistance: 6 months
70	Ind, Cons	2	None	N/A	Resistance: 4 months
56	Ind, Salv	3.5	D835	D835	Resistance: 4 months
60	Allo SCT	2	None	None	AC220 intolerance
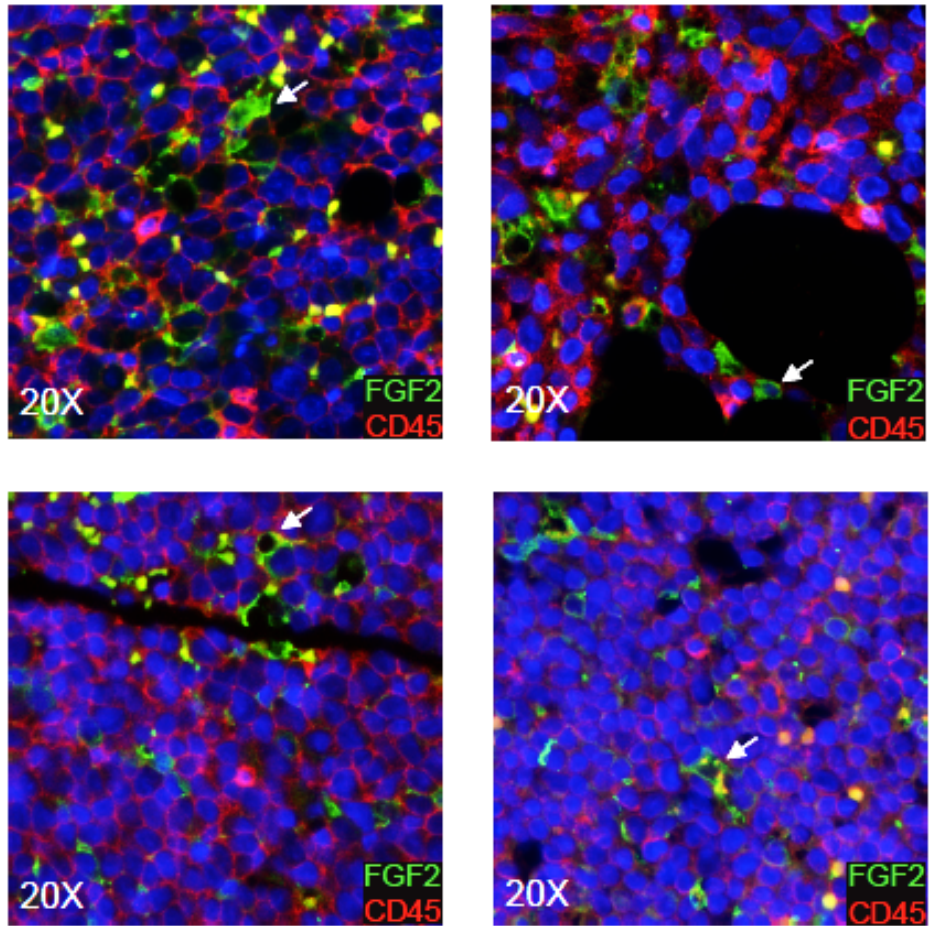
Figure 2.3.15 FGF2 is localized to bone marrow stromal cells and not in hematopoietic cells.
All patient specimens were obtained with informed consent of the patients on protocols approved by the Institutional Review Board of Oregon Health & Science University. Immunofluorescence for FGF2 (green) and CD45 (red) was performed as previously described{Traer, 2014 #193}. Representative bone marrow core biopsy sections of 4 FLT3-ITD AML patients are shown (see Figure 7).

	Sup.		Pellet	
Start	anti-FLT3	IgG	anti-FLT3	IgG

FLT3

FGFR1

* heavy chain
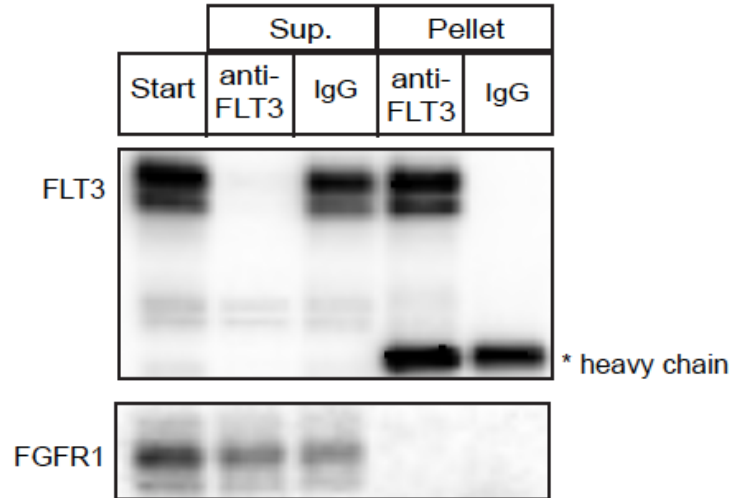
Figure 2.3.16 FGFR1 and FLT3 do not interact directly.

MOLM14 cell lysates were incubated with protein A beads coupled to anti-FLT3 antibody or control polyclonal antibody. The starting material (input) is shown in lane 1; the supernatant in lanes 2 and 3; and the immunoprecipitated protein in lanes 4 and 5. FLT3 immunoprecipitates with antibody but FGFR1 remains in the supernatant fraction.

3   Autocrine Function of FGF2 in Bone Marrow

Stroma

This chapter is based on one manuscript describing the secretion and delivery of FGF2 from bone marrow stroma to leukemia cells, and the autocrine function of FGF2 in maintaining a protective stromal phenotype.

3.1 FGF2 Regulates Release of Leukemia-Protective Exosomes from Bone Marrow Stromal Cells

Nathalie Javidi-Sharifi[†], Jacqueline Martinez[†], Isabel English, Shelton Viola, Danielle Jorgens, Brian Druker, and Elie Traer

[†]These authors contributed equally to this work.

Work not submitted for publication concerning signaling pathways downstream of FGFR1 involved in exosome production is presented in section 3.1.3.8.

3.1.1 Abstract

Bone marrow stromal cells communicate with leukemia cells and provide a protective niche during various forms of chemotherapy, including tyrosine kinase inhibitor (TKI) treatment. Protective signaling initiated by cytokines and growth factors in this niche may eventually lead to resistance and disease relapse. We previously identified fibroblast growth factor 2 (FGF2) as a protective signal in several types of leukemia and other malignancies during TKI therapy. FGF2 has previously been implicated as an autocrine regulator of bone marrow stromal growth and function. Here, we demonstrate that exosomes secreted by stromal cells in part account for the protective effect of stroma-conditioned media, and that FGF2 is contained in these exosomes. FGFR inhibition leads to reduced expansion of FGF2-expressing stroma and decreases secretion of FGF2-containing exosomes, resulting in attenuated protection of leukemia cells. We conclude that exosomes are important purveyors of protective signaling in the leukemia microenvironment. FGFR-inhibition may be a clinically relevant option to modulate stromal function and overcome microenvironment-mediated resistance.

3.1.2 Introduction

Tyrosine kinase inhibitors have revolutionized the treatment of chronic myeloid leukemia (CML) and show promise in acute myelogenous leukemia (AML) therapy.

175

However, resistance to single-agent therapy in AML develops within a few months. Cell-intrinsic resistance is often due to secondary mutations in the targeted kinase that prevent drug binding. In absence of these secondary mutations, resistance is frequently attributed to ligands in the tumor microenvironment that activate alternative survival pathways[131], [326]. This type of environment-mediated resistance, which also protects cells from the initial cytotoxic or cytostatic effects of therapy, may be essential for the development of any type of acquired resistance[266].

1.1.1.47 *FGF2 in maintenance of MSC function*

Mesenchymal stem cells (MSCs) are part of the bone marrow stroma and contribute to the niche that is important for normal hematopoiesis as well as for the maintenance of leukemic stem cells (LSCs)[255], [327]. The crosstalk between MSCs and LSCs has been implicated in cancer resistance, both to cytotoxic chemotherapy and to targeted agents. Previous studies into the mechanisms of resistance focused on soluble cytokines and growth factors secreted by normal stroma as the main paracrine protective agents[328]. However, evidence is mounting that hematologic malignancies are associated with profound phenotypic changes in the neighboring stromal cells, including altered differentiation potential and acquisition of features similar to cancer-associated fibroblasts[193], [329], [330].

We and others have demonstrated that fibroblast growth factor 2 (FGF2) protects hematologic malignancies from the effects of tyrosine kinase inhibitor (TKI) therapy[219], [220], [322]. In addition, FGF2 is essential for stress hematopoiesis after chemotherapy or irradiation[162], [281]. Despite its important roles in physiology and pathology, several aspects of FGF2 biology are poorly understood. FGF2 is not a classic secreted cytokine, and several mechanisms for cell-contact independent delivery have been proposed(Phosphatidylinositol 4,5-bisphosphate (PI(4,5)P2)-dependent oligomerization of fibroblast growth factor 2 (FGF2) triggers the formation of a lipidic membrane pore implicated in unconventional secretion[67], [68], [331]. Additionally, while FGF2 directly stimulates myeloid colony formation, there are also reports suggesting that FGF2 indirectly regulates hematopoiesis by stimulating stromal cells to produce cytokines.

In addition to soluble cytokines and direct cell-to-cell interactions, exosomes are increasingly understood to act as versatile messengers between stroma and leukemia cells. To date, inhibition of exosome secretion has not been proposed as a therapeutic target, and indeed no cell type-specific inhibitors exist. We present evidence that exosomes secreted by bone marrow stromal cells contain FGF2 and protect leukemia cells from the effects of targeted therapy. Further, FGFR signaling functions in an autocrine manner to promote the secretion of exosomes by stromal cells. Our findings

suggest that FGFR inhibition may be an attractive therapeutic target with the potential to disrupt the protective stroma-leukemia interaction and prevent drug resistance.

3.1.3   Results

1.1.1.48 Stromal cell extracellular vesicles protect leukemia

We previously noted that FGF2 is upregulated in bone marrow stromal cells of patients who developed resistance to TKI therapy in both CML and AML with internal tandem duplication in the receptor tyrosine kinase FLT3 (FLT3 ITD)[220]. The human stromal cell line HS-5 expresses high levels of FGF2 in addition to other soluble cytokines such as IL-5, IL-8 and HGF[316]. Since FGF2 is not a classically secreted cytokine, we hypothesized that the protective capacity of HS-5 conditioned media could be localized to the pelleted fraction after ultracentrifugation. HS-5 conditioned media was cleared of detached cells and large cell fragments by initial centrifugation and then ultracentrifuged at sufficient speed to sediment small extracellular vesicles (ECVs). The conditioned media was separated into a supernatant (S100) and a pellet fraction (P100). We compared the protective effect of unfractionated conditioned media, as well as S100 and P100 fractions on the proliferation of two leukemia cell lines, MOLM14 (FLT3 ITD+ AML) and K562 (CML), in the presence of their respective TKIs, quizartinib and imatinib (Figures 3.1.1 A and 1B). In both instances, the protective capacity of the S100 fraction was lower than complete conditioned media or P100. We observed no

significant difference in the capacity of complete conditioned media versus P100 to rescue proliferation of K562 after exposure to imatinib (Figure 3.1.1 A). Moreover, the P100 fraction protected MOLM14 cells even more effectively from the effects of quizartinib than complete conditioned media (Figure 3.1.1 B). These results indicate that the protective effect of HS-5 conditioned media is partly mediated by ECVs.

We next asked whether ECVs produced by HS-5 cells could be taken up by K562 and MOLM14 leukemia cells. Fluorescent confocal microscopy of HS-5 ECVs stained with a red lipophilic tracer (DiI) and added to K562 or MOLM14 cells (Figure 3.1.1 C) stained with a green lipophilic tracer (DiO) showed that ECVs were endocytosed whole and localized to the intracellular vesicle transport pathway. These experiments demonstrate that protective factors from bone marrow stroma can be conveyed to leukemia cells via ECVs.

1.1.1.49 *FGF2 in stromal cell exosomes*

As previously noted, we found high levels of FGF2 in the cell lysate of HS-5, while a non-protective stromal cell line from the same donor, HS-27, expressed no FGF2 (Figure 3.1.2 A). Having observed the strong protective effect of the pelleted fraction of HS-5 conditioned media, we now quantified FGF2 in S100 and P100 fractions of both HS-5 and HS-27 by Western Blot (Figure 3.1.2 B). As expected, FGF2 was not detected in the supernatant fractions, but remained in the pelleted fraction of HS-5 even after a wash

step. No FGF2 was detected in either supernatant or pellet of HS-27 conditioned media. This is in contrast to cytokines in HS-5 conditioned media that are found in the S100 fraction, such as stem cell factor, interleukin (IL)-6, IL-8, IL-11, macrophage colony-stimulating factor, and granulocyte macrophage colony-stimulating factor - all of which have been reported to contribute to the protective effect on leukemia cells[318], [328]: We compared the cytokine profiles of HS-5 S100 and P100 using a Luminex bead-based multiplexing assay (Figure 3.1.2 C). Of all cytokines included in the assay, only FGF2 was significantly enriched in the pellet fraction.

While ultracentrifugation separates soluble cytokines from insoluble factors, we wanted to determine whether a specific vesicle population or extracellular matrix (ECM) components conferred the protection. We therefore collected fractions of HS-5 P100 on a discontinuous sucrose gradient and quantified FGF2 and various cell compartment-specific molecular markers by immunoblot (Figure 3.1.2 D and pictorial in Figure 3.1.3 D). FGF2 was most highly enriched in the 15-30% sucrose fraction, which also contained the exosome-specific markers CD9 and tsg101. Conversely, fibronectin, an ECM component, did not co-localize with FGF2. Lamin A/C, calreticulin and Bcl-XL, markers of nuclear, endoplasmic reticulum and mitochondrial fractions respectively, were present at low levels in the starting material and were recovered in the 45-60% sucrose fraction. This fraction likely also contains larger microvesicles and apoptotic bodies.

Since FGF2 can be immobilized on the cell surface via heparan sulfate, it may be bound

to the exosome exterior or may be contained as cargo within the exosome. Proteins in organelles or vesicles are protected from proteases such as Proteinase K. We therefore incubated recombinant FGF2, exosomes isolated from HS-5 or HS-27 cells, as well as whole HS-5 cells with Proteinase K and probed for FGF2 by immunoblot (Figure 3.1.2 E). While recombinant FGF2 was entirely degraded, we observed a residual band at the molecular weight of undigested FGF2 in both HS-5 exosomes and whole cells. We repeated this experiment using only HS-5 exosomes, exposing either to Proteinase K alone or Proteinase K and a membrane-disrupting detergent, 0.1% Triton X-100. We again observed that a fraction of FGF2 was protected from digestion while exosomes remained intact, but not after the addition of 0.1% Triton X-100. We noted that the exosomal transmembrane proteins CD9 and tsg101 were degraded upon addition of Proteinase K with or without detergent. We concluded that FGF2 is localized both to the exosome membrane and the vesicle interior.

1.1.1.50 Protective stromal cells overproduce extracellular vesicles

In addition to the qualitative differences between conditioned media fractions from HS-5 and HS-27 cells, we suspected that extracellular vesicles might be more numerous in HS-5 conditioned media. Exosomes and other small vesicles can be quantified and characterized according to size, surface marker expression, content, and appearance on electron microscopy. We chose several orthogonal methods to quantify vesicles in conditioned media. First, we used nanoparticle tracking analysis to quantify and

compare ultracentrifuged conditioned media of HS-5 and HS-27 (Figure 3.1.3 A). We

consistently observed over twofold excess of vesicles produced by HS-5 compared to

HS-27 cells. In parallel, we employed a new flow cytometry-based technique using two

fluorescent dyes that bind hydrophobic proteins and nucleic acids (Figure 3.1.3 B).

Particles that contained both protein and nucleic acid were quantified in HS-5 and HS-

27 conditioned media and again confirmed to be more numerous in HS-5. Both flow-

based quantification as well as tracking analysis revealed a reproducible two-to-

threefold higher particle count in HS-5 compared to HS-27 conditioned media.

Although several new techniques such as the ones described above are emerging for the

quantification of small particles, electron microscopy still remains the gold standard.

We therefore performed negative stain transmission electron microscopy on HS-5 and

HS-27 ultracentrifuged conditioned media (Figure 3.1.3 C). Vesicles in both samples

exhibited the cup-shape appearance characteristic for exosomes, and lipid bilayers were

visible at high magnification. Vesicle shape and size (round, 30-100 nm diameter) also

conformed to the definition of exosomes. Quantification of exosomes on electron

microscopy confirmed an over 1.5-fold enrichment of exosomes in HS-5 conditioned

media over HS-27.

Finally, we performed sucrose gradient fractionation of HS-5 and HS-27 conditioned

media and detected cell compartment and exosome-specific markers by immunoblot

(Figure 3.1.3 E). Exosomes are expected to equilibrate primarily at the 15-30% sucrose

interface (Figure 3.1.3 D). Indeed, we found that the exosomal marker CD9 appeared in this fraction in both HS-5 and HS-27 samples. Although contaminants such as fibronectin, lamin A/C, calreticulin and Bcl-XL were more abundant in HS-27 starting material, CD9 was detected at much lower intensity and another exosomal marker, tsg101, could not be detected at all in HS-27 conditioned media. Actin was also more abundant in all vesicle fractions of HS-5 conditioned media, indicating that HS-5 cells may overproduce extracellular vesicles of varying sizes; however, FGF2 appears to be contained preferentially in exosomes over other vesicles. Overall, each quantification method revealed that HS-5 cells produce more extracellular vesicles, including a population that is consistent with the definition of exosomes as determined by size, appearance and molecular cargo.

1.1.1.51 FGF signaling regulates stromal cell growth and function

We previously observed that the protective effect of FGF2 on leukemia cells exposed to TKI could be eliminated by adding an FGFR inhibitor[220]. In Figures 3.1.1 and 3.1.2, we mapped the protective capacity of HS-5 cells to exosomes and demonstrated that FGF2 is contained in these vesicles. We hypothesized that if FGF2 delivered by exosomes was the main mediator of HS-5 protection, the addition of FGFR inhibitor PD173074 should block the protection. However, when adding the combination of HS-5 conditioned media and PD173074 to MOLM14 cells exposed to quizartinib, we observed only a minor reduction in protection compared to conditioned media alone

(Figure 3.1.4 A). Since HS-5 cells express high levels of both FGF2 (Figure 3.1.2 A) and FGFR1 (Figure 3.1.4 B), we suspected that FGFR signaling might regulate their protective phenotype in an autocrine manner. We therefore pre-treated HS-5 cells with PD173074 and added conditioned media to MOLM14 cells in the presence of quizartinib. Pre-treatment with an FGFR inhibitor led to a marked reduction in conditioned media protection (Figure 3.1.4 A).

We next sought to examine more closely the effect of FGFR inhibition on stromal cell growth and cellular phenotype. We confirmed that there was no significant decrease in viability or proliferation in either HS-5 or HS-27 cells after 72h exposure to PD173074 (Figure 3.1.4 C). However, when HS-5 cells were exposed to PD173074 continuously for 15 days, cell doubling time decreased dramatically (top panel Figure 3.1.4 D). In contrast, HS-27 cell doubling was unaffected by FGFR inhibition (bottom panel Figure 3.1.4 D). Lastly, we noted a pronounced change in morphology in HS-5 cells exposed to PD173074. HS-5 cells became less refractive and larger after FGFR inhibition (Figure 3.1.4 E). Size differences were quantified using CellProfiler software (Figure 3.1.4 F). Addition of PD173074 had no effect on HS-27 morphology or size (Figure 3.1.4 E and data not shown). Taken together, these results indicate that FGFR inhibition alters HS-5 cell growth dynamics, morphology, and protective capacity, but has no effect on FGF-low, non-protective HS-27 cells.

While we and others have demonstrated the importance of FGF signaling for stromal cell lines and ex vivo cultures, the endogenous expression of FGF2 and its receptors in stroma from AML patients is unknown. We utilized a collection of primary patient stroma cultured from leukemia patient bone marrow biopsies to determine the expression levels of FGF2 and FGFR family members by quantitative RT-PCR (Figure 3.1.4 G). We found that FGFR1 and FGF2 transcripts were present in primary stroma samples, while other FGFR family members were not expressed. We found a positive correlation between FGFR1 and FGF2 expression (Figure 3.1.4 H, r^2=0.5683 and p<0.0001 on nonparametric correlation). The finding both receptor and ligand are abundantly expressed in human stroma suggests that autocrine function of FGF2/FGFR1 signaling identified in our cell line model may be relevant to patients.

1.1.1.52 FGFR inhibition decreases stromal cell production of exosomes

Since FGFR inhibition did not kill HS-5 stromal cells but instead altered their morphology and protective capacity, we hypothesized that it might also decrease the production of protective extracellular vesicles. Consequently, we exposed HS-5 cells to different concentrations of PD173074 and measured vesicle production by nanoparticle tracking analysis (Figure 3.1.5 A). After 48 hours, we observed a dose-dependent decrease in the number of vesicles after FGFR inhibitor treatment. Notably, we saw a significant decrease in vesicle number as early as 6 hours after drug exposure (Figure 3.1.5 B). Given this short timeframe and the negligible effects of PD173074 on cell

proliferation during this time (Figure 3.1.4 C), these results suggest that FGFR inhibition results in a genuine reduction in vesicle production or release, rather than a secondary decrease due to inhibited cell growth.

Scanning electron microscopy of HS-5 cells revealed abundant budding of vesicles in untreated cells, while fewer nascent vesicles appeared on the cell surface of PD173074-exposed cells (Figure 3.1.4 C). We subjected conditioned media collected from HS-5 and HS-27 cells exposed to FGFR inhibitor to immunoblot analysis and found a reduction in exosome markers tsg101 and CD9, as well as exosomal FGF2 exclusively in HS-5 cells (Figure 3.1.4 D). We found a reduction of FGFR phosphorylation after PD173074 treatment, as well as an increase in FGFR1 receptor levels (data not shown). Intracellular levels of the exosome marker tsg101 remained unchanged after PD173074 treatment (data not shown). After sucrose fractionation of PD173074-treated and untreated HS-5 conditioned media, we found that the most profound reduction of exosomal markers and FGF2 occurred in the expected 15-30% interface fraction (Figure 3.1.5 E). We conclude that exosome production or secretion in HS-5 cells is dependent on FGFR activity and can be significantly reduced by FGFR inhibitor treatment.

1.1.1.53 FGFR1/FGF2 inhibition decreases exosome production

FGFR1 is the most abundant FGFR family member in HS-5 cells (data not shown) and in human bone marrow stroma (Figure 3.1.4 G). We therefore chose FGFR1 as the most

186

likely mediator of vesicle release and protective conditioned media production in HS-5

cells. Although PD173074 is considered a specific FGFR inhibitor, it has residual

activity against other receptor kinases, such as IGF1R and insulin receptor. PD173074 is

a more potent inhibitor of FGFR1, 2 and 3 over 4, but neither this drug nor any other

currently available small molecule is truly selective for individual FGFR family

members. We therefore aimed to demonstrate that reduced vesicle production in HS-5

is a result of FGFR1 inhibition by modulating receptor expression. We generated HS-5

CRISPR-Cas9 knockout cell lines for FGFR1 and FGF2. Without clonal selection, we

observed partial loss of FGFR1 or FGF2 expression in each of the four guide constructs

(Figure 3.1.6 A). Interestingly, we found that knockout of FGF2 led to increased FGFR1

levels, similar to the effect of FGFR inhibition with PD173074 (data not shown).

Conversely, we found that knockout of FGFR1 led to a dramatic reduction in FGF2

levels.

We next probed for exosomal markers in cell lysates and conditioned media of FGFR1

and FGF2 knockout cell lines (Figure 3.1.6 B). Again, we observed a partial reduction in

FGFR1 and FGF2 expression in cell lysates. Secretion of exosomes into conditioned

media was evaluated by quantification of CD9 and tsg101 levels (Figure 3.1.6 C).

Knockout of FGFR1 resulted in a 23% reduction of tsg101 and no reduction of CD9

compared to untreated HS-5 cells, while knockout of FGF2 led to an approximate 10-

fold reduction of tsg101 and threefold reduction of CD9. We conducted two

experiments to evaluate the protective capacity of conditioned media collected from the knockout cell lines. First, we exposed MOLM14 cells to 10nM quizartinib and overlaid a serial dilution of conditioned media (Figure 3.1.6 C). Conditioned media protection was concentration-dependent and significantly reduced in FGFR1 and FGF2 knockout cells compared to untreated HS-5 cells. Next, we plated MOLM14 cells in 50% conditioned media and added a concentration gradient of quizartinib (Figure 3.1.6 D). Again, protection was significantly reduced in media collected from FGFR1 or FGF2 knockout cells.

Having observed a decrease in vesicle secretion as early as 6 hours post FGFR inhibition (Figure 3.1.5 B), we chose siRNA/shRNA-mediated knockdown to investigate the short term effects of FGFR1/FGF2 loss. Flow-based particle analysis using Virocyt showed a reduction in particle counts after knockdown of FGFR1 and FGF2 (Figure 3.1.6 F, G). These experiments demonstrate that transient knockdown of FGFR1 or FGF2 is sufficient to reduce vesicle production in HS-5 cells. In addition, vesicle production remains inhibited in stable knockout cell lines, indicating that FGFR1 and FGF2 are essential for this process.

1.1.1.54 PLCgamma/PKC pathway in exosome release

Having observed that genetic or pharmacological inhibition of FGFR1 decreases exosome production in HS-5 cells, we hypothesized that activation of a pathway

downstream of FGFR1 may promote exosome biosynthesis and/or release. One of the well-established FGFR signaling intermediaries is phospholipase C, a membrane-associated enzyme that cleaves phospholipids into diacyl glycerol (DAG) and inositol 1,4,5-triphosphoate (IP_3). Secretory vesicle trafficking involves several steps that are controlled by DAG, including the fission of vesicles at the trans-Golgi network, the generation and maturation of multivesicular bodies, and the docking and fusion at the plasma membrane[332]-[335]. Previous reports have shown that DAG kinase α (DGKα) expression decreases the production of FasL-containing exosomes by T lymphocytes, and that inhibition of DGKα enhances the production[336]-[338]. DAG also activates protein kinase C (PKC), an enzyme which is recruited to the plasma membrane or to a number of intracellular compartments upon activation. PKC controls the endocytosis, trafficking and recycling of several receptor tyrosine kinases, notably EGFR, ErbB2, VEGFR and MET[339]-[342]. This may be a relevant mechanism for the regulation of endocytosis and subsequent routing to multivesicular bodies of FGFR1. Although PKC has not previously been shown to phosphorylate FGFR1, FGFR1 does possess C-terminal serine/threonine phosphorylation sites that are known to be important for regulation of endocytosis[343]. We therefore sought to test the roles of PLC and PKC in exosome release in HS-5 cells.

We first confirmed that FGFR1 and PLC interact directly in HS-5 cells by performing co-immunoprecipitation. Precipitation of FGFR1 led to immobilization of a small fraction

of the cellular PLC pool (Figure 3.1.7 A). However, FGFR1 did not co-immunoprecipitate with Rab11 or Rab27B, two Rabs associated with exosome biogenesis. We further wanted to determine whether FGF2 stimulation would lead to activation of PLC and PKC. We therefore exposed HS-5 cells to FGF2 or to PD173074 for 30 minutes and probed for phosphorylation of downstream signaling mediators on immunoblot. We observed increased phosphorylation of PLC upon FGF2 exposure, and decreased phosphorylation after treatment with an FGFR inhibitor (Figure 3.1.7 B). While MAPK phosphorylation behaved as expected, decreasing with inhibitor and increasing with ligand treatment, PKC phosphorylation was increased in both inhibitor and ligand samples compared to untreated.

We next examined the role of the PLC-PKC pathway in exosome production. A rise in intracellular calcium is necessary for regulated exocytosis of secretory granules and exosomes[344]. We therefore used the cell-permeable calcium ionophore ionomycin as a positive control for the regulation of exosome release. PD173074, which we confirmed as a negative regulator of exosome production in previous figures, served as a negative control. Phorbol 12-myristate 13-acetate (PMA) is a mimic of DAG and activates PKC. Over a timecourse of 72 hours, both PMA and ionomycin led to increased exosome production/release (Figure 3.1.7 C). PD173074 attenuated exosome production. Interestingly, this was not rescued by combined treatment with ionomycin, indicating an inhibition of early exosome biogenesis rather than release. Consistent with this, we

observed decreased vesicle concentrations after siRNA-mediated knockdown of PKCδ, the most abundant PKC isoform in HS-5 cells (data not shown) (Figure 3.1.7 D). While knockdown of PLCγ or FGFR1 did not significantly decrease vesicle production, combined knockdown with PKCδ achieved a more profound decrease in vesicle concentration. Of note, none of the siRNA conditions reduced HS-5 cell viability over the course of the experiment (data not shown).

Although short-term treatment of HS-5 cells with PKC inhibitor midostaurin did not reduce viability or proliferation (72-hour treatment, data not shown), we found that long-term culture in up to 500 nM midostaurin attenuated the growth of HS-5 cells (Figure 3.1.7 D). We re-plated equal numbers of these long term cultures without drug and collected conditioned media over the course of 3 hours. Media collected from cells grown in 500 nM midostaurin had significantly less protective effect on MOLM14 cells cultured with 100 nM AC220 compared to normal HS-5 media (Figure 3.1.7 E).

3.1.4 Discussion

Here, we demonstrate that exosomes are a major component of protective stromal cell conditioned medium. Exosomes have been identified as important mediators between surrounding tissue and tumor and have previously been implicated as paracrine effectors of MSCs. Cells in the tumor stroma, which includes bone marrow MSCs in leukemia, and their products play an important role in sustaining proliferative

signaling in cancer cells, evading growth suppressors, and supporting cancer stem

cells[25]. In hematologic malignancies, the bone marrow niche is known to be altered in

favor of leukemia stem cells (LSCs) over normal hematopoietic stem cells[167]. Stromal

cells derived from AML patient bone marrow biopsies exhibit altered gene expression

and cytokine secretion[329]. This altered microenvironment can protect leukemia cells

from virtually any type of therapy[317], [319], [328]. These cells are protected by

adhesion-dependent mechanisms, or through paracrine stimulation by soluble factors

[266].

1.1.1.55 Reciprocal exosome exchange between cancer and stroma

Most efforts have been focused on characterizing the delivery of cancer-derived

exosomes to normal tissue, and the suppression of normal function by microRNA

contained in exosomes[186], [193], [330], [345]. However, we found reciprocal exchange

of exosomes between leukemia and stromal cells (Figure 1 and data not shown). In

various disease models, exosome function appears to be similar to MSCs themselves,

such as reducing the size of myocardial infarctions, facilitating the repair of kidney

injury, and modulating immune responses[194]. MSC-derived exosomes have also been

implicated in oncogenesis, promoting multiple myeloma cell growth and resistance to

bortezomib[197]. Primary AML patient-derived bone marrow stroma exosomes are

enriched for TGFB1 and miR-155 and miR-375, all of which are independent risk factors

for disease recurrence[346].

1.1.1.56 Biology of FGF2 secretion

FGF2, a growth factor we previously found associated with resistance to targeted therapy in CML and AML[220], localizes to the exosomal fraction of HS-5 conditioned media. The finding that FGF2 is contained in exosomes is of special interest since FGF2 in serum and bone marrow supernatant has been implicated in hematologic malignancy progression and development of therapy resistance[103], [347]. Since the FGF2 transcript lacks signal sequences for endoplasmic reticulum translocation and integration into the classic secretory pathway, the mode of paracrine delivery is still unclear. Prior to the findings shown here, isolated reports suggested that FGF2 might be contained in extracellular vesicles[70], [348]. Alternatively, FGF2 has been reported to self-assemble into a pore-like structure on the cell membrane and mediate its own translocation with the help of extracellular heparan sulfate[68], [349]. Notably, high and low molecular weight isoforms of FGF2 may have different intracellular localization and mechanisms of export[69], [350]. Since our proteinase protection experiments demonstrated partial digestion of FGF2, it is possible that, as reported, the low molecular weight isoform is secreted and immobilized to the cell membrane via heparan sulfate, while the high molecular weight isoform remains cytoplasmic and is packaged inside the vesicle.

1.1.1.57 Clinical application of exosomes

We found that combining an FGFR inhibitor with conditioned media from HS-5 cells

only minimally reduced the protection conferred to leukemia cells exposed to a TKI.

Thus, the protective effect of exosomes is not limited to paracrine delivery of FGF2 and

activation of FGFRs on the recipient cells. HS-5 exosomes are likely to contain a

complex mixture of cytokines and microRNAs that contribute to protection. This

complexity presents a challenge to therapeutically target exosome-mediated resistance.

The most promising approach may be to target the cells producing protective exosomes,

or the mechanism of production itself. While the biology of exosome biogenesis is well

studied, we are not aware of any previous attempts to inhibit exosome production in a

specific cell type. Receptor-mediated endocytosis is the first step of exosome biogenesis.

This step may represent a neglected opportunity to target vesicle release given the

heterogeneity of receptor expression and activation among cell types and the

abundance of small molecule inhibitors against these receptors. In our stromal cell line

model, FGFR inhibition decreases production of extracellular vesicles. We found that

FGFR inhibition increased FGFR1 levels, consistent with previous reports that small

molecule kinase inhibitors alter receptor cycling and lead to accumulation at the cell

membrane. Similar to our observations, epidermal growth factor receptor has been

shown to be released on extracellular vesicles, and this release is increased after ligand

stimulation[178], [179]. Likewise, overexpression of oncogenic HER2 in breast cancer

cell lines resulted in qualitative differences in microvesicle content[351], suggesting a role for activated receptor tyrosine kinases in exosome production and secretion.

In summary, our finding that FGF2 has an autocrine function in regulating stromal cell proliferation and maintenance of a protective phenotype, combined with evidence for FGFR1/FGF2 expression in bone marrow stroma of AML patients, suggests that targeted inhibition of FGFRs could create a microenvironment that is less conducive to the development of TKI resistance.
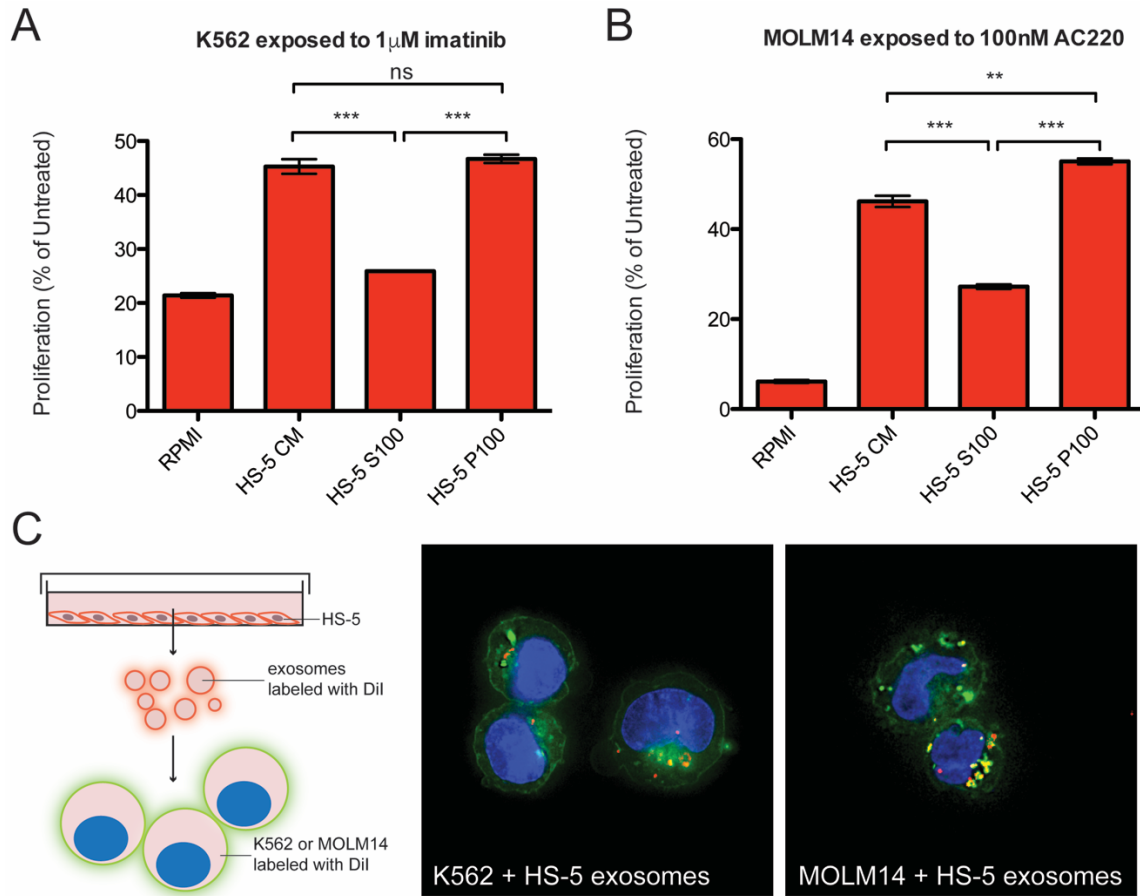
Figure 3.1.1 Extracellular vesicles secreted by HS-5 cells are internalized by and protect MOLM14 cells treated with AC220 and K562 cells treated with imatinib.
A, Proliferation of K562 cells after exposure to 1 μM imatinib and conditioned media fractions collected from HS-5 cells. B, Proliferation of MOLM14 cells after exposure to 100 nM AC220 and conditioned media fractions collected from HS-5 cells. Proliferation was measured using MTS reagent after 48 hours. Values were normalized to untreated cells. All wells were plated in triplicate and error bars indicate standard deviation. S100, HS-5 secreted soluble protein fraction; P100, HS-5 extracellular vesicle fraction. All experiments were done in triplicate, error bars represent standard deviation, p values are indicated by *<0.05, **<0.005, and ***=0.0007. C, MOLM14 and K562 cells were stained with DiO (green) tracer, washed, and immobilized on Poly-D-lysine coated chamber slides. HS-5 P100 fraction was stained with DiI (red) tracer and added to the cells for a 24-hour incubation. Slides were stained with Dapi (blue) and imaged by confocal fluorescent microscopy.
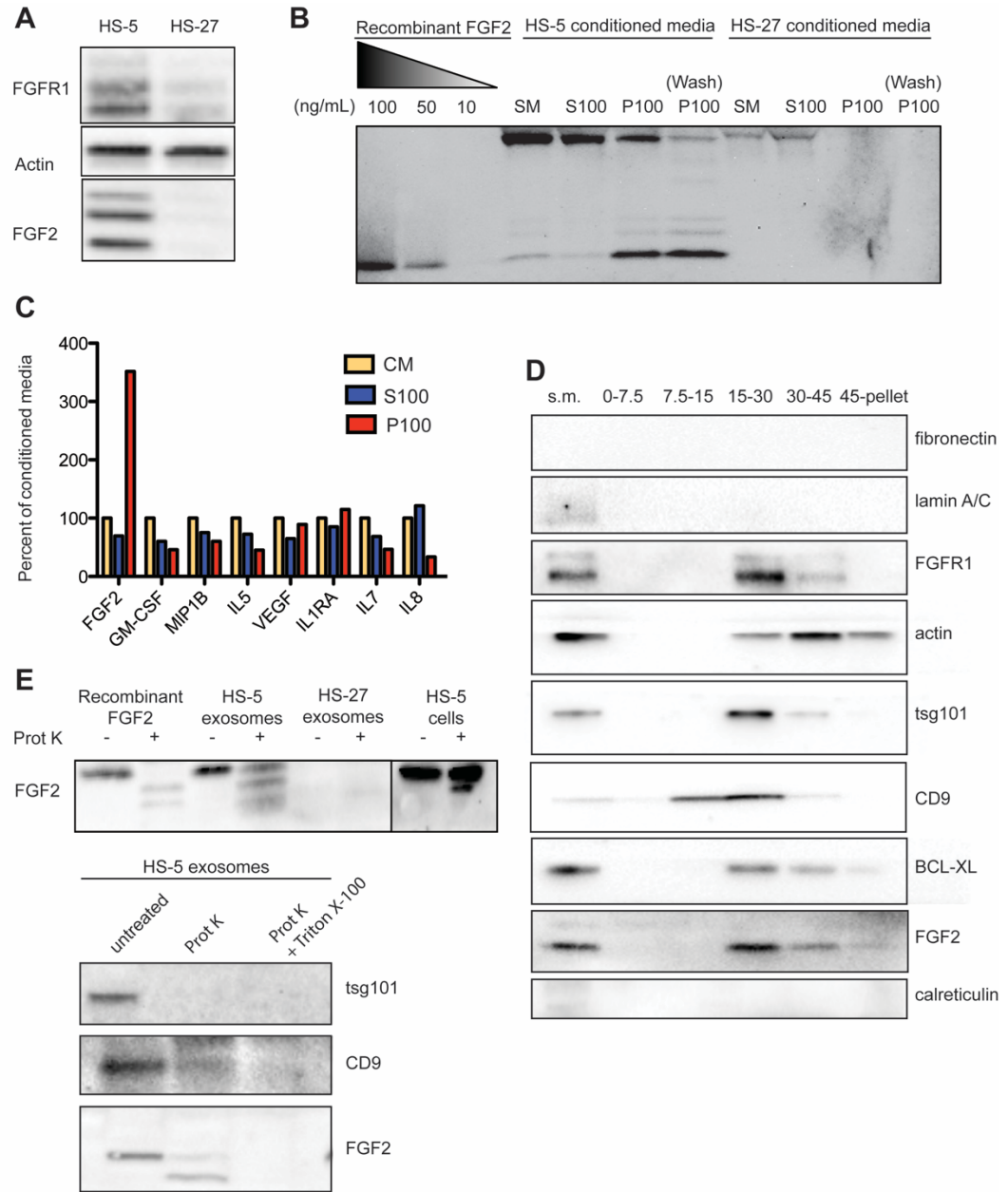
Figure 3.1.2 FGF2 is enriched in exosomes from HS-5 bone marrow stromal cells.
A, Western blot analysis of FGF2 in HS-5 and HS-27 whole cell lysates. B, HS-5 and HS-27 cells were incubated in R10 media for 3 hours. Cell supernatant was cleared of cells and ultracentrifuged at 100,000g for 2 hours at 4 degrees C. Starting material (SM), soluble protein (S100), and ECV (P100) fractions were lysed and analyzed by Western blot, using 10, 50, and 100 ng/mL recombinant FGF2 as controls. C, HS-5 conditioned media fractions were lysed in 0.1% NB40 and analyzed by ELISA on a bone marrow cytokine multiplex panel. D, HS-5 P100 fraction was further fractionated on a subsequent sucrose density gradient. Sucrose layer interfaces (0-7.5%, 7.5-15%, 15-30%, 30-45%, and 45%-pellet) were lysed and processed for Western blot analysis. Blots were probed with antibodies against the exosomal markers CD9 and tsg101, as

well as cell compartment markers fibronectin, lamin A/C, BCL-XL, and FGFR1 and FGF2. E, Following sucrose gradient purification, HS-5 and HS-27 exosomes, recombinant FGF2 and HS-5 cells were exposed to Proteinase K and analyzed by Western blot (top panel). In a separate experiment, HS-5 exosomes were exposed to Proteinase K with or without detergent (0.1% Triton X-100), and samples were subjected to Western Blot analysis using antibodies against tsg101, CD9 and FGF2.
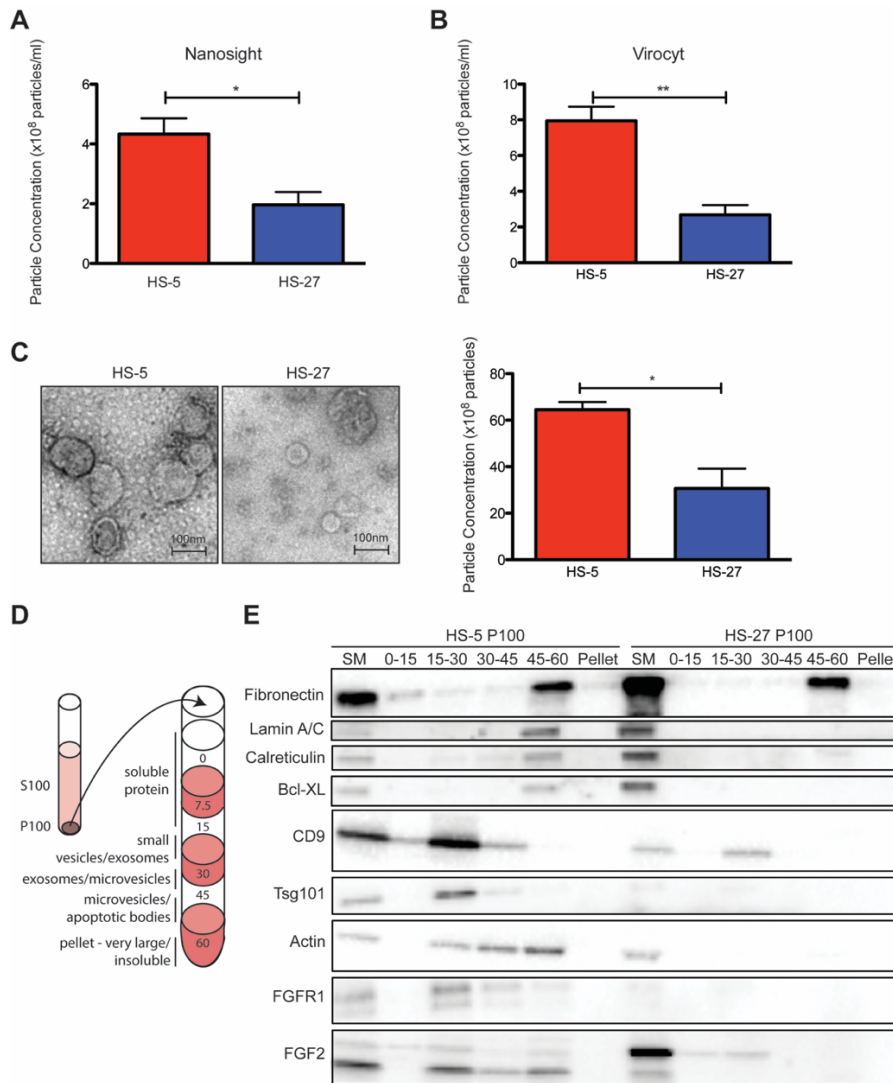
Figure 3.1.3 HS-5 cells secrete more exosomes than HS-27 cells.

Equal number of HS-5 and HS-27 cells were plated in RPMI with exosome-depleted FBS for 24 hours. The extracellular vesicle fraction was collected by ultracentrifugation at 100,000g for 2 hours at 4 degrees C and the pellet was resuspended in PBS. A, vesicle concentration was measured by nanovesicle tracking analysis. B, Vesicles were incubated with a proprietary combination of fluorescent dyes that stain both nucleic acid and protein and analyzed by flow cytometry (Virocyt). C, Transmission electron micrograph of HS-5 and HS-27 vesicles (left). Vesicles were quantified by counting in three 2x2 μm areas per sample (right). All experiments were done in triplicate, error bars represent standard deviation, p values are indicated by *<0.05, **<0.005. D, Illustration of sucrose density gradient used to fractionate pelleted fraction of conditioned media. E, HS-5 and HS-27 P100 fractions were obtained by ultracentrifugation, and the exosome fraction was further purified by a subsequent sucrose density gradient. Sucrose layer interfaces (0-7.5%, 7.5-15%, 15-30%, 30-45%, and 45%-pellet) were lysed and processed for Western blot analysis. Blots were probed with antibodies against the exosomal markers CD9 and tsg101, as well as cell compartment markers fibronectin, lamin A/C, BCL-XL, and FGFR1 and FGF2.
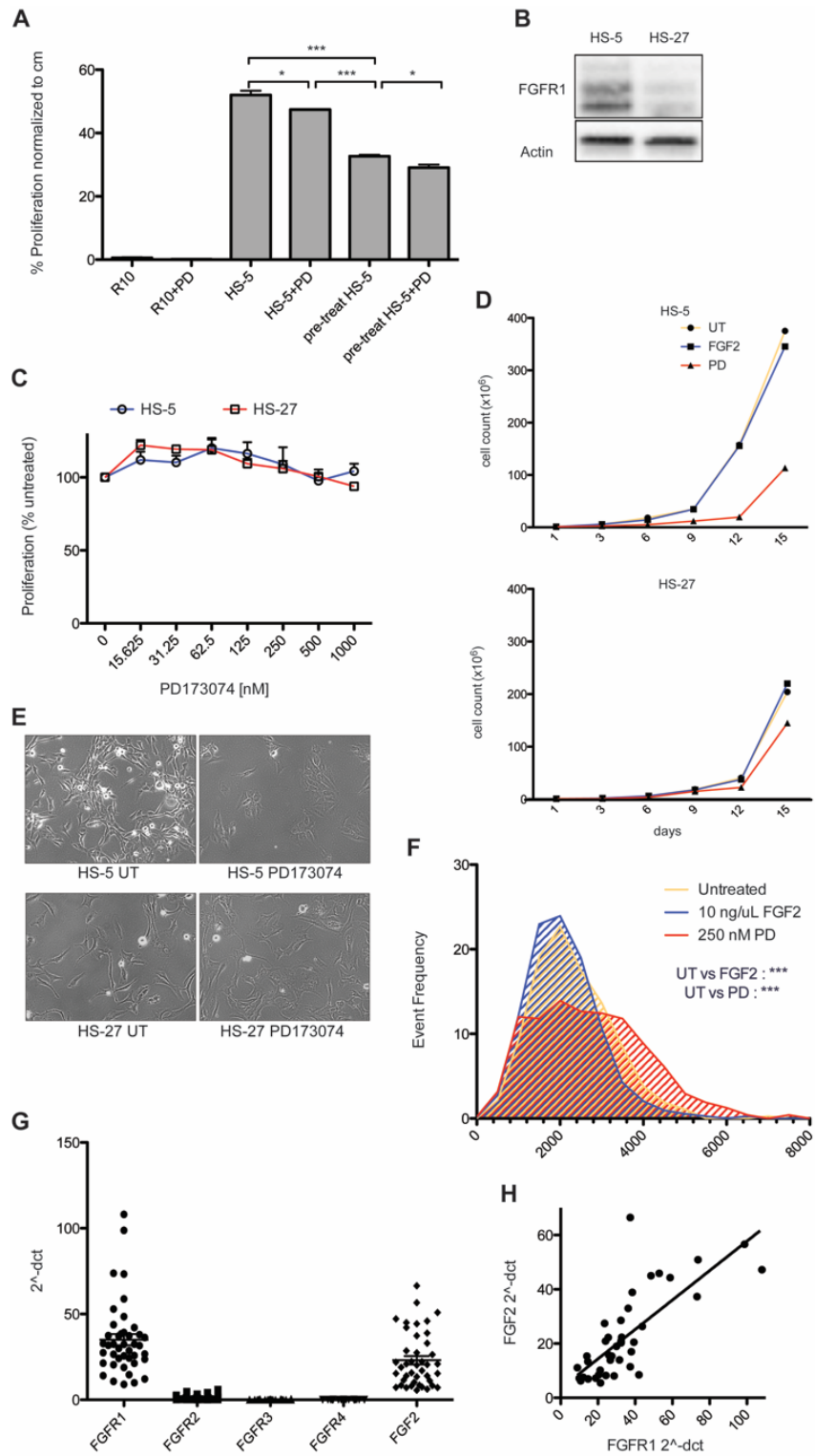
Figure 3.1.4 FGF2 is an autocrine growth factor in bone marrow stromal cells, and FGFR inhibition attenuates growth.

A, MOLM14 proliferation after 42h treatment with 100 nM AC220. HS-5 conditioned medium was collected over 3h after cells had been grown in medium or 250 nM PD173074 for one week. MOLM14 cells were resuspended in conditioned medium, and AC220 +/- 250 nM PD173074 was added. Proliferation was measured by MTS assay and values were normalized to untreated cells. Error bars represent standard deviation, p values are indicated by *<0.05, **<0.005, and ***=0.0007. B, Western blot analysis of FGFR1 and actin in HS-5 and HS-27 whole cell lysates. C, HS-5 and HS-27 cells were plated in triplicate on 96 well plates in a gradient of FGFR inhibitor PD173074. Proliferation was measured using MTS reagent after 72 hours. Error bars indicate standard deviation. D, HS-5 and HS-27 cells were incubated in R10 (UT), R10 + 10 ng/mL recombinant FGF2 protein, or R10 + 250 nM PD173074 (PD). cell Cell counts were obtained every 3 days over a 15-day period, with fresh media and cytokine added after 3 days. E, HS-5 and HS-27 cells were incubated in R10 (UT) or R10 + 1 µM PD173074 for 1 week. Brightfield microscopy images were obtained using 10X magnification. F, HS-5 cells were incubated in 4-well glass chamber slides in R10 (untreated), R10 + 10 ng/mL recombinant FGF2 protein, or 250 nM PD173074 (PD). Cells were stained with lipophilic tracer DiI, incubated for 24 hours, fixed, then stained with DAPI. Immunofluorescent images were taken at 10X and images were analyzed on Cell Profiler software. Cell size is expressed in ɰm2. G, Primary bone marrow stromal cells cultured from the red blood cell pellet of leukemia patient samples (n=42) were lysed for RNA extraction and cDNA synthesis. Taqman qPCR analysis was performed using FGFR1, FGFR2, FGFR3, FGFR4, and FGF2 Taqman primer assays. H, FGFR1 and FGF2 qPCR values ($2^{-\Delta CT}$) were plotted against each other. Linear regression produced a line fit with r2=0.5683 and slope significantly non-zero with p<0.0001.
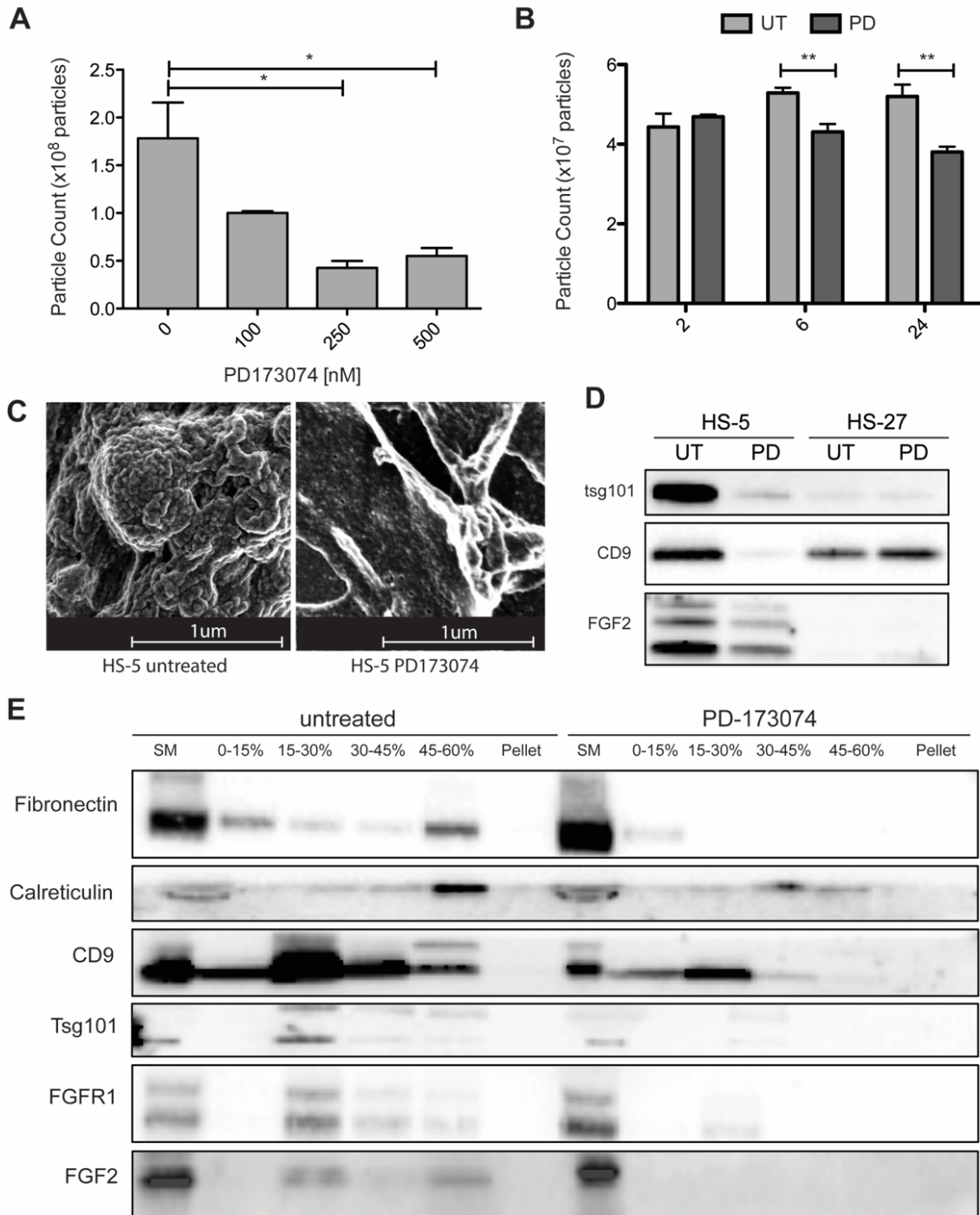
Figure 3.1.5 FGFR inhibition decreases exosome production in FGF2-expressing stroma.
A, Equal numbers of HS-5 cells were exposed to varying concentrations of PD173074 for 48 hours. Conditioned media was collected and extracellular vesicles were pelleted by ultracentrifugation. After resuspension in PBS, vesicles were quantified by nanoparticle tracking analysis. Error bars indicate standard deviation and p values are indicated by *<0.05. B, HS-5 cells were incubated in R10 (UT) or 1μM PD173074 (PD) for 2, 6, and 24 hours. Conditioned media was collected and

extracellular vesicles were pelleted by ultracentrifugation. After resuspension in PBS, vesicles were quantified by nanoparticle tracking analysis. Error bars indicate standard deviation and p values are indicated by *<0.005. C, HS-5 cells were plated in glass dishes in either R10 only (UT) or 1 µM PD173074 for 72 hours and imaged by electron microscopy. D, HS-5 and HS-27 cells were incubated in R10 (UT) or 1 µM PD173074 for 72 hours. Whole cells lysates were analyzed by Western blot and probed for exosome markers CD9 and tsg101 and FGF2. E, HS-5 cells were plated in R10 (UT) or 1 µM PD173074 for 72 hours. P100 fractions was obtained by ultracentrifugation, and the exosome fraction was further purified by a subsequent sucrose density gradient and ultracentrifugation. Sucrose layer interfaces (0-7.5%, 7.5-15%, 15-30%, 30-45%, and 45%-pellet) were lysed and processed for Western blot analysis. Exosome fractions (15-30% and 30-45% sucrose) were confirmed by co-expression of exosome markers CD9 and tsg101, as well as cell compartment markers fibronectin and calreticulin, and FGFR1 and FGF2.
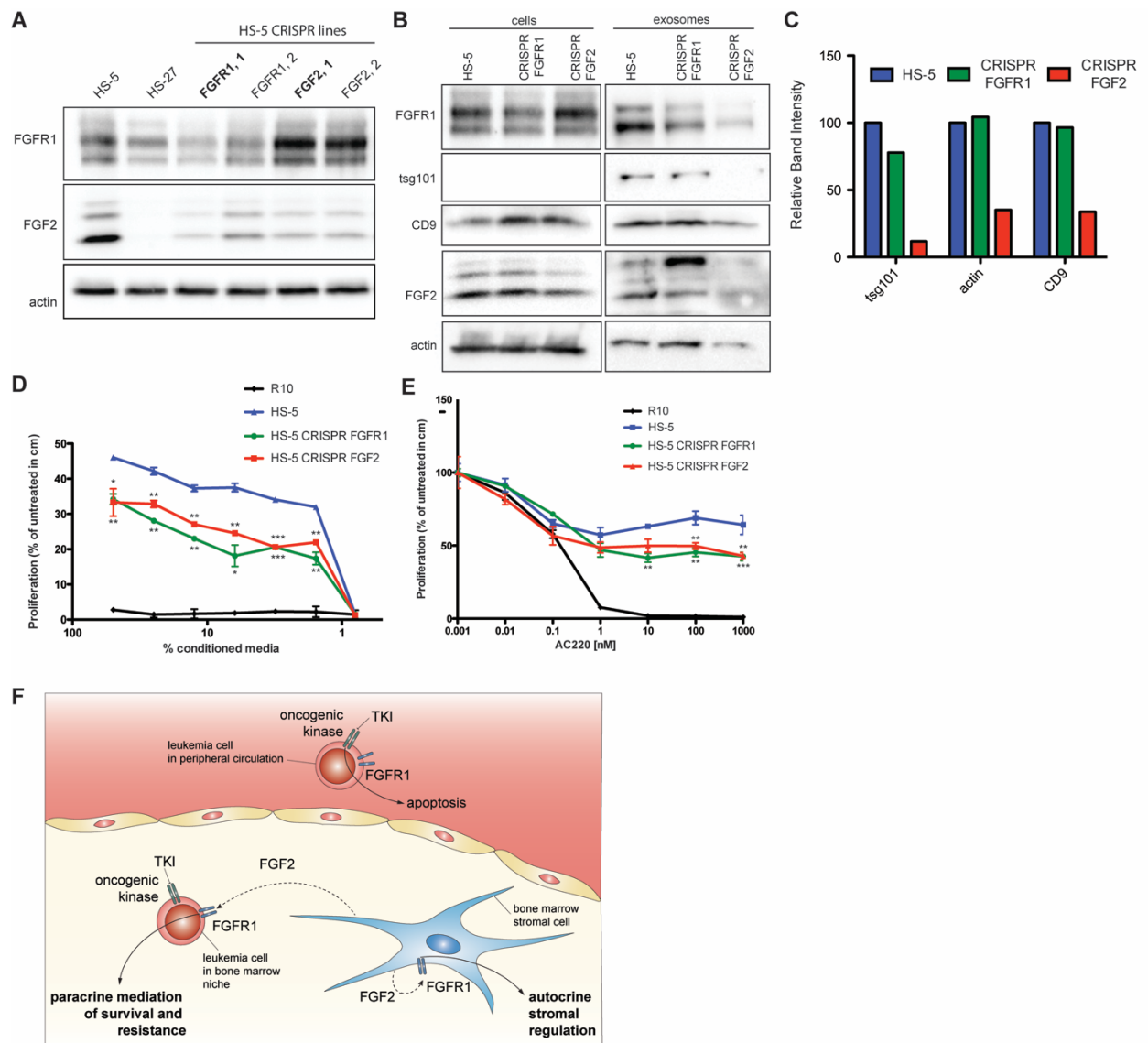
Figure 3.1.6 Silencing of FGFR1 or FGF2 expression in HS-5 cells attenuates the protective phenotype and decreases exosome production.

A, FGFR1 or FGF2 genes were knocked out in HS-5 cells by lentiviral CRISPR/Cas9 genome editing. Each gene was targeted with two single guide RNA sequences (labeled 1,2). Western blot analysis of whole cell lysates shown with antibodies against FGFR1, FGF2, and actin. B, Conditioned media from HS-5 cells and CRISPR/Cas9 HS-5 cells was harvested for exosome purification by ultracentrifugation and sucrose density gradient. Whole cell and exosome lysates were analyzed by Western blot with antibodies against FGFR1, tsg101, CD9, FGF2, and actin. C, Densitometry of exosome lysate bands normalized to cellular actin. D, Conditioned media was harvested from HS-5 cells, FGFR1 CRISPR/Cas9 HS-5 cells, and FGF2 CRISPR/Cas9 HS-5 cells after 72 hours. MOLM14 cells were plated in 100 nM AC220 and R10 or on a 1:10 gradient of conditioned media. Proliferation was measured using MTS reagent after 48 hours. E, MOLM14 cells were plated in

R10 or conditioned media on an AC220 gradient. Proliferation was measured using MTS reagent after 48 hours. Error bars indicate standard deviation. All experiments were done in triplicate and p values are indicated by *<0.05, **<0.005, ***=0.0007. F, Model showing both paracrine and autocrine pathways of FGFR1 stimulation by FGF2 in bone marrow stromal cells. The paracrine pathway mediates survival of leukemia cells in the bone marrow during targeted therapy.
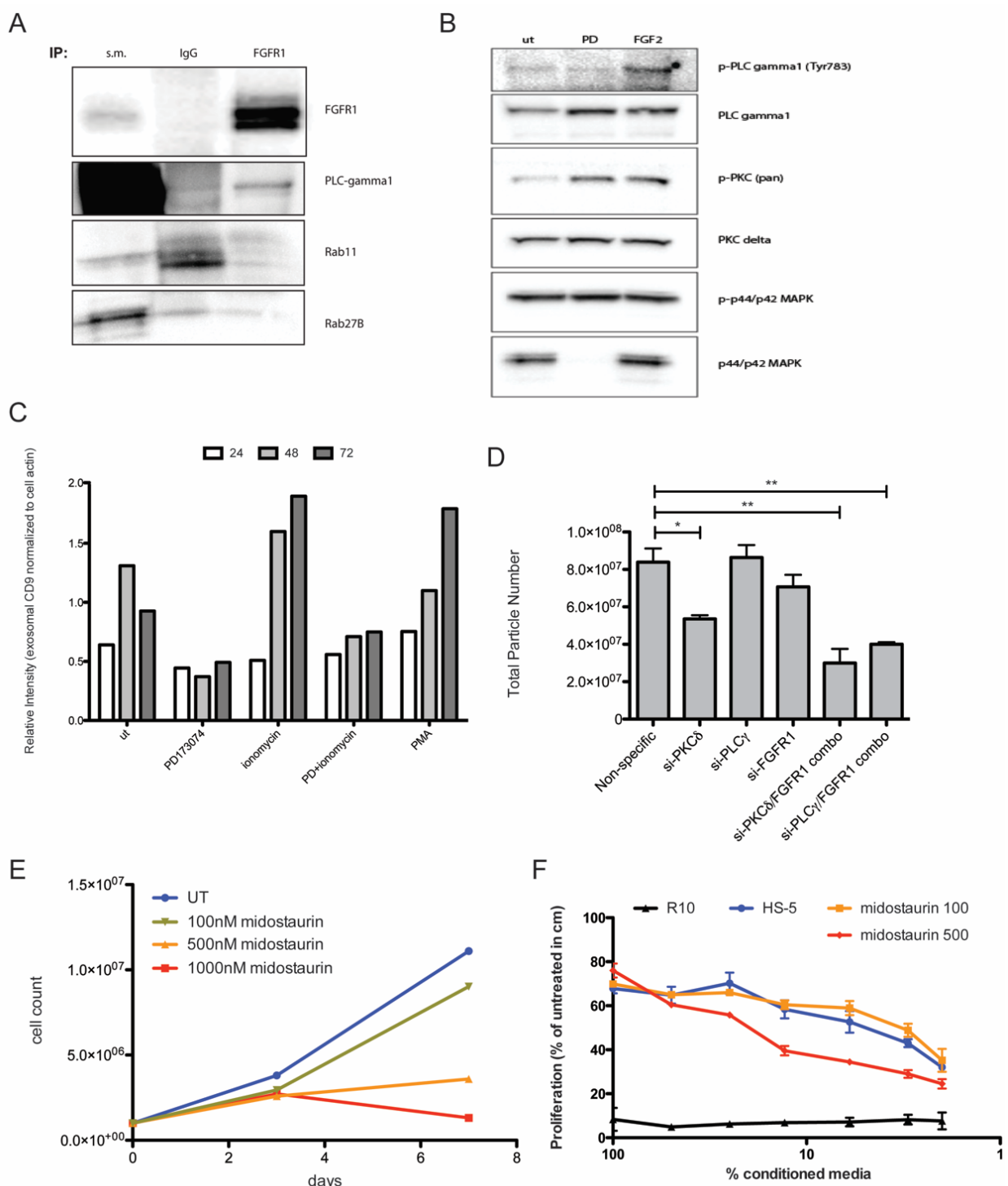
Figure 3.1.7 Activation of PLC/PKC by FGFR1 promotes exosome production in HS-5 cells.
A, Whole cell lysate and immunoprecipitates of FGFR1 from HS-5 lysate were analyzed on immunoblot for FGFR1, PLCγ, Rab11 and Rab27B. B, HS-5 cells were treated with 250 nM

206

PD173074 (PD), 10 ng/ml FGF2, or media (ut) for 30 minutes. Cell lysates were prepared for immunoblot analysis and blots were probed with antibodies against phospho- or total PLCγ, phospho- or total PKC,and phospho- or total p44/p42 MAPK.C, HS-5 cells were cultured with 1 μM PD173074, ionomycin or PMA for 24, 48, or 72 hours. Extracellular vesicles were harvested by ultracentrifugation, and cells and vesicles were prepared for immunoblot analysis. Band intensities of CD9 in extracellular vesicles were normalized to cellular actin as a relative measure of exosome production. D, HS-5 cells were transfected with siRNA against PKC, PLCγ, FGFR1, or a combination of two. After 72 hours, conditioned media was collected for vesicle quantification using the ViroCyt. Error bars indicate standard deviation. All experiments were done in triplicate and p values are indicated by *<0.05, **<0.005. E, HS-5 cells were cultured with varying concentrations of midostaurin. Cell counts were obtained every 3 days over a 7-day period, with fresh media and cytokine added after 3 days. F, HS-5 cells cultured in midostaurin for two weeks were replated at equal density, allowed to adhere over night, washed, and left to produce conditioned media over 3 hours. MOLM14 cells were plated in 100 nM AC220 and R1,0 or on a 1:10 gradient of conditioned media. Proliferation was measured using MTS reagent after 48 hours.

4 Materials and Methods

4.1 Cell culture and reagents

GIST T1 cells were treated with 10,000 nM imatinib for 2 months and GIST 10R grew out as a resistant colony. The cells were expanded and sequenced for KIT(exon 11-21) and PDGFRA, PDGFRB(exon 12,14 and 18). No secondary mutations were found in any of these receptor tyrosine kinases. MOLM14 cells were generously provided by Dr. Yoshinobu Matsuo (Fujisaki Cell Center, Hayashibara Biochemical Labs, Okayama, Japan)[352]. BAF3 cells with retrovirally introduced FLT3 ITD were created as previously described[312]. The cells were then retrovirally transfected with empty pMX vector or human FGFR1 cloned into a pMX vector; and transfected cells were selected with 1μg/ml puromycin. The human stromal cell lines HS-5 and HS-27a were kindly provided by Dr. Beverly Torok-Storb (Fred Hutchinson Cancer Research Center, Seattle, WA). The human CML cell line K562 was obtained from the American Type Culture Collection (Manassas, VA) and maintained in RPMI1640 media supplemented with 10% fetal bovine serum, 100 U/mL penicillin/100 μg/mL streptomycin, and 2 mM l-glutamine at 37°C in 5% CO_2, except MOLM13, which was grown in RPMI supplemented with 20% FBS (R20) and GIST T1, GIST 10R, and GIST 882 cells, which were supplemented with 15% FBS.

4.1.1 Proliferation assay

For proliferation assays, cells were plated in 96-well format and incubated for 48 hours with drug and 96 hours with siRNA, unless indicated otherwise. Viability assays were performed with CellTiter 96 AQueous One Solution Cell Proliferation Assay from Promega Corporation (Madison, WI, USA). Graphical and statistical data were generated using either Microsoft Excel or GraphPad Prism (GraphPad Software, Inc., La Jolla, CA, USA). Synergy Calculations were performed in the free software environment R for statistical computing and graphics using a script provided by Laura Heiser and Jim Korkola. Calculation of the CI values is based on the Chou-Talalay method for drug combination[353]. Recombinant SCF, FGF1, and FGF2 were purchased from Peprotech. Ligands were supplied at 10ng/ml for viability readouts. Unless indicated otherwise, MTS assays were performed 48 h after the addition of ligand. To detect receptor and downstream signaling activation, ligands were supplied at 100ng/ml for the indicated time before harvesting cell lysates for immunoblotting.

4.1.2 Transwell assay

HS-5 and HS-27 cells were plated at 1x105 cells in 6-well plates in 2 ml media. 1 ɥm transwells were then placed over the stromal cells and 1x105 MOLM14 cells were plated in 2 ml media (4 ml total). The co-cultures were then treated with AC220 10 nM and PD173074 250 nM individually or in combination. After two days, the transwells with

MOLM14 were removed and 2 ml fresh media and inhibitor added to stroma below. The co-cultures were incubated for another 2 days and MOLM14 cells assessed for annexin-5 staining by GuavaNexin (Millipore). The underlying stromal cultures were evaluated by MTS assay for viability. Co-cultures were performed in triplicate for each condition.

4.2 Exosome isolation

HS-5 cells were grown in R10 to 90-100% confluence in 15 cm dishes. Each plate was washed in 8 ml PBS, and 12 ml exosome-depleted R10 was added for an overnight (16 hour) incubation. The conditioned media was collected, cleared of cells (2 X 2000g spin for 10 min), and spun in an ultracentrifuge at 100,000g for 2 hr at 4°C. The resulting supernatant (S100) was poured off, and 100 ul PBS was added to the pellet (P100). This was shaken for 4 hr at 4°C at 2000 rpm. P100 was used fresh or stored at -80 C with 10% DMSO.

4.3 Sucrose density gradient

In an ultracentrifuge tube, we layered varying sucrose densities (60%, 45%, 30%, 15%, 7.5%, and 0%). P100 from HS-5 or HS-27 was added to the top of the tube, and the tube was ultracentrifuged at 100,000g for 90 min at 4°C. The interfaces (45-60, 30-45, 15-30, 7.5-15, 0-7.5) were collected with a micropipette and washed separately in PBS in an ultracentrifuge (100,000g for 2 hr at 4°C).

4.4 Exosome quantitation

Exosomes were quantitated either by Nanosight LM10 or by Virocyt Virus Counter 3100, according to respective manufacturers' protocols.

4.5 Transmission Electron Microscopy

Stromal cell exosomes were isolated and purified by sucrose density gradient as indicated above, then washed in filtered PBS. 10ul of the preparation was deposited onto glow discharged carbon formvar 400 mesh copper grids (Ted Pella 01822-F) for 3 min, rinsed 15 secs in water, wicked on Whatman filter paper 1, stained for 45 secs in filtered 1.33% (w/v) uranyl acetate, wicked and air dried. Samples were imaged at 120kV on a FEI Tecnai Spirit TEM system. Images were acquired as 2048x2048 pixel, 16-bit gray scale files using the FEI's TEM Imaging & Analysis (TIA) interface on an Eagle 2K CCD multiscan camera.

4.6 Fluorescent confocal microscopy

MOLM14 and K562 leukemia cells were stained with lipophilic tracer DiO (Thermo Fisher) according to manufacturer's protocol. HS-5 P100 was stained separately with lipophilic tracer DiI (Thermo Fisher). DiO-stained cells were combined with DiI-stained P100 and incubated for 24 hours. Cells were washed and added to poly-D-lysine coated chamber slides and DAPI-stained. Z-stack imaging was performed on an Olympus IX71 inverted microscope.

4.7   Proteinase K digestion

Exosomes were isolated and purified by sucrose density gradient as described above. Samples were incubated at room temperature with 5 µg/ml proteinase K for 1 hour. Digestion was terminated by adding Laemmli sample buffer with 2-mercaptoethanol and boiling samples for 5 minutes. Immunoblot analysis was performed as described above.

4.8   Cell morphology analysis

HS-5 and HS-27 cells were grown to 90% confluence in 8-well chamber microscope slides in the following conditions for 72 hours: R10; R10 supplemented with 10 ng/mL FGF2; or 250 nM PD173074 in R10. Cells were stained with lipophilic tracer DiI, washed, then stained for DAPI. Cells were imaged at 10X on a Zeiss Axio Observer fluorescent microscope using AxioVision software. Images were uploaded into Cell Profiler software and analyzed for statistical significance between untreated and treated conditions.

4.9   siRNA and kinase inhibitors

The RAPID siRNA library has been previously described[261], [262]. All siRNAs were from Thermo Fisher Scientific Dharmacon RNAi Technologies and cumulatively target the entire tyrosine kinase gene family as well as NRAS and KRAS (93 genes targeted total). Each well contained a pool of four siRNAs. Cells were aliquoted at 66 µL per well

in a 96-well plate and 34 μL of siRNA/OptiMEM/siRNA mixture was added to each

well. Oligofectamine and siRNA were used at a ratio of 1:6. MOLM14 cells were

washed in PBS, resuspended in siPORT (120 mM Trehalose, 20 mM HEPES, 1 mM Myo-

Inositol, 1 mM KCl, 1 mM MgCl2, 1 mM K2HPO4, 0.4 mM KH2PO4, 2.14 mM KOH and

1 mM Glutathione[262] at 1:6 dilution, and electroporated using a square wave protocol

(350V, 1.5 seconds, 2 pulses, 0.1s interval) in a BioRad Gene Pulser XCell (Hercules, CA,

USA). After 48 hours, FGF2 and quizartinib were added and viability was assessed with

MTS after another 48 hours.

For assessment of cell viability and proliferation, cells were subjected to the MTS assay

after 96 hours. PD173074, AZD-6244, and PI-103 were purchased from Selleck. Imatinib,

dasatinib, nilotinib, ponatinib, AC220 and CHIR-258 were purchased from LC

Laboratories (Woburn, MA).

4.10 Inducible shRNA

TRIPZ inducible lentiviral FGF2 and FGFR1 shRNA were purchased from Thermo

Fisher Scientific Dharmacon RNAi Technologies (Waltham, MA, USA), along with

Dharmacon's trans-lentiviral shRNA packaging kit with calcium phosphate transfection

reagent and HEK293T cells. HS-5 and HS-27 cells were transfected with either GIPZ

control, FGFR1 TRIPZ, or FGF2 TRIPZ inducible shRNA according to manufacturer's

protocol. Following puromycin selection, induction of TurboRFP/shRNA expression

was performed by incubating cells in R10 supplemented with 1 μg/mL doxycycline (Fisher). Cells were incubated for 48 hours, washed in PBS, and re-incubated with exosome-depleted R10 and 1 μg/mL doxycycline. Cell supernatant was collected for exosome isolation, and cells were harvested for immunoblot analysis.

4.11 CRISPR/Cas9 targeted genome editing.

The vector lentiCRISPRv2 was obtained from Addgene. This plasmid contains two expression cassettes, hSpCas9 and the chimeric guide RNA. Guide RNA sequences were obtained from genscript and manufactured by Fisher Scientific. The vector was digested and dephosphorylated, the plasmid was gel-purified and Oligos were ligated after annealing and phosphorylation. Plasmid was amplified in Stbl3 bacteria, purified, and lentivirus was generated in HEK293T cells. HS-5 cells were transduced and selected in puromycin for 5 days. Cells were cultured for an additional 5 days before assessing knockout.

4.12 Long-term resistant cultures

K562 cells were initially resuspended in 10 mL of fresh media at a concentration of 1 × 106 cells/mL. Media was supplemented with fibroblast growth factor 2 (FGF2), interferon-γ (IFN-γ), granulocyte colony-stimulating factor (G-CSF) at 10 ng/mL as indicated, and 1 μM imatinib. Media, recombinant protein, and IM were replaced every

2-3 days. Cell viability was evaluated every 2-3 days using Gauva ViaCount reagent

and cytometer (Millipore, Billerica, MA).

MOLM14 cells were initially resuspended in 10 ml of fresh media at a concentration of

1x106 cells/ml. Media was supplemented with FGF2 or FLT3 ligand (FL) at 10 ng/ml

and 10 nM quizartinib. Media, recombinant protein, and quizartinib were replaced

every 2-3 days. Cell viability was evaluated every 2-3 days using Guava ViaCount

reagent.

4.13 Blocking antibodies

FGF2 was diluted in media at 10 ng/mL and then blocking antibody (Ab) clone bFM-1

(Millipore) was added and incubated for 30 minutes at 37°C before addition of K562

cells and IM. Viability was assessed as described.

4.14 Immunoblotting

Cells were washed with PBS and lysed with 1 × Cell Signaling Lysis Buffer (Cell

Signaling Technology). Protein concentration was determined by BCA assay (Thermo

Scientific), and 30μg sample/lane was mixed with 3x SDS loading buffer containing β-

mercaptoethanol. Samples were separated by standard SDS-polyacrylamide gel

electrophoresis and transferred onto polyvinylidene fluoride (PVDF) membranes

(Millipore) and subjected to immunoblot analysis with antibodies specific for KIT,

phospho-KIT, FGFR3, TYK2, phospho-TYK2, STAT1, phospho-STAT1 (Cell Signaling

Technology), as well as phospho-FGFR3 (Y724), FGF2 (Santa Cruz Biotechnology), and β-actin (EMD Biosciences). For immunoprecipitation, 500µg protein was incubated with 2µg primary antibody overnight at 4 °C. Antibodies used were rabbit polyclonal anti-TYK2 (Cell Signaling Technology), mouse monoclonal anti-KIT (Santa Cruz Biotechnology), and rabbit and mouse isotype control antibodies (Santa Cruz Biotechnology). Samples were incubated for 1h with immobilized Protein A agarose bead slurry IPA300/S (Repligen) at 4 °C. Samples were subsequently prepared for immunoblotting as described above.

4.15 Patient tissue samples

All patient specimens were obtained with informed consent of the patients on protocols approved by the Institutional Review Board of Oregon Health & Science University. This study was conducted in accordance with the Declaration of Helsinki.

4.15.1 GIST samples

To prepare fresh-frozen GIST tissue samples for immunoblotting, tissue was dissected on dry ice using a razor blade. Four shavings per sample were sonicated three times for 3 seconds in 2× Cell Signaling Lysis Buffer.

4.15.2 Primary AML samples

Frozen viable cells from 18 FLT3 ITD AML patients were washed in IMDM with 20% heat-inactivated FBS and then cultured overnight in RPMI with 25% FBS, 100 U/mL

penicillin/100 µg/mL streptomycin, 2 mM L-glutamine, 10 ng/ml IL-3, 10 ng/ml SCF, 10 ng/ml G-CSF, and 10 ng/ml GM-CSF[354]. The cells were washed the following day. Fresh FLT3 ITD AML mononuclear cells were purified over Ficoll gradient as described[355]. 7x106 cells were plated in 96-well plates with R10 alone or supplemented with FGF2; and then treated with AC220. Viability was measured after 72 hours by MTS.

4.15.3 Primary bone marrow stromal culture

Primary bone marrow patient samples (how obtained?) were cleared of plasma and run on Ficoll. Red pellets were incubated on ice for 20 minutes with red blood cell lysis buffer ACK. Remaining cells were plated on 15 cm dishes in MEM-α supplemented with 20% FBS, L-glutamine, pen-strep, and fungizome. Adherent stromal cells were obtained from long-term (2 week) culture.

4.16 Real time RT-PCR

RNA was isolated from cells using the RNeasy Mini kit (Qiagen). RNA was transcribed to cDNA using Superscript III reverse transcriptase (Life Technologies), using undiluted RNA. Subsequently, cDNA was diluted 1:4 and quantified via real-time RT-PCR following the TaqMan Gene Expression Assay protocol (Life Technologies). Samples were plated in triplicate, and every assay included a water control.

4.17 Sequencing

Primers were used to amplify the FLT3 kinase domain and for sequencing as described[308]. Next-generation sequencing of resistant MOLM14 cells was performed as previously described[356].

4.18 Immunohistochemistry and Image Analysis

Antigen retrieval was performed by boiling samples in Dako Citrate buffer (10 mM sodium citrate, pH 6.0) for 30 minutes (Dako, Carpinteria, CA). Rabbit polyclonal anti-FGF2 Ab (SC-79) from Santa Cruz Biotechnology (Dallas, TX) was diluted 1:500 in Dako Ab Diluent with Background Reducing Reagents and incubated overnight at 4°C. The following day, secondary biotinylated anti-rabbit Ab (Vector Labs, Burlingame, CA) was added at 1:500 dilution and incubated for 1 hour at room temperature. Secondary Ab was detected using an avidin/biotinylated enzyme conjugate kit (Vectastain ABC kit;Vector Labs) according to the manufacturer's recommendations. The slides were dehydrated and mounted with Permount (VWR, Radnor, PA). Slides were scanned with an Aperio ScanScope AT microscope using ×20 objective (Vista, CA). The FGF2 staining was then quantitated with Aperio ImageScope software using a macro kindly provided by Dr Brian Ruffell in Dr Lisa Coussens' laboratory at Oregon Health & Science University.

4.19   Stromal cell cytokine ELISA

Stromal conditioned media fractions were prepared as described and incubated in 0.1% NP-40 for 30 min. Samples were spinned at 3,000 rpm for 10 mins to collect the supernatant. 50 ul supernatant was incubated with the magnetic beads overnight and samples were processed following manufacturer's instructions for a Luminex Multiplex magnetic beads 30-ples Assay (Life Technology).

4.20   Colony assays

All studies using human cells were approved by the Oregon Health & Science University Institutional Review Board and patients provided written informed consent before study participation. Previously isolated CD34+ cells (immunomagnetic beads; Miltenyi Biotech, Bergisch-Gladbach, Germany) were thawed and cultured overnight in Iscove modified Dulbecco media (Invitrogen, Carlsbad, CA) with 10% BIT9500 (Stem Cell Technologies, Vancouver, Canada), 10–4 M β-mercaptoethanol, 1 ng/mL G-CSF, 50 pg/mL leukemia inhibitory factor, 0.2 ng/mL granulocyte macrophage colony-stimulating factor, 0.2 ng/mL stem cell factor, 0.2 ng/mL macrophage inflammatory protein 1α, 1 ng/mL interleukin-6 (Stem Cell Technologies), and 100 U/mL penicillin/100 µg/mL streptomycin (Invitrogen). The cells were then plated in Methocult H4534 (Stem Cell Technologies) in triplicate with IM and FGF2 as indicated. Colony forming units–

granulocyte macrophage (CFU-GM) colonies were counted after 2 weeks of incubation at 37°C in 5% CO_2.

4.21 Statistical analyses

For cell proliferation assays, a Student t test was carried out for each treatment condition compared with untreated cells or appropriate controls. The P values for the t tests are indicated by asterisks: *, $0.01 \leq P < 0.05$; **, $0.001 \leq P < 0.01$; ***, $P < 0.001$. To determine the significance of combination indices to indicate synergy, upper and lower confidence limits were calculated. Data points for combinations with upper confidence limits below 1 were considered synergistic.

5   Summary and Conclusions

My thesis research evolved from the undetermined resistance of a gastrointestinal stromal tumor cell line to encompass several other malignancies in what I believe to be a broadly applicable mechanism. My work, integrated with observations made by others, indicates that fibroblast growth factor signaling is a physiologic damage response pathway that can be upregulated in many settings and many tissues, not only in response to cytotoxic chemotherapy or irradiation, but also kinase inhibitor therapy. While fibroblast growth factor signaling is essential for maintenance of tissue homeostasis and cellular function, as I and others have found to be the case in bone marrow stroma[162], it also creates a milieu that is permissive to survival and outgrowth of resistant disease. Here, I will summarize my findings presented in the previous four chapters, touch on concepts I have found particularly intriguing, and finally suggest future work

5.1   Crosstalk between KIT and FGFR3 Promotes Gastrointestinal Stromal Tumor Cell Growth and Drug Resistance.

Our inquiry into imatinib resistance in GIST started with a cell line generated by Dr. Brian Rubin from the commonly utilized cell line GIST T1. The new cell line, GIST 10R, had been grown in imatinib, and displayed no known mechanism of resistance on mutation or transcription analysis (Figure 2.1.1). This is of interest because the same is

true for a small subgroup of GIST patients, whose disease becomes refractory to imatinib despite no secondary mutations in KIT or upregulation of any known bypass pathway. We were hopeful that the GIST 10R cell line would serve as a model system for this disease group.

Upon siRNA-mediated knockdown of the tyrosine kinome, we observed that GIST 10R as well as its parent cell line GIST T1 was dependent on FGFR3 expression (Figures 2.1.2 and 2.1.3). We further discovered signaling crosstalk between KIT and FGFR3 (Figure 2.1.5). While we demonstrated that the two receptors might interact directly, we were not able to distinguish between direct crosstalk and a downstream mediator. We considered TYK2, a JAK family kinase that was essential for viability in both GIST cell lines. While we found evidence that TYK2 was activated by FGF2 stimulation and interacted directly with FGFR3, we found no evidence for activation after KIT stimulation, and no direct association with KIT (Figure 2.1.4). In addition, JAK inhibitors showed no synergy with imatinib in GIST 10R cells (data not shown). We also considered focal adhesion kinase (FAK), an intracellular kinase that can be activated by receptor tyrosine kinases as well as by extracellular matrix signaling, and that has been implicated in microenvironment-induced resistance. However, we found no evidence for interaction either with KIT or FGFR3, and no decrease in viability upon inhibition of FAK (data not shown). Thus, the signaling mediator between KIT and FGFR3, if there is one, remains to be discovered. Another candidate worthy of investigation would be

PKC, which fulfills the requirement of being activated downstream of both receptors and being able to modulate the activity of receptor tyrosine kinases by both inhibitory and activating Ser/Thr phosphorylations.

We next demonstrated that the crosstalk between KIT and FGFR3 could be exploited by GIST cells to maintain growth during imatinib exposure (Figure 2.1.7). In particular, activating of the MAPK pathway appeared to be essential for survival (Figure 2.1.12). This has been a theme in all settings of tyrosine kinase inhibitor resistance that I have studied to date. Likewise, the receptor crosstalk could be targeted in imatinib-resistant cells by combined inhibition of KIT and FGFRs, which re-sensitized cells and achieved remarkable synergy (Figure 2.1.10). Finally, we provided evidence that FGF2 is upregulated in GIST tumors undergoing imatinib treatment, possibly due to FGF2-expressing infiltrating immune cells, and that some cases of resistant disease develop autocrine FGF2 production (Figures 2.1.13 and 2.1.16)). These efforts were somewhat hampered by the difficulty in obtaining high numbers of GIST biopsies. Ideally, these would have been sequential biopsies before and during treatment, as well as after the onset of resistance. We decided that it was more feasible to examine the dynamics of FGF2 expression in human tissue in readily accessible bone marrow biopsies (see the next two manuscripts). Shortly after publication of this manuscript, a study identified FGFR1-depdent MAPK reactivation by FGF2 as a resistance mechanism in patient-derived GIST xenografts[226]. These data served as pre-clinical support for a clinical

trial to examine the effect of imatinib in combination with FGFR inhibitor BGJ398 for patients with advanced, treatment-naïve GIST (NCT02257541). This trial is still ongoing.

5.2 Ponatinib overcomes FGF2-mediated resistance in CML patients without kinase domain mutations.

The finding that FGF2 protects CML cells originated from a microenvironmental screen in which cytokines and growth factors were evaluated for their propensity to promote proliferation in cells exposed to imatinib (Figure 2.2.1). As in GIST, this effect was mediated by FGFR3 and led to reactivation of MAPK signaling (Figures 2.2.2 and 2.2.6). Unlike in GIST, where a resistant cell line had already been generated, CML cells were first cultured with imatinib and FGF2 for approximately three weeks, at which time they resumed exponential growth. With the exception of one culture, which re-activated BCR-ABL in the presence of imatinib, all long-term cultures displayed imatinib resistance that could be overcome by combined inhibition of BCR-ABL and FGFRs (Figures 2.2.3 and 2.2.4).

For this study, we had the opportunity to obtain bone marrow biopsies from CML patients enrolled in a trial for Ponatinib, a tyrosine kinase inhibitor that targets FGFRs as well as BCR-ABL. These patients had relapsed on imatinib and at least one other kinase inhibitor. Relapse was attributed either to a secondary mutation in BCR-ABL, or to a BCR-ABL-independent pathway. We obtained serial bone marrow biopsies: at

diagnosis, upon relapse but before Ponatinib, and after Ponatinib treatment had been initiated. We found that FGF2 expression was upregulated in CML patients, both treated and untreated, compared to normal controls (Figure 2.2.8). As discussed in chapter 1.2.5 of the introduction, this is a common feature in several hematologic malignancies and likely stems from activation of a stress response by bone marrow stroma that has become disrupted by leukemic stem cells. Furthermore, patients who relapsed without secondary mutations in BCR-ABL had dramatically increased FGF2 levels (Figure 2.2.8). In this group, Ponatinib treatment resulted in downregulation of FGF2 (Figure 2.2.8). Immunohistochemistry and immunofluorescence showed that FGF2 was localized to stromal cells as opposed to hematopoietic progenitors or leukemic blasts, although the staining pattern was diffuse in biopsies taken upon relapse (Figure 2.2.11). The observation that FGF2 levels decreased after FGFR inhibition was the first indication that stromal cells might have an autocrine positive feedback loop. We further explored this hypothesis in the final manuscript described in this thesis.

5.3 FGF2 from the bone marrow stroma promotes resistance to FLT3 inhibitors in acute myeloid leukemia

Already suspecting that FGF2 might serve as a protective growth factor in multiple settings of tyrosine kinase inhibition, we performed another microenvironmental screen on FLT3-ITD positive AML cells exposed to the FLT3 inhibitor AC220. This time, we

found that in addition to FGF2, FLT3 ligand (FL) could protect cells in the short term and promote outgrowth of resistant cultures in the long term (Figure 2.3.1). In another slight twist to the story, FGFR1 instead of FGFR3 was the most highly expressed receptor and mediated the protective effect of FGF2 (Figure 2.3.2). Our studies as well as others indicate that receptor expression level is a useful initial indicator for relevance to protective signaling.

Having access to a database of primary AML frozen viable cell samples, we sought to test the protective effect of FGF2 in a suitable subset. We selected samples with sensitivity to AC220 (IC50 more than two standard deviations below the mean), and with expression of FGFR1, which we had identified as the most highly expressed FGFR member in AML, by RNAseq. Despite the difficulty inherent in assessing viability of primary frozen samples, we found that approximately 24% of samples responded to FGF2 with a significant increase in viability (Figure 2.3.4). However, we found no correlation between degree of response and FGFR1 expression levels (data not shown), indicating that other factors besides receptor transcription levels determine the activating of protective pathways.

We again found that MAPK pathway reactivation was a feature of all resistant cultures, both those grown in FGF2 and in FL (Figure 2.3.7). In this study, we wanted to simulate the effects of a transient increase in FGF2 and FL in response to therapy, and ask whether ligand withdrawal would still permit outgrowth of resistant cultures. Indeed,

we found that cultures returned to exponential growth on average within less than a month, while initial outgrowth had required on average 2 months. This outgrowth experiment resulted in a good representation of resistance mechanisms seen in the patient population: All cultures grown without ligand or with FGF2 eventually developed secondary mutations in FLT3. Several cultures grown in FL also developed these mutations. 12/17 cultures in addition developed mutations in the MAPK pathway, specifically in KRAS and NRAS. We suspect that the KRAS mutation G13D pre-existed in naïve MOLM14 cells since it was detected in the majority of resistant cultures (Figure 2.3.10). This experiments strongly argues that 1) ligand-induced resistance cultures recapitulate the landscape of resistance mechanisms seen in the clinic and may be a more physiologic alternative to mutagenesis screens, and 2) resistance induced by microenvironmental factors is a two-step process; first allowing disease to linger in the presence of inhibitors, and then providing time and opportunity for the development of mutations that cause true resistance.

5.4 FGF2 Regulates Release of Leukemia-Protective Exosomes from Bone Marrow Stromal Cells

In the last two studies, we had detected FGF2 expression in bone marrow stromal cells. We found the changing levels of FGF2 in response to treatment and relapse intriguing and wondered whether there was a mechanism regulating the expression and release of FGF2 that could be targeted to therapeutic benefit. We worked with two well-

characterized human stromal cell lines, HS-5 and HS-27. These lines were isolated from

the same patient, but display different morphology and properties[316]. The HS-5 cell

line has long been known to produce conditioned media that supported hematopoietic

cells in culture and induced resistance to several kinds of chemotherapy[43], [318],

[319]. Several cytokines produced by HS-5 have been implicated in chemoresistance,

but FGF2, which is also dramatically enriched in HS-5 over HS-27, was not one of them.

We found that FGF2, which is not a classically secreted cytokine, was contained in

exosomes secreted by HS-5 cells (Figure 3.1.2). In addition, HS-5 cells produced

approximately twice the number of extracellular vesicles compared to HS-27 (Figure

3.1.3). From previous work, we suspected that the autocrine FGF2-FGFR1 loop may

regulate HS-5 protective properties. We confirmed this by demonstrating that HS-5 cells

cultured with an FGFR inhibitor produced less protective conditioned medium (Figure

3.1.4). Surprisingly, FGFR inhibition resulted in a decrease in exosome production

(Figure 3.1.5). We confirmed that this effect was specific to signaling through FGF2 and

FGFR1 by inhibiting expression of these proteins either by siRNA, inducible shRNA, or

CRISPR-Cas9 knockout (Figure 3.1.6). These experiments met with complications, as

long-term disruption of FGFR signaling led to senescence. This was also the case in the

culture of bone marrow stroma isolated from FGF2 knockout mice (data not shown).

5.5 Future Directions

At this time, several lines of inquiry are still open with regard to the connection between FGFR signaling, exosome production, and protective phenotype. Although we have demonstrated that the PLC-PKC pathway may mediate exosome production downstream of FGFR1, several intriguing questions remain open. Diacylglycerol, a metabolite of PLC, is implicated in exosome production and release[336]-[338]. DAG kinase further metabolizes and inactivates DAG. To test whether DAG is an important mediator of exosome biogenesis in HS-5 cells, we could combine a DGK inhibitor with FGFR inhibition and measure exosome release.

Another possible connection between FGFR activation and exosome biogenesis is represented by PKC. PKC has been shown to regulate endocytosis and intracellular trafficking of many receptor tyrosine kinases[340]-[342]. FGFR1 contains at least one C-terminal Ser/Thr phosphorylation site that is important for endocytosis[343], but PKC has not been demonstrated to interact with this site. An initial experiment would be detection of Ser/Thr phosphorylation on FGFR1 after PKC inhibition or knockdown.

What other components of HS-5 conditioned media are modulated by FGFR inhibition? This remains an important question to be answered. Given the strong connection between FGF2 and IL-6, my first step would be to assess IL-6 production after FGFR inhibition in HS-5 cells. Of course, the expression of other known protective cytokines,

such as IL-8 and HGF, should also be assessed. There is also to interesting possibility that entire activated receptor complexes could be transferred from stroma to leukemia cells. This has been observed in several instances, for example in GIST, where oncogenic KIT activates downstream pathways in tumor-associated smooth muscle cells[184].

Our findings reveal two important concepts that should be validated in additional models of cancer and therapy resistance: 1) Exosomes released from cells in the microenvironment protect cancer cells during therapy, and 2) Tyrosine kinase receptor activation is coupled to exosome release, which can therefore be modulated by tyrosine kinase inhibitors. Advances in technology will soon enable us to identify exosome populations secreted by a specific tissue or even cell type through the use of modified flow cytometry. With the help of this tool, we will be able to test the hypothesis that a population of protective exosomes is present or enriched in cancer therapy resistance in mouse models or human studies. In addition, we will be able to monitor the success of tyrosine kinase inhibitor treatment with the goal of reducing protective exosome secretion.

5.6   Outlook

Overall, my thesis research has succeeded in refining the question I had in mind at the beginning: how to choose combination therapy to overcome or prevent the development of resistance to tyrosine kinase inhibitors? The use of tyrosine kinase

inhibitors to reprogram the tumor microenvironment is a new approach to this problem, and believe that combination therapies that target cancer-intrinsic oncogenic drivers in addition to extracellular protective signaling will become and important area of research.

In future studies and application of our findings to the clinic, an understanding of tissue homeostasis will be essential, as many damage response pathways, like FGF-signaling outlined in this thesis, are bound to serve a dual role as essential guardians of stem cell pools and cancer-sheltering conspirators. Further research should thus focus on identifying the optimal timing for this intervention, as well as the most advantageous point of interference between cancer-microenvironmental crosstalk. Consideration of timing is especially important when a microenvironment modulator is proposed as an addition to cytotoxic chemotherapy. A better understanding of the dynamics of protective signaling will be necessary to prevent resistance without causing irreversible damage to normal stem cell populations. Potentially, that danger can also be circumvented by finding a unique targeting point in the cancer-microenvironment interaction. My research revealed FGFR inhibition has a possible point of contact to prevent the production of protective vesicles, however, this may not be the only point at which crosstalk between stroma and cancer can be successfully targeted. For example, a component downstream of FGFR, such as PKC, which appears to regulate vesicle release, may be another promising target. Another possibility is identifying signaling

originating from cancer cells that transform or stimulate stroma to adopt a protective

phenotype.

References

[1]   P. Rous, "A SARCOMA OF THE FOWL TRANSMISSIBLE BY AN AGENT SEPARABLE FROM THE TUMOR CELLS," *Journal of Experimental Medicine*, vol. 13, no. 4, pp. 397–411, Apr. 1911.

[2]   D. STEHELIN, H. E. VARMUS, J. M. BISHOP, and P. K. VOGT, "DNA related to the transforming gene(s) of avian sarcoma viruses is present in normal avian DNA," *Nature*, vol. 260, no. 5547, pp. 170–173, Mar. 1976.

[3]   T. Hunter and J. A. Cooper, "Protein-Tyrosine Kinases," *Annu. Rev. Biochem.*, vol. 54, no. 1, pp. 897–930, Jun. 1985.

[4]   G. Manning, D. B. Whyte, R. Martinez, T. Hunter, and S. Sudarsanam, "The protein kinase complement of the human genome.," *Science*, vol. 298, no. 5600, pp. 1912–1934, Dec. 2002.

[5]   A. Ullrich and J. Schlessinger, "Signal transduction by receptors with tyrosine kinase activity," *Cell*, vol. 61, no. 2, pp. 203–212, Apr. 1990.

[6]   W. J. Fantl, D. E. Johnson, and L. T. Williams, "Signalling by Receptor Tyrosine Kinases," *Annu. Rev. Biochem.*, vol. 62, no. 1, pp. 453–481, Jun. 1993.

[7]   T. Taniguchi, "Cytokine signaling through nonreceptor protein tyrosine kinases," *Science*, vol. 268, no. 5208, pp. 251–255, Apr. 1995.

[8]   S. R. Hubbard and J. H. Till, "Protein tyrosine kinase structure and function.," *Annu. Rev. Biochem.*, vol. 69, no. 1, pp. 373–398, 2000.

[9]   S. R. Hubbard, "Structural analysis of receptor tyrosine kinases.," *Prog. Biophys. Mol. Biol.*, vol. 71, no. 3, pp. 343–358, 1999.

[10]   C.-H. Heldin, "Dimerization of cell surface receptors in signal transduction," *Cell*, vol. 80, no. 2, pp. 213–223, Jan. 1995.

[11]   L. S. Argetsinger, G. S. Campbell, X. Yang, B. A. Witthuhn, O. Silvennoinen, J. N. Ihle, and C. Carter-Su, "Identification of JAK2 as a growth hormone receptor-associated tyrosine kinase," *Cell*, vol. 74, no. 2, pp. 237–244, Jul. 1993.

[12]   T. Kishimoto, T. Taga, and S. Akira, "Cytokine signal transduction," *Cell*, vol. 76, no. 2, pp. 253–262, Jan. 1994.

[13]   A. D. Keegan and W. E. Paul, "Multichain immune recognition receptors: similarities in structure and signaling pathways," *Immunology Today*, vol. 13, no. 2, pp. 63–68, Jan. 1992.

[14]   J. N. Ihle and I. M. Kerr, "Jaks and Stats in signaling by the cytokine receptor superfamily," *Trends in Genetics*, vol. 11, no. 2, pp. 69–74, Feb. 1995.

[15]   J. N. Ihle, B. A. Witthuhn, F. W. Quelle, K. Yamamoto, W. E. Thierfelder, B. Kreider, and O. Silvennoinen, "Signaling by the cytokine receptor superfamily: JAKs and STATs," *Trends in Biochemical Sciences*, vol. 19, no. 5, pp. 222–227, May 1994.

[16]   J. S. Biscardi, D. A. Tice, and S. J. Parsons, "c-Src, Receptor Tyrosine Kinases, and Human Cancer," vol. 76, Elsevier, 1999, pp. 61–119.

[17]   R. M. Stephens, D. M. Loeb, T. D. Copeland, T. Pawson, L. A. Greene, and D. R. Kaplan, "Trk receptors use redundant signal transduction pathways involving SHC and PLC-γ1 to mediate NGF responses," *Neuron*, vol. 12, no. 3, pp. 691–705, Mar. 1994.

[18]   E. G. Krebs, "The phosphorylation of proteins: a major mechanism for biological regulation. Fourteenth Sir Frederick Gowland Hopkins memorial lecture.," *Biochem. Soc. Trans*, vol. 13, no. 5, pp. 813–820, Oct. 1985.

[19]   N. K. Tonks and B. G. Neel, "From Form to Function: Signaling by Protein Tyrosine Phosphatases," *Cell*, vol. 87, no. 3, pp. 365–368, Nov. 1996.

[20]   M. A. Lemmon and J. Schlessinger, "Cell signaling by receptor tyrosine kinases.," *Cell*, vol. 141, no. 7, pp. 1117–1134, Jun. 2010.

[21]   G. A. Rodrigues and M. Park, "Oncogenic activation of tyrosine kinases," *Current Opinion in Genetics & Development*, vol. 4, no. 1, pp. 15–24, Feb. 1994.

[22]   R. M. Hudziak, J. Schlessinger, and A. Ullrich, "Increased expression of the putative growth factor receptor p185HER2 causes transformation and tumorigenesis of NIH 3T3 cells.," *Proc. Natl. Acad. Sci. U.S.A.*, vol. 84, no. 20, pp. 7159–7163, Oct. 1987.

[23]   P. P. Di Fiore, J. H. Pierce, T. P. Fleming, R. Hazan, A. Ullrich, C. R. King, J. Schlessinger, and S. A. Aaronson, "Overexpression of the human EGF receptor confers an EGF-dependent transformed phenotype to NIH 3T3 cells," *Cell*, vol. 51, no. 6, pp. 1063–1070, Dec. 1987.

[24]   E. D. Lynch, E. A. Ostermeyer, M. K. Lee, J. F. Arena, H. Ji, J. Dann, K. Swisshelm, D. Suchard, P. M. MacLeod, S. Kvinnsland, B. T. Gjertsen, K. Heimdal, H. Lubs, P. Møller, and M. C. King, "Inherited mutations in PTEN that are associated with breast cancer, cowden disease, and juvenile polyposis.," *Am. J. Hum. Genet.*, vol. 61, no. 6, pp. 1254–1260, Dec. 1997.

[25]   D. Hanahan and L. M. Coussens, "Accessories to the crime: functions of cells recruited to the tumor microenvironment.," *Cancer Cell*, vol. 21, no. 3, pp. 309–322, Mar. 2012.

[26]   D. Fabbro, S. Ruetz, E. Buchdunger, S. W. Cowan-Jacob, G. Fendrich, J. Liebetanz, J. Mestan, T. O'Reilly, P. Traxler, B. Chaudhuri, H. Fretz, J. Zimmermann, T. Meyer, G. Caravatti, P. Furet, and P. W. Manley, "Protein kinases as targets for

anticancer agents: from inhibitors to useful drugs.," *Pharmacology & Therapeutics*, vol. 93, no. 2, pp. 79–98, Feb. 2002.

[27]   P. Wu, T. E. Nielsen, and M. H. Clausen, "FDA-approved small-molecule kinase inhibitors.," *Trends Pharmacol. Sci.*, vol. 36, no. 7, pp. 422–439, Jul. 2015.

[28]   P. Wu, T. E. Nielsen, and M. H. Clausen, "Small-molecule kinase inhibitors: an analysis of FDA-approved drugs.," *Drug Discov. Today*, vol. 21, no. 1, pp. 5–10, Jan. 2016.

[29]   P. Yaish, A. Gazit, C. Gilon, and A. Levitzki, "Blocking of EGF-dependent cell proliferation by EGF receptor kinase inhibitors.," *Science*, vol. 242, no. 4880, pp. 933–935, Nov. 1988.

[30]   M. M. Gallogly and H. M. Lazarus, "Midostaurin: an emerging treatment for acute myeloid leukemia patients.," *J Blood Med*, vol. 7, pp. 73–83, 2016.

[31]   N. Feller, M. A. van der Pol, A. van Stijn, G. W. D. Weijers, A. H. Westra, B. W. Evertse, G. J. Ossenkoppele, and G. J. Schuurhuis, "MRD parameters using immunophenotypic detection methods are highly reliable in predicting survival in acute myeloid leukaemia," *Leukemia*, vol. 18, no. 8, pp. 1380–1390, Jun. 2004.

[32]   C. J. Hess, F. Denkers, G. J. Ossenkoppele, Q. Waisfisz, C. J. McElgunn, E. Eldering, J. P. Schouten, and G. J. Schuurhuis, "Gene expression profiling of minimal residual disease in acute myeloid leukaemia by novel multiplex-PCR-based method," *Leukemia*, vol. 18, no. 12, pp. 1981–1988, Oct. 2004.

[33]   J. Brisco, E. Hughes, S. H. Neoh, P. J. Sykes, K. Bradstock, A. Enno, J. Szer, K. McCaul, and A. A. Morley, "Relationship between minimal residual disease and outcome in adult acute lymphoblastic leukemia.," *Blood*, vol. 87, no. 12, pp. 5251–5256, Jun. 1996.

[34]   M. E. Gorre, M. Mohammed, K. Ellwood, N. Hsu, R. Paquette, P. N. Rao, and C. L. Sawyers, "Clinical resistance to STI-571 cancer therapy caused by BCR-ABL gene mutation or amplification.," *Science*, vol. 293, no. 5531, pp. 876–880, Aug. 2001.

[35]   L. Huang and L. Fu, "Mechanisms of resistance to EGFR tyrosine kinase inhibitors.," *Acta Pharm Sin B*, vol. 5, no. 5, pp. 390–401, Sep. 2015.

[36]   Y.-F. Chen and L.-W. Fu, "Mechanisms of acquired resistance to tyrosine kinase inhibitors," *Acta Pharm Sin B*, vol. 1, no. 4, pp. 197–207, Dec. 2011.

[37]   T. Matsunaga, N. Takemoto, T. Sato, R. Takimoto, I. Tanaka, A. Fujimi, T. Akiyama, H. Kuroda, Y. Kawano, M. Kobune, J. Kato, Y. Hirayama, S. Sakamaki, K. Kohda, K. Miyake, and Y. Niitsu, "Interaction between leukemic-cell VLA-4 and stromal fibronectin is a decisive factor for minimal residual disease of acute myelogenous leukemia," *Nat. Med.*, vol. 9, no. 9, pp. 1158–1165, Aug. 2003.

[38]   J. S. Damiano, A. E. Cress, L. A. Hazlehurst, A. A. Shtil, and W. S. Dalton, "Cell adhesion mediated drug resistance (CAM-DR): role of integrins and resistance to apoptosis in human myeloma cell lines.," *Blood*, vol. 93, no. 5, pp. 1658–1667, Mar. 1999.

[39]   M. B. Meads, L. A. Hazlehurst, and W. S. Dalton, "The Bone Marrow Microenvironment as a Tumor Sanctuary and Contributor to Drug Resistance," *Clin. Cancer Res.*, vol. 14, no. 9, pp. 2519–2526, May 2008.

[40]   L. A. Hazlehurst, R. F. Argilagos, and W. S. Dalton, "?1 integrin mediated adhesion increases Bim protein degradation and contributes to drug resistance in leukaemia cells," *Br. J. Haematol.*, vol. 136, no. 2, pp. 269–275, Jan. 2007.

[41]   T. Matsunaga, F. Fukai, S. Miura, Y. Nakane, T. Owaki, H. Kodama, M. Tanaka, T. Nagaya, R. Takimoto, T. Takayama, and Y. Niitsu, "Combination therapy of an anticancer drug with the FNIII14 peptide of fibronectin effectively overcomes cell adhesion-mediated drug resistance of acute myelogenous leukemia.," *Leukemia*, vol. 22, no. 2, pp. 353–360, Feb. 2008.

[42]   P. S. Becker, K. J. Kopecky, A. N. Wilks, S. Chien, J. M. Harlan, C. L. Willman, S. H. Petersdorf, D. L. Stirewalt, T. Papayannopoulou, and F. R. Appelbaum, "Very late antigen-4 function of myeloblasts correlates with improved overall survival for patients with acute myeloid leukemia.," *Blood*, vol. 113, no. 4, pp. 866–874, Jan. 2009.

[43]   Y. Nefedova, T. H. Landowski, and W. S. Dalton, "Bone marrow stromal-derived soluble factors and direct cell contact contribute to de novo drug resistance of myeloma cells by distinct mechanisms.," *Leukemia*, vol. 17, no. 6, pp. 1175–1182, Jun. 2003.

[44]   M. A. Frassanito, "Autocrine interleukin-6 production and highly malignant multiple myeloma: relation with resistance to drug-induced apoptosis," *Blood*, vol. 97, no. 2, pp. 483–489, Jan. 2001.

[45]   L. E. Perez, N. Parquet, K. Shain, R. Nimmanapalli, M. Alsina, C. Anasetti, and W. Dalton, "Bone marrow stroma confers resistance to Apo2 ligand/TRAIL in multiple myeloma in part by regulating c-FLIP.," *The Journal of Immunology*, vol. 180, no. 3, pp. 1545–1555, Feb. 2008.

[46]   P. M. Voorhees, Q. Chen, D. J. Kuhn, G. W. Small, S. A. Hunsucker, J. S. Strader, R. E. Corringham, M. H. Zaki, J. A. Nemeth, and R. Z. Orlowski, "Inhibition of interleukin-6 signaling with CNTO 328 enhances the activity of bortezomib in preclinical models of multiple myeloma.," *Clin. Cancer Res.*, vol. 13, no. 21, pp. 6469–6478, Nov. 2007.

[47]   Z.-G. Zhao, Y. Liang, K. Li, W.-M. Li, Q.-B. Li, Z.-C. Chen, and P. Zou, "Phenotypic and Functional Comparison of Mesenchymal Stem Cells Derived from the

Bone Marrow of Normal Adults and Patients with Hematologic Malignant Diseases," *Stem Cells Dev.*, vol. 16, no. 4, pp. 637–648, Aug. 2007.

[48]   D. Hanahan and R. A. Weinberg, "Hallmarks of cancer: the next generation.," vol. 144, no. 5, pp. 646–674, 2011.

[49]   Y. Mori, N. Shimizu, M. Dallas, M. Niewolna, B. Story, P. J. Williams, G. R. Mundy, and T. Yoneda, "Anti-alpha4 integrin antibody suppresses the development of multiple myeloma and associated osteoclastic osteolysis.," *Blood*, vol. 104, no. 7, pp. 2149–2154, Oct. 2004.

[50]   B. Lin, K. Podar, D. Gupta, Y.-T. Tai, S. Li, E. Weller, T. Hideshima, S. Lentzsch, F. Davies, C. Li, E. Weisberg, R. L. Schlossman, P. G. Richardson, J. D. Griffin, J. Wood, N. C. Munshi, and K. C. Anderson, "The vascular endothelial growth factor receptor tyrosine kinase inhibitor PTK787/ZK222584 inhibits growth and migration of multiple myeloma cells in the bone marrow microenvironment.," *Cancer Res.*, vol. 62, no. 17, pp. 5019–5026, Sep. 2002.

[51]   G. Bisping, D. Wenning, M. Kropff, D. Gustavus, C. Muller-Tidow, M. Stelljes, G. Munzert, F. Hilberg, G. J. Roth, M. Stefanic, S. Volpert, R. M. Mesters, W. E. Berdel, and J. Kienast, "Bortezomib, Dexamethasone, and Fibroblast Growth Factor Receptor 3-Specific Tyrosine Kinase Inhibitor in t(4;14) Myeloma," *Clin. Cancer Res.*, vol. 15, no. 2, pp. 520–531, Jan. 2009.

[52]   G. Bisping, R. Leo, D. Wenning, B. Dankbar, T. Padró, M. Kropff, C. Scheffold, M. Kröger, R. M. Mesters, W. E. Berdel, and J. Kienast, "Paracrine interactions of basic fibroblast growth factor and interleukin-6 in multiple myeloma.," *Blood*, vol. 101, no. 7, pp. 2775–2783, Apr. 2003.

[53]   A. Beenken and M. Mohammadi, "The FGF family: biology, pathophysiology and therapy," *Nature Reviews Drug Discovery*, vol. 8, no. 3, pp. 235–253, Mar. 2009.

[54]   C. Powers, "Fibroblast growth factors, their receptors and signaling," *Endocrine Related Cancer*, vol. 7, no. 3, pp. 165–197, Sep. 2000.

[55]   V. P. Eswarakumar, I. Lax, and J. Schlessinger, "Cellular signaling by fibroblast growth factor receptors.," *Cytokine & Growth Factor Reviews*, vol. 16, no. 2, pp. 139–149, Apr. 2005.

[56]   H. Kurosu, Y. Ogawa, M. Miyoshi, M. Yamamoto, A. Nandi, K. P. Rosenblatt, M. G. Baum, S. Schiavi, M.-C. Hu, O. W. Moe, and M. Kuro-o, "Regulation of fibroblast growth factor-23 signaling by klotho.," *Journal of Biological Chemistry*, vol. 281, no. 10, pp. 6120–6123, Mar. 2006.

[57]   B. C. Lin, M. Wang, C. Blackmore, and L. R. Desnoyers, "Liver-specific activities of FGF19 require Klotho beta.," *Journal of Biological Chemistry*, vol. 282, no. 37, pp. 27277–27284, Sep. 2007.

[58]   Y. Luo, C. Yang, W. Lu, R. Xie, C. Jin, P. Huang, F. Wang, and W. L. McKeehan, "Metabolic regulator betaKlotho interacts with fibroblast growth factor receptor 4 (FGFR4) to induce apoptosis and inhibit tumor cell proliferation.," *J. Biol. Chem.*, vol. 285, no. 39, pp. 30069–30078, Sep. 2010.

[59]   H. A. Armelin, "Pituitary extracts and steroid hormones in the control of 3T3 cell growth.," *Proc. Natl. Acad. Sci. U.S.A.*, vol. 70, no. 9, pp. 2702–2706, Sep. 1973.

[60]   D. Gospodarowicz, "Localisation of a fibroblast growth factor and its effect alone and with hydrocortisone on 3T3 cell growth.," *Nature*, vol. 249, no. 453, pp. 123–127, May 1974.

[61]   X. Li, C. Wang, J. Xiao, W. L. McKeehan, and F. Wang, "Fibroblast growth factors, old kids on the new block.," *Semin. Cell Dev. Biol.*, vol. 53, pp. 155–167, May 2016.

[62]   J. A. Hennessey, E. Q. Wei, and G. S. Pitt, "Fibroblast growth factor homologous factors modulate cardiac calcium channels.," *Circ. Res.*, vol. 113, no. 4, pp. 381–388, Aug. 2013.

[63]   C. Wang, C. Wang, E. G. Hoch, and G. S. Pitt, "Identification of novel interaction sites that determine specificity between fibroblast growth factor homologous factors and voltage-gated sodium channels.," *J. Biol. Chem.*, vol. 286, no. 27, pp. 24253–24263, Jul. 2011.

[64]   S. K. Olsen, M. Garbi, N. Zampieri, A. V. Eliseenkova, D. M. Ornitz, M. Goldfarb, and M. Mohammadi, "Fibroblast growth factor (FGF) homologous factors share structural but not functional homology with FGFs.," *Journal of Biological Chemistry*, vol. 278, no. 36, pp. 34226–34236, Sep. 2003.

[65]   V. Sørensen, T. Nilsen, and A. Wiedłocha, "Functional diversity of FGF-2 isoforms by intracellular sorting.," *Bioessays*, vol. 28, no. 5, pp. 504–514, May 2006.

[66]   M. Renko, N. Quarto, T. Morimoto, and D. B. Rifkin, "Nuclear and cytoplasmic localization of different basic fibroblast growth factor species.," *J. Cell. Physiol.*, vol. 144, no. 1, pp. 108–114, Jul. 1990.

[67]   W. Nickel, "The unconventional secretory machinery of fibroblast growth factor 2.," *Traffic*, vol. 12, no. 7, pp. 799–805, Jul. 2011.

[68]   J. P. Steringer, H.-M. Müller, and W. Nickel, "Unconventional secretion of fibroblast growth factor 2--a novel type of protein translocation across membranes?," *J. Mol. Biol.*, vol. 427, no. 6, pp. 1202–1210, Mar. 2015.

[69]   S. Taverna, G. Ghersi, A. Ginestra, S. Rigogliuso, S. Pecorella, G. Alaimo, F. Saladino, V. Dolo, P. Dell'Era, A. Pavan, G. Pizzolanti, P. Mignatti, M. Presta, and M. L. Vittorelli, "Shedding of membrane vesicles mediates fibroblast growth factor-2 release from cells.," *Journal of Biological Chemistry*, vol. 278, no. 51, pp. 51911–51919, Dec. 2003.

[70]   P. Proia, G. Schiera, M. Mineo, A. M. R. Ingrassia, G. Santoro, G. Savettieri, and I. Di Liegro, "Astrocytes shed extracellular vesicles that contain fibroblast growth factor-2 and vascular endothelial growth factor.," *Int. J. Mol. Med.*, vol. 21, no. 1, pp. 63–67, Jan. 2008.

[71]   M. Mohammadi, A. M. Honegger, D. Rotin, R. Fischer, F. Bellot, W. Li, C. A. Dionne, M. Jaye, M. Rubinstein, and J. Schlessinger, "A tyrosine-phosphorylated carboxy-terminal peptide of the fibroblast growth factor receptor (Flg) is a binding site for the SH2 domain of phospholipase C-gamma 1.," *Molecular and Cellular Biology*, vol. 11, no. 10, pp. 5068–5078, Oct. 1991.

[72]   S. H. Ong, G. R. Guy, Y. R. Hadari, S. Laks, N. Gotoh, J. Schlessinger, and I. Lax, "FRS2 proteins recruit intracellular signaling pathways by binding to diverse targets on fibroblast growth factor and nerve growth factor receptors.," *Molecular and Cellular Biology*, vol. 20, no. 3, pp. 979–989, Feb. 2000.

[73]   H. Larsson, P. Klint, E. Landgren, and L. Claesson-Welsh, "Fibroblast growth factor receptor-1-mediated endothelial cell proliferation is dependent on the Src homology (SH) 2/SH3 domain-containing adaptor protein Crk.," *Journal of Biological Chemistry*, vol. 274, no. 36, pp. 25726–25734, Sep. 1999.

[74]   W. L. McKeehan, F. Wang, and M. Kan, "The heparan sulfate-fibroblast growth factor family: diversity of structure and function.," *Prog. Nucleic Acid Res. Mol. Biol.*, vol. 59, pp. 135–176, 1998.

[75]   B. Matuszewska, M. Keogan, D. M. Fisher, K. A. Soper, C. M. Hoe, A. C. Huber, and J. V. Bondi, "Acidic fibroblast growth factor: evaluation of topical formulations in a diabetic mouse wound healing model.," *Pharm. Res.*, vol. 11, no. 1, pp. 65–71, Jan. 1994.

[76]   L. Xie, M. Zhang, B. Dong, M. Guan, M. Lu, Z. Huang, H. Gao, and X. Li, "Improved refractory wound healing with administration of acidic fibroblast growth factor in diabetic rats.," *Diabetes Res. Clin. Pract.*, vol. 93, no. 3, pp. 396–403, Sep. 2011.

[77]   N. T. Bennett and G. S. Schultz, "Growth factors and wound healing: biochemical properties of growth factors and their receptors.," *Am. J. Surg.*, vol. 165, no. 6, pp. 728–737, Jun. 1993.

[78]   B. Ma, D.-S. Cheng, Z.-F. Xia, D.-F. Ben, W. Lu, Z.-F. Cao, Q. Wang, J. He, J.-K. Chai, C.-A. Shen, Y.-H. Sun, G.-A. Zhang, and X.-H. Hu, "Randomized, multicenter, double-blind, and placebo-controlled trial using topical recombinant human acidic fibroblast growth factor for deep partial-thickness burns and skin graft donor site.," *Wound Repair Regen*, vol. 15, no. 6, pp. 795–799, Nov. 2007.

[79]   T. Sakurai, M. Tsuchida, P. D. Lampe, and M. Murakami, "Cardiomyocyte FGF signaling is required for Cx43 phosphorylation and cardiac gap junction maintenance.," *Experimental Cell Research*, vol. 319, no. 14, pp. 2152–2165, Aug. 2013.

[80]   M. Simons, B. H. Annex, R. J. Laham, N. Kleiman, T. Henry, H. Dauerman, J. E. Udelson, E. V. Gervino, M. Pike, M. J. Whitehouse, T. Moon, and N. A. Chronos, "Pharmacological treatment of coronary artery disease with recombinant fibroblast growth factor-2: double-blind, randomized, controlled clinical trial.," *Circulation*, vol. 105, no. 7, pp. 788–793, Feb. 2002.

[81]   R. J. Laham, N. A. Chronos, M. Pike, M. E. Leimbach, J. E. Udelson, J. D. Pearlman, R. I. Pettigrew, M. J. Whitehouse, C. Yoshizawa, and M. Simons, "Intracoronary basic fibroblast growth factor (FGF-2) in patients with severe ischemic heart disease: results of a phase I open-label dose escalation study.," *J. Am. Coll. Cardiol.*, vol. 36, no. 7, pp. 2132–2139, Dec. 2000.

[82]   Y. Sakakibara, K. Tambara, G. Sakaguchi, F. Lu, M. Yamamoto, K. Nishimura, Y. Tabata, and M. Komeda, "Toward surgical angiogenesis using slow-released basic fibroblast growth factor.," *Eur J Cardiothorac Surg*, vol. 24, no. 1, pp. 105–11– discussion 112, Jul. 2003.

[83]   W. Srisakuldee, M. M. Jeyaraman, B. E. Nickel, S. Tanguy, Z.-S. Jiang, and E. Kardami, "Phosphorylation of connexin-43 at serine 262 promotes a cardiac injury-resistant state.," *Cardiovasc. Res.*, vol. 83, no. 4, pp. 672–681, Sep. 2009.

[84]   J. Kastrup, "Gene therapy and angiogenesis in patients with coronary artery disease," *Expert Review of Cardiovascular Therapy*, vol. 8, no. 8, pp. 1127–1138, Jan. 2014.

[85]   M. J. Potthoff, S. A. Kliewer, and D. J. Mangelsdorf, "Endocrine fibroblast growth factors 15/19 and 21: from feast to famine.," *Genes Dev.*, vol. 26, no. 4, pp. 312–324, Feb. 2012.

[86]   A. Kharitonenkov, T. L. Shiyanova, A. Koester, A. M. Ford, R. Micanovic, E. J. Galbreath, G. E. Sandusky, L. J. Hammond, J. S. Moyers, R. A. Owens, J. Gromada, J. T. Brozinick, E. D. Hawkins, V. J. Wroblewski, D.-S. Li, F. Mehrbod, S. R. Jaskunas, and A. B. Shanafelt, "FGF-21 as a novel metabolic regulator.," *J. Clin. Invest.*, vol. 115, no. 6, pp. 1627–1635, Jun. 2005.

[87]   I. N. Foltz, S. Hu, C. King, X. Wu, C. Yang, W. Wang, J. Weiszmann, J. Stevens, J. S. Chen, N. Nuanmanee, J. Gupte, R. Komorowski, L. Sekirov, T. Hager, T. Arora, H. Ge, H. Baribault, F. Wang, J. Sheng, M. Karow, M. Wang, Y. Luo, W. McKeehan, Z. Wang, M. M. Véniant, and Y. Li, "Treating diabetes and obesity with an FGF21-mimetic antibody activating the βKlotho/FGFR1c receptor complex.," *Sci Transl Med*, vol. 4, no. 162, pp. 162ra153–162ra153, Nov. 2012.

[88]   Y. Luo and W. L. McKeehan, "Stressed Liver and Muscle Call on Adipocytes with FGF21.," *Front Endocrinol (Lausanne)*, vol. 4, p. 194, 2013.

[89]   T. P. Yamaguchi, K. Harpal, M. Henkemeyer, and J. Rossant, "fgfr-1 is required for embryonic growth and mesodermal patterning during mouse gastrulation.," *Genes Dev.*, vol. 8, no. 24, pp. 3032–3044, Dec. 1994.

[90]   C. Deng, M. Bedford, C. Li, X. Xu, X. Yang, J. Dunmore, and P. Leder, "Fibroblast growth factor receptor-1 (FGFR-1) is essential for normal neural tube and limb development.," *Dev. Biol.*, vol. 185, no. 1, pp. 42–54, May 1997.

[91]   C. X. Deng, A. Wynshaw-Boris, M. M. Shen, C. Daugherty, D. M. Ornitz, and P. Leder, "Murine FGFR-1 is required for early postimplantation growth and axial organization.," *Genes Dev.*, vol. 8, no. 24, pp. 3045–3057, Dec. 1994.

[92]   E. Arman, R. Haffner-Krausz, Y. Chen, J. K. Heath, and P. Lonai, "Targeted disruption of fibroblast growth factor (FGF) receptor 2 suggests a role for FGF signaling in pregastrulation mammalian development.," *Proc. Natl. Acad. Sci. U.S.A.*, vol. 95, no. 9, pp. 5082–5087, Apr. 1998.

[93]   A. Orr-Urtreger, M. T. Bedford, T. Burakova, E. Arman, Y. Zimmer, A. Yayon, D. Givol, and P. Lonai, "Developmental localization of the splicing alternatives of fibroblast growth factor receptor-2 (FGFR2).," *Dev. Biol.*, vol. 158, no. 2, pp. 475–486, Aug. 1993.

[94]   V. P. Eswarakumar, E. Monsonego-Ornan, M. Pines, I. Antonopoulou, G. M. Morriss-Kay, and P. Lonai, "The IIIc alternative of Fgfr2 is a positive regulator of bone formation.," *Development*, vol. 129, no. 16, pp. 3783–3793, Aug. 2002.

[95]   J. S. Colvin, B. A. Bohne, G. W. Harding, D. G. McEwen, and D. M. Ornitz, "Skeletal overgrowth and deafness in mice lacking fibroblast growth factor receptor 3.," *Nat. Genet.*, vol. 12, no. 4, pp. 390–397, Apr. 1996.

[96]   G. Valverde-Franco, H. Liu, D. Davidson, S. Chai, H. Valderrama-Carvajal, D. Goltzman, D. M. Ornitz, and J. E. Henderson, "Defective bone mineralization and osteopenia in young adult FGFR3-/- mice.," *Hum. Mol. Genet.*, vol. 13, no. 3, pp. 271–284, Feb. 2004.

[97]   S. Cool, R. Jackson, P. Pincus, I. Dickinson, and V. Nurcombe, "Fibroblast growth factor receptor 4 (FGFR4) expression in newborn murine calvaria and primary osteoblast cultures.," *Int. J. Dev. Biol.*, vol. 46, no. 4, pp. 519–523, 2002.

[98]   N. Hallinan, S. Finn, S. Cuffe, S. Rafee, K. O'Byrne, and K. Gately, "Targeting the fibroblast growth factor receptor family in cancer.," *Cancer Treatment Reviews*, vol. 46, pp. 51–62, May 2016.

[99]   G. Liang, G. Chen, X. Wei, Y. Zhao, and X. Li, "Small molecule inhibition of fibroblast growth factor receptors in cancer.," *Cytokine & Growth Factor Reviews*, vol. 24, no. 5, pp. 467–475, Oct. 2013.

[100]   A. A. Bakkar, H. Wallerand, F. Radvanyi, J.-B. Lahaye, S. Pissard, L. Lecerf, J. C. Kouyoumdjian, C. C. Abbou, J.-C. Pairon, M.-C. Jaurand, J.-P. Thiery, D. K. Chopin, and S. G. D. de Medina, "FGFR3 and TP53 gene mutations define two distinct pathways in urothelial cell carcinoma of the bladder.," *Cancer Res.*, vol. 63, no. 23, pp. 8108–8112, Dec. 2003.

[101]   Y. Mosesson, G. B. Mills, and Y. Yarden, "Derailed endocytosis: an emerging feature of cancer.," *Nat. Rev. Cancer*, vol. 8, no. 11, pp. 835–850, Nov. 2008.

[102]   K. Holzmann, T. Grunt, C. Heinzle, S. Sampl, H. Steinhoff, N. Reichmann, M. Kleiter, M. Hauck, and B. Marian, "Alternative Splicing of Fibroblast Growth Factor Receptor IgIII Loops in Cancer.," *J Nucleic Acids*, vol. 2012, no. 15, pp. 950508–12, 2012.

[103]   M. Chesi, L. A. Brents, S. A. Ely, C. Bais, D. F. Robbiani, E. A. Mesri, W. M. Kuehl, and P. L. Bergsagel, "Activated fibroblast growth factor receptor 3 is an oncogene that contributes to tumor progression in multiple myeloma.," *Blood*, vol. 97, no. 3, pp. 729–736, Feb. 2001.

[104]   Z. Li, Y. X. Zhu, E. E. Plowright, P. L. Bergsagel, M. Chesi, B. Patterson, T. S. Hawley, R. G. Hawley, and A. K. Stewart, "The myeloma-associated oncogene fibroblast growth factor receptor 3 is transforming in hematopoietic cells.," *Blood*, vol. 97, no. 8, pp. 2413–2419, Apr. 2001.

[105]   A. Vacca, "Bone marrow angiogenesis in patients with active multiple myeloma," *Semin. Oncol.*, vol. 28, no. 6, pp. 543–550, Dec. 2001.

[106]   M. A. Frassanito, L. Rao, M. Moschetta, R. Ria, L. Di Marzo, A. De Luisi, V. Racanelli, I. Catacchio, S. Berardi, A. Basile, E. Menu, S. Ruggieri, B. Nico, D. Ribatti, R. Fumarulo, F. Dammacco, K. Vanderkerken, and A. Vacca, "Bone marrow fibroblasts parallel multiple myeloma progression in patients and mice: in vitro and in vivo studies.," *Leukemia*, vol. 28, no. 4, pp. 904–916, Apr. 2014.

[107]   E. K. Grand, F. H. Grand, A. J. Chase, F. M. Ross, M. M. Corcoran, D. G. Oscier, and N. C. P. Cross, "Identification of a novel gene,FGFR1OP2, fused toFGFR1 in 8p11 myeloproliferative syndrome," *Genes Chromosomes Cancer*, vol. 40, no. 1, pp. 78–83, 2004.

[108]   M. R. Akl, P. Nagpal, N. M. Ayoub, B. Tai, S. A. Prabhu, C. M. Capac, M. Gliksman, A. Goy, and K. S. Suh, "Molecular and clinical significance of fibroblast growth factor 2 (FGF2 /bFGF) in malignancies of solid and hematological cancers for personalized therapies.," *Oncotarget*, vol. 5, no. 0, Mar. 2016.

[109]   V. J. Gnanapragasam, M. C. Robinson, C. Marsh, C. N. Robson, F. C. Hamdy, and H. Y. Leung, "FGF8 isoform b expression in human prostate cancer.," *Br J Cancer*, vol. 88, no. 9, pp. 1432–1438, May 2003.

[110]   B. Kwabi-Addo, M. Ozen, and M. Ittmann, "The role of fibroblast growth factors and their receptors in prostate cancer.," *Endocrine Related Cancer*, vol. 11, no. 4, pp. 709–724, Dec. 2004.

[111]   R. Aalinkeel, M. P. N. Nair, G. Sufrin, S. D. Mahajan, K. C. Chadha, R. P. Chawda, and S. A. Schwartz, "Gene expression of angiogenic factors correlates with metastatic potential of prostate cancer cells.," *Cancer Res.*, vol. 64, no. 15, pp. 5311–5321, Aug. 2004.

[112]   A. Gualandris, P. Dell'Era, M. Rusnati, R. Giuliani, E. Tanghetti, M. P. Molinari-Tosatti, M. Ziche, D. Ribatti, and M. Presta, "Autocrine Role of Basic Fibroblast Growth Factor (bFGF) in Angiogenesis and Angioproliferative Diseases," in *Angiogenesis*, no. 12, Boston, MA: Springer US, 1998, pp. 99–112.

[113]   M. Presta, L. Tiberio, M. Rusnati, P. Dell'Era, and G. Ragnotti, "Basic fibroblast growth factor requires a long-lasting activation of protein kinase C to induce cell proliferation in transformed fetal bovine aortic endothelial cells.," *Mol. Biol. Cell*, vol. 2, no. 9, pp. 719–726, Sep. 1991.

[114]   D. Hanahan, D. J. Hicklin, O. Casanovas, and G. Bergers, "Drug resistance by evasion of antiangiogenic targeting of VEGF signaling in late-stage pancreatic islet tumors.," *Cancer Cell*, vol. 8, no. 4, pp. 299–309, Oct. 2005.

[115]   R. Gharbaran, A. Goy, T. Tanaka, J. Park, C. Kim, N. Hasan, S. Vemulapalli, S. Sarojini, M. Tuluc, K. Nalley, P. Bhattacharyya, A. Pecora, and K. Suh, "Fibroblast growth factor-2 (FGF2) and syndecan-1 (SDC1) are potential biomarkers for putative circulating CD15+/CD30+ cells in poor outcome Hodgkin lymphoma patients," *J Hematol Oncol*, vol. 6, no. 1, p. 62, 2013.

[116]   D. Khnykin, G. Troen, J.-M. Berner, and J. Delabie, "The expression of fibroblast growth factors and their receptors in Hodgkin's lymphoma," *The Journal of Pathology*, vol. 208, no. 3, pp. 431–438, 2006.

[117]   A. R. Perez-Atayde, S. E. Sallan, U. Tedrow, S. Connors, E. Allred, and J. Folkman, "Spectrum of tumor angiogenesis in the bone marrow of children with acute lymphoblastic leukemia.," *Am. J. Pathol.*, vol. 150, no. 3, pp. 815–821, Mar. 1997.

[118]   L. Smolej, C. Andrýs, V. Maisnar, L. Pour, and J. Malý, "Plasma concentrations of vascular endothelial growth factor and basic fibroblast growth factor in lymphoproliferative disorders.," *Acta Medica (Hradec Kralove)*, vol. 48, no. 1, pp. 57–58, 2005.

[119]   A. Aguayo, H. Kantarjian, T. Manshouri, C. Gidel, E. Estey, D. Thomas, C. Koller, Z. Estrov, S. O'Brien, M. Keating, E. Freireich, and M. Albitar, "Angiogenesis in acute and chronic leukemias and myelodysplastic syndromes.," *Blood*, vol. 96, no. 6, pp. 2240–2245, Sep. 2000.

[120]   A. Aguayo, F. Giles, and M. Albitar, "Vascularity, Angiogenesis and Angiogenic Factors in Leukemias and Myelodysplastic Syndromes," *Leuk. Lymphoma*, vol. 44, no. 2, pp. 213–222, Jul. 2009.

[121]   H. Ishikawa, N. Tsuyama, S. Liu, S. Abroun, F.-J. Li, K.-I. Otsuyama, X. Zheng, Z. Ma, Y. Maki, M. S. Iqbal, M. Obata, and M. M. Kawano, "Accelerated proliferation of myeloma cells by

interleukin-6 cooperating with fibroblast growth factor receptor 3-mediated signals," *Oncogene*, vol. 24, no. 41, pp. 6328–6332, Jun. 2005.

[122] Y. Gan, M. G. Wientjes, and J. L.-S. Au, "Expression of basic fibroblast growth factor correlates with resistance to paclitaxel in human patient tumors.," *Pharm. Res.*, vol. 23, no. 6, pp. 1324–1331, Jun. 2006.

[123] T. Menzel, Z. Rahman, E. Calleja, K. White, E. L. Wilson, R. Wieder, and J. Gabrilove, "Elevated intracellular level of basic fibroblast growth factor correlates with stage of chronic lymphocytic leukemia and is associated with resistance to fludarabine.," *Blood*, vol. 87, no. 3, pp. 1056–1063, Feb. 1996.

[124] O. E. Pardo, N. Sebire, F. Bowen, J. Downward, M. Aubert, I. T. Gout, V. V. Filonenko, P. J. Parker, R. Marais, C. Wellbrock, U. K. Khanzada, I. Arozarena, S. Davidson, and M. J. Seckl, "FGF-2 protects small cell lung cancer cells from apoptosis through a complex involving PKCepsilon, B-Raf and S6K2.," *EMBO J*, vol. 25, no. 13, pp. 3078–3088, Jul. 2006.

[125] Z. Fuks, R. S. Persaud, A. Alfieri, M. McLoughlin, D. Ehleiter, J. L. Schwartz, A. P. Seddon, C. Cordon-Cardo, and A. Haimovitz-Friedman, "Basic fibroblast growth factor protects endothelial cells against radiation-induced programmed cell death in vitro and in vivo.," *Cancer Res.*, vol. 54, no. 10, pp. 2582–2590, May 1994.

[126] A. Karsan, E. Yee, G. G. Poirier, P. Zhou, R. Craig, and J. M. Harlan, "Fibroblast growth factor-2 inhibits endothelial cell apoptosis by Bcl-2-dependent and independent mechanisms.," *Am. J. Pathol.*, vol. 151, no. 6, pp. 1775–1784, Dec. 1997.

[127] E. Chavakis, "Regulation of Endothelial Cell Survival and Apoptosis During Angiogenesis," *Arteriosclerosis, Thrombosis, and Vascular Biology*, vol. 22, no. 6, pp. 887–893, Apr. 2002.

[128] K. E. Ware, C. T. Cummings, D. Astling, T. K. Hinz, E. Kleczko, K. R. Singleton, L. A. Marek, B. A. Helfrich, D. K. Graham, A.-C. Tan, and L. E. Heasley, "A mechanism of resistance to gefitinib mediated by cellular reprogramming and the acquisition of an FGF2-FGFR1 autocrine growth loop.," *Oncogenesis*, vol. 2, no. 3, p. e39, 2013.

[129] H. Terai, K. Soejima, H. Yasuda, S. Nakayama, J. Hamamoto, D. Arai, K. Ishioka, K. Ohgino, S. Ikemura, T. Sato, S. Yoda, R. Satomi, K. Naoki, and T. Betsuyaku, "Activation of the FGF2-FGFR1 autocrine pathway: a novel mechanism of acquired resistance to gefitinib in NSCLC.," *Mol. Cancer Res.*, vol. 11, no. 7, pp. 759–767, Jul. 2013.

[130] V. Yadav, X. Zhang, J. Liu, S. Estrem, S. Li, X.-Q. Gong, S. Buchanan, J. R. Henry, J. J. Starling, and S.-B. Peng, "Reactivation of mitogen-activated protein kinase (MAPK) pathway by FGF receptor 3 (FGFR3)/Ras mediates resistance to vemurafenib in human B-RAF V600E mutant melanoma.," *J. Biol. Chem.*, vol. 287, no. 33, pp. 28087–28098, Aug. 2012.

[131] T. R. Wilson, J. Fridlyand, Y. Yan, E. Penuel, L. Burton, E. Chan, J. Peng, E. Lin, Y. Wang, J. Sosman, A. Ribas, J. Li, J. Moffat, D. P. Sutherlin, H. Koeppen, M. Merchant, R. Neve, and J. Settleman, "Widespread potential for growth-factor-driven resistance to anticancer kinase inhibitors.," *Nature*, vol. 487, no. 7408, pp. 505–509, Jul. 2012.

[132]   L. Tan, J. Wang, J. Tanizaki, Z. Huang, A. R. Aref, M. Rusan, S.-J. Zhu, Y. Zhang, D. Ercan, R. G. Liao, M. Capelletti, W. Zhou, W. Hur, N. Kim, T. Sim, S. Gaudet, D. A. Barbie, J.-R. J. Yeh, C.-H. Yun, P. S. Hammerman, M. Mohammadi, P. A. Jänne, and N. S. Gray, "Development of covalent inhibitors that can overcome resistance to first-generation FGFR kinase inhibitors," *Proc. Natl. Acad. Sci. U.S.A.*, vol. 111, no. 45, pp. E4869–E4877, Nov. 2014.

[133]   H. Sootome, Y. Fujioka, A. Miura, H. Fujita, H. Hirai, and T. Utsugi, "Abstract A271: TAS-120, an irreversible FGFR inhibitor, was effective in tumors harboring FGFR mutations, refractory or resistant to ATP competitive inhibitors .," *Molecular Cancer Therapeutics*, vol. 12, no. 11, pp. A271–A271, Jan. 2014.

[134]   F. Andre, T. Bachelot, M. Campone, F. Dalenc, J. M. Perez-Garcia, S. A. Hurvitz, N. Turner, H. Rugo, J. W. Smith, S. Deudon, M. Shi, Y. Zhang, A. Kay, D. Graus-Porta, A. Yovine, and J. Baselga, "Targeting FGFR with Dovitinib (TKI258): Preclinical and Clinical Data in Breast Cancer," *Clin. Cancer Res.*, vol. 19, no. 13, pp. 3693–3702, Jun. 2013.

[135]   M. Abu-Khalaf, I. Mayer, J. B. Litten, M. Raponi, A. R. Allen, L. Pusztai, and C. L. Arteaga, "Abstract OT1-1-13: A Phase 2, randomized, open-label, multicenter, safety and efficacy study of oral lucitanib in patients with metastatic breast cancer with alterations in the FGF pathway," *Cancer Res.*, vol. 75, no. 9, pp. OT1–1–13–OT1–1–13, Apr. 2015.

[136]   J. C. Soria, F. DeBraud, R. Bahleda, B. Adamo, F. Andre, R. Dientsmann, A. Delmonte, R. Cereda, J. Isaacson, J. Litten, A. Allen, F. Dubois, C. Saba, R. Robert, M. D'Incalci, M. Zucchetti, M. G. Camboni, and J. Tabernero, "Phase I/IIa study evaluating the safety, efficacy, pharmacokinetics, and pharmacodynamics of lucitanib in advanced solid tumors," *Annals of Oncology*, vol. 25, no. 11, pp. 2244–2251, Oct. 2014.

[137]   P. R. Gavine, L. Mooney, E. Kilgour, A. P. Thomas, K. Al-Kadhimi, S. Beck, C. Rooney, T. Coleman, D. Baker, M. J. Mellor, A. N. Brooks, and T. Klinowska, "AZD4547: An Orally Bioavailable, Potent, and Selective Inhibitor of the Fibroblast Growth Factor Receptor Tyrosine Kinase Family," *Cancer Res.*, vol. 72, no. 8, pp. 2045–2056, Apr. 2012.

[138]   V. Guagnano, C. Stamm, J. Brueggen, J. Murray, M. Wartmann, C. Spanka, A. Zimmerlin, P. Furet, V. Bordas, M. Le Douget, M. R. Jensen, C. Schnell, H. Schmid, J. Berghausen, P. Drueckes, D. Bussiere, and D. Graus Porta, "Discovery of 3-(2,6-dichloro-3,5-dimethoxy-phenyl)-1-{6-[4-(4-ethyl-piperazin-1-yl)-phenylamino]-pyrimidin-4-yl}-1-methyl-urea (NVP-BGJ398), a potent and selective inhibitor of the fibroblast growth factor receptor family of receptor tyrosine kinase.," *J. Med. Chem.*, vol. 54, no. 20, pp. 7066–7083, Oct. 2011.

[139]   V. Guagnano, A. Kauffmann, S. Wöhrle, C. Stamm, M. Ito, L. Barys, A. Pornon, Y. Yao, F. Li, Y. Zhang, Z. Chen, C. J. Wilson, V. Bordas, M. Le Douget, L. A. Gaither, J. Borawski, J. E. Monahan, K. Venkatesan, T. Brümmendorf, D. M. Thomas, C. Garcia-Echeverria, F. Hofmann, W. R. Sellers, and D. Graus Porta, "FGFR genetic alterations predict for sensitivity to NVP-BGJ398, a selective pan-FGFR inhibitor.," *Cancer Discovery*, vol. 2, no. 12, pp. 1118–1133, Dec. 2012.

[140]   F. Göke, A. Franzen, T. K. Hinz, L. A. Marek, P. Yoon, R. Sharma, M. Bode, A. von Maessenhausen, B. Lankat-Buttgereit, A. Göke, C. Golletz, R. Kirsten, D. Boehm, W. Vogel, E. K. Kleczko, J. R. Eagles, F. R. Hirsch, T. Van Bremen, F. Bootz, A. Schroeck, J. Kim, A.-C. Tan, A.

Jimeno, L. E. Heasley, and S. Perner, "FGFR1 Expression Levels Predict BGJ398 Sensitivity of FGFR1-Dependent Head and Neck Squamous Cell Cancers.," *Clin. Cancer Res.*, May 2015.

[141]   R. Dienstmann, R. Bahleda, B. Adamo, J. Rodon, A. Varga, A. Gazzah, S. Platero, H. Smit, T. Perera, B. Zhong, K. Stuyckens, Y. Elsayed, C. Takimoto, V. Peddareddigari, J. Tabernero, F. R. Luo, and J.-C. Soria, "Abstract CT325: First in human study of JNJ-42756493, a potent pan fibroblast growth factor receptor (FGFR) inhibitor in patients with advanced solid tumors," *Cancer Res.*, vol. 74, no. 19, pp. CT325–CT325, Sep. 2014.

[142]   J. Tabernero, R. Bahleda, R. Dienstmann, J. R. Infante, A. Mita, A. Italiano, E. Calvo, V. Moreno, B. Adamo, A. Gazzah, B. Zhong, S. J. Platero, J. W. Smit, K. Stuyckens, M. Chatterjee-Kishore, J. Rodon, V. Peddareddigari, F. R. Luo, and J. C. Soria, "Phase I Dose-Escalation Study of JNJ-42756493, an Oral Pan-Fibroblast Growth Factor Receptor Inhibitor, in Patients With Advanced Solid Tumors," *Journal of Clinical Oncology*, vol. 33, no. 30, pp. 3401–3408, Oct. 2015.

[143]   P. C. Liu, L. Wu, H. Koblish, K. Bowman, Y. Zhang, R. Klabe, L. Leffet, D. DiMatteo, M. Rupar, K. Gallagher, M. Hansbury, C. Zhang, C. He, P. Collier, M. Covington, R. Wynn, S. Yeleswaram, K. Vaddi, T. Burn, W. Yao, R. Huber, P. Scherle, and G. Hollis, "Abstract 771: Preclinical characterization of the selective FGFR inhibitor INCB054828," *Cancer Res.*, vol. 75, no. 15, pp. 771–771, Aug. 2015.

[144]   M. Touat, E. Ileana, S. Postel-Vinay, F. André, and J.-C. Soria, "Targeting FGFR Signaling in Cancer.," *Clin. Cancer Res.*, vol. 21, no. 12, pp. 2684–2694, Jun. 2015.

[145]   P. ODonnell, J. W. Goldman, M. S. Gordon, K. Shih, Y. J. Choi, D. Lu, O. Kabbarah, W. Ho, I. Rooney, and E. T. Lam, "621 A Phase I Dose-escalation Study of MFGR1877S, a Human Monoclonal Anti-fibroblast Growth Factor Receptor 3 (FGFR3) Antibody, in Patients (pts) with Advanced Solid Tumors," *European Journal of Cancer*, vol. 48, pp. 191–192, Nov. 2012.

[146]   E. A. R. Sison and P. Brown, "The bone marrow microenvironment and leukemia: biology and therapeutic targeting.," *Expert Rev Hematol*, vol. 4, no. 3, pp. 271–283, Jun. 2011.

[147]   S. J. Morrison and D. T. Scadden, "The bone marrow niche for haematopoietic stem cells," *Nature*, vol. 505, no. 7483, pp. 327–334, Jan. 2014.

[148]   S. Méndez-Ferrer, T. V. Michurina, F. Ferraro, A. R. Mazloom, B. D. MacArthur, S. A. Lira, D. T. Scadden, A. Ma'ayan, G. N. Enikolopov, and P. S. Frenette, "Mesenchymal and haematopoietic stem cells form a unique bone marrow niche," *Nature*, vol. 466, no. 7308, pp. 829–834, Aug. 2010.

[149]   T. Sugiyama, H. Kohara, M. Noda, and T. Nagasawa, "Maintenance of the Hematopoietic Stem Cell Pool by CXCL12-CXCR4 Chemokine Signaling in Bone Marrow Stromal Cell Niches," *Immunity*, vol. 25, no. 6, pp. 977–988, Dec. 2006.

[150]   L. Ding, T. L. Saunders, G. Enikolopov, and S. J. Morrison, "Endothelial and perivascular cells maintain haematopoietic stem cells," *Nature*, vol. 481, no. 7382, pp. 457–462, Jan. 2012.

[151]   F.-J. Lv, R. S. Tuan, K. M. C. Cheung, and V. Y. L. Leung, "Concise review: the surface markers and identity of human mesenchymal stem cells.," *Stem Cells*, vol. 32, no. 6, pp. 1408–1419, Jun. 2014.

[152]   K. Akiyama, Y.-O. You, T. Yamaza, C. Chen, L. Tang, Y. Jin, X.-D. Chen, S. Gronthos, and S. Shi, "Characterization of bone marrow derived mesenchymal stem cells in suspension.," *Stem Cell Res Ther*, vol. 3, no. 5, p. 40, 2012.

[153]   K. E. Schwab and C. E. Gargett, "Co-expression of two perivascular cell markers isolates mesenchymal stem-like cells from human endometrium," *Human Reproduction*, vol. 22, no. 11, pp. 2903–2911, Sep. 2007.

[154]   S. J. Morrison and D. T. Scadden, "The bone marrow niche for haematopoietic stem cells," *Nature*, vol. 505, no. 7483, pp. 327–334, Jan. 2014.

[155]   M. Allouche, "Basic fibroblast growth factor and hematopoiesis.," *Leukemia*, vol. 9, no. 6, pp. 937–942, Jun. 1995.

[156]   G. de Haan, E. Weersing, B. Dontje, R. van Os, L. V. Bystrykh, E. Vellenga, and G. Miller, "In vitro generation of long-term repopulating hematopoietic stem cells by fibroblast growth factor-1.," *Dev. Cell*, vol. 4, no. 2, pp. 241–251, Feb. 2003.

[157]   S. Emami, W. Merrill, V. Cherington, G. G. Chiang, M. Kirchgesser, J. M. Appel, M. Hansen, P. H. Levine, J. S. Greenberger, and D. R. Hurwitz, "Enhanced growth of canine bone marrow stromal cell cultures in the presence of acidic fibroblast growth factor and heparin," *In Vitro Cellular & Developmental Biology - Animal*, vol. 33, no. 7, pp. 503–511, Jul. 1997.

[158]   Q. Chen, P. Shou, C. Zheng, M. Jiang, G. Cao, Q. Yang, J. Cao, N. Xie, T. Velletri, X. Zhang, C. Xu, L. Zhang, H. Yang, J. Hou, Y. Wang, and Y. Shi, "Fate decision of mesenchymal stem cells: adipocytes or osteoblasts?," *Cell Death Differ.*, vol. 23, no. 7, pp. 1128–1139, Jul. 2016.

[159]   K. Woei Ng, T. Speicher, C. Dombrowski, T. Helledie, L. M. Haupt, V. Nurcombe, and S. M. Cool, "Osteogenic Differentiation of Murine Embryonic Stem Cells is Mediated by Fibroblast Growth Factor Receptors," *Stem Cells Dev.*, vol. 16, no. 2, pp. 305–318, Apr. 2007.

[160]   L. Ling, S. Murali, C. Dombrowski, L. M. Haupt, G. S. Stein, A. J. van Wijnen, V. Nurcombe, and S. M. Cool, "Sulfated glycosaminoglycans mediate the effects of FGF2 on the osteogenic potential of rat calvarial osteoprogenitor cells," *J. Cell. Physiol.*, vol. 209, no. 3, pp. 811–825, 2006.

[161]   M. Neubauer, C. Fischbach, P. Bauer-Kreisel, E. Lieb, M. Hacker, J. Tessmar, M. B. Schulz, A. Goepferich, and T. Blunk, "Basic fibroblast growth factor enhances PPARγ ligand-induced adipogenesis of mesenchymal stem cells," *FEBS Lett.*, vol. 577, no. 1, pp. 277–283, Oct. 2004.

[162]   T. Itkin, A. Ludin, B. Gradus, S. Gur-Cohen, A. Kalinkovich, A. Schajnovitz, Y. Ovadya, O. Kollet, J. Canaani, E. Shezen, D. J. Coffin, G. N. Enikolopov, T. Berg, W. Piacibello, E. Hornstein, and T. Lapidot, "FGF-2 expands murine hematopoietic stem and progenitor cells via proliferation of stromal cells, c-Kit activation, and CXCL12 down-regulation.," *Blood*, vol. 120, no. 9, pp. 1843–1855, Aug. 2012.

[163]   T. Itkin, S. Gur-Cohen, J. A. Spencer, A. Schajnovitz, S. K. Ramasamy, A. P. Kusumbe, G. Ledergor, Y. Jung, I. Milo, M. G. Poulos, A. Kalinkovich, A. Ludin, O. Kollet, G. Shakhar, J. M. Butler, S. Rafii, R. H. Adams, D. T. Scadden, C. P. Lin, and T. Lapidot, "Distinct bone marrow

blood vessels differentially regulate haematopoiesis.," *Nature*, vol. 532, no. 7599, pp. 323–328, Apr. 2016.

[164]   Y. Tabe and M. Konopleva, "Role of Microenvironment in Resistance to Therapy in AML.," *Curr Hematol Malig Rep*, vol. 10, no. 2, pp. 96–103, Jun. 2015.

[165]   A. Avigdor, P. Goichberg, S. Shivtiel, A. Dar, A. Peled, S. Samira, O. Kollet, R. Hershkoviz, R. Alon, I. Hardan, H. Ben-Hur, D. Naor, A. Nagler, and T. Lapidot, "CD44 and hyaluronic acid cooperate with SDF-1 in the trafficking of human CD34+ stem/progenitor cells to bone marrow.," *Blood*, vol. 103, no. 8, pp. 2981–2989, Apr. 2004.

[166]   L. Jin, K. J. Hope, Q. Zhai, F. Smadja-Joffe, and J. E. Dick, "Targeting of CD44 eradicates human acute myeloid leukemic stem cells," *Nat. Med.*, vol. 12, no. 10, pp. 1167–1174, Sep. 2006.

[167]   A. Rashidi and J. F. DiPersio, "Targeting the leukemia-stroma interaction in acute myeloid leukemia: rationale and latest evidence.," *Ther Adv Hematol*, vol. 7, no. 1, pp. 40–51, Feb. 2016.

[168]   C. R. Walkley, G. H. Olsen, S. Dworkin, S. A. Fabb, J. Swann, G. A. McArthur, S. V. Westmoreland, P. Chambon, D. T. Scadden, and L. E. Purton, "A Microenvironment-Induced Myeloproliferative Syndrome Caused by Retinoic Acid Receptor γ Deficiency," *Cell*, vol. 129, no. 6, pp. 1097–1110, Jun. 2007.

[169]   M. H. G. P. Raaijmakers, S. Mukherjee, S. Guo, S. Zhang, T. Kobayashi, J. A. Schoonmaker, B. L. Ebert, F. Al-Shahrour, R. P. Hasserjian, E. O. Scadden, Z. Aung, M. Matza, M. Merkenschlager, C. Lin, J. M. Rommens, and D. T. Scadden, "Bone progenitor dysfunction induces myelodysplasia and secondary leukaemia," *Nature*, vol. 464, no. 7290, pp. 852–857, Mar. 2010.

[170]   C. Théry, L. Zitvogel, and S. Amigorena, "Exosomes: composition, biogenesis and function," *Nature Reviews Immunology*, 2002.

[171]   P.-Y. Mantel and M. Marti, "The role of extracellular vesicles in Plasmodium and other protozoan parasites.," *Cell. Microbiol.*, vol. 16, no. 3, pp. 344–354, Mar. 2014.

[172]   G. van Niel, "Exosomes: A Common Pathway for a Specialized Function," *J. Biochem.*, vol. 140, no. 1, pp. 13–21, Jul. 2006.

[173]   K. Trajkovic, C. Hsu, S. Chiantia, L. Rajendran, D. Wenzel, F. Wieland, P. Schwille, B. Brügger, and M. Simons, "Ceramide triggers budding of exosome vesicles into multivesicular endosomes.," *Science*, vol. 319, no. 5867, pp. 1244–1247, Feb. 2008.

[174]   M. A. Antonyak, B. Li, L. K. Boroughs, J. L. Johnson, J. E. Druso, K. L. Bryant, D. A. Holowka, and R. A. Cerione, "Cancer cell-derived microvesicles induce transformation by transferring tissue transglutaminase and fibronectin to recipient cells.," *Proc. Natl. Acad. Sci. U.S.A.*, vol. 108, no. 12, pp. 4852–4857, Mar. 2011.

[175]   E. Hosseini-Beheshti, S. Pham, H. Adomat, N. Li, and E. S. Tomlinson Guns, "Exosomes as biomarker enriched microvesicles: characterization of exosomal proteins derived from a panel

of prostate cell lines with distinct AR phenotypes.," *Mol. Cell Proteomics*, vol. 11, no. 10, pp. 863–885, Oct. 2012.

[176] B. Costa-Silva, N. M. Aiello, A. J. Ocean, S. Singh, H. Zhang, B. K. Thakur, A. Becker, A. Hoshino, M. T. Mark, H. Molina, J. Xiang, T. Zhang, T.-M. Theilen, G. García-Santos, C. Williams, Y. Ararso, Y. Huang, G. Rodrigues, T.-L. Shen, K. J. Labori, I. M. B. Lothe, E. H. Kure, J. Hernandez, A. Doussot, S. H. Ebbesen, P. M. Grandgenett, M. A. Hollingsworth, M. Jain, K. Mallya, S. K. Batra, W. R. Jarnagin, R. E. Schwartz, I. Matei, H. Peinado, B. Z. Stanger, J. Bromberg, and D. Lyden, "Pancreatic cancer exosomes initiate pre-metastatic niche formation in the liver.," *Nat. Cell Biol.*, vol. 17, no. 6, pp. 816–826, Jun. 2015.

[177] M. C. Boelens, T. J. Wu, B. Y. Nabet, B. Xu, Y. Qiu, T. Yoon, D. J. Azzam, C. Twyman-Saint Victor, B. Z. Wiemann, H. Ishwaran, P. J. Ter Brugge, J. Jonkers, J. Slingerland, and A. J. Minn, "Exosome transfer from stromal to breast cancer cells regulates therapy resistance pathways.," *Cell*, vol. 159, no. 3, pp. 499–513, Oct. 2014.

[178] M. Perez-Torres, B. L. Valle, N. J. Maihle, L. Negron-Vega, R. Nieves-Alicea, and E. M. Cora, "Shedding of epidermal growth factor receptor is a regulated process that occurs with overexpression in malignant cells.," *Experimental Cell Research*, vol. 314, no. 16, pp. 2907–2918, Oct. 2008.

[179] M. P. Sanderson, S. Keller, A. Alonso, S. Riedle, P. J. Dempsey, and P. Altevogt, "Generation of novel, secreted epidermal growth factor receptor (EGFR/ErbB1) isoforms via metalloprotease-dependent ectodomain shedding and exosome secretion.," *J. Cell. Biochem.*, vol. 103, no. 6, pp. 1783–1797, Apr. 2008.

[180] P. Kharaziha, S. Ceder, Q. Li, and T. Panaretakis, "Tumor cell-derived exosomes: A message in a bottle," *Biochimica et Biophysica Acta (BBA) - Reviews on Cancer*, vol. 1826, no. 1, pp. 103–111, Aug. 2012.

[181] J. Skog, T. Würdinger, S. van Rijn, D. H. Meijer, L. Gainche, M. Sena-Esteves, W. T. Curry, B. S. Carter, A. M. Krichevsky, and X. O. Breakefield, "Glioblastoma microvesicles transport RNA and proteins that promote tumour growth and provide diagnostic biomarkers.," *Nat. Cell Biol.*, vol. 10, no. 12, pp. 1470–1476, Dec. 2008.

[182] K. Al-Nedawi, B. Meehan, J. Micallef, V. Lhotak, L. May, A. Guha, and J. Rak, "Intercellular transfer of the oncogenic receptor EGFRvIII by microvesicles derived from tumour cells," *Nat. Cell Biol.*, vol. 10, no. 5, pp. 619–624, Apr. 2008.

[183] A. Riches, E. Campbell, E. Borger, and S. Powis, "Regulation of exosome release from mammary epithelial and breast cancer cells - a new regulatory pathway.," *Eur. J. Cancer*, vol. 50, no. 5, pp. 1025–1034, Mar. 2014.

[184] S. Atay, S. Banskota, J. Crow, G. Sethi, L. Rink, and A. K. Godwin, "Oncogenic KIT-containing exosomes increase gastrointestinal stromal tumor cell invasion.," *Proc. Natl. Acad. Sci. U.S.A.*, vol. 111, no. 2, pp. 711–716, Jan. 2014.

[185] L. R. Languino, A. Singh, M. Prisco, G. J. Inman, A. Luginbuhl, J. M. Curry, and A. P. South, "Exosome-mediated transfer from the tumor microenvironment increases TGFβ signaling in squamous cell carcinoma.," *Am J Transl Res*, vol. 8, no. 5, pp. 2432–2437, 2016.

[186]   H. Peinado, M. Alečković, S. Lavotshkin, I. Matei, B. Costa-Silva, G. Moreno-Bueno, M. Hergueta-Redondo, C. Williams, G. García-Santos, C. Ghajar, A. Nitadori-Hoshino, C. Hoffman, K. Badal, B. A. Garcia, M. K. Callahan, J. Yuan, V. R. Martins, J. Skog, R. N. Kaplan, M. S. Brady, J. D. Wolchok, P. B. Chapman, Y. Kang, J. Bromberg, and D. Lyden, "Melanoma exosomes educate bone marrow progenitor cells toward a pro-metastatic phenotype through MET.," *Nat. Med.*, vol. 18, no. 6, pp. 883–891, Jun. 2012.

[187]   A. Hoshino, B. Costa-Silva, T.-L. Shen, G. Rodrigues, A. Hashimoto, M. Tesic Mark, H. Molina, S. Kohsaka, A. Di Giannatale, S. Ceder, S. Singh, C. Williams, N. Soplop, K. Uryu, L. Pharmer, T. King, L. Bojmar, A. E. Davies, Y. Ararso, T. Zhang, H. Zhang, J. Hernandez, J. M. Weiss, V. D. Dumont-Cole, K. Kramer, L. H. Wexler, A. Narendran, G. K. Schwartz, J. H. Healey, P. Sandstrom, K. J. Labori, E. H. Kure, P. M. Grandgenett, M. A. Hollingsworth, M. de Sousa, S. Kaur, M. Jain, K. Mallya, S. K. Batra, W. R. Jarnagin, M. S. Brady, O. Fodstad, V. Muller, K. Pantel, A. J. Minn, M. J. Bissell, B. A. Garcia, Y. Kang, V. K. Rajasekhar, C. M. Ghajar, I. Matei, H. Peinado, J. Bromberg, and D. Lyden, "Tumour exosome integrins determine organotropic metastasis.," *Nature*, vol. 527, no. 7578, pp. 329–335, Nov. 2015.

[188]   N. I. Hornick, J. Huan, B. Doron, N. A. Goloviznina, J. Lapidus, B. H. Chang, and P. Kurre, "Serum Exosome MicroRNA as a Minimally-Invasive Early Biomarker of AML.," *Sci Rep*, vol. 5, p. 11295, 2015.

[189]   M. Davila, A. Amirkhosravi, E. Coll, H. Desai, L. Robles, J. Colon, C. H. Baker, and J. L. Francis, "Tissue factor-bearing microparticles derived from tumor cells: impact on coagulation activation.," *J. Thromb. Haemost.*, vol. 6, no. 9, pp. 1517–1524, Sep. 2008.

[190]   J. E. Geddings and N. Mackman, "Tumor-derived tissue factor-positive microparticles and venous thrombosis in cancer patients.," *Blood*, vol. 122, no. 11, pp. 1873–1880, Sep. 2013.

[191]   M. C. Martínez, A. Tesse, F. Zobairi, and R. Andriantsitohaina, "Shed membrane microparticles from circulating and vascular cells in regulating vascular function.," *Am. J. Physiol. Heart Circ. Physiol.*, vol. 288, no. 3, pp. H1004–9, Mar. 2005.

[192]   J. Huan, N. I. Hornick, N. A. Goloviznina, A. N. Kamimae-Lanning, L. L. David, P. A. Wilmarth, T. Mori, J. R. Chevillet, A. Narla, C. T. Roberts, M. M. Loriaux, B. H. Chang, and P. Kurre, "Coordinate regulation of residual bone marrow function by paracrine trafficking of AML exosomes.," *Leukemia*, Jun. 2015.

[193]   J. Paggetti, F. Haderk, M. Seiffert, B. Janji, U. Distler, W. Ammerlaan, Y. J. Kim, J. Adam, P. Lichter, E. Solary, G. Berchem, and E. Moussay, "Exosomes released by chronic lymphocytic leukemia cells induce the transition of stromal cells into cancer-associated fibroblasts.," *Blood*, vol. 126, no. 9, pp. 1106–1117, Jun. 2015.

[194]   B. Yu, X. Zhang, and X. Li, "Exosomes derived from mesenchymal stem cells.," *Int J Mol Sci*, vol. 15, no. 3, pp. 4142–4157, 2014.

[195]   B. Zhang, Y. Yin, R. C. Lai, S. S. Tan, A. B. H. Choo, and S. K. Lim, "Mesenchymal Stem Cells Secrete Immunologically Active Exosomes," *Stem Cells Dev.*, vol. 23, no. 11, pp. 1233–1244, Jun. 2014.

[196]   R. C. Lai, F. Arslan, S. S. Tan, B. Tan, A. Choo, M. M. Lee, T. S. Chen, B. J. Teh, J. K. L. Eng, H. Sidik, V. Tanavde, W. S. Hwang, C. N. Lee, R. M. El Oakley, G. Pasterkamp, D. P. V. de Kleijn, K. H. Tan, and S. K. Lim, "Derivation and characterization of human fetal MSCs: an alternative cell source for large-scale production of cardioprotective microparticles.," *J. Mol. Cell. Cardiol.*, vol. 48, no. 6, pp. 1215–1224, Jun. 2010.

[197]   J. Wang, A. Hendrix, S. Hernot, M. Lemaire, E. De Bruyne, E. Van Valckenborgh, T. Lahoutte, O. De Wever, K. Vanderkerken, and E. Menu, "Bone marrow stromal cell-derived exosomes as communicators in drug resistance in multiple myeloma cells.," *Blood*, vol. 124, no. 4, pp. 555–566, Jul. 2014.

[198]   S. S. Tan, Y. Yin, T. Lee, R. C. Lai, R. W. Y. Yeo, B. Zhang, A. Choo, and S. K. Lim, "Therapeutic MSC exosomes are derived from lipid raft microdomains in the plasma membrane.," *J Extracell Vesicles*, vol. 2, no. 0, p. 141, 2013.

[199]   A. Bobrie, S. Krumeich, F. Reyal, C. Recchi, L. F. Moita, M. C. Seabra, M. Ostrowski, and C. Théry, "Rab27a Supports Exosome-Dependent and -Independent Mechanisms That Modify the Tumor Microenvironment and Can Promote Tumor Progression," *Cancer Res.*, vol. 72, no. 19, pp. 4920–4930, Sep. 2012.

[200]   A. Hendrix, W. Westbroek, M. Bracke, and O. De Wever, "An ex(o)citing machinery for invasive tumor growth.," *Cancer Res.*, vol. 70, no. 23, pp. 9533–9537, Dec. 2010.

[201]   F. Chalmin, S. Ladoire, G. Mignot, J. Vincent, M. Bruchard, J.-P. Remy-Martin, W. Boireau, A. Rouleau, B. Simon, D. Lanneau, A. De Thonel, G. Multhoff, A. Hamman, F. Martin, B. Chauffert, E. Solary, L. Zitvogel, C. Garrido, B. Ryffel, C. Borg, L. Apetoh, C. Rébé, and F. Ghiringhelli, "Membrane-associated Hsp72 from tumor-derived exosomes mediates STAT3-dependent immunosuppressive function of mouse and human myeloid-derived suppressor cells.," *J. Clin. Invest.*, vol. 120, no. 2, pp. 457–471, Feb. 2010.

[202]   L. G. Kindblom, H. E. Remotti, F. Aldenborg, and J. M. Meis-Kindblom, "Gastrointestinal pacemaker cell tumor (GIPACT): gastrointestinal stromal tumors show phenotypic characteristics of the interstitial cells of Cajal.," *Am. J. Pathol.*, vol. 152, no. 5, pp. 1259–1269, May 1998.

[203]   M. Miettinen and J. Lasota, "Gastrointestinal stromal tumors: review on morphology, molecular pathology, prognosis, and differential diagnosis.," *Archives of Pathology & Laboratory Medicine*, vol. 130, no. 10, pp. 1466–1478, Oct. 2006.

[204]   S. Hirota, T. Nishida, K. Isozaki, M. Taniguchi, J. Nakamura, T. Okazaki, and Y. Kitamura, "Gain-of-function mutation at the extracellular domain of KIT in gastrointestinal stromal tumours.," vol. 193, no. 4, pp. 505–510, 2001.

[205]   M. C. Heinrich, C. L. Corless, A. Duensing, L. McGreevey, C.-J. Chen, N. Joseph, S. Singer, D. J. Griffith, A. Haley, A. Town, G. D. Demetri, C. D. M. Fletcher, and J. A. Fletcher, "PDGFRA activating mutations in gastrointestinal stromal tumors.," *Science*, vol. 299, no. 5607. pp. 708–710, 31-Jan-2003.

[206]   S. Hirota, A. Ohashi, T. Nishida, K. Isozaki, K. Isozaki, K. Kinoshita, K. Kinoshita, Y. Shinomura, Y. Shinomura, Y. Kitamura, and Y. Kitamura, "Gain-of-function mutations of

platelet-derived growth factor receptor α gene in gastrointestinal stromal tumors," *Gastroenterology*, vol. 125, no. 3, pp. 660–667, Sep. 2003.

[207]   A. Duensing, F. Medeiros, B. McConarty, N. E. Joseph, D. Panigrahy, S. Singer, C. D. M. Fletcher, G. D. Demetri, and J. A. Fletcher, "Mechanisms of oncogenic KIT signal transduction in primary gastrointestinal stromal tumors (GISTs).," *Oncogene*, vol. 23, no. 22, pp. 3999–4006, May 2004.

[208]   P. Chi, Y. Chen, L. Zhang, X. Guo, J. Wongvipat, T. Shamu, J. A. Fletcher, S. Dewell, R. G. Maki, D. Zheng, C. R. Antonescu, C. D. Allis, and C. L. Sawyers, "ETV1 is a lineage survival factor that cooperates with KIT in gastrointestinal stromal tumours.," *Nature*, vol. 467, no. 7317, pp. 849–853, Oct. 2010.

[209]   D. T. Patil and B. P. Rubin, "Gastrointestinal stromal tumor: advances in diagnosis and management.," *Archives of Pathology & Laboratory Medicine*, vol. 135, no. 10, pp. 1298–1310, Oct. 2011.

[210]   S. Bauer, M. Schlemmer, C. Hosius, P. Reichardt, R. Schütte, J. T. Hartmann, C. Bokemeyer, R. Schütte, and J. T. Hartmann, "Activity and side effects of imatinib in patients with gastrointestinal stromal tumors: data from a german multicenter trial," *Eur J Med Res*, vol. 16, no. 5, p. 206, 2011.

[211]   J. A. Polikoff, R. P. DeMatteo, S. Patel, C. D. Blanke, G. D. Demetri, B. R. Tan, R. G. Maki, K. V. Ballman, C. R. Antonescu, P. W. T. Pisters, M. E. Blackstein, M. von Mehren, M. F. Brennan, M. D. McCarter, K. Owzar, American College of Surgeons Oncology Group (ACOSOG) Intergroup Adjuvant GIST Study Team, "Adjuvant imatinib mesylate after resection of localised, primary gastrointestinal stromal tumour: a randomised, double-blind, placebo-controlled trial.," *Lancet*, vol. 373, no. 9669, pp. 1097–1104, Mar. 2009.

[212]   S. Bauer, A. Duensing, G. D. Demetri, and J. A. Fletcher, "KIT oncogenic signaling mechanisms in imatinib-resistant gastrointestinal stromal tumor: PI3-kinase/AKT is a crucial survival pathway.," *Oncogene*, vol. 26, no. 54, pp. 7560–7568, Nov. 2007.

[213]   C. D. Blanke, C. Rankin, G. D. Demetri, C. W. Ryan, M. von Mehren, R. S. Benjamin, A. K. Raymond, V. H. C. Bramwell, L. H. Baker, R. G. Maki, M. Tanaka, J. R. Hecht, M. C. Heinrich, C. D. M. Fletcher, J. J. Crowley, and E. C. Borden, "Phase III randomized, intergroup trial assessing imatinib mesylate at two dose levels in patients with unresectable or metastatic gastrointestinal stromal tumors expressing the kit receptor tyrosine kinase: S0033.," *J. Clin. Oncol.*, vol. 26, no. 4, pp. 626–632, Feb. 2008.

[214]   G. D. Demetri, J. Desai, I. R. Judson, S. George, J. A. Morgan, G. McArthur, C. D. Fletcher, J. Verweij, A. T. van Oosterom, C. R. Garrett, M. E. Blackstein, M. H. Shah, M. C. Heinrich, C. L. Bello, X. Huang, C. M. Baum, and P. G. Casali, "Efficacy and safety of sunitinib in patients with advanced gastrointestinal stromal tumour after failure of imatinib: a randomised controlled trial.," *Lancet*, vol. 368, no. 9544, pp. 1329–1338, Oct. 2006.

[215]   S. George, Q. Wang, M. C. Heinrich, C. L. Corless, M. Zhu, J. E. Butrynski, J. A. Morgan, A. J. Wagner, E. Choy, W. D. Tap, J. T. Yap, A. D. Van den Abbeele, J. B. Manola, S. M. Solomon, J. A. Fletcher, M. von Mehren, and G. D. Demetri, "Efficacy and safety of regorafenib in patients

with metastatic and/or unresectable GI stromal tumor after failure of imatinib and sunitinib: a multicenter phase II trial.," *J. Clin. Oncol.*, vol. 30, no. 19, pp. 2401–2407, Jul. 2012.

[216]   I. Kuss, D. Laurent, T. Nishida, S. Bauer, B. B. Nguyen, P. G. Casali, P. Schöffski, G. D. Demetri, C. Kappeler, J. Xu, P. Reichardt, Y.-K. Kang, J.-Y. Blay, P. Rutkowski, H. Gelderblom, P. Hohenberger, M. Leahy, M. von Mehren, H. Joensuu, G. Badalamenti, M. Blackstein, A. Le Cesne, R. G. Maki, J. Chung, GRID study investigators, "Efficacy and safety of regorafenib for advanced gastrointestinal stromal tumours after failure of imatinib and sunitinib (GRID): an international, multicentre, randomised, placebo-controlled, phase 3 trial.," *Lancet*, vol. 381, no. 9863, pp. 295–302, Jan. 2013.

[217]   M. A. Pantaleo, A. Astolfi, M. Nannini, and G. Biasco, "The emerging role of insulin-like growth factor 1 receptor (IGF1r) in gastrointestinal stromal tumors (GISTs).," *J Transl Med*, vol. 8, no. 1, p. 117, 2010.

[218]   T. Taguchi, H. Sonobe, S.-I. Toyonaga, and I. Yamasaki, "B RIEF M ETHOD Conventional and Molecular Cytogenetic Characterization of a New Human Cell Line , GIST-T1 , Established from Gastrointestinal Stromal Tumor," vol. 82, no. 5, pp. 663–665, 2002.

[219]   K. E. Ware, P. Hercule, L. E. Heasley, B. A. Helfrich, L. Marek, A. Fritzsche, W. R. Helton, J. E. Smith, L. A. Mcdermott, C. D. Coldren, R. A. Nemenoff, D. T. Merrick, and P. A. Bunn, "Fibroblast Growth Factor (FGF) and FGF Receptor-Mediated Autocrine Signaling in Non – Small-Cell Lung Cancer Cells," *Cell Proliferation*, vol. 75, no. 1, pp. 196–207, 2009.

[220]   E. Traer, N. Javidi-Sharifi, A. Agarwal, J. Dunlap, I. English, J. Martinez, J. W. Tyner, M. Wong, and B. J. Druker, "Ponatinib overcomes FGF2-mediated resistance in CML patients without kinase domain mutations," *Blood*, vol. 123, no. 10, pp. 1516–1524, Mar. 2014.

[221]   Z. Qu, R. J. Kayton, P. Ahmadi, J. M. Liebler, M. R. Powers, S. R. Planck, and J. T. Rosenbaum, "Ultrastructural Immunolocalization of Basic Fibroblast Growth Factor in Mast Cell Secretory Granules: Morphological Evidence for bFGF Release Through Degranulation," *Journal of Histochemistry & Cytochemistry*, vol. 46, no. 10, pp. 1119–1128, Oct. 1998.

[222]   L. E. Haddad, L. B. Khzam, F. Hajjar, Y. Merhi, and M. G. Sirois, "Characterization of FGF receptor expression in human neutrophils and their contribution to chemotaxis.," *Am. J. Physiol., Cell Physiol.*, vol. 301, no. 5, pp. C1036–45, Nov. 2011.

[223]   B. Styp-Rekowska, N. Gross, F. Salm, A. Arcaro, A. Ghosal, I. Zlobec, S. C. Schäfer, P. Cwiek, A. Lucia Buccarello, F. Largey, C. Wotzkow, K. Höland, V. Djonov, N. Bodmer, and F. Westermann, "RNA interference screening identifies a novel role for autocrine fibroblast growth factor signaling in neuroblastoma chemoresistance.," *Oncogene*, vol. 32, no. 34, pp. 3944–3953, Aug. 2013.

[224]   K. E. Ware, M. E. Marshall, L. R. Heasley, L. Marek, T. K. Hinz, P. Hercule, B. A. Helfrich, R. C. Doebele, and L. E. Heasley, "Rapidly acquired resistance to EGFR tyrosine kinase inhibitors in NSCLC cell lines through de-repression of FGFR2 and FGFR3 expression.," *PLoS ONE*, vol. 5, no. 11, p. e14117, 2010.

[225]   H. Huynh, J. W. J. Lee, P. K. H. Chow, V. C. Ngo, G. B. Lew, I. W. L. Lam, H. S. Ong, A. Chung, and K. C. Soo, "Sorafenib induces growth suppression in mouse models of

gastrointestinal stromal tumor.," *Molecular Cancer Therapeutics*, vol. 8, no. 1, pp. 152–159, Jan. 2009.

[226]   F. Li, H. Huynh, X. Li, D. A. Ruddy, Y. Wang, R. Ong, P. Chow, S. Qiu, A. Tam, D. P. Rakiec, R. Schlegel, J. E. Monahan, and A. Huang, "FGFR-Mediated Reactivation of MAPK Signaling Attenuates Antitumor Effects of Imatinib in Gastrointestinal Stromal Tumors.," *Cancer Discovery*, vol. 5, no. 4, pp. 438–451, Apr. 2015.

[227]   G. P. Paner, S. Alkan, G. V. Aranha, G. Hartman, S. Silberman, and K. C. Micetich, "Analysis of signal transducer and activator of transcription 3 (STAT3) in gastrointestinal stromal tumors.," vol. 23, no. 3, pp. 2253–2260.

[228]   C. R. Carmo, J. Lyons-Lewis, M. J. Seckl, and A. P. Costa-Pereira, "A novel requirement for Janus kinases as mediators of drug resistance induced by fibroblast growth factor-2 in human cancer cells.," *PLoS ONE*, vol. 6, no. 5, p. e19861, 2011.

[229]   M. V. Karamouzis, P. A. Konstantinopoulos, and A. G. Papavassiliou, "Targeting MET as a strategy to overcome crosstalk-related resistance to EGFR inhibitors.," *The Lancet Oncology*, vol. 10, no. 7, pp. 709–717, Jul. 2009.

[230]   H. Yokote, X. Yan, K. Sakaguchi, K. Fujita, T. Sawada, S. Liang, L. Yao, J. Schlessinger, Y. Zhang, and X. Jing, "Trans-activation of EphA4 and FGF receptors mediated by direct interactions between their cytoplasmic domains.," vol. 102, no. 52, pp. 18866–18871, 2005.

[231]   Virchow, "Weisses Blut," *Frorieps Notizen*, no. 36, pp. 151–156, 1845.

[232]   J. H. BENNETT, "18. Case of Suppuration of the Blood, independent of Inflammation," *The American Journal of the Medical Sciences*, vol. 20, p. 444, Oct. 1845.

[233]   C. L. Sawyers, "Chronic Myeloid Leukemia," *N. Engl. J. Med.*, vol. 340, no. 17, pp. 1330–1340, Apr. 1999.

[234]   S. Faderl, "Chronic Myelogenous Leukemia: Biology and Therapy," *Annals of Internal Medicine*, vol. 131, no. 3, pp. 207–219, Aug. 1999.

[235]   P. C. NOWELL, "The minute chromosome (Phl) in chronic granulocytic leukemia.," *Blut*, vol. 8, pp. 65–66, Apr. 1962.

[236]   J. D. Rowley, "Letter: A new consistent chromosomal abnormality in chronic myelogenous leukaemia identified by quinacrine fluorescence and Giemsa staining.," *Nature*, vol. 243, no. 5405, pp. 290–293, Jun. 1973.

[237]   N. Rosenberg and O. N. Witte, "The viral and cellular forms of the Abelson (abl) oncogene.," *Adv. Virus Res.*, vol. 35, pp. 39–81, 1988.

[238]   J. B. Konopka, S. M. Watanabe, and O. N. Witte, "An alteration of the human c-abl protein in K562 leukemia cells unmasks associated tyrosine kinase activity.," *Cell*, vol. 37, no. 3, pp. 1035–1042, Jul. 1984.

[239]   T. G. Lugo, A. M. Pendergast, A. J. Muller, and O. N. Witte, "Tyrosine kinase activity and transformation potency of bcr-abl oncogene products.," *Science*, vol. 247, no. 4946, pp. 1079–1082, Mar. 1990.

[240] N. Heisterkamp, G. Jenster, J. ten Hoeve, D. Zovich, P. K. Pattengale, and J. Groffen, "Acute leukaemia in bcr/abl transgenic mice," *Nature*, vol. 344, no. 6263, pp. 251–253, Mar. 1990.

[241] G. Q. Daley, R. A. Van Etten, and D. Baltimore, "Induction of chronic myelogenous leukemia in mice by the P210bcr/abl gene of the Philadelphia chromosome.," *Science*, vol. 247, no. 4944, pp. 824–830, Feb. 1990.

[242] M. Y. Gordon, C. R. Dowding, G. P. Riley, J. M. Goldman, and M. F. Greaves, "Altered adhesive interactions with marrow stroma of haematopoietic progenitor cells in chronic myeloid leukaemia.," *Nature*, vol. 328, no. 6128, pp. 342–344, Jul. 1987.

[243] M. W. Deininger, J. M. Goldman, and J. V. Melo, "The molecular biology of chronic myeloid leukemia.," *Blood*, vol. 96, no. 10, pp. 3343–3356, Nov. 2000.

[244] L. Puil, J. Liu, G. Gish, G. Mbamalu, D. Bowtell, P. G. Pelicci, R. Arlinghaus, and T. Pawson, "Bcr-Abl oncoproteins bind directly to activators of the Ras signalling pathway.," *EMBO J*, vol. 13, no. 4, pp. 764–773, Feb. 1994.

[245] A. Bedi, B. A. Zehnbauer, J. P. Barber, S. J. Sharkis, and R. J. Jones, "Inhibition of apoptosis by BCR-ABL in chronic myeloid leukemia.," *Blood*, vol. 83, no. 8, pp. 2038–2044, Apr. 1994.

[246] H. M. Kantarjian, M. J. Keating, M. Talpaz, R. S. Walters, T. L. Smith, A. Cork, K. B. McCredie, and E. J. Freireich, "Chronic myelogenous leukemia in blast crisis. Analysis of 242 patients.," *Am. J. Med.*, vol. 83, no. 3, pp. 445–454, Sep. 1987.

[247] S. Sacchi, H. M. Kantarjian, S. O'Brien, J. Cortes, M. B. Rios, F. J. Giles, M. Beran, C. A. Koller, M. J. Keating, and M. Talpaz, "Chronic myelogenous leukemia in nonlymphoid blastic phase: analysis of the results of first salvage therapy with three different treatment approaches for 162 patients.," *Cancer*, vol. 86, no. 12, pp. 2632–2641, Dec. 1999.

[248] B. J. Druker, S. Tamura, E. Buchdunger, S. Ohno, G. M. Segal, S. Fanning, J. Zimmermann, and N. B. Lydon, "Effects of a selective inhibitor of the Abl tyrosine kinase on the growth of Bcr-Abl positive cells.," *Nat. Med.*, vol. 2, no. 5, pp. 561–566, May 1996.

[249] P. le Coutre, L. Mologni, L. Cleris, E. Marchesi, E. Buchdunger, R. Giardini, F. Formelli, and C. Gambacorti-Passerini, "In vivo eradication of human BCR/ABL-positive leukemia cells with an ABL kinase inhibitor.," *J. Natl. Cancer Inst.*, vol. 91, no. 2, pp. 163–168, Jan. 1999.

[250] S. G. O'Brien, F. Guilhot, R. A. Larson, I. Gathmann, M. Baccarani, F. Cervantes, J. J. Cornelissen, T. Fischer, A. Hochhaus, T. Hughes, K. Lechner, J. L. Nielsen, P. Rousselot, J. Reiffers, G. Saglio, J. Shepherd, B. Simonsson, A. Gratwohl, J. M. Goldman, H. Kantarjian, K. Taylor, G. Verhoef, A. E. Bolton, R. Capdeville, B. J. Druker, IRIS Investigators, "Imatinib compared with interferon and low-dose cytarabine for newly diagnosed chronic-phase chronic myeloid leukemia.," *N. Engl. J. Med.*, vol. 348, no. 11, pp. 994–1004, Mar. 2003.

[251] T. P. Hughes, J. Kaeda, S. Branford, Z. Rudzki, A. Hochhaus, M. L. Hensley, I. Gathmann, A. E. Bolton, I. C. van Hoomissen, J. M. Goldman, J. P. Radich, International Randomised Study of Interferon versus STI571 (IRIS) Study Group, "Frequency of major molecular responses to

imatinib or interferon alfa plus cytarabine in newly diagnosed chronic myeloid leukemia.," *N. Engl. J. Med.*, vol. 349, no. 15, pp. 1423–1432, Oct. 2003.

[252]	D. Frame, "New strategies in controlling drug resistance in chronic myeloid leukemia.," *Am J Health Syst Pharm*, vol. 64, no. 24, pp. S16–21, Dec. 2007.

[253]	M. Talpaz, N. P. Shah, H. Kantarjian, N. Donato, J. Nicoll, R. Paquette, J. Cortes, S. O'Brien, C. Nicaise, E. Bleickardt, M. A. Blackwood-Chirchir, V. Iyer, T.-T. Chen, F. Huang, A. P. Decillis, and C. L. Sawyers, "Dasatinib in imatinib-resistant Philadelphia chromosome-positive leukemias.," *N. Engl. J. Med.*, vol. 354, no. 24, pp. 2531–2541, Jun. 2006.

[254]	J. E. Cortes, D.-W. Kim, J. Pinilla-Ibarz, P. le Coutre, R. Paquette, C. Chuah, F. E. Nicolini, J. F. Apperley, H. J. Khoury, M. Talpaz, J. DiPersio, D. J. DeAngelo, E. Abruzzese, D. Rea, M. Baccarani, M. C. Müller, C. Gambacorti-Passerini, S. Wong, S. Lustgarten, V. M. Rivera, T. Clackson, C. D. Turner, F. G. Haluska, F. Guilhot, M. W. Deininger, A. Hochhaus, T. Hughes, J. M. Goldman, N. P. Shah, H. Kantarjian, PACE Investigators, "A phase 2 trial of ponatinib in Philadelphia chromosome-positive leukemias.," *N. Engl. J. Med.*, vol. 369, no. 19, pp. 1783–1796, Nov. 2013.

[255]	F. Ayala, R. Dewar, M. Kieran, and R. Kalluri, "Contribution of bone microenvironment to leukemogenesis and leukemia progression.," *Leukemia*, vol. 23, no. 12, pp. 2233–2241, Dec. 2009.

[256]	R. Schofield, "The relationship between the spleen colony-forming cell and the haemopoietic stem cell.," *Blood Cells*, vol. 4, no. 1, pp. 7–25, 1978.

[257]	D. Reynaud, E. Pietras, K. Barry-Holson, A. Mir, M. Binnewies, M. Jeanne, O. Sala-Torra, J. P. Radich, and E. Passegué, "IL-6 controls leukemic multipotent progenitor cell fate and contributes to chronic myelogenous leukemia development.," *Cancer Cell*, vol. 20, no. 5, pp. 661–673, Nov. 2011.

[258]	D. K. Hiwase, D. L. White, J. A. Powell, V. A. Saunders, S. A. Zrim, A. K. Frede, M. A. Guthridge, A. F. Lopez, R. J. D'Andrea, L. B. To, J. V. Melo, S. Kumar, and T. P. Hughes, "Blocking cytokine signaling along with intense Bcr-Abl kinase inhibition induces apoptosis in primary CML progenitors.," *Leukemia*, vol. 24, no. 4, pp. 771–778, Apr. 2010.

[259]	Y. Wang, D. Cai, C. Brendel, C. Barett, P. Erben, P. W. Manley, A. Hochhaus, A. Neubauer, and A. Burchert, "Adaptive secretion of granulocyte-macrophage colony-stimulating factor (GM-CSF) mediates imatinib and nilotinib resistance in BCR/ABL+ progenitors via JAK-2/STAT-5 pathway activation.," *Blood*, vol. 109, no. 5, pp. 2147–2155, Mar. 2007.

[260]	T. Schmidt, B. Kharabi Masouleh, S. Loges, S. Cauwenberghs, P. Fraisl, C. Maes, B. Jonckx, K. De Keersmaecker, M. Kleppe, M. Tjwa, T. Schenk, S. Vinckier, R. Fragoso, M. De Mol, K. Beel, S. Dias, C. Verfaillie, R. E. Clark, T. H. Brümmendorf, P. Vandenberghe, S. Rafii, T. Holyoake, A. Hochhaus, J. Cools, M. Karin, G. Carmeliet, M. Dewerchin, and P. Carmeliet, "Loss or inhibition of stromal-derived PlGF prolongs survival of mice with imatinib-resistant Bcr-Abl1(+) leukemia.," *Cancer Cell*, vol. 19, no. 6, pp. 740–753, Jun. 2011.

[261]	J. W. Tyner, M. W. Deininger, M. M. Loriaux, B. H. Chang, J. R. Gotlib, S. G. Willis, H. Erickson, T. Kovacsovics, T. O'Hare, M. C. Heinrich, and B. J. Druker, "RNAi screen for rapid

therapeutic target identification in leukemia patients.," *Proc. Natl. Acad. Sci. U.S.A.*, vol. 106, no. 21, pp. 8695–8700, May 2009.

[262]   J. W. Tyner, D. K. Walters, S. G. Willis, M. Luttropp, J. Oost, M. Loriaux, H. Erickson, A. S. Corbin, T. O'Hare, M. C. Heinrich, M. W. Deininger, and B. J. Druker, "RNAi screening of the tyrosine kinome identifies therapeutic targets in acute myeloid leukemia.," *Blood*, vol. 111, no. 4, pp. 2238–2245, Feb. 2008.

[263]   T. O'Hare, W. C. Shakespeare, X. Zhu, C. A. Eide, V. M. Rivera, F. Wang, L. T. Adrian, T. Zhou, W.-S. Huang, Q. Xu, C. A. Metcalf, J. W. Tyner, M. M. Loriaux, A. S. Corbin, S. Wardwell, Y. Ning, J. A. Keats, Y. Wang, R. Sundaramoorthi, M. Thomas, D. Zhou, J. Snodgrass, L. Commodore, T. K. Sawyer, D. C. Dalgarno, M. W. N. Deininger, B. J. Druker, and T. Clackson, "AP24534, a pan-BCR-ABL inhibitor for chronic myeloid leukemia, potently inhibits the T315I mutant and overcomes mutation-based resistance.," *Cancer Cell*, vol. 16, no. 5, pp. 401–412, Nov. 2009.

[264]   J. M. Gozgit, M. J. Wong, L. Moran, S. Wardwell, Q. K. Mohemmad, N. I. Narasimhan, W. C. Shakespeare, F. Wang, T. Clackson, and V. M. Rivera, "Ponatinib (AP24534), a multitargeted pan-FGFR inhibitor with activity in multiple FGFR-amplified or mutated cancer models.," *Molecular Cancer Therapeutics*, vol. 11, no. 3, pp. 690–699, Mar. 2012.

[265]   M. Ren, H. Qin, R. Ren, and J. K. Cowell, "Ponatinib suppresses the development of myeloid and lymphoid malignancies associated with FGFR1 abnormalities.," *Leukemia*, vol. 27, no. 1, pp. 32–40, Jan. 2013.

[266]   M. B. Meads, R. A. Gatenby, and W. S. Dalton, "Environment-mediated drug resistance: a major contributor to minimal residual disease.," *Nat. Rev. Cancer*, vol. 9, no. 9, pp. 665–674, Sep. 2009.

[267]   C. R. Degnin, M. B. Laederich, and W. A. Horton, "Ligand activation leads to regulated intramembrane proteolysis of fibroblast growth factor receptor 3.," *Mol. Biol. Cell*, vol. 22, no. 20, pp. 3861–3873, Oct. 2011.

[268]   T. Ernst, P. La Rosée, M. C. Müller, and A. Hochhaus, "BCR-ABL mutations in chronic myeloid leukemia.," *Hematol. Oncol. Clin. North Am.*, vol. 25, no. 5, pp. 997–1008– v–vi, Oct. 2011.

[269]   S. Y. Yoon, A. Tefferi, and C. Y. Li, "Bone marrow stromal cell distribution of basic fibroblast growth factor in chronic myeloid disorders.," *Haematologica*, vol. 86, no. 1, pp. 52–57, Jan. 2001.

[270]   J. M. Chou, C.-Y. Li, and A. Tefferi, "Bone marrow immunohistochemical studies of angiogenic cytokines and their receptors in myelofibrosis with myeloid metaplasia.," *Leuk. Res.*, vol. 27, no. 6, pp. 499–504, Jun. 2003.

[271]   R. C. Inhorn, J. C. Aster, S. A. Roach, C. A. Slapak, R. Soiffer, R. Tantravahi, and R. M. Stone, "A syndrome of lymphoblastic lymphoma, eosinophilia, and myeloid hyperplasia/malignancy associated with t(8;13)(p11;q11): description of a distinctive clinicopathologic entity.," *Blood*, vol. 85, no. 7, pp. 1881–1887, Apr. 1995.

[272] J. Sohal, A. Chase, S. Mould, M. Corcoran, D. Oscier, S. Iqbal, S. Parker, J. Welborn, R. I. Harris, G. Martinelli, V. Montefusco, P. Sinclair, B. S. Wilkins, H. van den Berg, D. Vanstraelen, J. M. Goldman, and N. C. Cross, "Identification of four new translocations involving FGFR1 in myeloid disorders.," *Genes Chromosomes Cancer*, vol. 32, no. 2, pp. 155–163, Oct. 2001.

[273] M. Chesi, E. Nardini, L. A. Brents, E. Schröck, T. Ried, W. M. Kuehl, and P. L. Bergsagel, "Frequent translocation t(4;14)(p16.3;q32.3) in multiple myeloma is associated with increased expression and activating mutations of fibroblast growth factor receptor 3.," *Nat. Genet.*, vol. 16, no. 3, pp. 260–264, Jul. 1997.

[274] R. Richelda, D. Ronchetti, L. Baldini, L. Cro, L. Viggiano, R. Marzella, M. Rocchi, T. Otsuki, L. Lombardi, A. T. Maiolo, and A. Neri, "A novel chromosomal translocation t(4; 14)(p16.3; q32) in multiple myeloma involves the fibroblast growth-factor receptor 3 gene.," *Blood*, vol. 90, no. 10, pp. 4062–4070, Nov. 1997.

[275] D. Cappellen, C. De Oliveira, D. Ricol, S. de Medina, J. Bourdin, X. Sastre-Garau, D. Chopin, J. P. Thiery, and F. Radvanyi, "Frequent activating mutations of FGFR3 in human bladder and cervix carcinomas.," *Nat. Genet.*, vol. 23, no. 1, pp. 18–20, Sep. 1999.

[276] D. Singh, J. M. Chan, P. Zoppoli, F. Niola, R. Sullivan, A. Castano, E. M. Liu, J. Reichel, P. Porrati, S. Pellegatta, K. Qiu, Z. Gao, M. Ceccarelli, R. Riccardi, D. J. Brat, A. Guha, K. Aldape, J. G. Golfinos, D. Zagzag, T. Mikkelsen, G. Finocchiaro, A. Lasorella, R. Rabadan, and A. Iavarone, "Transforming fusions of FGFR and TACC genes in human glioblastoma.," *Science*, vol. 337, no. 6099, pp. 1231–1235, Sep. 2012.

[277] J. S. G. Yeoh, R. van Os, E. Weersing, A. Ausema, B. Dontje, E. Vellenga, and G. de Haan, "Fibroblast growth factor-1 and -2 preserve long-term repopulating ability of hematopoietic stem cells in serum-free cultures.," *Stem Cells*, vol. 24, no. 6, pp. 1564–1572, Jun. 2006.

[278] I. Kashiwakura and T. A. Takahashi, "Basic fibroblast growth factor-stimulated ex vivo expansion of haematopoietic progenitor cells from human placental and umbilical cord blood.," *Br. J. Haematol.*, vol. 122, no. 3, pp. 479–488, Aug. 2003.

[279] G. Brunner, H. Nguyen, J. Gabrilove, D. B. Rifkin, and E. L. Wilson, "Basic fibroblast growth factor expression in human bone marrow and peripheral blood cells.," *Blood*, vol. 81, no. 3, pp. 631–638, Feb. 1993.

[280] A. Montero, Y. Okada, M. Tomita, M. Ito, H. Tsurukami, T. Nakamura, T. Doetschman, J. D. Coffin, and M. M. Hurley, "Disruption of the fibroblast growth factor-2 gene results in decreased bone mass and bone formation.," *J. Clin. Invest.*, vol. 105, no. 8, pp. 1085–1093, Apr. 2000.

[281] M. Zhao, J. T. Ross, T. Itkin, J. M. Perry, A. Venkatraman, J. S. Haug, M. J. Hembree, C.-X. Deng, T. Lapidot, X. C. He, and L. Li, "FGF signaling facilitates postinjury recovery of mouse hematopoietic system.," *Blood*, vol. 120, no. 9, pp. 1831–1842, Aug. 2012.

[282] T. Itkin, K. B. Kaufmann, S. Gur-Cohen, A. Ludin, and T. Lapidot, "Fibroblast growth factor signaling promotes physiological bone remodeling and stem cell self-renewal," *Curr. Opin. Hematol.*, vol. 20, no. 3, pp. 237–244, May 2013.

[283]   B. J. Druker, F. Guilhot, S. G. O'Brien, I. Gathmann, H. Kantarjian, N. Gattermann, M. W. N. Deininger, R. T. Silver, J. M. Goldman, R. M. Stone, F. Cervantes, A. Hochhaus, B. L. Powell, J. L. Gabrilove, P. Rousselot, J. Reiffers, J. J. Cornelissen, T. Hughes, H. Agis, T. Fischer, G. Verhoef, J. Shepherd, G. Saglio, A. Gratwohl, J. L. Nielsen, J. P. Radich, B. Simonsson, K. Taylor, M. Baccarani, C. So, L. Letvak, R. A. Larson, IRIS Investigators, "Five-year follow-up of patients receiving imatinib for chronic myeloid leukemia.," *N. Engl. J. Med.*, vol. 355, no. 23, pp. 2408–2417, Dec. 2006.

[284]   G. D. Demetri, M. von Mehren, C. D. Blanke, A. D. Van den Abbeele, B. Eisenberg, P. J. Roberts, M. C. Heinrich, D. A. Tuveson, S. Singer, M. Janicek, J. A. Fletcher, S. G. Silverman, S. L. Silberman, R. Capdeville, B. Kiese, B. Peng, S. Dimitrijevic, B. J. Druker, C. Corless, C. D. M. Fletcher, and H. Joensuu, "Efficacy and safety of imatinib mesylate in advanced gastrointestinal stromal tumors.," *N. Engl. J. Med.*, vol. 347, no. 7, pp. 472–480, Aug. 2002.

[285]   S.-H. I. Ou, E. L. Kwak, C. Siwak-Tapp, J. Dy, K. Bergethon, J. W. Clark, D. R. Camidge, B. J. Solomon, R. G. Maki, Y.-J. Bang, D.-W. Kim, J. Christensen, W. Tan, K. D. Wilner, R. Salgia, and A. J. Iafrate, "Activity of crizotinib (PF02341066), a dual mesenchymal-epithelial transition (MET) and anaplastic lymphoma kinase (ALK) inhibitor, in a non-small cell lung cancer patient with de novo MET amplification.," *J Thorac Oncol*, vol. 6, no. 5, pp. 942–946, May 2011.

[286]   J. K. Lennerz, E. L. Kwak, A. Ackerman, M. Michael, S. B. Fox, K. Bergethon, G. Y. Lauwers, J. G. Christensen, K. D. Wilner, D. A. Haber, R. Salgia, Y.-J. Bang, J. W. Clark, B. J. Solomon, and A. J. Iafrate, "MET amplification identifies a small and aggressive subgroup of esophagogastric adenocarcinoma with evidence of responsiveness to crizotinib.," *J. Clin. Oncol.*, vol. 29, no. 36, pp. 4803–4810, Dec. 2011.

[287]   J. G. Paez, P. A. Jänne, J. C. Lee, S. Tracy, H. Greulich, S. Gabriel, P. Herman, F. J. Kaye, N. Lindeman, T. J. Boggon, K. Naoki, H. Sasaki, Y. Fujii, M. J. Eck, W. R. Sellers, B. E. Johnson, and M. Meyerson, "EGFR mutations in lung cancer: correlation with clinical response to gefitinib therapy.," *Science*, vol. 304, no. 5676, pp. 1497–1500, Jun. 2004.

[288]   T. J. Lynch, D. W. Bell, R. Sordella, S. Gurubhagavatula, R. A. Okimoto, B. W. Brannigan, P. L. Harris, S. M. Haserlat, J. G. Supko, F. G. Haluska, D. N. Louis, D. C. Christiani, J. Settleman, and D. A. Haber, "Activating mutations in the epidermal growth factor receptor underlying responsiveness of non-small-cell lung cancer to gefitinib.," *N. Engl. J. Med.*, vol. 350, no. 21, pp. 2129–2139, May 2004.

[289]   D. J. Slamon, B. Leyland-Jones, S. Shak, H. Fuchs, V. Paton, A. Bajamonde, T. Fleming, W. Eiermann, J. Wolter, M. Pegram, J. Baselga, and L. Norton, "Use of chemotherapy plus a monoclonal antibody against HER2 for metastatic breast cancer that overexpresses HER2.," *N. Engl. J. Med.*, vol. 344, no. 11, pp. 783–792, Mar. 2001.

[290]   K. T. Flaherty, I. Puzanov, K. B. Kim, A. Ribas, G. A. McArthur, J. A. Sosman, P. J. O'Dwyer, R. J. Lee, J. F. Grippo, K. Nolop, and P. B. Chapman, "Inhibition of mutated, activated BRAF in metastatic melanoma.," *N. Engl. J. Med.*, vol. 363, no. 9, pp. 809–819, Aug. 2010.

[291]   B. D. Smith, M. Levis, M. Beran, F. Giles, H. Kantarjian, K. Berg, K. M. Murphy, T. Dauses, J. Allebach, and D. Small, "Single-agent CEP-701, a novel FLT3 inhibitor, shows biologic and

clinical activity in patients with relapsed or refractory acute myeloid leukemia.," *Blood*, vol. 103, no. 10, pp. 3669–3676, May 2004.

[292]   R. M. Stone, D. J. DeAngelo, V. Klimek, I. Galinsky, E. Estey, S. D. Nimer, W. Grandin, D. Lebwohl, Y. Wang, P. Cohen, E. A. Fox, D. Neuberg, J. Clark, D. G. Gilliland, and J. D. Griffin, "Patients with acute myeloid leukemia and an activating mutation in FLT3 respond to a small-molecule FLT3 tyrosine kinase inhibitor, PKC412.," *Blood*, vol. 105, no. 1, pp. 54–60, Jan. 2005.

[293]   C. Thiede, C. Steudel, B. Mohr, M. Schaich, U. Schäkel, U. Platzbecker, M. Wermke, M. Bornhäuser, M. Ritter, A. Neubauer, G. Ehninger, and T. Illmer, "Analysis of FLT3-activating mutations in 979 patients with acute myelogenous leukemia: association with FAB subtypes and identification of subgroups with poor prognosis.," *Blood*, vol. 99, no. 12, pp. 4326–4335, Jun. 2002.

[294]   P. D. Kottaridis, R. E. Gale, M. E. Frew, G. Harrison, S. E. Langabeer, A. A. Belton, H. Walker, K. Wheatley, D. T. Bowen, A. K. Burnett, A. H. Goldstone, and D. C. Linch, "The presence of a FLT3 internal tandem duplication in patients with acute myeloid leukemia (AML) adds important prognostic information to cytogenetic risk group and response to the first cycle of chemotherapy: analysis of 854 patients from the United Kingdom Medical Research Council AML 10 and 12 trials.," *Blood*, vol. 98, no. 6, pp. 1752–1759, Sep. 2001.

[295]   M. Levis, F. Ravandi, E. S. Wang, M. R. Baer, A. Perl, S. Coutre, H. Erba, R. K. Stuart, M. Baccarani, L. D. Cripe, M. S. Tallman, G. Meloni, L. A. Godley, A. A. Langston, S. Amadori, I. D. Lewis, A. Nagler, R. Stone, K. Yee, A. Advani, D. Douer, W. Wiktor-Jedrzejczak, G. Juliusson, M. R. Litzow, S. Petersdorf, M. Sanz, H. M. Kantarjian, T. Sato, L. Tremmel, D. M. Bensen-Kennedy, D. Small, and B. D. Smith, "Results from a randomized trial of salvage chemotherapy followed by lestaurtinib for patients with FLT3 mutant AML in first relapse.," *Blood*, vol. 117, no. 12, pp. 3294–3301, Mar. 2011.

[296]   F. Ravandi, H. Kantarjian, S. Faderl, G. Garcia-Manero, S. O'Brien, C. Koller, S. Pierce, M. Brandt, D. Kennedy, J. Cortes, and M. Beran, "Outcome of patients with FLT3-mutated acute myeloid leukemia in first relapse.," *Leuk. Res.*, vol. 34, no. 6, pp. 752–756, Jun. 2010.

[297]   S. D. Lyman, L. James, T. Vanden Bos, P. de Vries, K. Brasel, B. Gliniak, L. T. Hollingsworth, K. S. Picha, H. J. McKenna, and R. R. Splett, "Molecular cloning of a ligand for the flt3/flk-2 tyrosine kinase receptor: a proliferative factor for primitive hematopoietic cells.," *Cell*, vol. 75, no. 6, pp. 1157–1167, Dec. 1993.

[298]   M. Nakao, S. Yokota, T. Iwai, H. Kaneko, S. Horiike, K. Kashima, Y. Sonoda, T. Fujimoto, and S. Misawa, "Internal tandem duplication of the flt3 gene found in acute myeloid leukemia.," *Leukemia*, vol. 10, no. 12, pp. 1911–1918, Dec. 1996.

[299]   J. Griffith, J. Black, C. Faerman, L. Swenson, M. Wynn, F. Lu, J. Lippke, and K. Saxena, "The structural basis for autoinhibition of FLT3 by the juxtamembrane domain.," *Mol. Cell*, vol. 13, no. 2, pp. 169–178, Jan. 2004.

[300]   F. M. Abu-Duhier, A. C. Goodeve, G. A. Wilson, M. A. Gari, I. R. Peake, D. C. Rees, E. A. Vandenberghe, P. R. Winship, and J. T. Reilly, "FLT3 internal tandem duplication mutations in

adult acute myeloid leukaemia define a high-risk group.," *Br. J. Haematol.*, vol. 111, no. 1, pp. 190–195, Oct. 2000.

[301]   F. M. Abu-Duhier, A. C. Goodeve, G. A. Wilson, R. S. Care, I. R. Peake, and J. T. Reilly, "Identification of novel FLT-3 Asp835 mutations in adult acute myeloid leukaemia.," *Br. J. Haematol.*, vol. 113, no. 4, pp. 983–988, Jun. 2001.

[302]   Y. Yamamoto, H. Kiyoi, Y. Nakano, R. Suzuki, Y. Kodera, S. Miyawaki, N. Asou, K. Kuriyama, F. Yagasaki, C. Shimazaki, H. Akiyama, K. Saito, M. Nishimura, T. Motoji, K. Shinagawa, A. Takeshita, H. Saito, R. Ueda, R. Ohno, and T. Naoe, "Activating mutation of D835 within the activation loop of FLT3 in human hematologic malignancies.," *Blood*, vol. 97, no. 8, pp. 2434–2439, Apr. 2001.

[303]   T. Fischer, R. M. Stone, D. J. DeAngelo, I. Galinsky, E. Estey, C. Lanza, E. Fox, G. Ehninger, E. J. Feldman, G. J. Schiller, V. M. Klimek, S. D. Nimer, D. G. Gilliland, C. Dutreix, A. Huntsman-Labed, J. Virkus, and F. J. Giles, "Phase IIB trial of oral Midostaurin (PKC412), the FMS-like tyrosine kinase 3 receptor (FLT3) and multi-targeted kinase inhibitor, in patients with acute myeloid leukemia and high-risk myelodysplastic syndrome with either wild-type or mutated FLT3.," *J. Clin. Oncol.*, vol. 28, no. 28, pp. 4339–4345, Oct. 2010.

[304]   R. M. Stone, T. Fischer, R. Paquette, G. Schiller, C. A. Schiffer, G. Ehninger, J. Cortes, H. M. Kantarjian, D. J. DeAngelo, A. Huntsman-Labed, C. Dutreix, A. del Corral, and F. Giles, "Phase IB study of the FLT3 kinase inhibitor midostaurin with chemotherapy in younger newly diagnosed adult patients with acute myeloid leukemia.," *Leukemia*, vol. 26, no. 9, pp. 2061–2068, Sep. 2012.

[305]   C. B. Williams, S. Kambhampati, W. Fiskus, J. Wick, C. Dutreix, S. Ganguly, O. Aljitawi, R. Reyes, A. Fleming, S. Abhyankar, K. N. Bhalla, and J. P. McGuirk, "Preclinical and phase I results of decitabine in combination with midostaurin (PKC412) for newly diagnosed elderly or relapsed/refractory adult patients with acute myeloid leukemia.," *Pharmacotherapy*, vol. 33, no. 12, pp. 1341–1352, Dec. 2013.

[306]   C. H. Man, T. K. Fung, C. Ho, H. H. C. Han, H. C. H. Chow, A. C. H. Ma, W. W. L. Choi, S. Lok, A. M. S. Cheung, C. Eaves, Y. L. Kwong, and A. Y. H. Leung, "Sorafenib treatment of FLT3-ITD(+) acute myeloid leukemia: favorable initial outcome and mechanisms of subsequent nonresponsiveness associated with the emergence of a D835 mutation.," *Blood*, vol. 119, no. 22, pp. 5133–5143, May 2012.

[307]   J. E. Cortes, H. Kantarjian, J. M. Foran, D. Ghirdaladze, M. Zodelava, G. Borthakur, G. Gammon, D. Trone, R. C. Armstrong, J. James, and M. Levis, "Phase I study of quizartinib administered daily to patients with relapsed or refractory acute myeloid leukemia irrespective of FMS-like tyrosine kinase 3-internal tandem duplication status.," *J. Clin. Oncol.*, vol. 31, no. 29, pp. 3681–3687, Oct. 2013.

[308]   C. C. Smith, Q. Wang, C.-S. Chin, S. Salerno, L. E. Damon, M. J. Levis, A. E. Perl, K. J. Travers, S. Wang, J. P. Hunt, P. P. Zarrinkar, E. E. Schadt, A. Kasarskis, J. Kuriyan, and N. P. Shah, "Validation of ITD mutations in FLT3 as a therapeutic target in human acute myeloid leukaemia.," *Nature*, vol. 485, no. 7397, pp. 260–263, May 2012.

[309]   Y. Alvarado, H. M. Kantarjian, R. Luthra, F. Ravandi, G. Borthakur, G. Garcia-Manero, M. Konopleva, Z. Estrov, M. Andreeff, and J. E. Cortes, "Treatment with FLT3 inhibitor in patients with FLT3-mutated acute myeloid leukemia is associated with development of secondary FLT3-tyrosine kinase domain mutations.," *Cancer*, vol. 120, no. 14, pp. 2142–2149, Jul. 2014.

[310]   T. Sato, X. Yang, S. Knapper, P. White, B. D. Smith, S. Galkin, D. Small, A. Burnett, and M. Levis, "FLT3 ligand impedes the efficacy of FLT3 inhibitors in vitro and in vivo.," *Blood*, vol. 117, no. 12, pp. 3286–3293, Mar. 2011.

[311]   D. M. Ornitz and P. Leder, "Ligand specificity and heparin dependence of fibroblast growth factor receptors 1 and 3.," *Journal of Biological Chemistry*, vol. 267, no. 23, pp. 16305–16311, Aug. 1992.

[312]   K. W. H. Yee, M. Schittenhelm, A.-M. O'Farrell, A. R. Town, L. McGreevey, T. Bainbridge, J. M. Cherrington, and M. C. Heinrich, "Synergistic effect of SU11248 with cytarabine or daunorubicin on FLT3 ITD-positive leukemic cells.," *Blood*, vol. 104, no. 13, pp. 4202–4209, Dec. 2004.

[313]   I. Ben-Batalla, A. Schultze, M. Wroblewski, R. Erdmann, M. Heuser, J. S. Waizenegger, K. Riecken, M. Binder, D. Schewe, S. Sawall, V. Witzke, M. Cubas-Cordova, M. Janning, J. Wellbrock, B. Fehse, C. Hagel, J. Krauter, A. Ganser, J. B. Lorens, W. Fiedler, P. Carmeliet, K. Pantel, C. Bokemeyer, and S. Loges, "Axl, a prognostic and therapeutic target in acute myeloid leukemia mediates paracrine crosstalk of leukemia cells with bone marrow stroma.," *Blood*, vol. 122, no. 14, pp. 2443–2452, Oct. 2013.

[314]   I.-K. Park, A. Mishra, J. Chandler, S. P. Whitman, G. Marcucci, and M. A. Caligiuri, "Inhibition of the receptor tyrosine kinase Axl impedes activation of the FLT3 internal tandem duplication in human acute myeloid leukemia: implications for Axl as a potential therapeutic target.," *Blood*, vol. 121, no. 11, pp. 2064–2073, Mar. 2013.

[315]   E. I. Zimmerman, D. C. Turner, J. Buaboonnam, S. Hu, S. Orwick, M. S. Roberts, L. J. Janke, A. Ramachandran, C. F. Stewart, H. Inaba, and S. D. Baker, "Crenolanib is active against models of drug-resistant FLT3-ITD-positive acute myeloid leukemia.," *Blood*, vol. 122, no. 22, pp. 3607–3615, Nov. 2013.

[316]   B. A. Roecklein and B. Torok-Storb, "Functionally distinct human marrow stromal cell lines immortalized by transduction with the human papilloma virus E6/E7 genes.," *Blood*, vol. 85, no. 4, pp. 997–1005, Feb. 1995.

[317]   A. Parmar, S. Marz, S. Rushton, C. Holzwarth, K. Lind, S. Kayser, K. Döhner, C. Peschel, R. A. J. Oostendorp, and K. S. Götze, "Stromal niche cells protect early leukemic FLT3-ITD+ progenitor cells against first-generation FLT3 tyrosine kinase inhibitors.," *Cancer Res.*, vol. 71, no. 13, pp. 4696–4706, Jul. 2011.

[318]   E. Weisberg, R. D. Wright, D. W. McMillin, C. Mitsiades, A. Ray, R. Barrett, S. Adamia, R. Stone, I. Galinsky, A. L. Kung, and J. D. Griffin, "Stromal-mediated protection of tyrosine kinase inhibitor-treated BCR-ABL-expressing leukemia cells.," *Molecular Cancer Therapeutics*, vol. 7, no. 5, pp. 1121–1129, May 2008.

[319]   X. Yang, A. Sexauer, and M. Levis, "Bone marrow stroma-mediated resistance to FLT3 inhibitors in FLT3-ITD AML is mediated by persistent activation of extracellular regulated kinase.," *Br. J. Haematol.*, vol. 164, no. 1, pp. 61–72, Jan. 2014.

[320]   O. Piloto, M. Wright, P. Brown, K.-T. Kim, M. Levis, and D. Small, "Prolonged exposure to FLT3 inhibitors leads to resistance via activation of parallel signaling pathways.," *Blood*, vol. 109, no. 4, pp. 1643–1652, Feb. 2007.

[321]   E. Traer, N. Javidi-Sharifi, A. Agarwal, J. Dunlap, I. English, J. Martinez, J. W. Tyner, M. Wong, and B. J. Druker, "Ponatinib overcomes FGF2-mediated resistance in CML patients without kinase domain mutations.," *Blood*, vol. 123, no. 10, pp. 1516–1524, Mar. 2014.

[322]   N. Javidi-Sharifi, E. Traer, J. Martinez, A. Gupta, T. Taguchi, J. Dunlap, M. C. Heinrich, C. L. Corless, B. P. Rubin, B. J. Druker, and J. W. Tyner, "Crosstalk between KIT and FGFR3 Promotes Gastrointestinal Stromal Tumor Cell Growth and Drug Resistance.," *Cancer Res.*, vol. 75, no. 5, pp. 880–891, Mar. 2015.

[323]   R. Straussman, T. Morikawa, K. Shee, M. Barzily-Rokni, Z. R. Qian, J. Du, A. Davis, M. M. Mongare, J. Gould, D. T. Frederick, Z. A. Cooper, P. B. Chapman, D. B. Solit, A. Ribas, R. S. Lo, K. T. Flaherty, S. Ogino, J. A. Wargo, and T. R. Golub, "Tumour micro-environment elicits innate resistance to RAF inhibitors through HGF secretion.," *Nature*, vol. 487, no. 7408, pp. 500–504, Jul. 2012.

[324]   Z. Zhang, J. C. Lee, L. Lin, V. Olivas, V. Au, T. LaFramboise, M. Abdel-Rahman, X. Wang, A. D. Levine, J. K. Rho, Y. J. Choi, C.-M. Choi, S.-W. Kim, S. J. Jang, Y. S. Park, W. S. Kim, D. H. Lee, J.-S. Lee, V. A. Miller, M. Arcila, M. Ladanyi, P. Moonsamy, C. Sawyers, T. J. Boggon, P. C. Ma, C. Costa, M. Taron, R. Rosell, B. Halmos, and T. G. Bivona, "Activation of the AXL kinase causes resistance to EGFR-targeted therapy in lung cancer.," *Nat. Genet.*, vol. 44, no. 8, pp. 852–860, Aug. 2012.

[325]   K. H. Metzeler, M. Hummel, C. D. Bloomfield, K. Spiekermann, J. Braess, M.-C. Sauerland, A. Heinecke, M. Radmacher, G. Marcucci, S. P. Whitman, K. Maharry, P. Paschka, R. A. Larson, W. E. Berdel, T. Büchner, B. Wörmann, U. Mansmann, W. Hiddemann, S. K. Bohlander, C. Buske, Cancer and Leukemia Group B, German AML Cooperative Group, "An 86-probe-set gene-expression signature predicts survival in cytogenetically normal acute myeloid leukemia.," *Blood*, vol. 112, no. 10, pp. 4193–4201, Nov. 2008.

[326]   E. Traer, R. MacKenzie, J. Snead, A. Agarwal, A. M. Eiring, T. O'Hare, B. J. Druker, and M. W. Deininger, "Blockade of JAK2-mediated extrinsic survival signals restores sensitivity of CML cells to ABL inhibitors.," *Leukemia*, vol. 26, no. 5, pp. 1140–1143, May 2012.

[327]   A. Colmone, M. Amorim, A. L. Pontier, S. Wang, E. Jablonski, and D. A. Sipkins, "Leukemic cells create bone marrow niches that disrupt the behavior of normal hematopoietic progenitor cells.," *Science*, vol. 322, no. 5909, pp. 1861–1865, Dec. 2008.

[328]   T. Manshouri, Z. Estrov, A. Quintás-Cardama, J. Burger, Y. Zhang, A. Livun, L. Knez, D. Harris, C. J. Creighton, H. M. Kantarjian, and S. Verstovsek, "Bone marrow stroma-secreted cytokines protect JAK2(V617F)-mutated cells from the effects of a JAK2 inhibitor.," *Cancer Res.*, vol. 71, no. 11, pp. 3831–3840, Jun. 2011.

[329]   J. C. Huang, S. K. Basu, X. Zhao, S. Chien, M. Fang, V. G. Oehler, F. R. Appelbaum, and P. S. Becker, "Mesenchymal stromal cells derived from acute myeloid leukemia bone marrow exhibit aberrant cytogenetics and cytokine elaboration.," *Blood Cancer J*, vol. 5, no. 4, p. e302, 2015.

[330]   J. Huan, N. I. Hornick, N. A. Goloviznina, A. N. Kamimae-Lanning, L. L. David, P. A. Wilmarth, T. Mori, J. R. Chevillet, A. Narla, C. T. Roberts, M. M. Loriaux, B. H. Chang, and P. Kurre, "Coordinate regulation of residual bone marrow function by paracrine trafficking of AML exosomes.," *Leukemia*, Jun. 2015.

[331]   S. Zacherl, G. La Venuta, H.-M. Müller, S. Wegehingel, E. Dimou, P. Sehr, J. D. Lewis, H. Erfle, R. Pepperkok, and W. Nickel, "A direct role for ATP1A1 in unconventional secretion of fibroblast growth factor 2.," *J. Biol. Chem.*, vol. 290, no. 6, pp. 3654–3665, Feb. 2015.

[332]   H. Sprong, P. van der Sluijs, and G. van Meer, "How proteins move lipids and lipids move proteins.," *Nat Rev Mol Cell Biol*, vol. 2, no. 7, pp. 504–513, Jul. 2001.

[333]   C. L. Baron and V. Malhotra, "Role of diacylglycerol in PKD recruitment to the TGN and protein transport to the plasma membrane.," *Science*, vol. 295, no. 5553, pp. 325–328, Jan. 2002.

[334]   M. G. Roth, "Lipid regulators of membrane traffic through the Golgi complex.," *Trends Cell Biol.*, vol. 9, no. 5, pp. 174–179, May 1999.

[335]   E. J. Quann, E. Merino, T. Furuta, and M. Huse, "Localized diacylglycerol drives the polarization of the microtubule-organizing center in T cells.," *Nat. Immunol.*, vol. 10, no. 6, pp. 627–635, Jun. 2009.

[336]   R. Alonso, C. Mazzeo, I. Mérida, and M. Izquierdo, "A new role of diacylglycerol kinase alpha on the secretion of lethal exosomes bearing Fas ligand during activation-induced cell death of T lymphocytes.," *Biochimie*, vol. 89, no. 2, pp. 213–221, Feb. 2007.

[337]   R. Alonso, C. Mazzeo, M. C. Rodriguez, M. Marsh, A. Fraile-Ramos, V. Calvo, A. Avila-Flores, I. Merida, and M. Izquierdo, "Diacylglycerol kinase α regulates the formation and polarisation of mature multivesicular bodies involved in the secretion of Fas ligand-containing exosomes in T lymphocytes.," *Cell Death Differ.*, vol. 18, no. 7, pp. 1161–1173, Jul. 2011.

[338]   R. Alonso, M. C. Rodríguez, J. Pindado, E. Merino, I. Mérida, and M. Izquierdo, "Diacylglycerol kinase alpha regulates the secretion of lethal exosomes bearing Fas ligand during activation-induced cell death of T lymphocytes.," *Journal of Biological Chemistry*, vol. 280, no. 31, pp. 28439–28450, Aug. 2005.

[339]   J. Bao, I. Alroy, H. Waterman, E. D. Schejter, C. Brodie, J. Gruenberg, and Y. Yarden, "Threonine phosphorylation diverts internalized epidermal growth factor receptors from a degradative pathway to the recycling endosome.," *Journal of Biological Chemistry*, vol. 275, no. 34, pp. 26178–26186, Aug. 2000.

[340]   T. A. Bailey, H. Luan, E. Tom, T. A. Bielecki, B. Mohapatra, G. Ahmad, M. George, D. L. Kelly, A. Natarajan, S. M. Raja, V. Band, and H. Band, "A kinase inhibitor screen reveals protein

kinase C-dependent endocytic recycling of ErbB2 in breast cancer cells.," *J. Biol. Chem.*, vol. 289, no. 44, pp. 30443–30458, Oct. 2014.

[341]   A. J. Singh, R. D. Meyer, H. Band, and N. Rahimi, "The carboxyl terminus of VEGFR-2 is required for PKC-mediated down-regulation.," *Mol. Biol. Cell*, vol. 16, no. 4, pp. 2106–2118, Apr. 2005.

[342]   S. Kermorgant, D. Zicha, and P. J. Parker, "PKC controls HGF-dependent c-Met traffic, signalling and cell migration.," *EMBO J*, vol. 23, no. 19, pp. 3721–3734, Oct. 2004.

[343]   B. Nadratowska-Wesolowska, E. M. Haugsten, M. Zakrzewska, P. Jakimowicz, Y. Zhen, D. Pajdzik, J. Wesche, and A. Wiedlocha, "RSK2 regulates endocytosis of FGF receptor 1 by phosphorylation on serine 789.," *Oncogene*, vol. 33, no. 40, pp. 4823–4836, Oct. 2014.

[344]   A. Savina, M. Furlán, M. Vidal, and M. I. Colombo, "Exosome release is regulated by a calcium-dependent mechanism in K562 cells.," *Journal of Biological Chemistry*, vol. 278, no. 22, pp. 20083–20090, May 2003.

[345]   P. Filipazzi, M. Bürdek, A. Villa, L. Rivoltini, and V. Huber, "Recent advances on the role of tumor exosomes in immunosuppression and disease progression.," *Semin. Cancer Biol.*, vol. 22, no. 4, pp. 342–349, Aug. 2012.

[346]   S. Viola, E. Traer, J. Huan, N. I. Hornick, J. W. Tyner, A. Agarwal, M. Loriaux, B. Johnstone, and P. Kurre, "Alterations in acute myeloid leukaemia bone marrow stromal cell exosome content coincide with gains in tyrosine kinase inhibitor resistance.," *Br. J. Haematol.*, pp. n/a–n/a, Jun. 2015.

[347]   N. Sato, Y. Hattori, D. Wenlin, T. Yamada, T. Kamata, T. Kakimoto, S. Okamoto, C. Kawamura, M. Kizaki, N. Shimada, Y. Ote, J.-I. Hata, and Y. Ikeda, "Elevated level of plasma basic fibroblast growth factor in multiple myeloma correlates with increased disease activity.," *Jpn. J. Cancer Res.*, vol. 93, no. 4, pp. 459–466, Apr. 2002.

[348]   J. S. Choi, H. I. Yoon, K. S. Lee, Y. C. Choi, S. H. Yang, I.-S. Kim, and Y. W. Cho, "Exosomes from differentiating human skeletal muscle cells trigger myogenesis of stem cells and provide biochemical cues for skeletal muscle regeneration.," *J Control Release*, vol. 222, pp. 107–115, Jan. 2016.

[349]   T. Schäfer, H. Zentgraf, C. Zehe, B. Brügger, J. Bernhagen, and W. Nickel, "Unconventional secretion of fibroblast growth factor 2 is mediated by direct translocation across the plasma membrane of mammalian cells.," *Journal of Biological Chemistry*, vol. 279, no. 8, pp. 6244–6251, Feb. 2004.

[350]   I. Delrieu, "The high molecular weight isoforms of basic fibroblast growth factor (FGF-2): an insight into an intracrine mechanism.," *FEBS Lett.*, vol. 468, no. 1, pp. 6–10, Feb. 2000.

[351]   M. Amorim, G. Fernandes, P. Oliveira, D. Martins-de-Souza, E. Dias-Neto, and D. Nunes, "The overexpression of a single oncogene (ERBB2/HER2) alters the proteomic landscape of extracellular vesicles." *Proteomics*, vol. 14, no. 12, pp. 1472–1479, Jun. 2014.

[352]   Y. Matsuoka, R. Nakatsuka, K. Sumide, H. Kawamura, M. Takahashi, T. Fujioka, Y. Uemura, H. Asano, Y. Sasaki, M. Inoue, H. Ogawa, T. Takahashi, M. Hino, and Y. Sonoda,

"Prospectively Isolated Human Bone Marrow Cell-Derived MSCs Support Primitive Human CD34-Negative Hematopoietic Stem Cells.," *Stem Cells*, vol. 33, no. 5, pp. 1554–1565, May 2015.

[353]   T. C. Chou and P. Talalay, "Quantitative analysis of dose-effect relationships: the combined effects of multiple drugs or enzyme inhibitors.," *Advances in enzyme regulation*, vol. 22, pp. 27–55, 1984.

[354]   M. degnin, K. tarlock, A. Agarwal, S. meshinchi, C. Tognon, and B. J. Druker, "Novel Method to Perform Functional Drug Screens on Frozen Primary Leukemia Samples," *American Society of Hematology*. 03-Dec-2015.

[355]   J. W. Tyner, W. F. Yang, A. Bankhead, G. Fan, L. B. Fletcher, J. Bryant, J. M. Glover, B. H. Chang, S. E. Spurgeon, W. H. Fleming, T. Kovacsovics, J. R. Gotlib, S. T. Oh, M. W. Deininger, C. M. Zwaan, M. L. Den Boer, M. M. van den Heuvel-Eibrink, T. O'Hare, B. J. Druker, and M. M. Loriaux, "Kinase pathway dependence in primary human leukemias determined by rapid inhibitor screening.," *Cancer Res.*, vol. 73, no. 1, pp. 285–296, Jan. 2013.

[356]   J. Dunlap, C. Beadling, A. Warrick, T. Neff, W. H. Fleming, M. Loriaux, M. C. Heinrich, T. Kovacsovics, K. Kelemen, N. Leeborg, K. Gatter, R. M. Braziel, R. Press, C. L. Corless, and G. Fan, "Multiplex high-throughput gene mutation analysis in acute myeloid leukemia.," *Human Pathology*, vol. 43, no. 12, pp. 2167–2176, Dec. 2012.